PLANKTONIC FORAMINIFERAL BIOSTRATIGRAPHY, SEQUENCE STRATIGRAPHY AND FORAMINIFERAL RESPONSE TO SEDIMENTARY CYCLICITY IN THE UPPER CRETACEOUS-PALEOCENE OF THE HAYMANA BASIN (CENTRAL ANATOLIA, TURKEY)

A THESIS SUBMITTED TO
THE GRADUATE SCHOOL OF NATURAL AND APPLIED SCIENCES
OF
MIDDLE EAST TECHNICAL UNIVERSITY

BY

ELNUR AMIROV

IN PARTIAL FULFILLMENT OF THE REQUIREMENTS
FOR
THE DEGREE OF MASTER OF SCIENCE
IN
GEOLOGICAL ENGINEERING

NOVEMBER 2008

Approval of thesis:

PLANKTONIC FORAMINIFERAL BIOSTRATIGRAPHY, SEQUENCE STRATIGRAPHY AND FORAMINIFERAL RESPONSE TO SEDIMENTARY CYCLICITY IN THE UPPER CRETACEOUS-PALEOCENE OF THE HAYMANA BASIN (CENTRAL ANATOLIA, TURKEY)

submitted by **ELNUR AMIROV** in partial fulfillment of the requirements for the degree of **Master of Science in Geological Engineering Department, Middle East Technical University** by,

Prof. Dr. Canan Özgen _____
Dean, Graduate School of **Natural and Applied Sciences**

Prof. Dr. Zeki Çamur _____
Head of Department, **Geological Engineering**

Assoc. Prof. Dr. Sevinç Özkan Altıner _____
Supervisor, **Geological Engineering Dept., METU**

Prof. Dr. Demir Altıner _____
Co-Supervisor, **Geological Engineering Dept., METU**

Examining Committee Members:

Prof. Dr. Asuman Günal-Türkmenoğlu _____
Geological Engineering Dept., METU

Assoc. Prof. Dr. Sevinç Özkan Altıner _____
Geological Engineering Dept., METU

Assoc. Prof. Dr. Bora Rojay _____
Geological Engineering Dept., METU

Assist. Prof. Dr. İsmail Ömer Yılmaz _____
Geological Engineering Dept., METU

Dr. Zühtü Batı _____
Turkish Petroleum Corporation

Date: 21.11.2008

I hereby declare that all information in this document has been obtained and presented in accordance with academic rules and ethical conduct. I also declare that, as required by these rules and conduct, I have fully cited and referenced all material and results that are not original to this work.

Name, Last Name: Elnur AMIROV

Signature:

ABSTRACT

PLANKTONIC FORAMINIFERAL BIOSTRATIGRAPHY, SEQUENCE STRATIGRAPHY AND FORAMINIFERAL RESPONSE TO SEDIMENTARY CYCLICITY IN THE UPPER CRETACEOUS-PALEOCENE OF THE HAYMANA BASIN (CENTRAL ANATOLIA, TURKEY)

Amirov, Elnur
M.Sc., Department of Geological Engineering
Supervisor: Assoc. Prof. Dr. Sevinç Özkan Altıner
Co-Supervisor: Prof. Dr. Demir Altıner

November 2008, 213 pages

The aim of this study is to establish the planktonic foraminiferal biozonation, to construct the sequence stratigraphical framework and to determine the foraminiferal response to sedimentary cyclicity in the sedimentary sequence spanning Upper Cretaceous-Paleocene in the Haymana basin (Central Anatolia, Turkey).

In order to achieve this study, the stratigraphic section was measured from sedimentary sequence of the Haymana, Beyobası and Yeşilyurt formations. The sedimentary sequence is mainly characterized by flyschoidal sequence that is composed of alternating of siliciclastic and carbonate units.

On the account of the detailed taxonomic study of planktonic foraminifers, the biostratigraphic framework was established for the Maastrichtian-Paleocene interval. The biozonation includes 7 zones; *Pseudoguembelina hariaensis*, Pα, P1, P2, P3, P4 and P5 zones. The Cretaceous-Paleogene (K/P) boundary was delinated between the samples HEA-105 and 106.

In order to construct the sequence-stratigraphical framework, the A, B, C and D-type meter-scale cycles were identified. Based on the stacking patterns of

them, six depositional sequences, six third and two second order cycles were determined. Third order cycles coincide with the Global Sea Level Change Curve.

On the account of the conducted petrographic analysis sandstone, mudstone, marl, limestone and muddy-limestone lithofacies were recorded in the studied samples. In order to demostrate the response of foraminifers to cyclicity, quantitative analysis has been carried out by counting the individuals of planktonic, benthonic foraminifers and ostracods. The best response to sedimentary cyclicity was revealed from planktonic foraminifers. The average abundance of planktonic foraminifers increases in the transgressive systems tract and decreases in the highstand systems tract.

Keywords: Planktonic Foraminifers, Biostratigraphy, Sequence Stratigraphy, Upper Cretaceous-Paleocene, Haymana basin (Central Anatolia, Turkey).

ÖZ

HAYMANA BASENİNDEKİ (ORTA ANADOLU, TÜRKİYE) ÜST KRETASE-PALEOSEN PLANKTONİK FORAMİNİFER BİYOSTRATİGRAFİSİ, SEKANS STRATİGRAFİSİ VE FORAMİNİFERLERİN SEDİMANTER DEVİRSELLİĞE TEPKİSİ

Amirov, Elnur
Yüksek Lisans, Jeoloji Mühendisliği Bölümü
Tez Yöneticisi: Doç. Dr. Sevinç Özkan Altıner
Yardımcı tez Yöneticisi: Prof. Dr. Demir Altıner

Kasım 2008, 213 sayfa

Bu çalışmanın amacı, Haymana Basenindeki (Orta Anadolu, Türkiye) Üst Kretase-Paleosen sedimenter istifinin planktonik foraminifer biyozonasyonunu kurmak, sekans stratigrafi çatısını oluşturmak, ve foraminiferlerin sedimanter devirselliğe karşı tepkilerini belirlemektir.

Bu çalışmayı gerçekleştirmek için, Haymana, Beyobası, ve Yeşilyurt formasyonlarının sedimanter istifinden kesit ölçülmüştür. Sedimanter istif silisiklastik ve karbonat birimlerinin ardalanmasından oluşan flişoidal istif ile karakterize edilir.

Planktonik foraminiferlerin detaylı taksonomik çalışılmasıyla, Maastrihtiyen-Paleosen aralığı için biyostratigrafik çatı kurulmuştur. Bu zonasyon 7 zon içerir; *Pseudoguembelina hariaensis*, Pα, P1, P2, P3, P4 and P5 zonları. Kretase-Paleojen (K/P) sınırı HEA-105 ve HEA-106 örnekleri arasından çizilmiştir.

Sekans stratigrafik çatıyı oluşturmak için A, B, C ve D-tipi metre ölçekli devirler tanımlanmıştır. Bunların dikey birlikteliklerinden, altı sedimanter istif,

altı üçüncü ve iki ikinci dereceden devir belirlenmiştir. Üçüncü derece devirler global deniz seviyesi değişimleri ile uyum göstermektedir.

Petrografik analizler sonucu, çalışılan örneklerde kumtaşı, çamurtaşı, marn, kireştaşı ve killi-kireştaşı litofasiyesleri kaydedilmiştir. Foraminiferlerin devirselliğe tepkisinin belirlenmesi için, planktonik ve bentonik foraminiferler ile ostrakod bireyleri sayılarak kantitatif analiz yapılmıştır. Sedimanter devirselliğe en iyi tepkiyi planktonik foraminiferler göstermiştir. Planktonik foraminiferlerin ortalama bolluğu Transgresif Sistem Traktta artmakta ve Highstand Sistem Traktta azalmaktadır.

Anahtar kelimeler: Planktonik Foraminifer, Biyostratigrafi, Sekans Stratigrafi, Üst Kretase-Paleocene, Haymana Havzası (Orta Anadolu, Türkiye).

To my beloved parents and sister…

ACKNOWLEDGEMENTS

I would like to express my deepest gratitude to my supervisor. It is a highly rewarding experience gained by working under the supervision of Assoc. Prof. Dr. Sevinç ÖZKAN ALTINER, to whom I am indebted for her valuable advice, encouragement, theoretical support and criticism during the field studies and the preparation of this thesis.

I would like to thank to Prof. Dr. Demir ALTINER for his attention and constructive recommendations during my studies and for his encouragements and for making me highly motivated during my education.

I would like to express my gratitude to Assist. Prof. Dr. I. Ömer YILMAZ for his advises and for his scientific explanations for Carbonate Petrology.

I would like to thank to Mr. Orhan KARAMAN for his help in the preparation of my thin sections.

I would like to thank to all my teachers from Azerbaijan for their valuable advises and encouragements as well, especially for Mr. Akif ALIZADE, Mrs. Elmira ALIYEVA, Mrs. Aliya BABAZADEH, Mr. Vahid AGAYEV, Mr. Nazim IMAMVERDIYEV and Mr. Aydin MAMMEDOV.

I am most grateful to all my friends for their friendships and endless encouragements. Especially, I would like to thank to Afgan HUSEYNOV, Rufat AGAYEV, Mejid AMIROV, Elnur BINYATOV, Farid BABAYEV, Aysel MAJIDOVA, Selen ESMERAY, Ayşe ATAKUL ÖZDEMİR and Aydın ÇIÇEK for their helps and encouragements.

Finally, at last but not the least, I would like to express my grateful appreciation to my mother Mrs. Sevda AMIROVA, to my father Mr. Fikret AMIROV and my sister Ms. Aynura AMIROVA for their support and encouragements during my studies.

I would like to note that this scrupulous research work have been possible due to financial support of British Petroleum Caspian Sea Exploration and that is

why I would like to express my grateful appreciation to Mr. David DAY, to all teams of Azerbaijan Busines Unit and to all HR team for this opportunity given to me.

TABLE OF CONTENTS

LIST OF TABLES

LIST OF FIGURES

CHAPTER 1

INTRODUCTION

1.1 Purpose and Scope

Planktonic foraminifers are ideal index fossils. Their rapid evolution, their cosmopolitan nature and their great abundance in many deep marine sedimentary rocks make them excellent biostratigraphic tools for precise world-wide correlation. They are also used for recognition of environmental changes and the estimation of the ancient climatic and oceanographic conditions.

The present study primarily concerns with an analysis of the Maastrichtian-Paleocene planktonic foraminifers of a sedimentary succession from the Haymana basin, Central Anatolia, Turkey. The recovery of many species from samples provides the basis on the taxonomy and biostratigraphy. The purpose of this study is:

- To describe and illustrate the planktonic foraminifers occurring in the uppermost Cretaceous-Paleocene succession;
- To establish the biostratigraphic zonation based on the planktonic foraminifers;
- To correlate the biostratigraphic study with the established worldwide planktonic foraminiferal zonation;
- To delineate the Cretaceous-Paleogene boundary in the studied succession by using the resulting zonation;
- To point out the response of foraminifers to the environmental changes by using the ratio of relative abundance of benthonic foraminifers to planktonic foraminifers;
- To analyze the microfacies of the studied samples;

- To determine the depositional cycles by using stacking pattern of these microfacies and;
- to construct the sequence stratigraphic framework and compare with the Global Sea Level Change Curve.

To achieve these objectives, a stratigraphic section was measured from the uppermost Cretaceous-Paleogene sedimentary sequence in the Haymana region. Since the Upper Cretaceous-Lower Tertiary succession is complete and well exposed in the Haymana region, this area was chosen as the studied area. A total of 106 samples were collected. Several studies were performed based on different disciplines of geology including lithostratigraphy, taxonomy, biostratigraphy, microfacies analysis and the sequence stratigraphy. Concerning the scope of the study, a semi-quantitative analysis based on the relative abundances of foraminifers has been also carried out to present an account on response of planktonic and benthonic foraminifers to sedimentary cyclicity.

1.2 Geographic Setting

The Haymana basin (presently 60 × 60 km in size) is located at approximately about 70 km SW of Ankara in Central Anatolia (Figure 1, Figure 2). It is situated in the topographic map of Ankara of 1:500000 scales. The studied section was measured southwest of the Haymana (Figure 1). By the GPS recordings, the section starts at coordinates 36454254 E – 4363267 N (elevation 1202 m, 39° 25' 01 N – 032° 28' 07 E) and finishes at 36453997 E – 4363156 N (elevation 1272 m, 39° 24' 58 N – 032° 27' 55 E) (Figure 2).

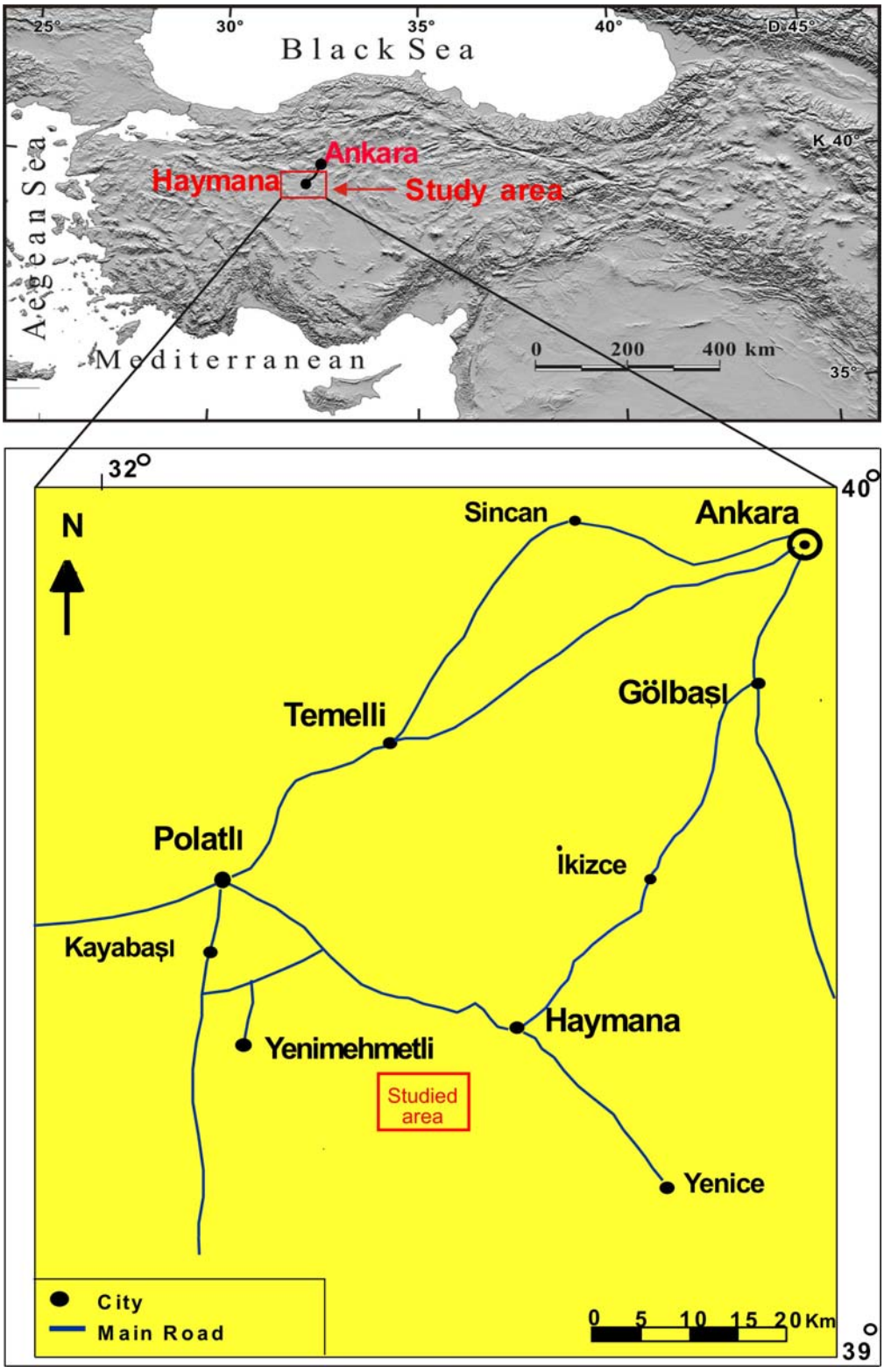

Figure 1. Geographic setting of the study area and the location of the measured section.

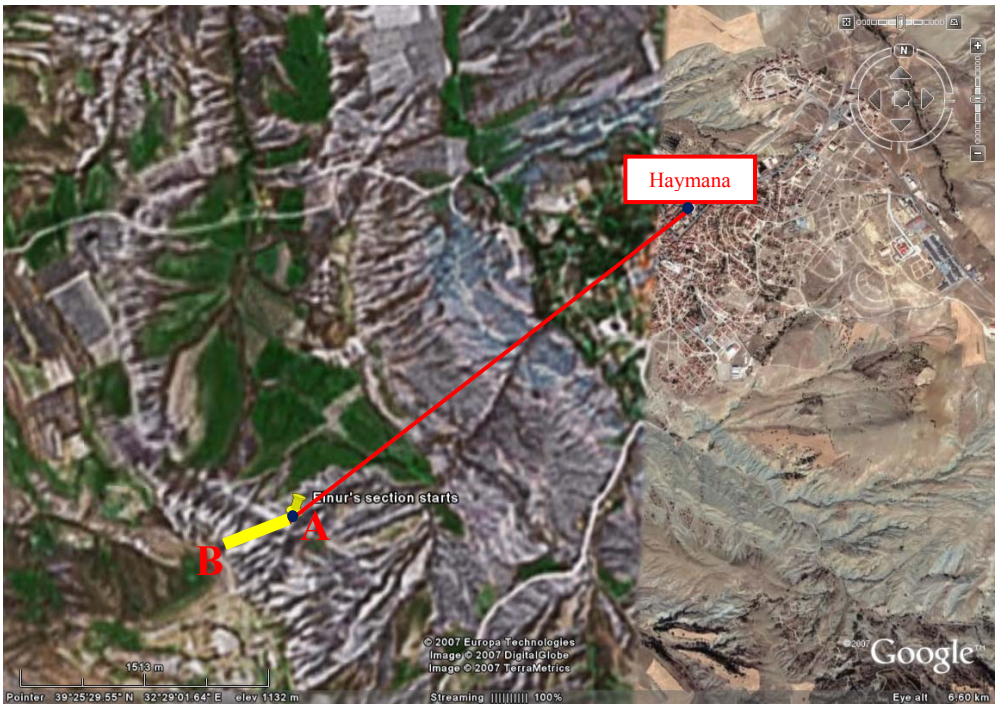

Figure 2. Satellite snapshot of the measured section (yellow line, A-section start point, B-section end point) (Google Earth Software).

1.3 Method of Study

This study included field and laboratory works. In the field study, a stratigraphic section was measured through the succession, which was 162 m in thickness. The succession is mainly composed of rhythmic alternation of mudstone and marl deposits (Figure 3). During the field work, the studied succession was examined bed by bed, lithological properties and fossil content were recognized by hand lens and 106 samples were collected nearly from each bed along the section. Actually two stratigraphic sections were measured. First HEA section was measured on 31st May 2007 and a total 53 samples (HEA-1-53) were collected. Following a rapid examination of the samples, the age of the succession was determined as Paleocene. In order to delineate the boundary between Cretaceous-Paleogene, the lower part of the succession were measured and collected samples (HEA-101-153) during the second field-work on 25th June

2007. As a result, a composite section has been obtained which represents the latest Cretaceous-Paleocene interval.

The laboratory work included the preparation of thin sections and the application of different washing methods. In order to recognize the faunal content and microfacies of the studied succession, oriented thin-sections (all samples were marked according to top to bottom of the bed in the field study) were prepared from all of the samples collected.

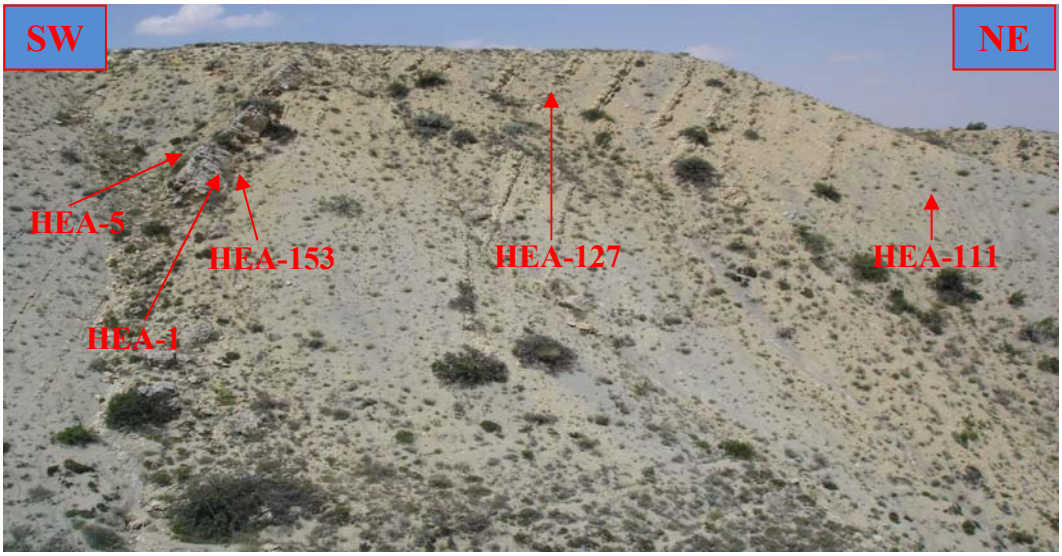

Figure 3. The generalized view of the studied stratigraphic section (numbers indicate the stratigraphic position of collected samples across the succession).

The various washing methods were applied on all 106 samples for extracting the individual planktonic foraminifers from the rock. First of all standard washing techniques, such as hydrogen peroxide treatment, were applied to extract the individual forms. Since this method was not proper for marl and limestone samples, different washing methods were compiled from different articles (Knitter, 1979; Canudo, 1997; Arenillas *et al*., 2000; Tur *et al*., 2001; Weber *et al*., 2001; Keller *et al*., 2002; Luciani, 2002). All those methods were applied and the best result was obtained from the method described below:

For limestones, 20 gr per each samples were broken into small pieces and placed into the glass jars. 50% of acetic acid (CH_3COOH) solution was added

onto the samples up to a level to cover the whole sample and after 20 ml of chloroform ($CHCL_3$) was added to each jar, tap of the jars was closed tightly. The amount of chloroform was determined as to be the same as the weight of the sample (like 20 ml of chloroform for 20 gr of sample). After waiting 2, 4, 6, 12 and 24 hours, the lids were opened and the samples were washed under tap water by standard method and picked from the 63, 125, 250 μm size aperture sieve with the elimination of the particle size greater than 425 μm. The best results were obtained when samples kept in solution 12 hours.

For the marls, two different methods were applied. The first method is to wash the samples with standard hydrogen peroxide (H_2O_2) method. Treated with 50% of hydrogen peroxide solution for 2, 4, 6, 12, 24, 48 and 72 hours, the samples were washed within 63, 125, 250 and 425 μm size aperture sieve. The best results were obtained when samples were kept in solution 72 hours but this method alone did not give a perfect solution in cleaning. For this reason samples were dried and kept in acetic acid (CH_3COOH) and at this time the waiting period was the same 2, 4, 6, 12 and 24 hours. The best result was when the samples were kept in acetic acid (CH_3COOH) for 12 hours. In other cases preservation of fossils were very poor.

On the other hand, for the mudstones, two different methods were applied as well. Samples were kept in acetic acid (CH_3COOH) for 2, 4, 6, 12 and 24 hours but preservation of fossils were not very good. That is why samples were kept in 50% of hydrogen peroxide (H_2O_2) for 2, 4, 6, 12, 24, 48 and 72 hours and outcome was excellent. The best results were obtained when samples were kept in solution 72 hours.

After extracting fossils by those methods, laboratory works were carried out by picking up the specimens. The identification of the planktonic foraminifers was performed from the washing samples. Washing of a 20 gm sample was enough since the samples are rich in planktonic foraminifers. On the other hand, the foraminifers from all samples were cleaned from attached particles by ultrasonic cleaning techniques. The best time for cleaning of foraminifers is 2 minutes.

After washing the sydied samples, all individuals of planktonic, benthonic foraminifers and ostracods were picked up from washing residue and collected in microfossil holders and counted one by one in order to reveal their response to sedimentary cyclicity and figure out the changes in relative abundances of planktonic and benthonic foraminifers.

SEM analysis was carried out in order to identify and illustrate morphology of planktonic foraminifers in detail at the Department of Metallurgical and Materials Engineering in the Middle East Technical University. All identified species of foraminifers for the SEM study were placed in holders (aluminum disc) held with carbon paint, dried and gold coated in a vacuum with sputter coater (model Anatech LTD, Sputtering System Hummer VII). The coated samples were subsequently scanned with the SEM (model JEOL JSM-6400 SM) under electron beam not greater than 20KV.

In the laboratory work, approximately 1500 points of all thin sections were counted for petrographic analysis of the studied samples by using J. Swift Co. apparatus in order to identify the percentage of bioclasts, grains of quartz, plagioclase, muscovite and biotite in microfacies. The point counting analysis was carried out in order to classify the sandstone from 2 samples, namely HEA-102 and HEA-103. Predictions on a provenance of sandstones were carried out by using of these data as well.

1.4 Previous Works

In the Haymana basin various geological studies have been carried out for different purposes by many researchers over the last century. In this thesis only some of them have been cited because their researches interconnected with the purpose of the thesis.

Ünalan *et al*. (1976) established the stratigraphy of the succession in the Haymana-Polatlı region that the deposits ranging from Late Cretaceous to Early Tertiary in age. At the base of these deposits there are Temirözü, Mollaresul, Dereköy formations. Neogene unconformably overlies all these formations. The

thickness of the Upper Cretaceous-Lower Tertiary deposits is approximately 5800 m in the region. Deposition was continuous with the exception of the local unconformity between the Çayraz and Eskipolatlı formations in the north of Haymana. Lateral and vertical facies changes were highly developed. Interpretation of the facies studies shows that there existed a semicircle-shaped shelf near Haymana; the Çaldağ formation and Çayraz formation were deposited on this shelf. Behind the shelf partly continental units, the Kartal formation, and the Beldede formation and in front of the shelf flysch units, the Haymana formation, the Yeşilyurt formation, and the Yamak formation were deposited. Throughout Late Cretaceous - Early Tertiary times, the Haymana-Polatlı basin was believed to be joined with the Tuz Gölü basin toward the southeast, and flysch deposits were accumulated in this part of the region. Their investigation shows that the north and west parts of the region were filled with sediments and were uplifted afterwards.

Görür *et al.* (1984) studied the palaeotectonic evolution of the Tuz Gölü basin complex, Central Turkey and sedimentary record of a Neo-Tethyan closure. They found out that the Tuz Gölü basin complex represents a cluster of epi-sutural depressions nested on the Ankara Knot in the Central Anatolia, where several sutures converge. According to this study the basin complex consists mainly of two sub-basins, the Haymana and the Tuzgölü depressions. During the Late Cretaceous to the Late Paleocene, the Tuzgölü and the Haymana sub-basins evolved coevally, but independently as fore-arc basins along the active margins of the Sakarya continent and the Kırşehir Block. Turbidites were accumulated in the basin interiors, with shallow marine and terrestrial deposition near the basin margins. This paper shed light to the paleotectonic evolution in the Haymana region in the Late Cretaceous to the Late Paleocene time.

Koçyiğit *et al*. (1988) studied an example of an accretionary forearc basin from northern Central Anatolia and its implications for the history of subduction of Neo-Tethys in Turkey. He interpreted deformed sedimentary sequences of Late Cretaceous-Middle Eocene age located between the Sakarya continent and the Anatolian complex as the fill of a forearc basin. He tested and elaborated upon

this interpretation on the basis of three basic outcrop areas of Upper Cretaceous-Lower Tertiary sedimentary sequences confined to a northeast-southwest-trending belt in northwest Ankara.

The first study on the cyclicity was made by Çiner *et al*. (1996). They studied cyclicity in the Middle Eocene Çayraz formation of the Haymana basin in the Central Anatolia, Turkey. According to them, the Haymana basin developed on a fore-arc accretionary wedge during the Late Cretaceous and the Middle Eocene. Turbidite deposits fill the center of the basin and grade northwestward into shallow marine clastics and carbonates, which in turn pass into lacustrine and fluvial deposits toward the margin. At the scale of basic sequences and shelf systems, the lateral and vertical distribution of the sequences, and the presence of onlap structures strongly suggest sea-level changes.

In the Haymana basin the hydrocarbon potential has also attracted the attention of many scientists in the middle of 1950s. The important studies related to the oil exploration in the basin were carried out simultaneously with the sedimentological studies. Arıkan (1975) carried out a detailed study about the geology and hydrocarbon potential of the Tuz Gölü. In conducted study, Haymana basin and Tuz Gölü considered to be connected during the Late Senonian to Middle Eocene and are defined as intercontinental basins.

The paleontologic studies based on the planktonic and benthonic foraminifers in the Haymana succession was first established by Sirel and Gündüz (1976), Toker (1979) and Sirel (1999). Yüksel (1970) has just reported the *Globotruncanita calcarata* biozone from the northern flank of the Haymana anticline, just above the conglomerates of the Haymana Formation. Sirel and Gündüz (1976) studied the description and stratigraphical distribution of some species of the genera *Nummulites*, *Assilina* and *Alveolina* from the Ilerdian, Cuisian and Lutetian of the Haymana region (south Ankara). They found out that the rock units of Late Cretaceous (Maastrichtian), Paleogene and Neogene ages crop out in the region. Maastrichtian sequence is composed of alternating sandstone, marl, conglomerate and sandy limestone. The upper part of the Maastrichtian sequence contains abundant foraminifer species, such as *Orbitoides*

medius (d'Archiac), *Siderolites calcitropoides* Lamarck, *Cuvillierina sözerii* Sirel in large amount. Lower Paleocene (Montian) sequence overlies comformable the Maastrichtian, and it is composed of an alternating of algal limestones and marl. The algal limestones contain species of the foraminifera such as *Laffitteina bibensis* Marie and *Cuvillierina* sp.

Toker (1979) studied Upper Cretaceous planktonic foraminifers from the Haymana and the Kavak formations. She distinguished twenty-seven planktonic foraminifer species and established the biostratigraphic zonation including *Globotruncana elevata*, *Globotruncana havanensis*, *Globotruncana gansseri*, *Globotruncana mayaroensis* biozones of Campanian-Maastrichtian.

Sirel (1999) described four new genera: *Haymanella* (Lituolidae), type species *Haymanella paleocenica*; *Kayseriella* (Hauerinidae), type species *Kayseriella decastroi*; *Elazigella* (Spiroloculinidae), type species *Elazigella altineri* and *Orduella* (Orduellinidae n. fam.), type species *Orduella sphaerica* from the Paleocene of the Haymana region. One new foraminiferal species *Hottingerina anatolica* from the Thanetian was described by Sirel (1999). One new foraminiferal family, Orduellinidae (type genus *Orduella* n. gen.) in the superfamily Orbitoidacea was described by Sirel (1999).

Özcan and Özkan-Altıner (1997) studied Late Campanian-Maastrichtian evolution of orbitoidal foraminifera in the Haymana basin succession (Ankara, Central Turkey). Evolution of *Lepidorbitoides* and *Orbitoides* concerning embryonic features and the initial chamber arrangement has been investigated in the Late Cretaceous part of this succession. Previously unrecognized assemblages of *L. campaniensis* - "primitive stage" of *O. megaloformis* of Late Campanian, *L. bisambergensis* - "advanced stage" of *O. megaloformis* of Early Maastrichtian and *L. socialis* - *O. apiculata/O. gensacicus* of Late Maastrichtian age have been documented with their biometric aspects. Chambers of the *Orbitoides* specimens in the same and successive populations has been observed. According to the results of this study, *Lepidorbitoides* is more reliable than *Orbitoides* in aging the populations at least during Late Campanian-Early Maastrichtian time interval.

Related to the topic of this thesis, the important study was carried out by Özkan-Altıner and Özcan (1999) concerning the Upper Cretaceous planktonic foraminifers biostratigraphy. They studied planktonic and larger benthonic foraminifers of the Upper Cretaceous (Santonian-Maastrichtian)-Lower Tertiary (Danian) rock units from north, northwest and Central Anatolian fore-arc basin in order to improve the biostratigraphic resolution of this time interval. Planktonic foraminiferal zonation which was determined with Özkan-Altıner and Özcan (1999) from bottom to top of the succession consists of zones defined by *Dicarinella concavata, Dicarinella asymetrica, Globotruncanita elevata, Globotruncana ventricosa, Radotruncana calcarata, Globotruncanella havanensis, Globotruncana aegyptiaca, Gansserina gansseri, Abathomphalus mayaroensis* and *Morozovella pseudobulloides.* Ten *Orbitoides* and *Lepidorbitoides* species have been identified. The different phylogenetic development stages of *Orbitoides* and *Lepidorbitoides* populations and other larger benthonic foraminifers, *Pseudosiderolites vidali, Siderolites calcitrapoides, Siderolites denticulatus, Omphalocyclus macroporus, Cideina sozerii, Hellenocyclina peotica,* and *Clypeorbis mamillata* have been calibrated with the planktonic foraminiferal zonation established in the same successions.

Following studies of Özcan and Özkan-Altıner (1999) described the evolution of *Lepidorbitoides* and stratigraphic significance in some flysch basins of Anatolia. Phylogenetic developmental stages of *Lepidorbitoides* were correlated with the planktonic foraminiferal zones recorded in the same sample. This study displayed populations with highly asymmetric quadriserial nepionts recorded stratigraphically below the symmetric ones in Early Maastrichtian.

Özcan *et al*. (2001) studied Late Paleocene *Orthophragminae* (benthonic foraminifer) from the Haymana-Polatlı basin (Central Turkey) and described a new taxon, *Orbitoclypeus haymanaensis.* Özcan *et al*. (2001) studied *Orthophragminae* in oriented sections and grouped them into four categories considering the qualitative and quantitative aspects of megalospheric embryo and morphologic elements of equatorial and lateral chamberlets in equatorial and partly vertical sections. Thus, *Discocyclina seunesi*, *Orbitoclypeus neumannae*

and *Discocyclina sp*. were identified and a new species, *Orbitoclypeus haymanaensis*, is erected. These assemblages were dated to Thanetian based upon the calcareous nannofossil and planktonic foraminifera identified in the overlying basinal sediments and also the benthonic foraminifera either associated with *Orthophragminae* or present in different horizons of the shallow-marine succession.

Özcan and Özkan-Altıner (2001) carried out another very interesting study. They described an early ontogenetic evolutionary step in *Lepidorbitoides*: *Lepidorbitoides bisambergensis asymmetrica* new subsp., Early Maastrichtian (Central Turkey). The asymmetric specimens of *Lepidorbitoides bisambergensis* were commonly identified in stratigraphic horizons below the symmetric ones after the introduction of a new auxiliary chamberlet and progressively replaced by symmetric ones in the younger populations. Asymmetric quadriserial specimens representing the early phylogenetic stage of *L. bisambergensis* described in the stratigraphic horizons corresponding to G. *havanensis* and *G. aegyptiaca* zones were thought to deserve a particular taxonomic status and were attributed to new subspecies *Lepidorbitoides bisambergensis asymmetrica.*

Under the light of all these mentioned studies, this study with a high resolution approach has been undertaken in order to delineate the Cretaceous/Paleogene boundary by means of planktonic foraminifera, to conduct a high resolution planktonic foraminiferal biozonation for Paleocene, analyze microfacies and investigate the response of foraminifers to sedimentary cyclicity by analyzing the quantitative composition and benthonic to planktonic foraminifer ratio in the Upper Cretaceous-Paleocene successions of the Haymana basin. Previously conducted researches helped to deliniate the position of the studied succession and prooved that Haymana formation starts with Maastrichtian and ends with Yeşilyurt formation of the Thanetian age. Sequence stratigraphic concepts have also been applied in order to compare the sea-level fluctuations of studied section with the Global Sea Level Change Curve and understand the response of the deep and shallow water facies to sea-level fluctuations.

1.5 Regional Geological Setting

The Haymana basin is located about 70 SW of Ankara in Central Anatolia (Figure 4). Dickinson and Selly (1979) interpreted it as forearc basin that formed on an accretionary wedge. The age of the formation of this wedge ranges from Late Cretaceous to Late Eocene. It was formed by the convergence and collision of the Eurasian continent to the north and the intervening Sakarya continent on the oceanic crust of the northern branch of Neo-Tethys (İzmir-Ankara Suture Zone) (Fourquin, 1975; Sengör and Yılmaz, 1981; Görür *et al*., 1984; Koçyiğit *et al*., 1988; Koçyiğit 1991) (Figure 4, Figure 5).

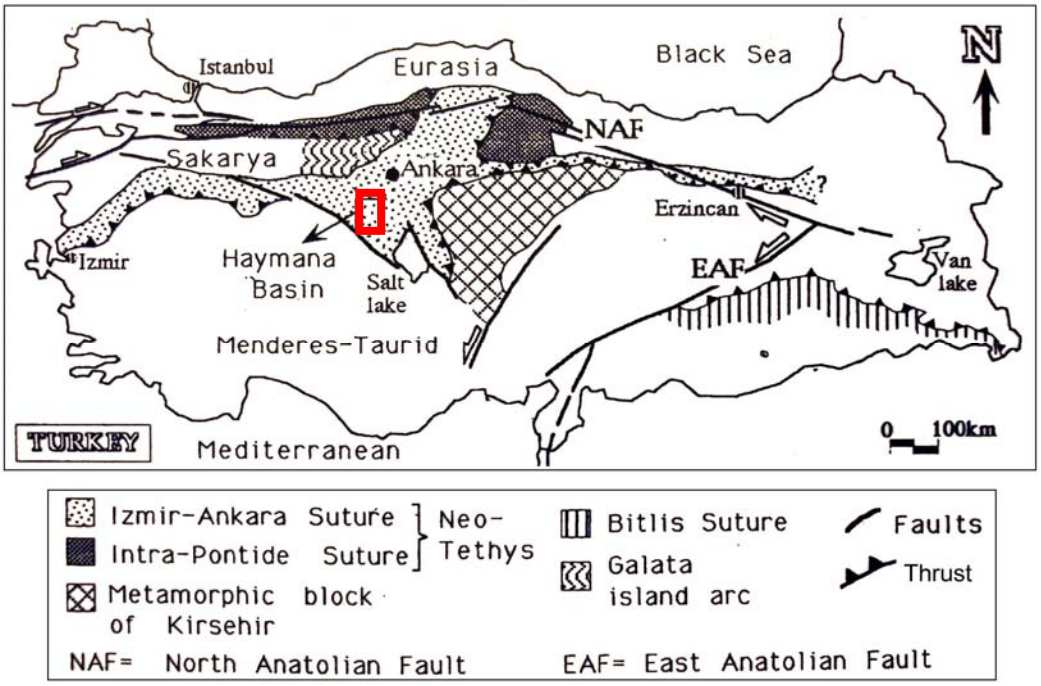

Figure 4. Main structural features of Turkey and location of the Haymana basin (from Koçyiğit, 1991).

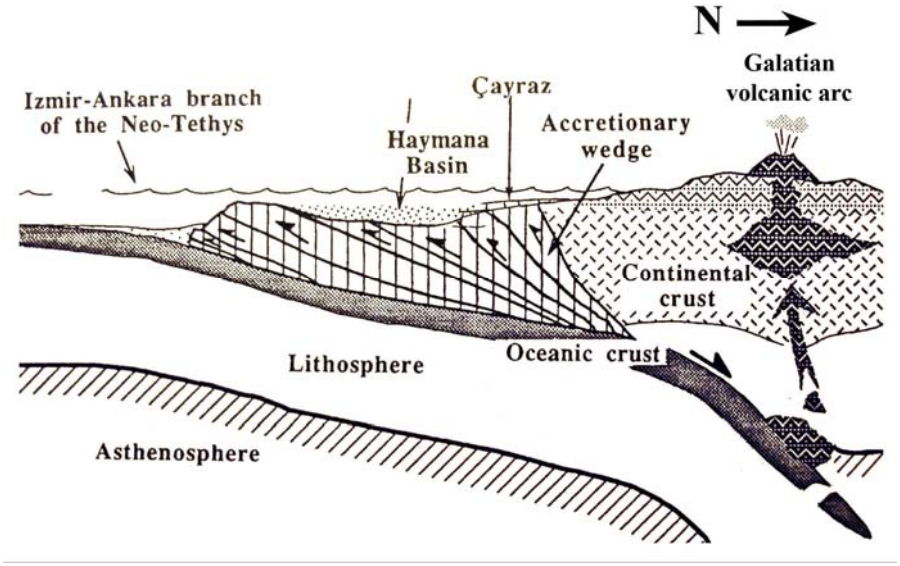

Figure 5. Schematic cross section (not to scale) showing the structural setting of the Haymana basin during the Campanian to the Lutetian time interval (from Koçyiğit, 1991).

Deformation continued until the Late Pliocene after the closure of the north Neo-Tethys Ocean (Koçyiğit, 1991). The studied succession is spanning in age from Late Cretaceous to Paleocene in the Haymana basin (Figure 6).

In the Haymana region a thick sedimentary succession of Santonian/Campanian-Eocene in age crops out. The basement of this basin is composed of the Jurassic-Upper Cretaceous carbonates cover of the Sakarya Continent, in which the total thickness of the Maastrichtian-Tertiary deposits reaches thousands of meters (Şengör and Yılmaz 1981), the pre-Jurassic basement of the Sakarya Continent consists of Karakaya Complex (Şengör and Yılmaz, 1981) and the Ankara Melange (Bailey and McCallian 1953, Ünalan *et al.*, 1976) (Figure 7).

The composite basement is unconformably overlain by the Upper Cretaceous Çaltepe formation which is composed of the thick bedded limestones (Hüseynov, 2007). The Upper Cretaceous Seyran formation which consists of limestones, shales, and breccia unconconformably overlies the Upper Cretaceous Çaltepe formation. On the other hand, this formation is overlain by the red-pink

limestones of the Upper Cretaceous Kocatepe formation unconformably (Figure 7).

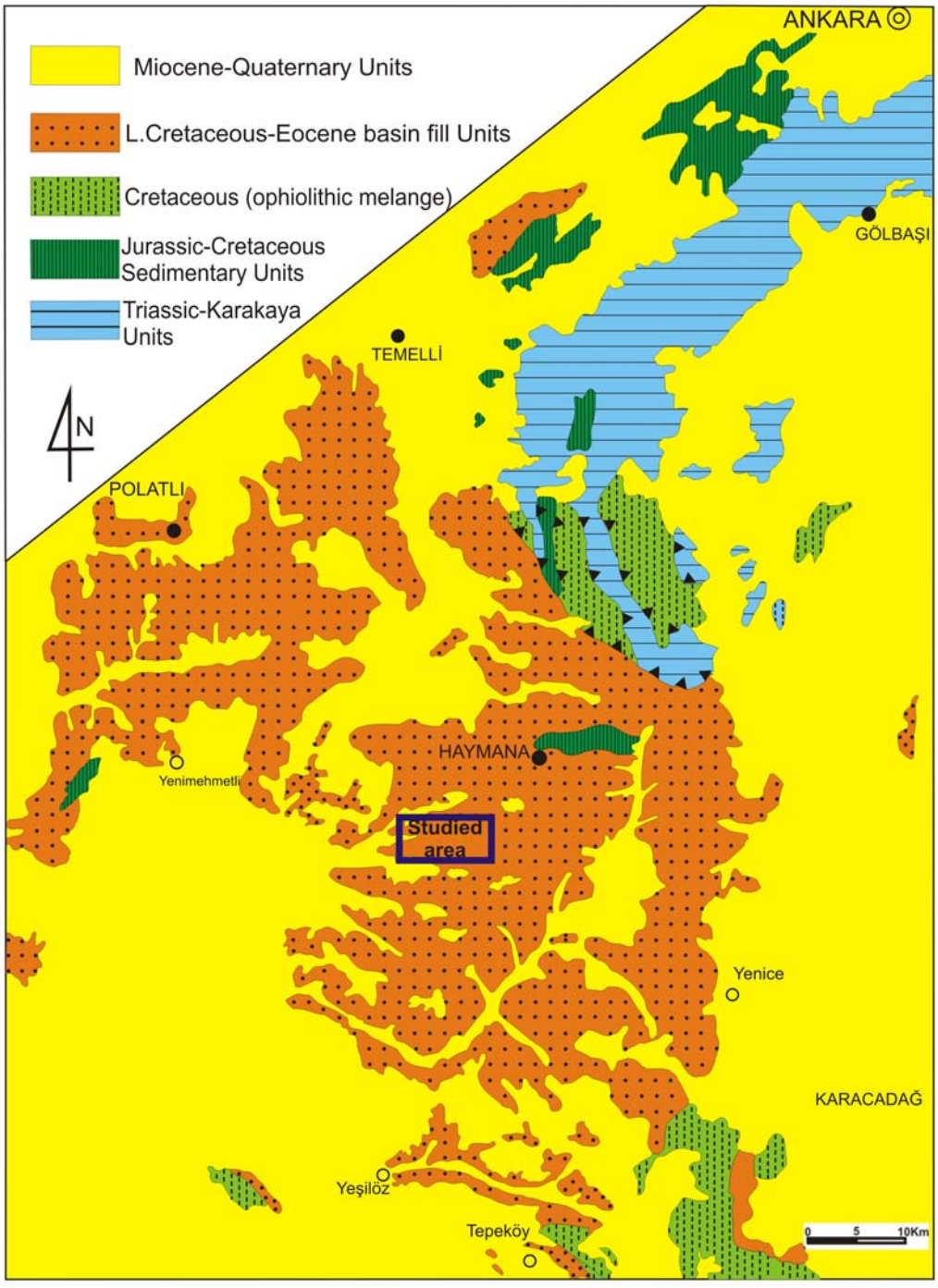

Figure 6. Generalized geologic map of the Haymana basin and location of the study area (modified from 1/500000 Turkey).

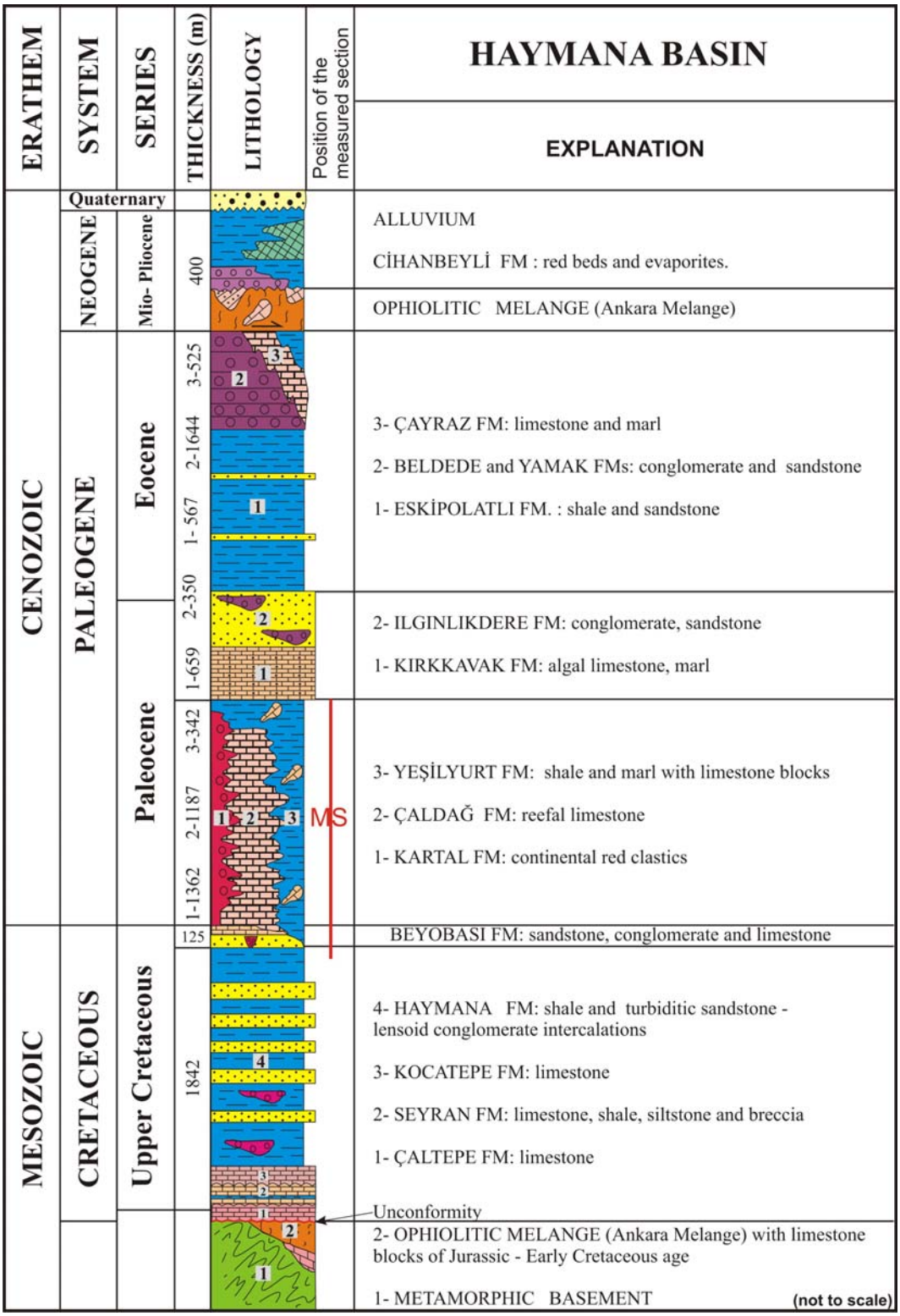

Figure 7. Generalized columnar section of the study area (Haymana basin). The measured section (MS) is shown by the red line (modified from Ünalan *et al*., 1976).

The flyschoidal succession of the Haymana formation of Late Maastrichtian age overlies the Kocatepe formation (Figure 7). The Haymana formation consists of sandstone-shale intercalations with frequent conglomerates, olistostromes and debris-flow deposits. These clastics mainly consists of texturally and mineralogically immature ultramafic and mafic rocks of ophiolitic origin, which derived probably from the Karakaya Complex, the Ankara Mélange and metamorphic rock fragments, including composite quartz, potassic and sodic feldspars derived from the basement of the Sakarya Continent (Ünalan *et al.*, 1976).

These deep-sea deposits pass laterally and vertically into richly fossiliferous shallow marine sandstones, shales and limestones around the basin margins with *Cyclolites* sp., orbitoids, gastropods and lamellibranches shell of *Hippurites* sp.. This unit is named as the Beyobası formation (Ünalan *et al*., 1976) (Figure 7).

Deposition of continental red beds of the Kartal formation and reefal limestones of the Çaldağ formation during the Paleocene age characterized the basin edges. The red beds of the Kartal formation contain clasts of radiolarian cherts, limestones and ophiolites (Görür & Derman, 1978). The relatively deep water shale-marl intercalations of the Yeşilyurt formation were deposited in the interior part of the basin with limestone blocks. The Kırkkavak formation overlies the Yeşilyurt formation and represented with algal limestone and marl. The Kırkkavak formation overlain by the Ilgınlıkdere formation and consists of conglomerate and sandstone (Ünalan *et al*., 1976) (Figure 7).

The deposition of thick turbidite successions in the central parts of the basin in Early and Middle Eocene was occupied a larger area than in Paleocene. During the Eocene time, the depositional areas of the Çaldağ reefal limestones were filled up with turbidites and as a result the shoreline retreated away from the basin centre. Turbidites of the Haymana basin constitute the Eski Polatlı formation of Eocene age and contain clasts of serpentinite, dunite, peridotite, diabase, basalt, radiolarian chert and glaucophane schist. Most probably they were derived from the ophiolits of the Ankara mélange, as well as micaschists and amphibolites from

the ophiolitic mélange and the Sakarya basement and rhyolitic lava flows from the Sakarya magmatic arc (Ünalan *et al*. 1976) (Figure 7).

The turbiditic depositional areas of the Haymana basin began to shrink rapidly by the end of the Middle Eocene. Turbidites graded vertically and laterally into shallow marine nummulitic limestones of the Çayraz formation and the terrestrial clastic sediments of the Beldede and Yamak formations during Eocene. Both the nappe of Ankara mélange and the units underlying it were later covered unconformably by terrestrial conglomerates, marls, sandstones, evaporates and the tuffs of the Cihanbeyli formation during Mio-Pliocene (Ünalan *et al*.1976) (Figure 7).

Within this regional geological content, the studied section measured in a sedimentary succession which covers the Haymana, Beyobası and Yeşilyurt formations (Figure 7).

CHAPTER 2

LITHOSTRATIGRAPHY AND BIOSTRATIGRAPHY

2.1 Lithostratigraphy

The deposits of the Haymana basin are mainly characterized by Upper Cretaceous to Eocene marine sequences and the total thickness of these deposits is about 5000 m (Ünalan *et al*. 1976). The Upper Cretaceous-Paleocene part of this succession, which is the main target of this thesis work, is characterized by alternating pelagic and neritic sediments.

Based on Ünalan *et al*. (1976) studies, the Haymana formation consists of shale and sandstone intercalations with frequent conglomerates and debris flow deposits. In studied succession, the Haymana formation at the base starts by a mudstone deposits. According to Ünalan *et al*. (1976) the Haymana formation at the upper contact is overlain by the Beyobası formation, which consists of sandstone, conglomerate and limestone (see Figure 7) and Beyobası formation is overlain by the Yeşilyurt formation which consists of alternation of shale and marl with limestone blocks. In the studied area Beyobası formation is represented only by a sandstone and mudstone deposits (Figure 8) and is overlain by the Yeşilyurt formation which composed of mudstone, marl and limestone alternation (Figure 8). According to Ünalan *et al*. (1976) the Yeşilyurt formation laterally passes into the Kartal and Çaldağ formations which actually are the basin edges. Kartal formation consists of continental red clastics and Çaldağ formation consists of reefal limestone.

In the studied area, the Upper Cretaceous to Upper Paleocene succession of the Haymana basin is widely exposed. Approximately 162 m thick lithological section was measured in the field and was studied in detail.

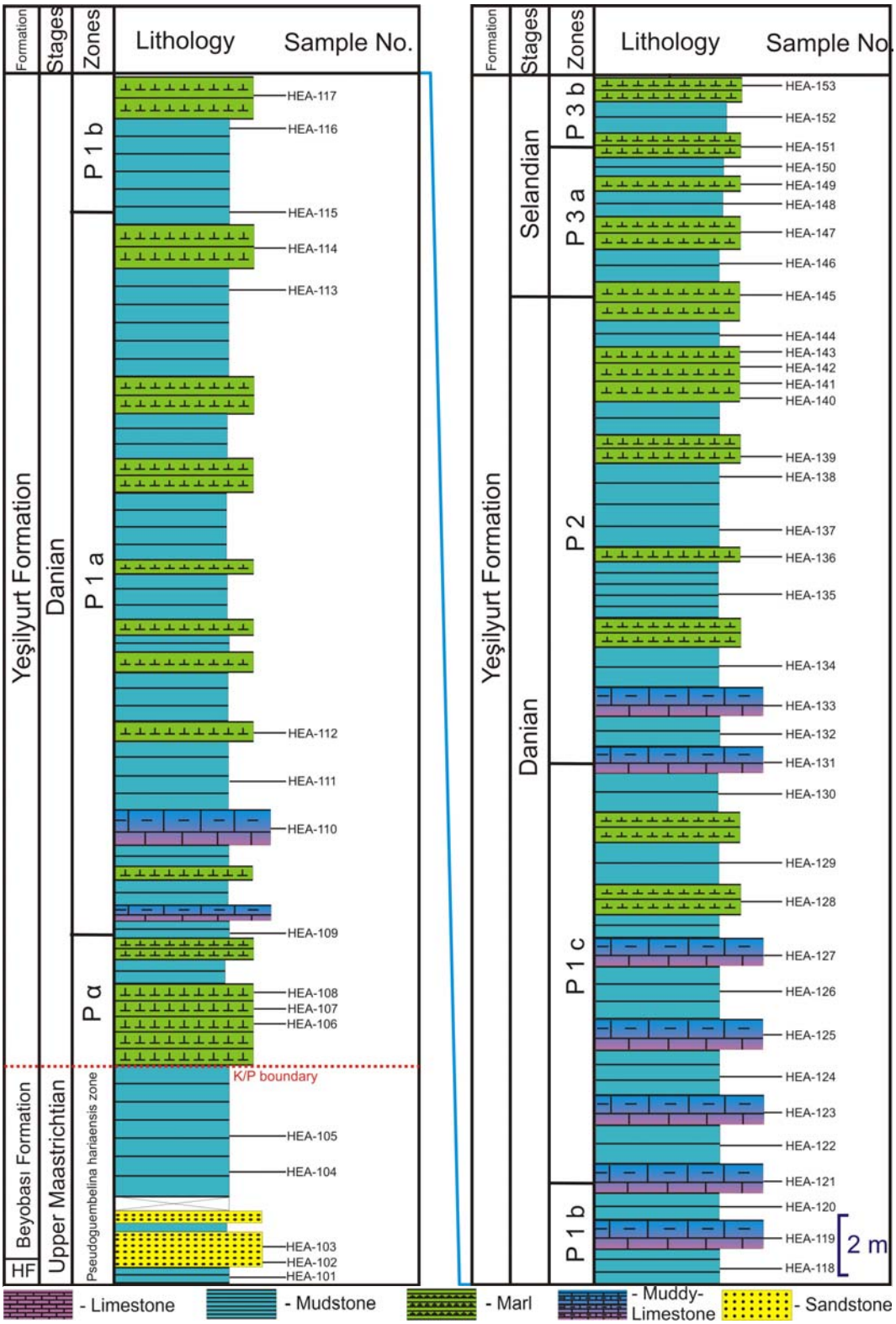

HF-Haymana formation

Figure 8. Lithostratigraphy of the measured section (for detailed section see appendix A).

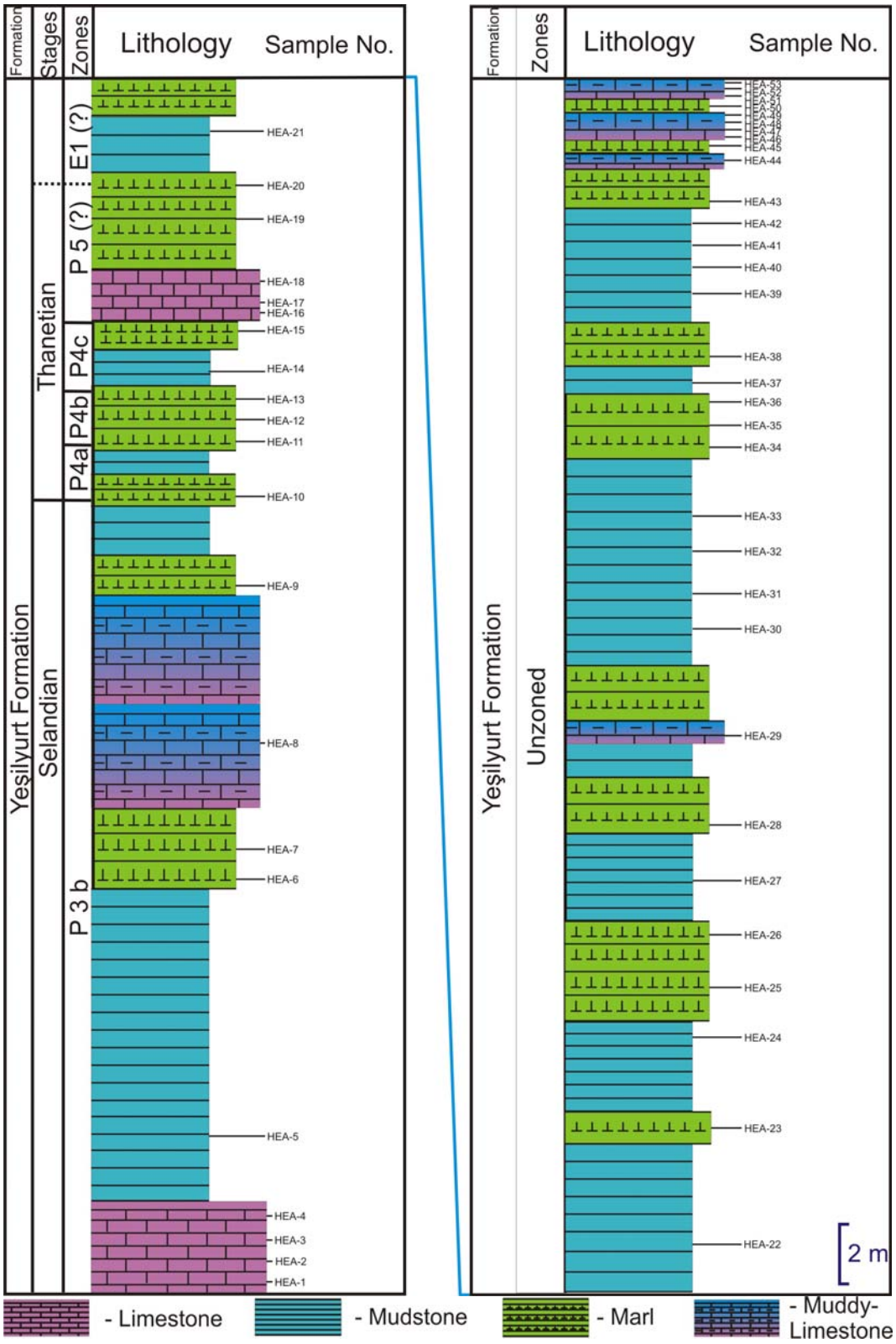

Figure 8. Continued.

All studied deposits have been interpreted to be deposited in the alternation of shallow and deep water environments, where deposition has continued from Late Cretaceous to Early Tertiary time.

The studied section of the Haymana and Beyobası formations starts at the base with alternation of mudstone and dark colored sandstone (Figure 9, samples from HEA-101 to HEA-103) passing into mudstone - marl rhythmic alternations (Figure 10), whereas the middle part of the section mainly consists of the limestone beds.

In the lower parts of the measured section, dark grayish sandstone beds are laminated and thickess 90 cm but towards top there is a gradual decrease in their thickness which reaches 20 cm (Figure 9, samples from HEA-101 to HEA-103). The grain size of sandstones decreases upward along the succession and sandstone facies are composed of litharenites.

The section continues with alternation of yellowish to grayish, thick to medium (3.50 m-30 cm) bedded marls and thick to thin (2 m-10 cm) dark colored mudstones (Appendix A, samples from HEA-106 to HEA-117). Mudstones are more frequent through all measured section. They look like massive but at closer look, they consist of thin to medium and thick mudstone layers. Their color at the upper part of section varies from dark brownish and greenish to black and grayish.

The marl and mudstone facies is mainly composed of wackestone and mudstone microfacies alternations (Appendix A) and in general composed of silt and sand sized fossil fragments consisting mainly of planktonic, benthonic foraminifers and ostracods. This part is followed by 40 m portion of the formation which is characterized by alternation of mudstone, muddy-limestone and marl (Figure 11, Appendix A, samples from HEA-117 to HEA-153). This part is followed by thick layer of limestone with 126 cm in thickness (Figure 12, Appendix A, samples from HEA-1 to HEA-4). This part is overlain again by alternation of marl and mudstone facies with 15 m in thickness (Appendix A, samples from HEA-4 to HEA-15). This part is followed again by thick layer of limestone with 145 cm in thickness (Appendix A, samples from HEA-16 to HEA-18). This part is overlain again by alternation of marl and mudstone facies with 60

m in thickness (Appendix A, samples from HEA-19 to HEA-42). Upper part of the studied section finishes with an alternation of marl and muddy-limestone facies with 392 cm in thickness (Figure 13, Appendix A, samples from HEA-43 to HEA-53).

In the previous studies the age of the Haymana formation has been defined as Maastrichtian, based on *Tritaxia trilatera* Cushman, *Dorothia bulletta* Carsey, *Blumina carseyae* Plummer, *Globotruncana arca* Cushman, *Globotruncana conica* White, *Globotruncana stuarti* De Lapparent etc. (Ünalan *et al*., 1976). Our studied portion of the succession comprises the Haymana, Beyobası and Yeşilyurt formations which have been divided into Maastrichtian, Danian, Selandian and Thanetian (see biostratigraphy chapter).

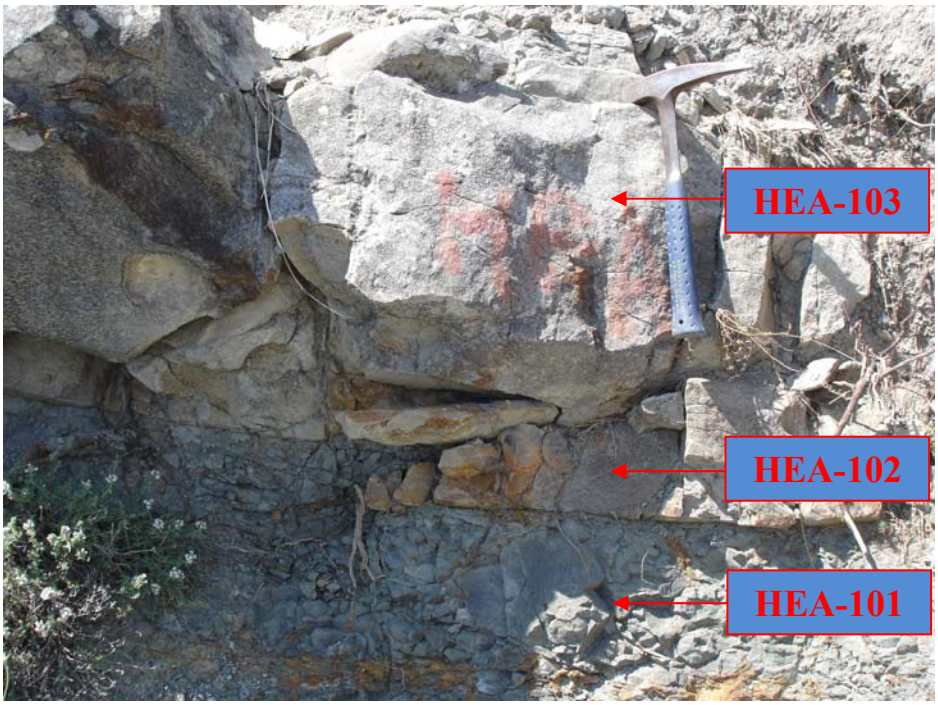

Figure 9. Close-up view of sandstone-mudstone alternations in the lower part of the measured section (HEA-101, HEA-102 and HEA-103 indicates the position of samples).

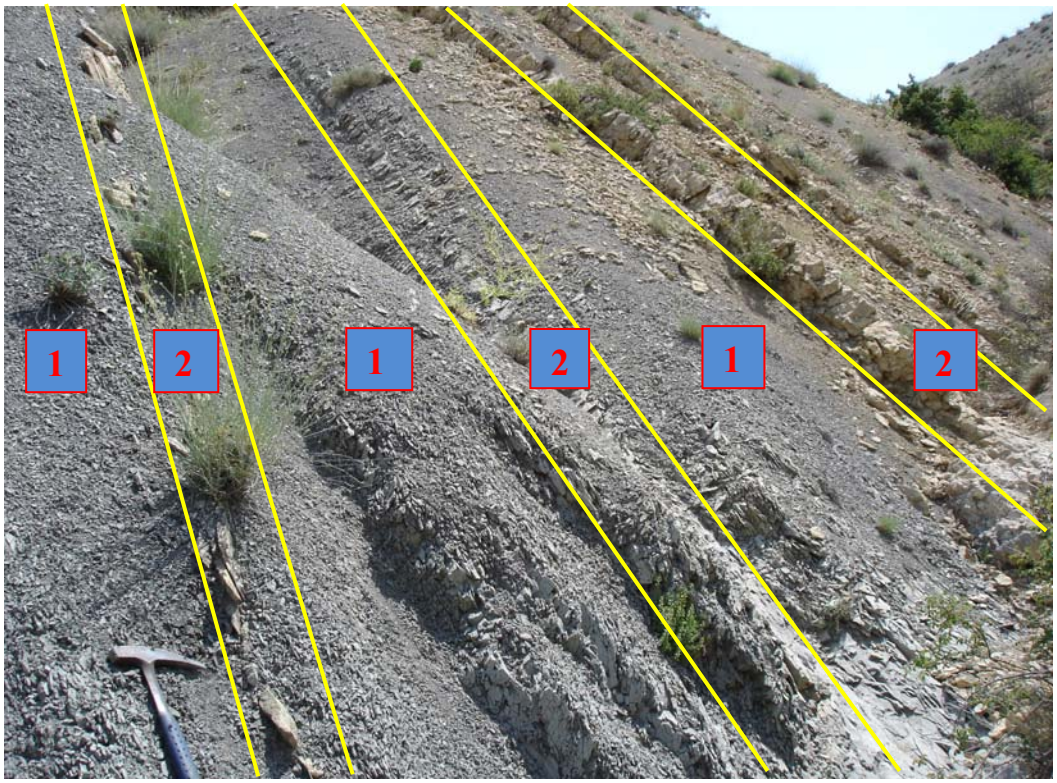

Figure 10. Close-up view of mudstone-marl alternations (1- mudstone, 2- marl).

Figure 11. An alternating mudstone and muddy-limestone in the lower part of the measured section (Number 127 indicates the position of sample HEA-127).

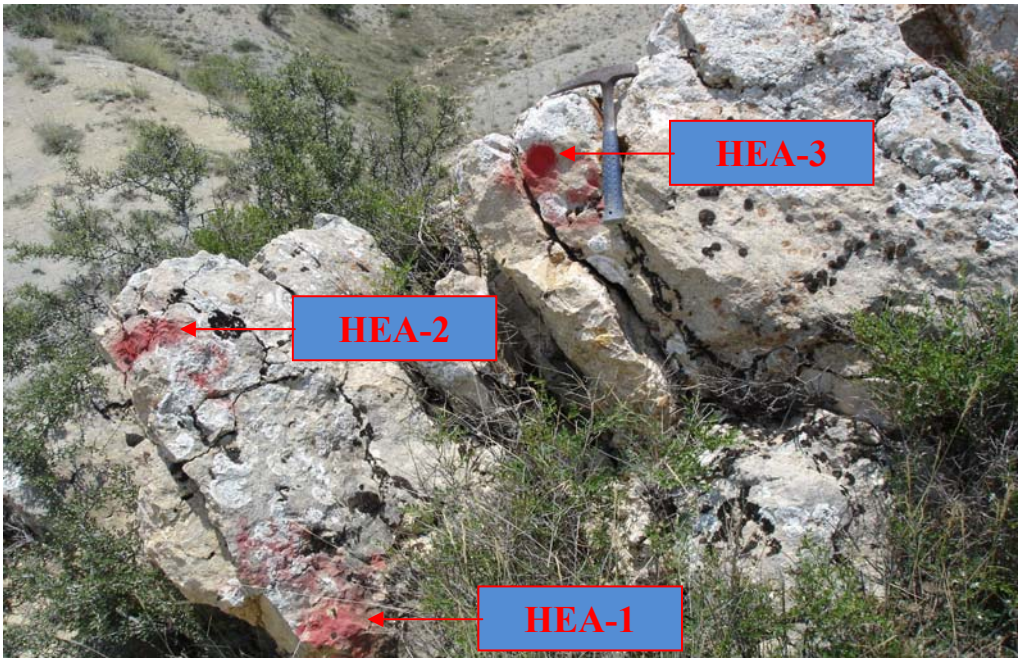

Figure 12. Close-up view of limestone in the middle part of the measured section (HEA-1, 2 and 3 indicates the position of samples).

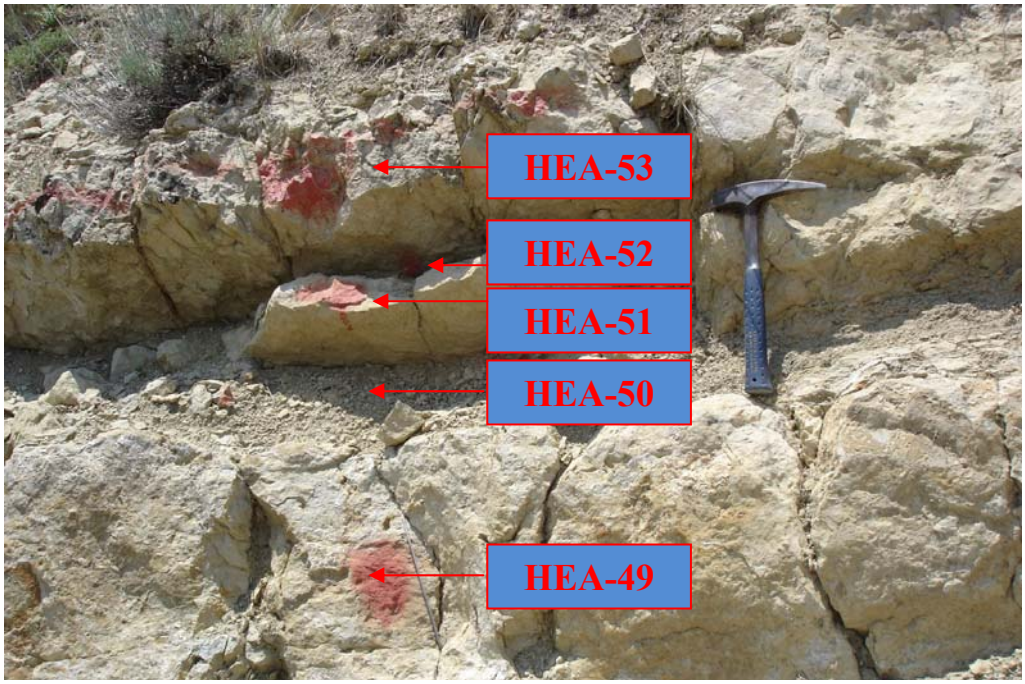

Figure 13. Close-up view of marl and muddy-limestone alternations in the upper part of the measured section (HEA-49, 50, 51, 52 and 53 indicates the position of samples).

2.2 Biostratigraphy

The detailed planktonic foraminiferal study of the Upper Maastrichtian-Paleocene sequence which exposes in the Haymana region has revealed a total of 67 species belonging to 29 genera (Table 1). The samples in this study have yielded a great diversification from moderate to poor preservation of the specimens. Preservation of small forms for instance as *Parvularugoglobigerina eugubina* is quite poor, most of the specimens are fragmented and display traces of dissolution.

The studied sequence has been divided into several stages (Uppermost Maastrichtian, Danian, Selandian and Tanetian stages) based on the biostratigraphic data obtained from the samples collected along the measured section, namely from the Haymana, Beyobası and Yeşilyurt formations by means of planktonic foraminifers.

By investigation and determination of foraminifers genera under the microscope, the Cretaceous/Paleogene boundary in the studied succession has been pinpointed (Figure 14, between the samples HEA-105 and HEA-106; Table 1), which is indicating the mass extinction of Cretaceous foraminifers such as *Globotruncana, Globotruncanita, Pseudoguembelina, Pseudotextularia, Planoglobulina, Heterohelix, Laeviheterohelix, Racemiguembelina, Rugoglobigerina, Trinitella* and appearance new ones in the Tertiary such as *Eoglobigerina, Chiloguembelina, Globanomalina, Parasubbotina, Praemurica, Parvularugoglobigerina, Igorina, Globoconusa, Woodringina* and etc.

One of the most important biostratigraphic studies using the Cretaceous planktonic foraminifers was carried out by Robaszynski *et al.* (1984). They separated Maastrichtian stage into three zones by using globotruncanids: *Globotruncana falsostuarti*, *Gansserina gansseri* and *Abathomphalus mayaroensis* interval zones. Robaszynski (1998) also separated Maastrichtian stage into three zones by using heterohelicids: *Planoglobulina acervulinoides*, *Racemiguembelina fructicosa* and *Pseudoguembelina hariaensis* zones.

Table 1. Stratigraphical distributions of planktonic foraminifers and biostratigraphical zonal scheme from the studied section.

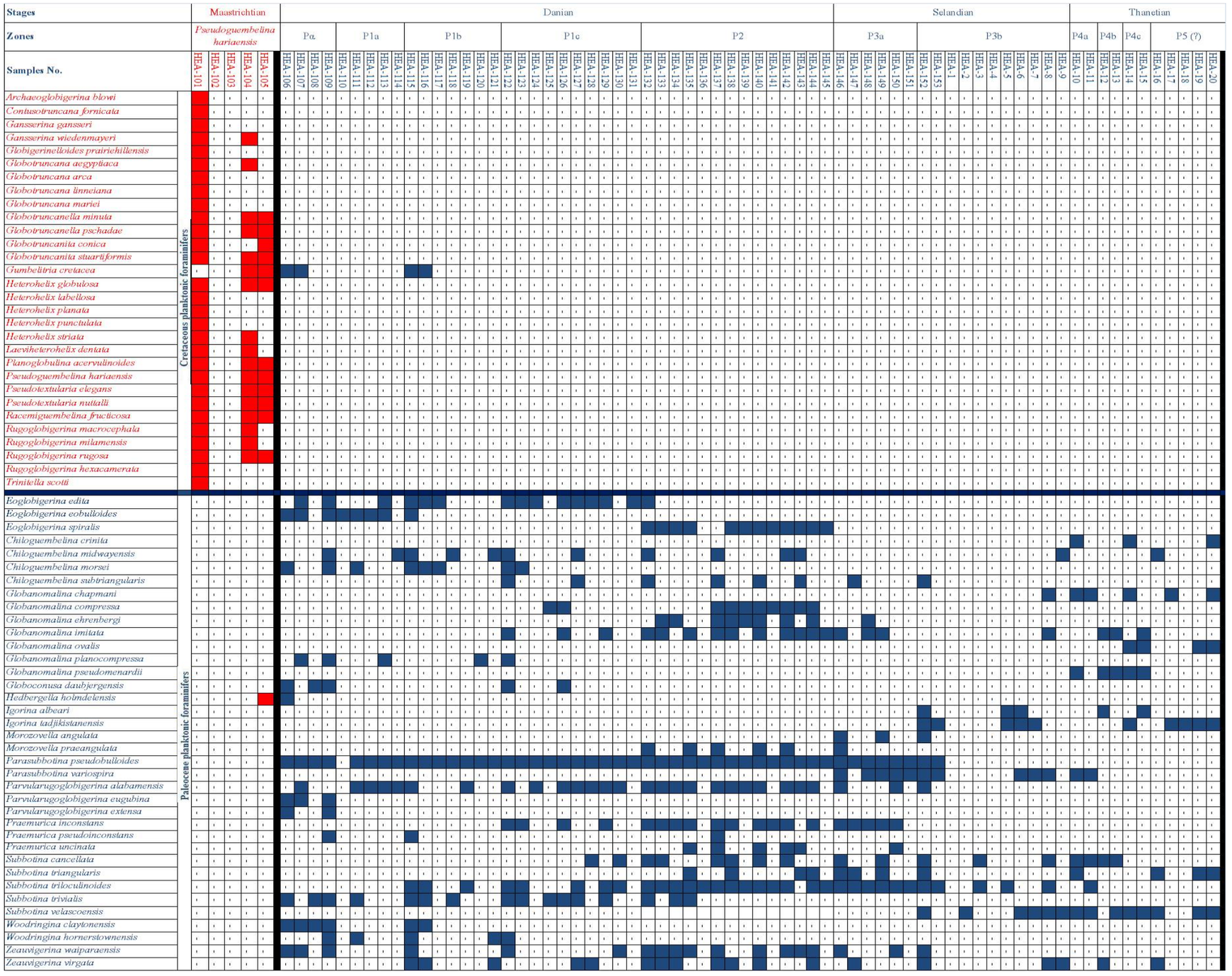

In this study, because of the rareness of the globotruncanids forms in the studied samples, the biostratigraphic framework was established by using heterohelicid forms (Table 1). At the base of the section, only the *Pseudoguembelina hariaensis* biozone (samples from HEA-101 to HEA-105) was determined. After the detailed studies of Nederbragt (1990, 1991) on the heterohelicids, there has been a limited usage of those forms on the Upper Cretaceous biozonation (Li and Keller, 1998; Robasyznski, 1998; Obaidalla, 2005).

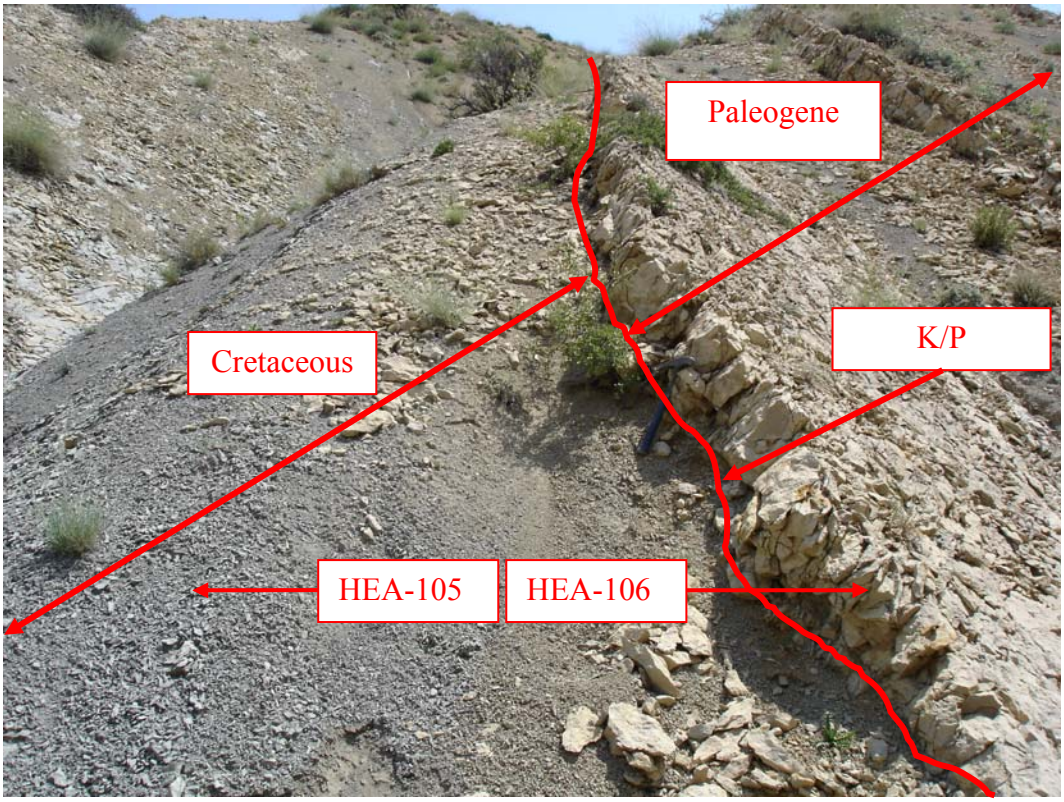

Figure 14. K/P boundary location in the field (HEA-105 is the last Cretaceous sample and HEA-106 is the first Paleocene sample).

The heterohelicid biozonation in which Maastrichtian is divided just into *Pseudoguembelina hariaensis* zone is established by using the biostratigraphic study of Robaszynski (1998) (Table 1). Table 2 shows the correlation of planktonic foraminiferal biozonations in uppermost Maastrichtian from different localities.

Table 2. Correlation of planktonic foraminiferal biozonations in the uppermost Maastrichtian from different localities.

Stages	Robaszynski, 1984 Tethyan realm	Caron, 1985 Atlantic ocean	Özkan-Altıner&Özcan, 1999 Central Turkey	Premoli-Silva and Sliter, 1999 Pacific Basin	Li&Keller, 1998 DSDP 525A (S. Atlantic)	Arenillas *et al*., 2000 Tunisia	Gardin *et al*., 2001 Central Italy	Chacon *et al*., 2004 SE Spain	Obaidalla, 2005 SE Sinai, Egypt	This Study, Haymana, Central Anatolia, Turkey
Maastrichtian	*Abathomphalus mayaroensis*	*Abathomphalus mayaroensis*	*Abathomphalus mayaroensis*	*Abathomphalus mayaroensis*	*P.palpebra* *P.hariensis*	*Plummerita hantkeninoides*	*Abathomphalus mayaroensis*	*Abathomphalus mayaroensis*	*Plummerita hantkeninoides*	*Pseudoguembelina hariaensis*
	Gansserina gansseri	*Gansserina gansseri*	*Gansserina gansseri*	*C. contusa-Rc. Fructicosa*	*Gansserina gansseri*	*Abathomphalus mayaroensis*	*C. contusa-Rc. Fructicosa*	*C. contusa*	*Abathomphalus mayaroensis*	not revealed

Biozonation for Paleocene was carried out by many authors such as Bolli (1966), Canudo *et al*. (1991), Berggren *et al*. (1995), Keller *et al*. (1995), Lucciani (1997), Pardo *et al*. (1999), Olsson *et al*. (1999), Obaidalla (2005) and etc. In this research we used the biostratigraphic study and taxonomy which was compiled by Olsson *et al*. (1999), mainly because of that this study is more recent and peer reviewed by many authors. They divided Paleocene into 7 zones and 8 subzones (Table 3). In this study Paleocene was divided just into 6 zones and 8 subzones respectively (Figure 15, Table 1): Pα, P1 (Subzones-P1a, P1b, P1c), P2, P3 (Subzones-P3a, P3b), P4 (Subzones-P4a, P4b, P4c) and P5. Table 4 shows the correlation of planktonic foraminiferal biozonations for Danian from different localities.

2.2.1 *Pseudoguembelina hariaensis* Zone

Definition: Interval of total range of *Pseudoguembelina hariaensis* (see Figure 15).

Author: Li and Keller, 1998.

Remarks: In this study, *Abathomphalus mayaroensis* has not been recorded in any sample. The absence of this marker zone could be explained by rareness of this species. Instead of the *Abathomphalus mayaroensis* Zone, the uppermost heterohelicid zone, *Pseudoguembelina hariaensis* zone has been recorded in this study. In general the preservation of forms is very good. Actually all species from this zone was picked up from samples washed through 125 and 250 μm seive, mainly because Cretaceous species relatively big in size and well preserved. In this zone *Globotruncanella minuta, Globotruncanella pschadae, Globotruncanita conica, Globotruncanita stuartiformis, Heterohelix globulosa, Planoglobulina acervulinoides, Pseudoguembelina hariaensis, Pseudotextularia elegans, Pseudotextularia nuttalli, Racemiguembelina fructicosa* and *Rugoglobigerina rugosa* shows almost a continuous distribution.

Table 3. Biostratigraphic range chart of planktonic foraminiers for Paleocene (Olsson *et. al.,* 1999).

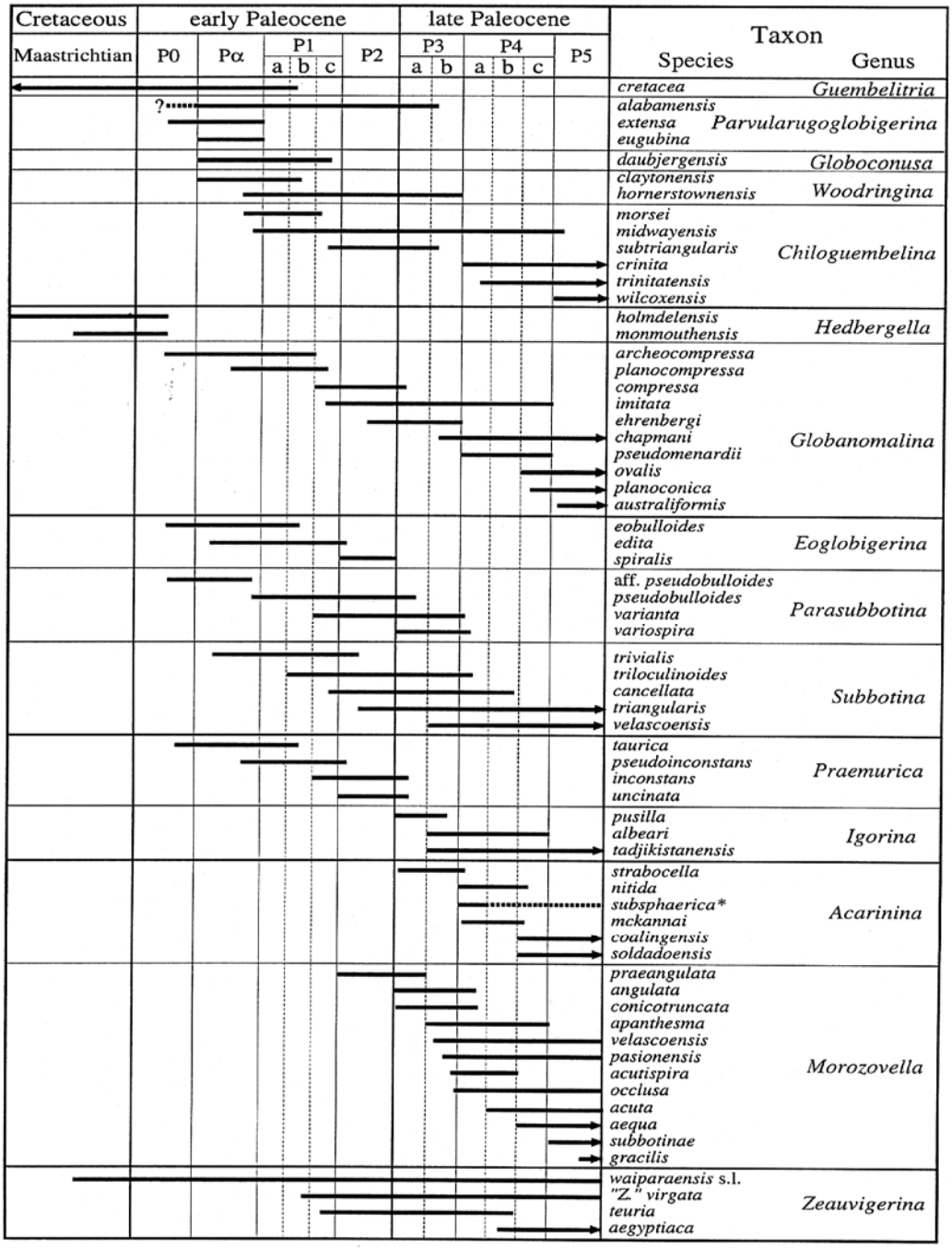

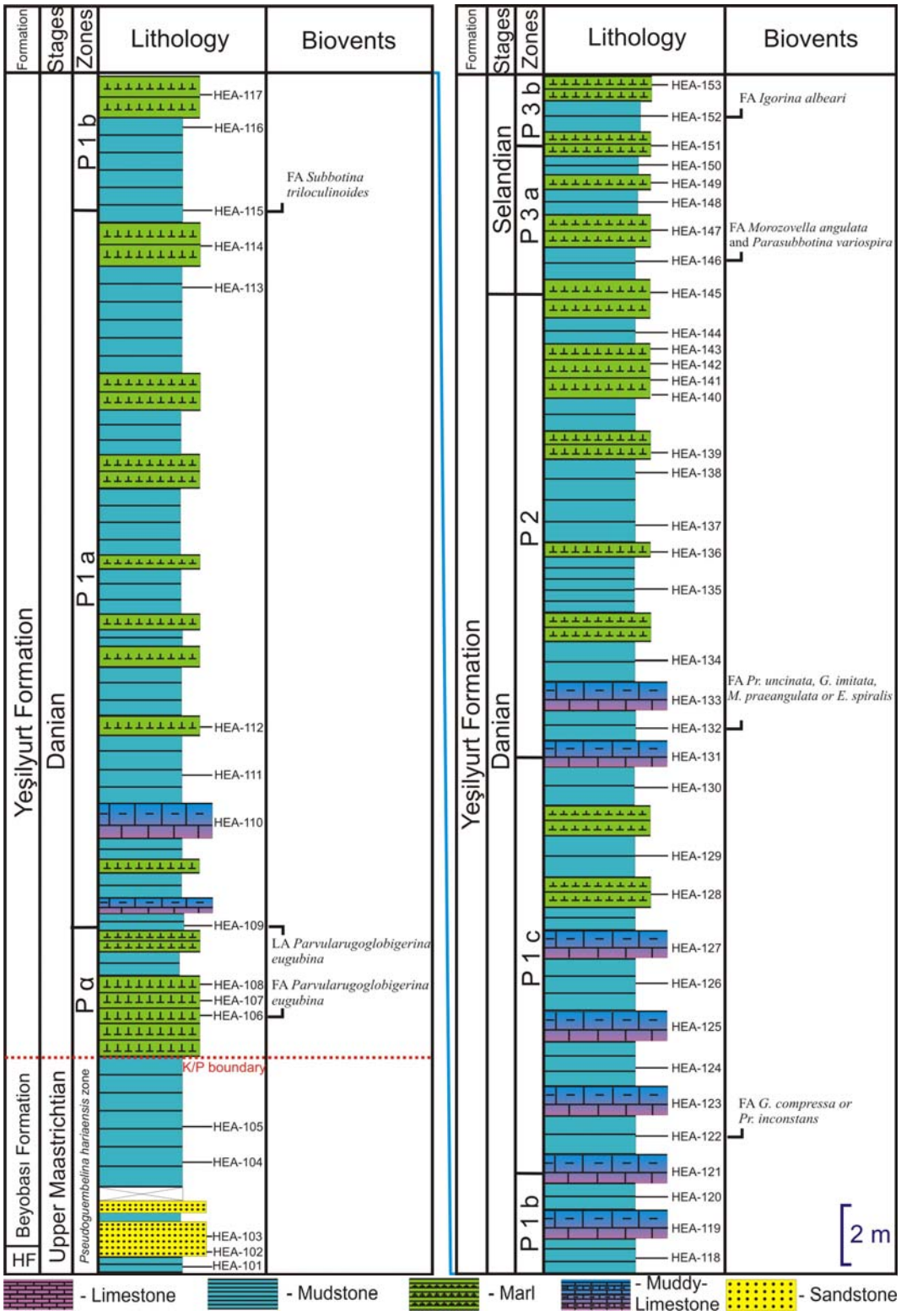

-| - FA (first appearance), |- -LA (last appearance), HF-Haymana formation

Figure 15. Planktonic foraminiferal bioevents recorded in the measured section.

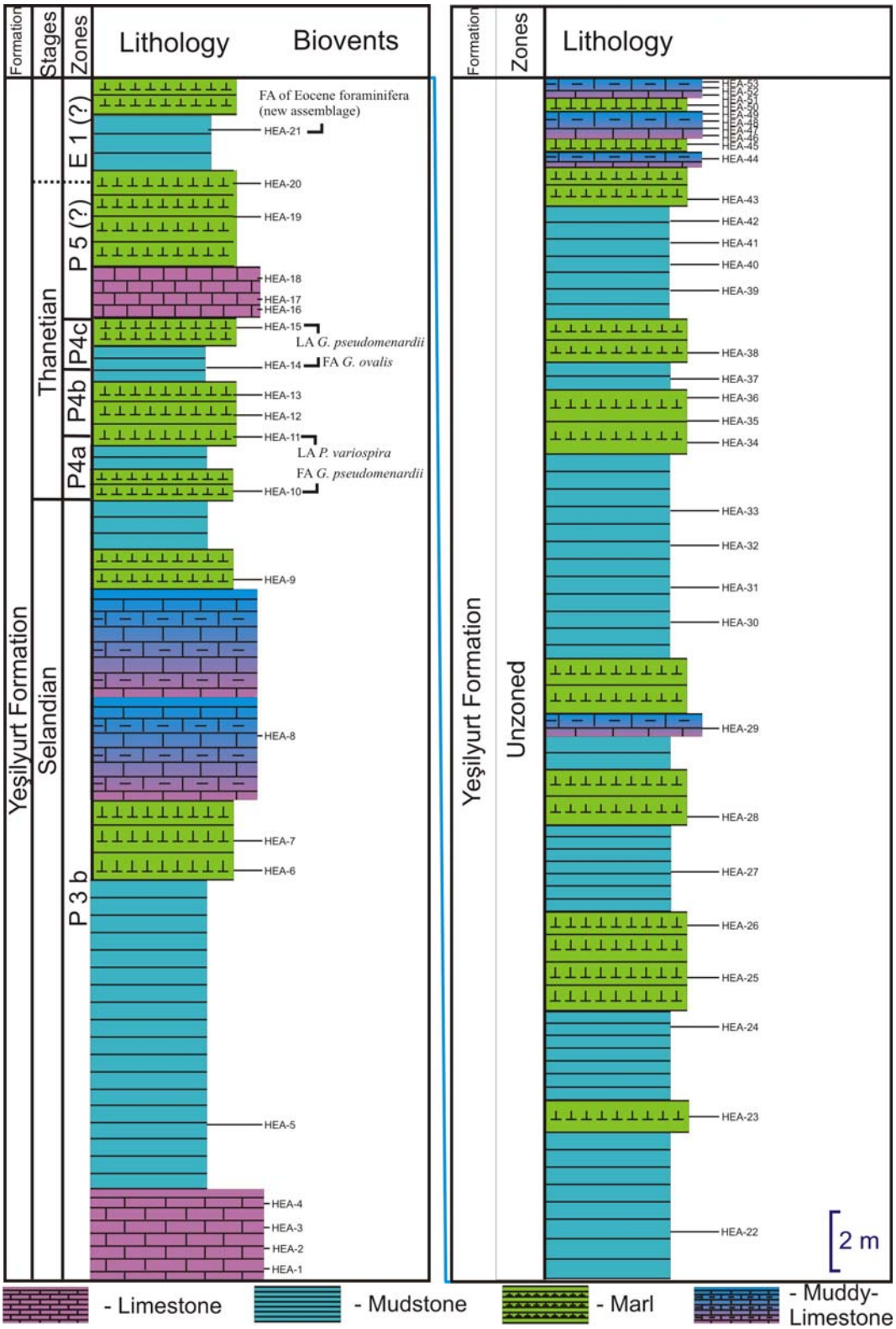

⌟- FA (first appearance), ⌝-LA (last appearance).

Figure 15. Continued.

Table 4. Correlation of planktonic foraminiferal biozonations in Danian from different localities.

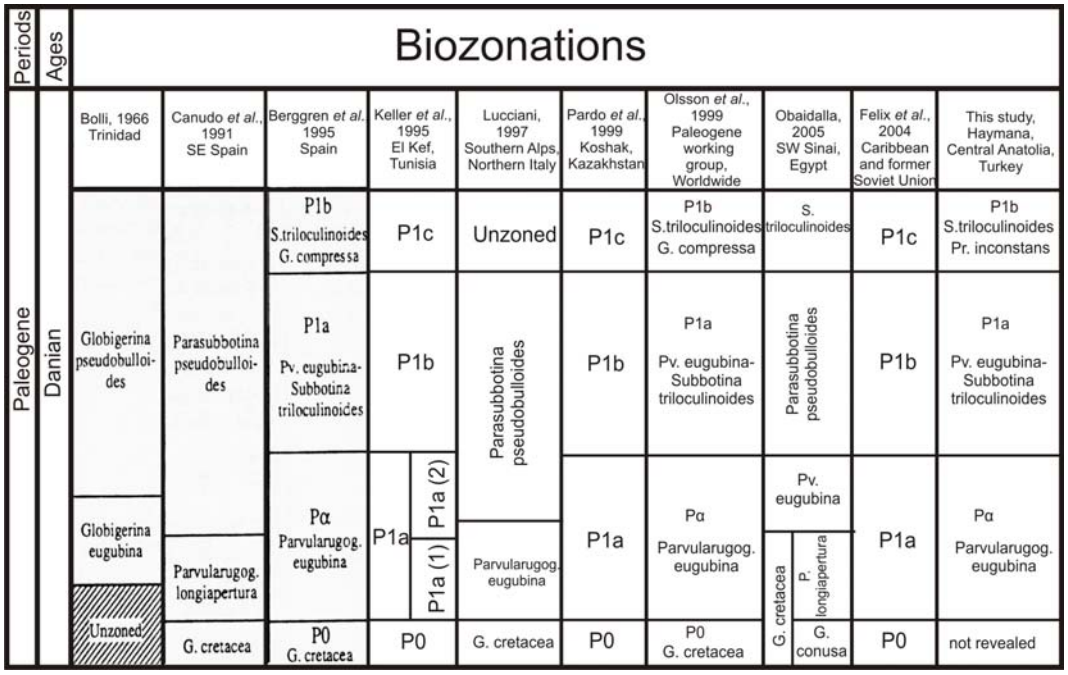

This interval comprises the planktonic foraminiferal assemblages below (Table 1): *Archaeoglobigerina blowi, Contusotruncana fornicata, Gansserina gansseri, Gansserina wiedenmayeri, Globigerinelloides prairiehillensis, Globotruncana aegyptiaca, Globotruncana arca, Globotruncana linneiana, Globotruncana mariei, Gumbelitria cretacea, Hedbergella holmdelensis, Heterohelix labellosa, Heterohelix planata, Heterohelix punctulata, Heterohelix striata, Laeviheterohelix dentata, Rugoglobigerina macrocephala, Rugoglobigerina milamensis, Rugoglobigerina hexacamerata* and *Trinitella scotti.* This zone mainly consists of mudstone and sandstone (Figure 15). It was not possible to extract any foraminifers from the sandstone samples HEA-102 and HEA-103 because of lithology and that is why there is no any data from those samples in foraminiferal distribution chart.

Stratigraphic distribution: From the sample HEA 101 to the sample HEA 105.

Age: Latest Maastrichtian.

2.2.2 Pα. *Parvularugoglobigerina eugubin*a Total Range Zone

Definition: Interval characterized by the total range of the *Parvularugoglobigerina eugubin*a (Figure 15).

Author: Liu, 1993, emended of Pα of Blow, 1979; Luterbacher and Premoli Silva, 1964.

Remarks: This zone is the lowest recorded Paleocene zone (Danian) in this study. It was not possible to reveal P0 Zone in the studied section, because of the sampling interval. The Cretaceous-Paleogene boundary (HEA-105 / 106) has been delineated within 4.75 m interval. If the sampling interval was smaller than this interval, P0 zone might be precisely recognized somewhere between the sample HEA-105 and the sampleHEA-106. The Danian part of the section starts directly with the Pα Zone. It was difficult to extract some good preserved small species from samples in this zone. Actually all species from Pα Zone was picked up from samples washed through 63 μm seive, mainly because first appeared species were too small in size. Different authors named this zone as P1a or *Parvularugoglobigerina longiapertura* (Table 4). In this research we used the taxonomy which was compiled by Olsson *et al*. (1999), mainly because it is more recent and peer reviewed by many authors. The following species have been recognized in this zone: *Eoglobigerina eobulloides*, *Globoconusa daubjergensis, Parasubbotina pseudobulloides, Parvularugoglobigerina eugubina, Woodringina claytonensis* and *Zeauvigerina waiparaensis.* They show almost a continuous distribution. This interval comprises the following planktonic foraminiferal assemblages (Table 1): *Eoglobigerina edita*, *Chiloguembelina midwayensis, Chiloguembelina morsei, Globanomalina planocompressa, Hedbergella holmdelensis, Parvularugoglobigerina alabamensis, Parvularugoglobigerina extensa, Praemurica pseudoinconstans, Subbotina trivialis* and *Woodringina hornerstownensis*. This zone mainly consists of marl and mudstone alternation (Figure 15). It should be noted that it was difficult to extract good preserved foraminifer tests from marl facies.

Stratigraphic distribution: From the sample HEA-106 to the sample HEA-109.

Age: Earliest Paleocene (early Danian).

2.2.3 P1. *Parvularugoglobigerina eugubina - Praemurica uncinata* Interval Zone

Definition: Interval between the LAD (Last Appearance Datum) of *Parvularugoglobigerina eugubina* and the FAD (First Appearance Datum) of *Praemurica uncinata* and/or *Eoglobigerina spiralis* (Figure 15).

Author: Berggren *et al*., 1995, emended of Berggren and Miller, 1988.

Remarks: The lower part of this interval zone in studied section delineated by the last appearance of *Parvularugoglobigerina eugubina* and the upper part defined by the first appearance of *Eoglobigerina spiralis.* Different authors named this zone as *Globigerina pseudobulloides* and *Parasubbotina pseudobulloides* (Table 4). In this research we used the taxonomy which was compiled by Olsson *et al*. (1999). For that reason this zone was named as *Parvularugoglobigerina eugubina-Praemurica uncinata* Interval Zone. In this Inteval Zone *Eoglobigerina edita*, *Parasubbotina pseudobulloides, Parvularugoglobigerina alabamensis, Subbotina triloculinoides* and *Subbotina trivialis* shows almost a continuous distribution. This interval comprises the following planktonic foraminiferal assemblages (Table 1): *Eoglobigerina eobulloides*, *Chiloguembelina midwayensis, Chiloguembelina morsei, Chiloguembelina subtriangularis, Globanomalina compressa, Globanomalina imitata, Globanomalina planocompressa, Globoconusa daubjergensis, Praemurica inconstans, Praemurica pseudoinconstans, Subbotina cancellata, Woodringina claytonensis, Woodringina hornerstownensis, Zeauvigerina waiparaensis* and *Zeauvigerina virgata.* This zone mainly consists of mudstone, marl and muddy-limestone alternation (Figure 15).

Stratigraphic distribution: From the sample HEA-110 to the sample HEA-131.

Age: Early Paleocene (Danian).

2.2.3.1 P1a. *Parvularugoglobigerina eugubina - Subbotina triloculinoides* Interval Subzone

Definition: Interval between the LAD of *Parvularugoglobigerina eugubina* and the FAD of *Subbotina triloculinoides* (Figure 15).

Author: Berggren *et al*., 1995

Remarks: It was not so difficult to delineate the upper boundary of this zone, because the preservation of *Subbotina triloculinoides* is quite good in mudstone facies. Keller *et al*. (1995) and Pardo *et al*. (1999) named this subzone as P1b but many authors and Olsson *et al*. (1999) named this subzone as a P1a (*Parvularugoglobigerina eugubina-Subbotina triloculinoides* Interval Subzone) (Table 4). In this subzone *Eoglobigerina eobulloides*, *Parasubbotina pseudobulloides* and *Parvularugoglobigerina alabamensis* show almost a continuous distribution. This interval comprises the following planktonic foraminiferal assemblages (Table 1): *Chiloguembelina morsei, Subbotina trivialis* and *Woodringina hornerstownensis.* This subzone mainly consists of mudstone and muddy-limestone alternation (Figure 15). The preservation of specimens in muddy-limestone facies is poor whereas it is quite good in mudstone facies.

Stratigraphic distribution: From the sample HEA-110 to the sample HEA-112.

Age: Early Paleocene (Early Danian).

2.2.3.2 P1b. *Subbotina triloculinoides - Globanomalina compressa*/*Praemurica inconstans* Interval Subzone

Definition: Interval between the FAD of *Subbotina triloculinoides* and the FAD of *Globanomalina compressa* and/or *Praemurica inconstans* (Figure 15).

Author: Berggren and Miller, 1988.

Remarks: The upper part of subzone in the studied section is defined by first appearance of *Praemurica inconstans* instead of *Globanomalina compressa,* mainly because *Praemurica inconstans* is more abundant, well preserved and appeared in the section earlier than *Globanomalina compressa.* Keller *et al*. (1995) and Pardo *et al*. (1999) named this subzone as P1c but Berggren *et al*. (1995) and Olsson *et al*. (1999) named this subzone as a P1b (*Subbotina*

triloculinoides - *Globanomalina compressa* Interval Subzone) (Table 4). In this subzone *Chiloguembelina midwayensis, Parasubbotina pseudobulloides, Parvularugoglobigerina alabamensis* and *Subbotina triloculinoides* shows almost a continuous distribution. This interval comprises the following planktonic foraminiferal assemblages (Table 1): *Eoglobigerina edita, Eoglobigerina eobulloides, Chiloguembelina morsei, Globanomalina planocompressa, Praemurica pseudoinconstans, Subbotina trivialis, Woodringina claytonensis, Woodringina hornerstownensis, Zeauvigerina waiparaensis* and *Zeauvigerina virgata.* This subzone mainly consists of mudstone, marl and muddy-limestone facies alternation (Figure 15).

Stratigraphic distribution: From the sample HEA-115 to the sample HEA-121.

Age: Early Paleocene (middle Danian).

2.2.3.3 P1c. *Globanomalina compressa*/*Praemurica inconstans-Praemurica uncinata* Interval Subzone

Definition: Interval between the FAD of *Globanomalina compressa* and/or *Praemurica inconstans* and the FAD of *Praemurica uncinata* and/or *Eoglobigerina spiralis* (Figure 15).

Author: Berggren and Miller, 1988.

Remarks: This subzone in the studied section starts with the first appearance of *Praemurica inconstans*. The first appearance of *Globanomalina compressa* was not used as the start point of the subzone, because it appeared in the studied section later than *Praemurica inconstans.* The end of the subzone was delineated by the first appearance of *Eoglobigerina spiralis.* The *Praemurica uncinata* was not used to deliniate the upper boundary of this subzone because it appeared later than *Eoglobigerina spiralis* in the studied section. In this subzone *Eoglobigerina edita*, *Parasubbotina pseudobulloides, Parvularugoglobigerina alabamensis, Praemurica inconstans, Subbotina cancellata, Subbotina triloculinoides* and *Subbotina trivialis* shows almost a continuous distribution. This interval comprises the following planktonic foraminiferal assemblages (Table 1): *Chiloguembelina midwayensis, Chiloguembelina subtriangularis, Globanomalina*

compressa, Globanomalina imitata, Globanomalina planocompressa, Globoconusa daubjergensis, Zeauvigerina waiparaensis and *Zeauvigerina virgata.* This subzone mainly consists of mudstone, marl and muddy-limestone facies alternation (Figure 15). Well preserved forms extracted mainly from the mudstone facies.

Stratigraphic distribution: From the sample HEA-122 to the sample HEA 131.

Age: Early Paleocene (late Danian).

2.2.4 P2. *Praemurica uncinata/Eoglobigerina spiralis-Morozovella angulata* Interval Zone

Definition: Interval between the FAD of *Praemurica uncinata* and/or *Eoglobigerina spiralis* and the FAD of *Morozovella angulata* or LAD of *Eoglobigerina spiralis* (Figure 15).

Author: Berggren and Miller, 1988.

Remarks: This Zone in the studied section starts with the first appearance of *Eoglobigerina spiralis*. We did not use the first appearance of *Praemurica uncinata* as the start point of this zone, mainly because it appeared in the section 3 samples later than *Eoglobigerina spiralis.* However, *Eoglobigerina spiralis* also very good indicative of the start point of P2 Zone (Table 3). Preservation and abundance of *Eoglobigerina spiralis* shells in samples also high than the *Praemurica uncinata.* In this zone *Eoglobigerina spiralis, Globanomalina compressa, Globanomalina ehrenbergi, Globanomalina imitata, Parasubbotina pseudobulloides, Parvularugoglobigerina alabamensis, Praemurica inconstans, Praemurica uncinata, Subbotina cancellata, Subbotina triloculinoides, Zeauvigerina waiparaensis* and *Zeauvigerina virgata* shows almost a continuous distribution. This interval comprises the planktonic foraminiferal assemblages below (Table 1): *Chiloguembelina midwayensis, Chiloguembelina subtriangularis, Morozovella praeangulata, Praemurica pseudoinconstans* and *Subbotina triangularis.* This zone mainly consists of mudstone and marl alterrnation (Figure 15). It was possible to extract well preserved forms from both mudstone and marl facies.

Stratigraphic distribution: From the sample HEA-132 to the sample HEA-145.

Age: Early Paleocene (late Danian).

2.2.5 P3. *Morozovella angulata-Globanomalina pseudomenardii* Interval Zone

Definition: Interval between the FAD of *Morozovella angulata* and/or *Parasubbotina variospira* and the FAD of *Globanomalina pseudomenardii* (Figure 15).

Author: Berggren and Miller, 1988.

Remarks: The lower boundary of this zone is defined by the first appearance of both *Morozovella angulata* and *Parasubbotina variospira.* However, the upper boundary of this zone is recognized by the first appearance of *Globanomalina pseudomenardii*. In this zone *Parasubbotina pseudobulloides, Parasubbotina variospira, Subbotina cancellata, Subbotina triloculinoides, Subbotina velascoensis* and *Zeauvigerina virgata* shows almost a continuous distribution. This interval comprises the following planktonic foraminiferal assemblages (Table 1): *Chiloguembelina midwayensis, Chiloguembelina subtriangularis, Globanomalina chapmani, Globanomalina ehrenbergi, Globanomalina imitata, Igorina albeari, Igorina tadjikistanensis, Morozovella angulata, Parvularugoglobigerina alabamensis, Praemurica inconstans, Praemurica uncinata, Subbotina triangularis* and *Zeauvigerina waiparaensis*. This zone mainly consists of mudstone and marl alternation (Figure 15).

Stratigraphic distribution: From the sample HEA-146 to the sample HEA-9.

Age: Middle Paleocene (Selandian).

2.2.5.1 P3a. *Morozovella angulata-Igorina albeari* Interval Subzone

Definition: Interval between FAD of *Morozovella angulata* and/or *Parasubbotina variospira* and FAD of *Igorina albeari* (Figure 15).

Author: Berggren *et al*., 1995.

Remarks: The lower boundary of this subzone is recognized by the first appearance of both *Morozovella angulata* and *Parasubbotina variospira.*

However, the upper boundary of this subzone is defined by the first appearance of *Igorina albeari*. It should be noted that abundance of planktonic foraminifers in this subzone is relatively poor. In this subzone *Parasubbotina pseudobulloides, Parasubbotina variospira, Praemurica inconstans* and *Subbotina triloculinoides* shows almost a continuous distribution. This interval comprises the following planktonic foraminiferal assemblages (Table 1): *Chiloguembelina subtriangularis, Globanomalina ehrenbergi, Globanomalina imitata, Morozovella angulata, Morozovella praeangulata, Parvularugoglobigerina alabamensis, Praemurica uncinata, Subbotina cancellata, Subbotina triangularis, Zeauvigerina waiparaensis* and *Zeauvigerina virgata.* This subzone mainly consists of mudstone and marl alternation (Figure 15). It was difficult to extract well preserved planktonic foraminifers from marl facies and because of this identification of some species is difficult.

Stratigraphic distribution: From the sample HEA-146 to the sample HEA-151.

Age: Middle Paleocene (Selandian).

2.2.5.2 P3b. *Igorina albeari-Globanomalina pseudomenardii* Interval Subzone

Definition: Interval between FAD of *Igorina albeari* and the FAD of *Globanomalina pseudomenardii* (Figure 15).

Author: Berggren *et al*., 1995.

Remarks: The lower boundary of this subzone is recorded by the first appearance of *Igorina albeari* and the upper boundary is defined by the first appearance of *Globanomalina pseudomenardii*. The preservation and abundance of which is very low. In this subzone *Igorina albeari, Igorina tadjikistanensis, Parasubbotina variospira, Subbotina triloculinoides* and *Subbotina velascoensis* are recognized. This interval comprises the following planktonic foraminiferal assemblages (Table 1): *Chiloguembelina midwayensis, Chiloguembelina subtriangularis, Globanomalina chapmani, Globanomalina imitata, Subbotina cancellata* and *Zeauvigerina virgata.* This subzone mainly consists of mudstone, marl, muddy-limestone and limestone alternation (Figure 15). Since it was very difficult to

extract planktonic foraminifers from marl, muddy-limestone and limestone facies, the preservation of forms is poor.

Stratigraphic distribution: From the sample HEA-152 to the sample HEA-9.

Age: Middle Paleocene (Selandian).

2.2.6 P4. *Globanomalina pseudomenardii* Total Range Zone

Definition: Interval of the total range of the nominate taxon, *Globanomalina pseudomenardii* (Figure 15).

Author: Bolli, 1957a.

Remarks: The lower and upper boundaries of this zone are defined by respectively first and last appearances of *Globanomalina pseudomenardii*. Since the abundance of *Globanomalina pseudomenardii* in this zone is relatively high it was not so difficult to delineate the upper and lower boundary of the zone. In this zone *Globanomalina imitata, Globanomalina pseudomenardii, Subbotina cancellata* and *Subbotina velascoensis* are recorded. This interval comprises the following planktonic foraminiferal assemblages (Table 1): *Chiloguembelina crinita, Globanomalina chapmani, Globanomalina ovalis, Igorina albeari, Igorina tadjikistanensis, Parasubbotina variospira, Subbotina triloculinoides* and *Zeauvigerina virgata.* This zone mainly consists of mudstone and marl facies alternation (Figure 15).

Stratigraphic distribution: From the sample HEA-10 to the sample HEA-15.

Age: Middle part of late Paleocene (late Selandian-Thanetian).

2.2.6.1 P4a. *Globanomalina pseudomenardii*/*Acarinina subsphaerica* Concurrent Range Subzone

Definition: Interval characterized by the concurrent range of the three nominate taxa between the FAD of *Globanomalina pseudomenardii* and the LAD of *Acarinina subsphaerica* and/or *Parasubbotina variospira* (Figure 15).

Author: Berggren *et al*., 1995.

Remarks: The lower boundary of this subzone is recorded by the first appearance of *Globanomalina pseudomenardii* and the upper boundary is defined by the last appearances of *Acarinina subsphaerica* and/or *Parasubbotina variospira.* It was

not difficult to delineate the start point of this Zone because of relatively high abundance and good preservation of *Globanomalina pseudomenardii* but it was difficult to delineate the end of subzone. The upper boundary of this P4a subzone was recognized by the last appearance of *Parasubbotina variospira* because the *Acarinina subsphaerica* was not recorded. In this subzone *Globanomalina chapmani, Globanomalina pseudomenardii, Parasubbotina variospira, Subbotina cancellata* and *Subbotina velascoensis* were recorded with almost continuous distribution. This interval comprises the following planktonic foraminiferal assemblages (Table 1): *Chiloguembelina crinita, Subbotina triangularis* and *Subbotina triloculinoides.* This subzone mainly consists of mudstone and marl facies (Figure 15).

Stratigraphic distribution: From the sample HEA-10 to the sample HEA-11.

Age: Late Paleocene (Thanetian).

2.2.6.2 P4b. *Acarinina subsphaerica-Acarinina soldadoensis* Interval Subzone

Definition: Interval from the LAD of *Acarinina subsphaerica* and/or *Parasubbotina variospira* to the FAD of *Acarinina soldadoensis* and/or *Globanomalina ovalis*.

Author: Berggren *et al*., 1995.

Remarks: The lower boundary of this zone is recorded by the last appearance of *Acarinina subsphaerica* and/or *Parasubbotina variospira* and the upper boundary is defined by the last appearances of *Acarinina soldadoensis* and/or *Globanomalina ovalis*. Because of the absence of *Acarinina soldadoensis,* the first appearance of it was not used for the definition of upper boundary of this subzone. Instead of this species, the first appearance of *Globanomalina ovalis,* which indicate the beginning of P4c subzone (Table 3) was used. In this subzone *Globanomalina imitata, Globanomalina pseudomenardii* and *Subbotina cancellata* were recorded with almost a continuous distribution. This interval comprises the following planktonic foraminiferal assemblages (Table 1): *Igorina albeari, Subbotina velascoensis* and *Zeauvigerina virgata*. This subzone consists of mudstone and marl facies (Figure 15).

Stratigraphic distribution: From the sample HEA-12 to the sample HEA-13.

Age: Late Paleocene (Thanetian).

2.2.6.3 P4c. *Acarinina soldadoensis-Globanomalina pseudomenardii* Concurrent range Subzone

Definition: Interval containing the concurrent range of the nominate taxa from the FAD of *Acarinina soldadoensis* and/or *Globanomalina ovalis* to the LAD of *Globanomalina pseudomenardii* (Figure 15).

Author: Berggren *et al*., 1995.

Remarks: This subzone in the studied section starts with the first appearance of *Globanomalina ovalis*. The end point of this subzone delineated by the last appearance of *Globanomalina pseudomenardii.* In this subzone *Globanomalina ovalis, Globanomalina pseudomenardii* and *Subbotina velascoensis* shows almost a continuous distribution. This interval comprises the following planktonic foraminiferal assemblages (Table 1): *Chiloguembelina crinita, Globanomalina chapmani, Globanomalina imitata, Igorina albeari* and *Igorina tadjikistanensis*. This subzone mainly consists of mudstone and marl facies (Figure 15).

Stratigraphic distribution: From the sample HEA-14 to the sample HEA-15.

Age: Late Paleocene (late Thanetian).

2.2.6.4 P5. *Morozovella velascoensis* Interval Zone

Definition: Interval between the LAD of *Globanomalina pseudomenardii* and the LAD of *Morozovella velascoensis* and/or FAD of *Morozovella alisonensis* (Figure 15).

Author: Bolli, 1957a.

Remarks: Although the lower boundary of this zone is delineated by the last appearance of *Globanomalina pseudomenardii,* the upper boundary of this zone could not be defined. The existences of *Morozovella velascoensis* and *Morozovella alisonensis* are not clear in the studied samples because of the poor preservation of specimens. However, the upper boundary of this zone is roughly delineated by the appearance of new assemblage of planktonic foraminifers in the sample HEA-21. Because of this unclear definition, the upper boundary is marked with question mark. More precisely the end of this zone can be delineated in

future research by the first appearance of Eocene planktonic foraminifer species. In this zone *Globanomalina chapmani, Globanomalina ovalis, Igorina tadjikistanensis* and *Subbotina triangularis* shows almost a continuous distribution. This interval comprises the following planktonic foraminiferal assemblages (Table 1): *Chiloguembelina crinita* and *Subbotina velascoensis.* This zone mainly consists of limestone and marl (Figure 15).

Stratigraphic distribution: From the sample HEA-16 to the sample HEA-20.

Age: Late Paleocene (late Thanetian ?).

2.2.7 Cretaceous - Paleogene boundary across the measured section

Cretaceous-Paleogene boundary sections are one of the interesting and most studied sequences in the world. Various fossil assemblages were used for determining the age and depositional environments of the sequences, such as planktonic and benthonic foraminifers, calcareous nannofossils, belemnites and ammonites (Canudo, 1997; Ginsburg, 1997; Keller, 1997; Kouwenhoven, 1997; Lipps, 1997; Keller, 2001; Luciani, 2002; Masters, 1997; Olsson, 1997; Smit and Nederbragt, 1997, etc.).

Since the Cretaceous-Paleogene boundary shows a great extension of mass extinctions, causes and characteristics of these enormous extinctions have become an important discussion. The first theory was the bolide impact that suddenly obliterated the life on Earth. The crater in the Yucatan (Mexico) and the distinct clay level with an iridium anomaly through the boundaries in measured sections in the world verify this idea. However, by the following detailed studies, it is argued that the bolide impact wasn't the only main cause of the mass extinction and there became long period extinction events around the boundary due to the changes in the environmental conditions (Canudo, 1997; Keller, 2001; Keller, 1997; Luciani, 2002; Masters, 1997; Olsson, 1997; Smit and Nederbragt, 1997).

Among the continuing discussion, another point is whether the K/P extinction was a single event or kept on as gradual, stepwise events. Due to conducted research in the studied section, it seems that mass extinction was a single event.

Some researchers defended that most of the species became extinct as a result of bolide impact and the observed Cretaceous species in the Danian samples were the result of reworking. Other groups argued that many species survived from the extinction event and continued to live in Paleocene (Keller, 1988; Keller *et al*., 2002; Obaidalla, 2005). The specimens of some Cretaceous species are smaller than the original. Cretaceous species that has been observed above the boundary can be thought as "survivors" (Keller *et al*., 2002). On the other hand, the pre-boundary extinction is thought to be resulted from the insufficient sampling in the studies or differences in the taxonomic nomenclature for different authors. El Kef blind test is one of the most significant projects in this manner. A blind test was carried out to find out the characteristics of the Cretaceous - Paleogene extinction by numerous authors (Canudo, 1997; Ginsburg, 1997; Keller, 1997; Kouwenhoven, 1997; Lipps, 1997; Masters, 1997; Olsson, 1997; Orue-etxebarria, 1997; Smit and Nederbragt, 1997). However, in this project, the authors have not reached an agreement on these subjects yet and the discussions are going on.

During the fieldwork in the study area, it was difficult to define the Cretaceous-Paleogene boundary, since there is not any change in the lithology of the measured sequence. However, during the laboratory studies, by the data of both thin sections and the washing specimens from the collected samples, a detailed observation has been carried out and exact level of K/P boundary was delineated. The interval between the sample HEA-105 and the sample HEA-106 where K/P boundary was pinpointed is 4.75 m in thickness (Figure 16, Appendix A). Throughout conducted laboratory work, in the studied section the Cretaceous-Paleogene boundary is determined with the complete disappearance of the Cretaceous forms and appearance of new ones in the Paleocene (Figure 17). Paleocene species are smaller forms in size with globular chambers and they are not bearing keels or any other complex structures as a Cretaceous species. Thus, all through the measured section HEA-101 was determined as first Cretaceous sample and HEA-105 as the last Cretaceous sample, HEA-106 as the first Paleocene sample and HEA-20 as the last Paleocene sample.

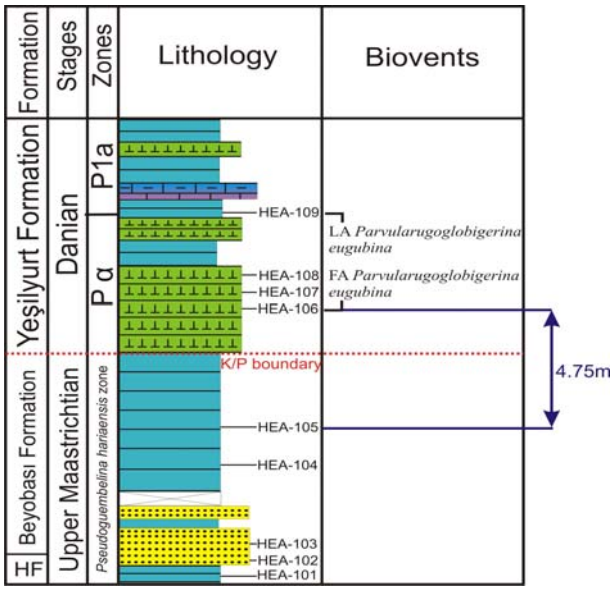

Figure 16. The K/P boundary was pinpointed between the interval (4.75 m in thickness), between the sample HEA-105 and 106.

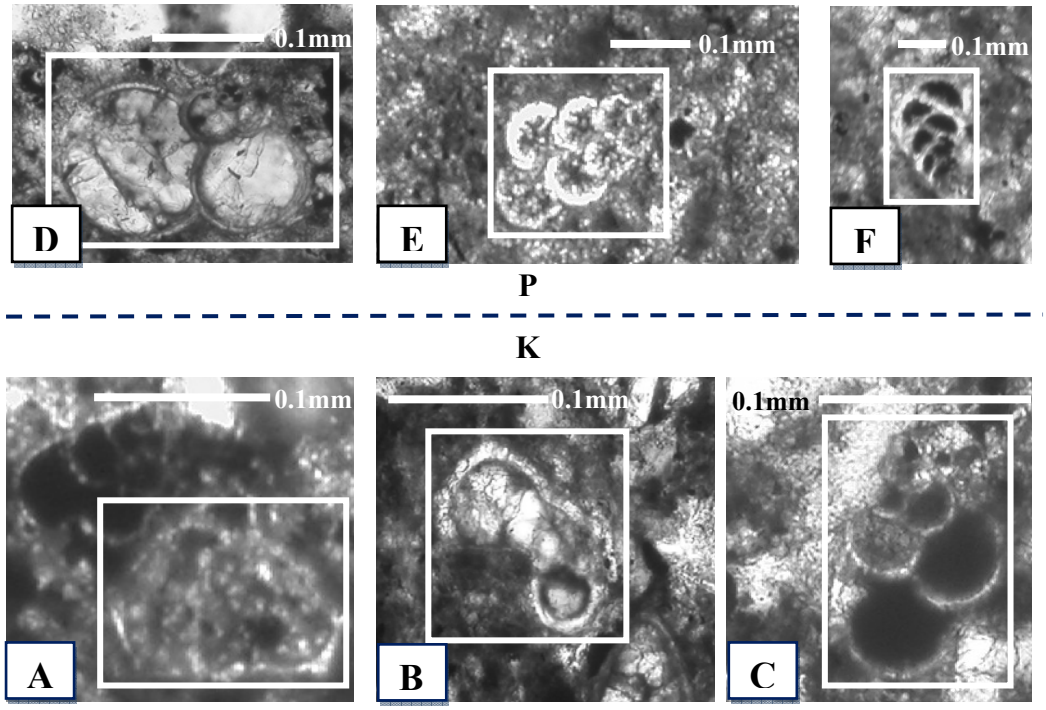

Figure 17. Changes in the planktonic foraminiferal assemblages at the K/P (Cretaceous-Paleogene) boundary: A, B, C: High diversity of Maastrichtian forms with complex morphologies such as double keels (A: HEA-101), single-keel (B: HEA-104) and biserial form (C: HEA-104); D, E, F: Danian species with simple morphology such as globular chambers in trochospiral form (D: HEA-106) and small biserial forms (E, F: HEA-114, 115).

CHAPTER 3

SEQUENCE STRATIGRAPHY

3.1 Historical Preview

Sequence stratigraphy is a subdiscipline of stratigraphy and most recent paradigm in geological thought. Sequence stratigraphy is often regarded as a relatively new science, evolving in the 1970s from seismic stratigraphy. Seismic stratigraphy emerged in 1970's with the work of Vail *et al*. (1977). The seismic stratigraphic analysis stimulated a revolution in stratigraphy. This new method together with the global cycle chart was published by Vail *et al*. (1977). Seismic stratigraphy is a geologic approach to the stratigraphic interpretation of seismic data (Vail and Mitchum, 1977). Seismic sequence analysis is based on the depositional sequences. Depositional sequence is defined as a stratigraphic unit composed of a relatively conformable succession of genetically related strata and bounded at its top and base by unconformities or their correlative conformities (Mitchum *et al*., 1977). However, in 1963 Sloss had defined the sequence as an unconformity bounded rock-stratigraphic units of higher rank.

Sequence stratigraphy provides a powerful tool for stratigraphic analysis of marine clastic systems when it is combined with an appreciation of the variability in processes and depositional products of marine settings. This combined approach based on sequence stratigraphy and sedimentary processes has advanced from early studies of the late 1970s, which emphasized simple model-driven interpretations of marine clastic systems based on seismic data (Mitchum *et al*., 1977; Vail *et al*., 1977; Posamentier *et al*., 1988; Van Wagoner *et al*., 1990).

Sequence stratigraphy is defined as the study of rock relationships within a chronostratigraphic framework of repetitive, genetically related strata bounded by surfaces of erosion or nondeposition, or their correlative conformities (Van

Wagoner *et al*., 1988). Sequence is the fundamental unit of sequence stratigraphy. A sequence can be subdivided into system tracts which are composed of depositional systems, 3D assemblages of lithofacies (Van Wagoner *et al*., 1988). System tracts are defined by stacking patterns of parasequence sets or cycles. Cycle is defined as a relatively conformable succession of genetically related beds or bed sets bounded by marine flooding surfaces and their correlative surfaces (Van Wagoner *et al*., 1988). Meter-scale depositional cycles are fundamental stratigraphic units. Cyclicity is defined by the stratal repetition of physical and chemical characters of sedimentary rocks, such as, lithofacies and biofacies (Yang *et al*., 1998).

This study documents a detailed study of cyclic sedimentation in the shallow-marine carbonate and deep-marine siliciclastic deposits of the Upper – Cretaceous and Paleocene successions of the Haymana, Beyobası and Yeşilyurt formations.

In order to define cyclic sedimentation in these depositional systems of the studied area, firstly detailed vertical lithofacies association have been carried out and documented in the field. Secondly more detailed microfacies analysis have been performed in the laboratory based on thin section analysis, which was discussed in the petrographic analysis of the studied samples chapter.

3.2 Meter-scale Cycles

The parasequence is a relatively conformable succession of bed or bedsets bounded by marine flooding surfaces and their correlative surfaces (Van Wagoner *et al*., 1988). Because a parasequence is bounded by flooding surfaces, recognition of flooding surfaces is the key for establishing a parasequence. In shallow water environments, it is possible to recognize flooding surfaces because small changes in water depths (for instance, a few m) are reflected in the deposits. However in deep marine settings minor changes in water depths cannot be easily recognized in all cases and care must be taken in definition of these surfaces (Shanmugam, 1997).

In our study area, where the Upper Cretaceous-Paleocene succession of the Haymana basin is well exposed, perfect repetition of meter-scale units (cycles) can be seen and limestone or lime-rich intervals within studied section were interpreted as an increase in water depths (Sarg, 1988). The total thickness of the measured section is 162 m and contains depositional systems and its smaller subdivisions. According to detailed lithofacies analysis and their vertical association, the whole section, which is 162 m thick can be divided into several meter-scale cycles by the combination of five main lithologies recognized along the section (Figure 18). Lithologies are namely limestone, muddy or clayey limestone, marl, mudstone (or shale) and the sandstone. In our measured section the meter-scale cycles are of four main types (Figure 19, Figure 20). A-type is only seen at the base of the section and basically composed of mudstone overlain by a sandstone. B-type is one of the most common cycle types in the section and characterized by mudstones capped by marls. C-type is the combination of mudstone and muddy-limestone associations. D-type cycles are generally characterized by the combination of three types of lithologies in contrast to A, B and C cycles. Within D-type cycles three subtypes are distinguished. D-1 cycles start at the base with mudstones and are overlain by marls. Cycle tops are capped by pure limestones. D-2 type cycles start with mudstones and continue upwards with marls. However, in this subtype, with a slight variation in lithology, the upper capping lithology which is limestone is followed by a marl deposition at the top of the cycle. D-3 type cycles exhibit a similar organization consisting of mudstones followed by marls in the lower part of the cycle and muddy-limestones and marls as the capping lithologies.

Sequence architecture of the measured section is constructed by the stacking pattern of these meter-scale cycles which are basically characterized by the capping limy facies at their tops, which indicate the highstand conditions during the sea level oscillations.

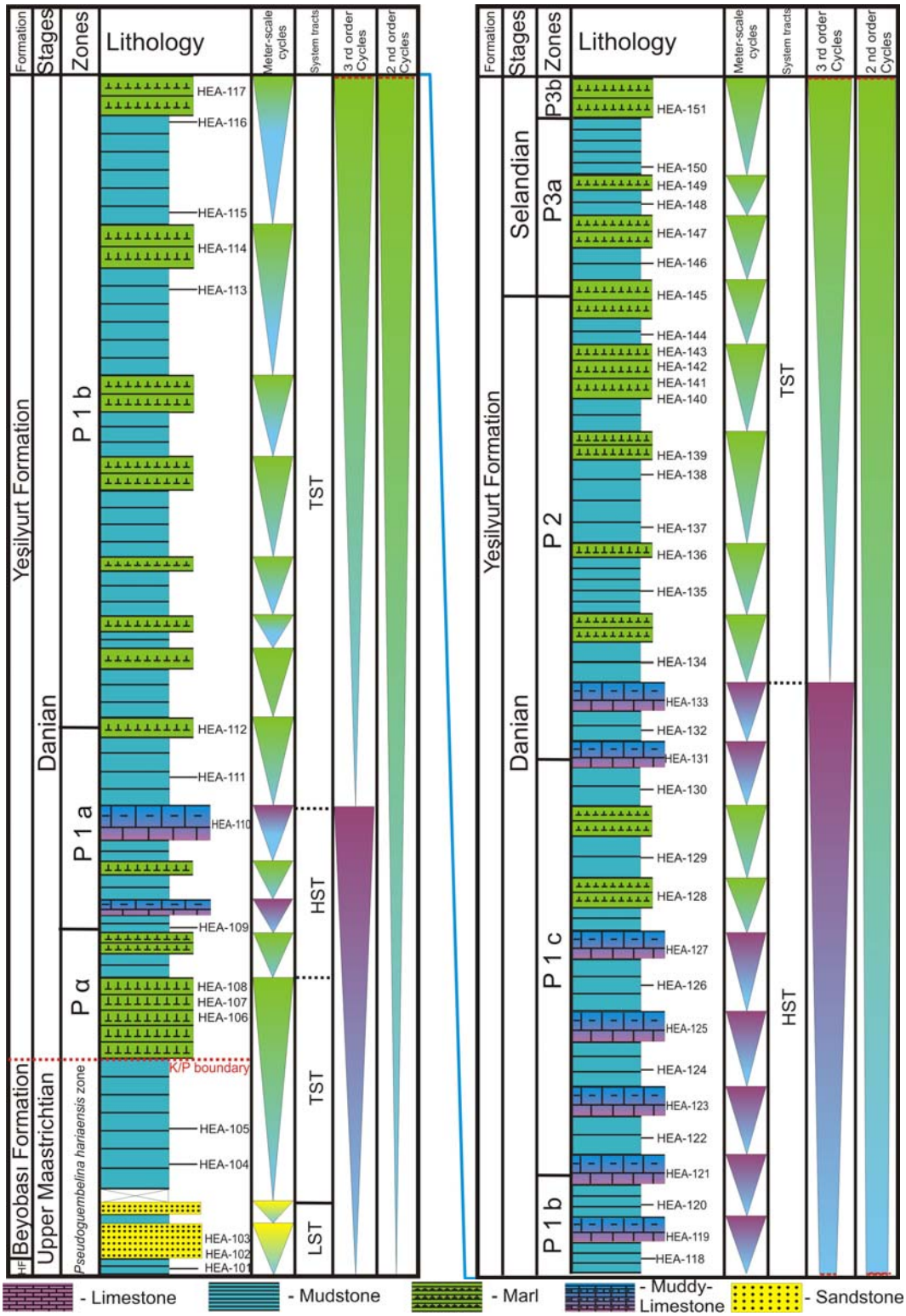

Figure 18. Meter-scale cycles and system tracts recorded in the studied section.

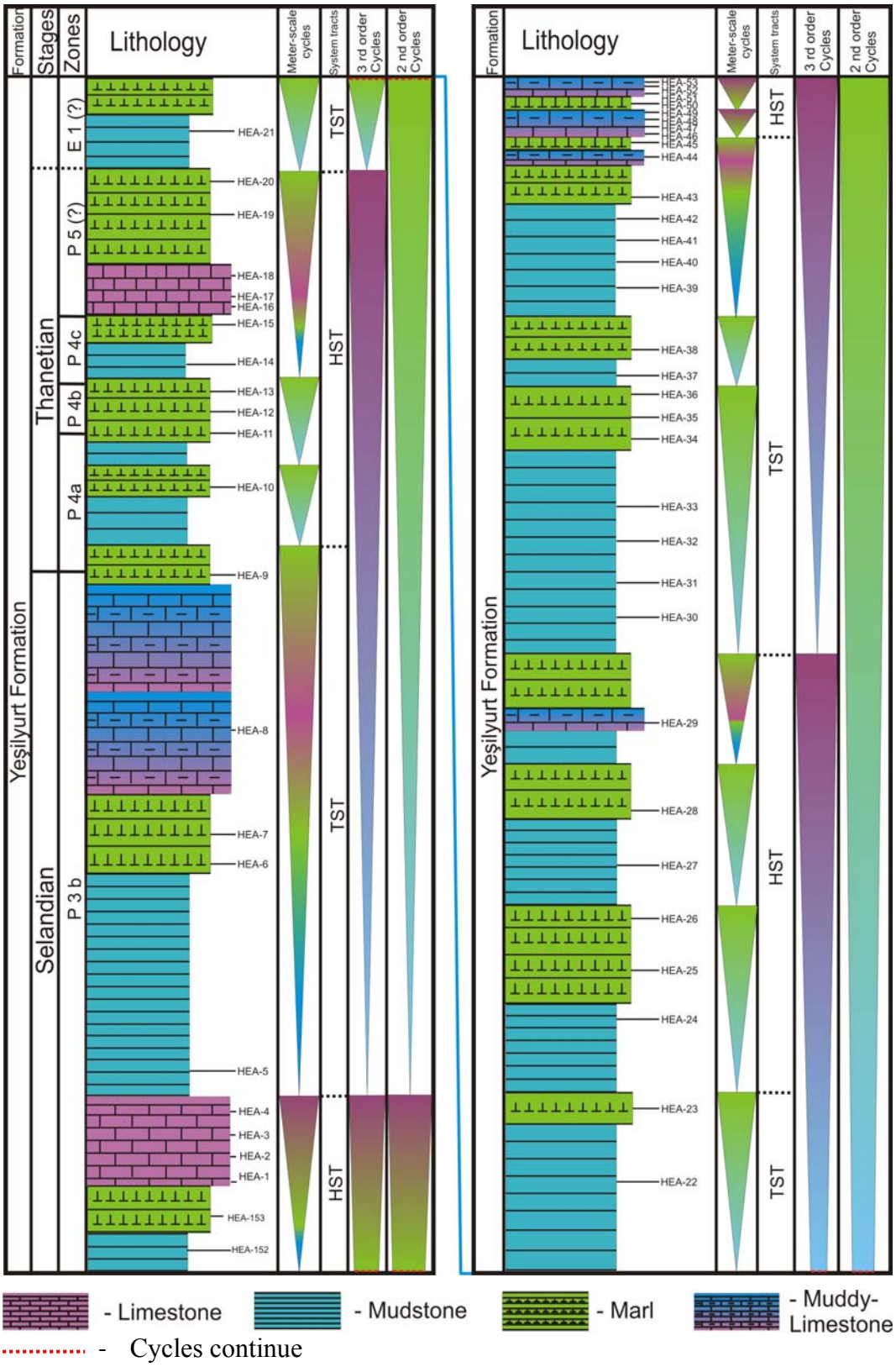

Figure 18. Continued.

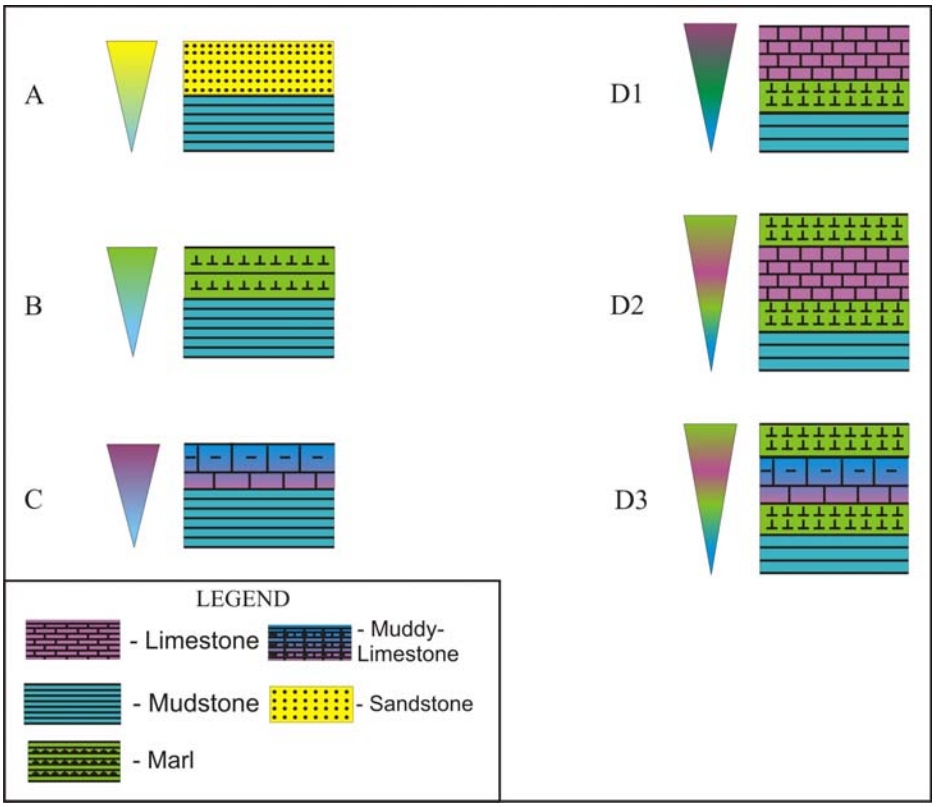

Figure 19. Types of meter-scale cycles.

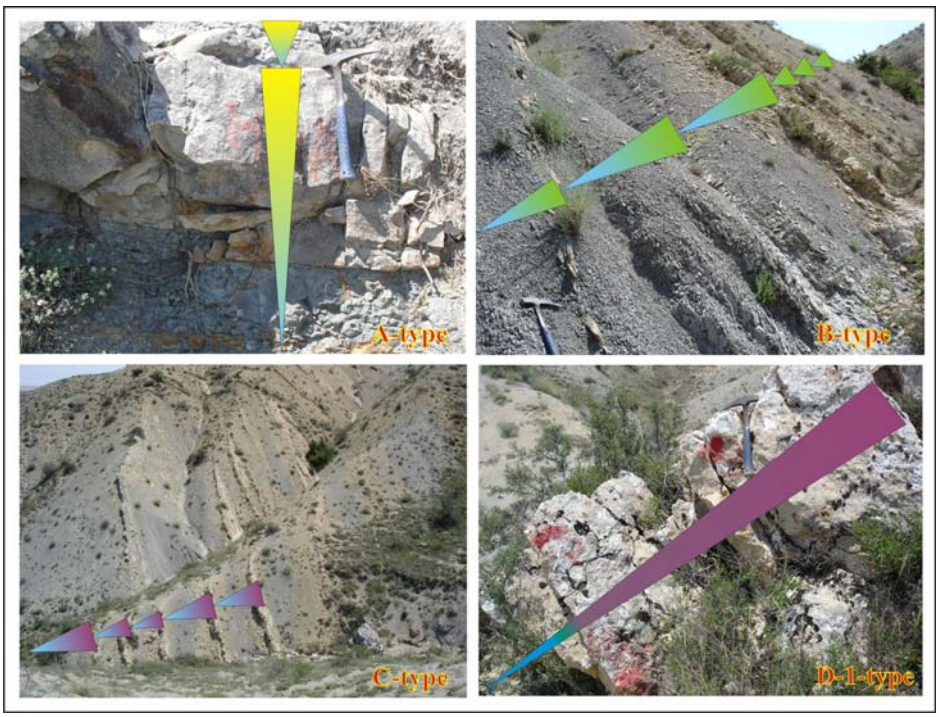

Figure 20. Different types of meter-scale cycles recorded in the studied section.

3.3 Higher Order Sequences and Interpretation

As a result of conducted sequence stratigraphical analysis, it was also possible to reveal 6 third-order and 2 second-order depositional cycles in the studied succession (Figure 18). The vertical evaluation of lithofacies, their bounding surfaces, packing and interaction of cycle types within the section is examined to define system tracts and possible sequence boundaries in the measured section. In the studied sequences, the lowermost one is characterized by a lowstand systems tract deposit laid down over a type-1 sequence boundary. The rest of the sequences examined in the studied section are of type-2 sequences, consisting probably of shelf margin wedge deposits at their base. Because of the difficulty of distingushing progradational to aggradational shelf margin wedge deposits from transgressive systems tract deposits we have interpreted the lower parts of these sequences as transgressive system tracts deposits including also shelf margin wedge deposits.

Based on our interpretations, the first depositional sequence is complete and represented by a lowstand systems tract (LST), transgressive systems tract (TST) and highstand system tract (HST) (Figure 18). The succession starts at the base with sandstone deposits (Samples HEA-102, 103) which corresponding to LST, which means a considerable fell in sea level and sediment bypassing. Under these conditions, the shoreline and environments close to the shoreline should have shift in the seaward direction. The LST deposits of this depositional sequence is characterized by dark colored sandstones and the A-type meter-scale cycle (Figure 18, Figure 19, Figure 20). A sequence boundary should lie immediately below these lowstand systems tract deposits. The TST of this depositional sequence is characterized by dark colored mudstone deposits which are print of a B-type meter-scale cycle (Figure 18, Figure 19, Figure 20). Samples from HEA-104 to 108 corresponds to a transgressive systems tract deposit, which means at this time corresponding to the Cretaceous-Paleogene boundary sea level drastically rose, basin enlarged and retrogradation took place. Mud which was present in suspension started to precipitate. The TST of this depositional sequence was overlain by the HST deposits which are characterized by the alternation of

yellowish marl, muddy-limestone and mudstone deposits. The cyclic organization was characterized by a B and C-type cycles (Figure 18, Figure 19, Figure 20). This means that accommodation space started to decrease in the carbonate generating areas of the basin and limestone deposits started to prograde towards the basin.

After a sequence boundary the sea level increased again and mudstone deposits started to precipitate alternating with marl facies. This interval is composed of the stacking of B-type meter-scale cycles of the second depositional sequence and covers the samples from HEA-111 to 117 corresponding to the TST. The HST of the second depositional sequence starts with the mainly alternation of muddy-limestone and mudstone deposits, characterized by a C-type meter scale cycles. The muddy-limestone capping these cycles prograded into the basin. The HST deposits continued till the level HEA-133 (Figure 18). Just below the level HEA-134, the third sequence boundary was defined (Figure 18). The TST started to get deposited above this level and is also characterized by a B-type meter-scale cycles (Figure 18). The HST deposits of the third depositional sequence are characterized by a D1-type meter-scale cycles which are capped by a prominent limestone level (the sample HEA 1-4, Figure 18, Figure 19).

The fourth depositional sequence is composed of TST and HST deposits. The TST deposits are represented by an alternation of mudstone, marl and muddy-limestone deposits, defined as a D-3-type meter-scale cycle. Thick mudstone deposits (sample HEA-5) correspond to the relative sea level rise. The TST continues till the level HEA-9 (Figure 18) and the HST of the fourth depositional sequence starts with a B-type meter-scale cycles and ends with a D-2-type cycle capped by a prominent limestone level (Figure 18).

The fifth depositional sequence is composed of TST and HST deposits. The TST of the fifth depositional sequence is represented by the alternation of marl and mudstone deposits, represented by a B-type meter-scale cycles. The TST covers the interval from HEA-21 to the level HEA-23 (Figure 18). The HST of the fifth depositional sequence starts above the level HEA-23 and a D-3-type cycle caps the HST deposits (Figure 18).

The sixth depositional sequence is incomplete and again consists of the TST and HST deposits. The TST of the sixth depositional sequence again represented by the alternation of marl, mudstone and muddy-limestone deposits of a B-type meter-scale cycles. The TST starts above the level HEA-29 which also corresponds to a sequence boundary. The TST deposits continues till the level HEA-45 and a D-3-type cycle caps the TST deposits (Figure 18). The HST of the depositional sequence starts above the level HEA-45 and consists of a D-type cycles (Figure 18).

We made comparisons between the cycles recognized in the studied section and the Global Sea Level Change Curve (Felix *et al*., 2004) (Figure 21).

The biozonations of Olsson *et al.* (1999) and Felix *et al*. (2004) are not so different from each other. The insignificant difference exists only in the zones Pα (Olsson *et al.*, 1999) and the P1a (Felix *et al*., 2004). Olsson *et al.* (1999) defined the base of the Pα Zone by the first appearance of *Parvularugoglobigerina eugubina* and the top by the last appearance of *Parvularugoglobigerina eugubina*. Felix *et al*. (2004) defined this zone as P1a. The base of the P1b Zone is indicated by the first appearance of *Subbotina triloculinoides*, whereas bases of P3b and P4b Zones are defined by the first appearances of *Igorina albeari* and *Parasubbotina variospira*, respectively.

When we compare the sea level curve of Haq *et al*. (1988) and Felix *et al*. (2004) it is possible to see that main transgressions and regressions occured mostly in the same biozones. For instance, according to Haq *et al*. (1988) (Figure 22) one of the main regression and sea level fall occurred in the *Abathomphalus mayaroensis* (*Pseudoquembelina hariaensis* zone in our section) and the following ones in the P1a, P1c, P3a, P4a and P5 Zones but according to Felix *et al*. (2004) the main sea level falls occurred in the P1a, P1c, P2, P3a, P4a and P5 Zones (Figure 21, Figure 22). This means that, according to Haq *et al*. (1988) no sea level fall was recorded in the P2 Zone. Our sequence boundaries roughly coincide with the main sequence boundaries of Felix *et al*. (2004) (Figure 21). Falls indicated in the P1c, P2 and P5 Zones are directly correlatable with our

sequence boundaries, because in studied section we also have the same sea level falls (Figure 21).

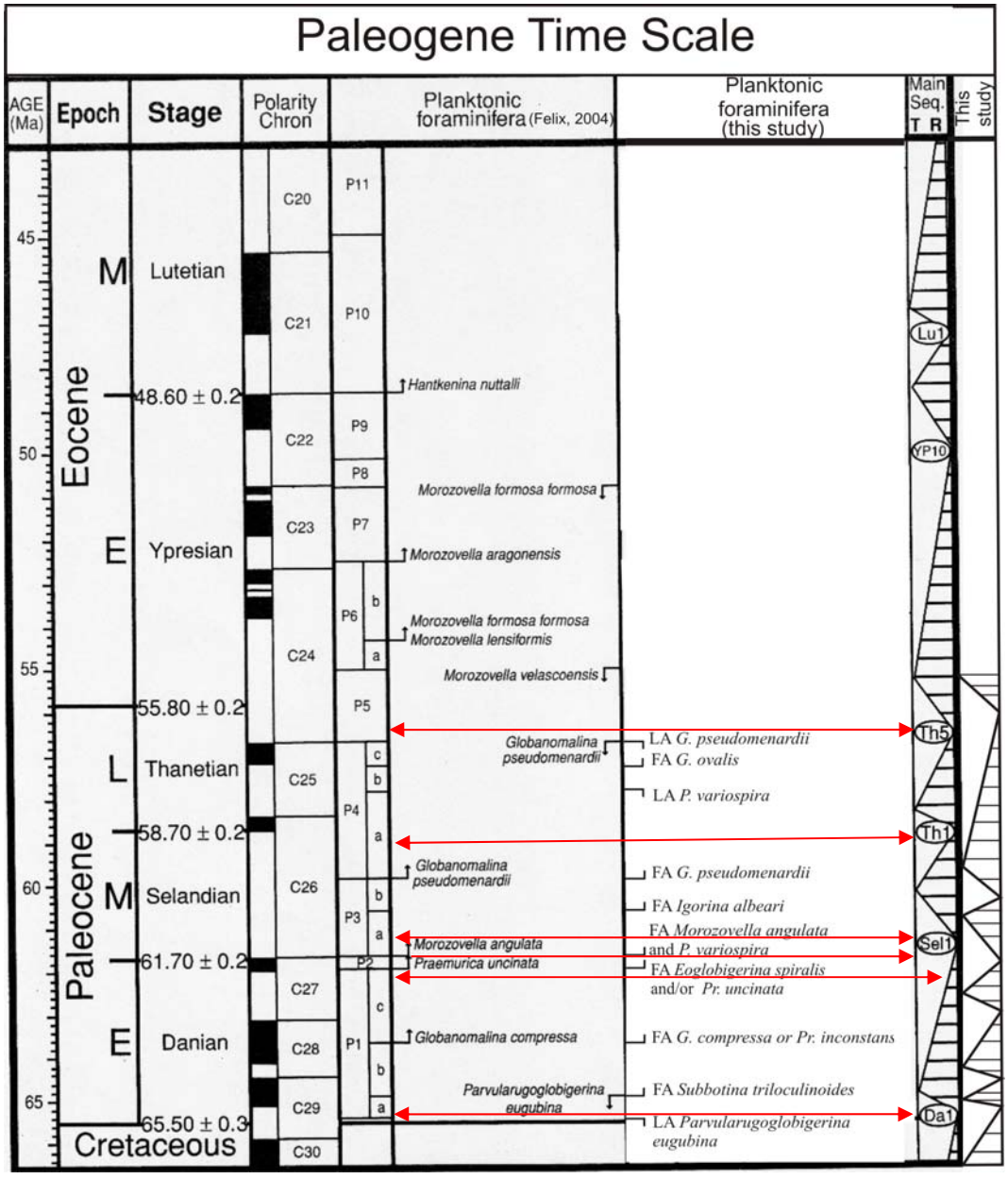

⌟- FA (first appearance), ⌝-LA (last appearance).

Figure 21. Paleogene Time Scale and main sequences (modified from Felix *et al.*, 2004).

In the studied succession we have detected the sea level falls in the *Pseudoquembelina hariaensis*, P1a, P1b, P1c, P2, P3b and P5 Zones. No sea level falls were detected in the P3a and P4a Zones. The reason why we have these discrepancies may be because of autocyclic events, for instance, because of tectonism in the Haymana basin at this time. If sea level falls in our succession do not sometime coincide to the zones correlated with the Global Sea Level Change Curve, we can think that the shifts might be due to the effect of tectonism. We also figure out that the sea level fall in the P2 Zone of our section, is absent in the curve of Haq *et al*. (1988) (Figure 22).

Based on the defined system tracts, the K/P boundary in the Haymana basin is located between the sample HEA-105 and 106, namely in a TST which coincides with the TST of the sequence on the chronostratigraphic chart of Haq *et al*., (1988) (Figure 22).

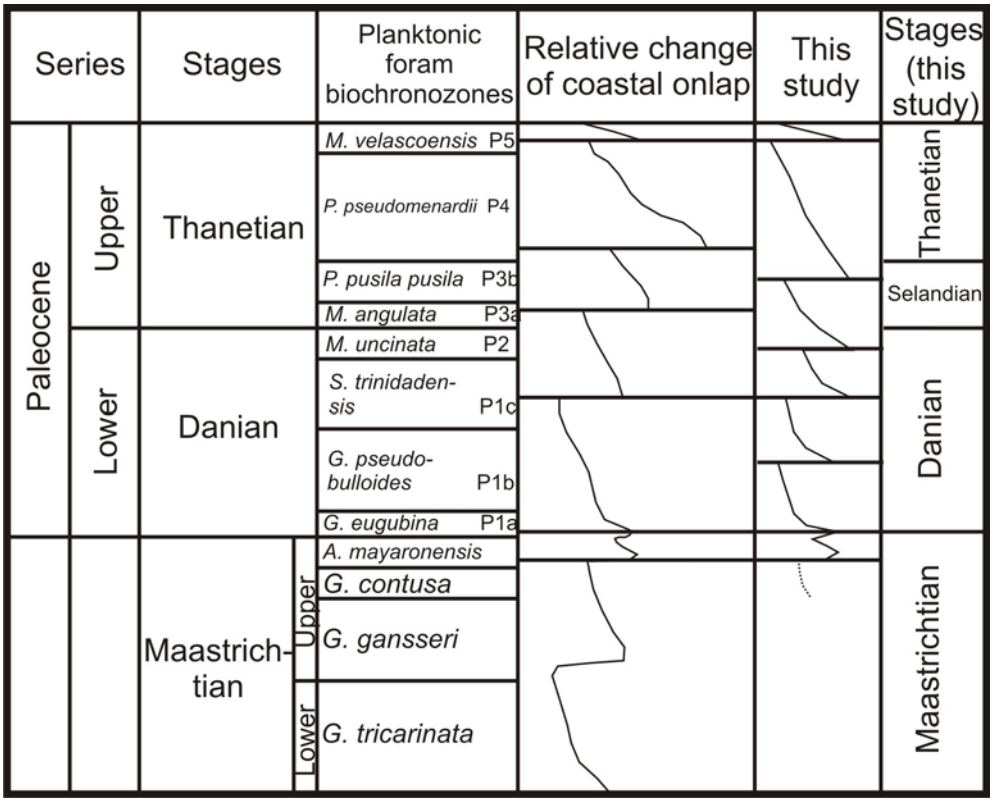

Figure 22. Paleocene chronostratigraphic chart (modified from Haq *et al*., 1988).

Moreover, when we compare our sequences from the studied section with the Paleocene sequence stratigraphy of De Graciansky, it is possible to see that we have 6 depositional cycles in the Paleocene as in the chart of De Graciansky (1998) (Figure 23).

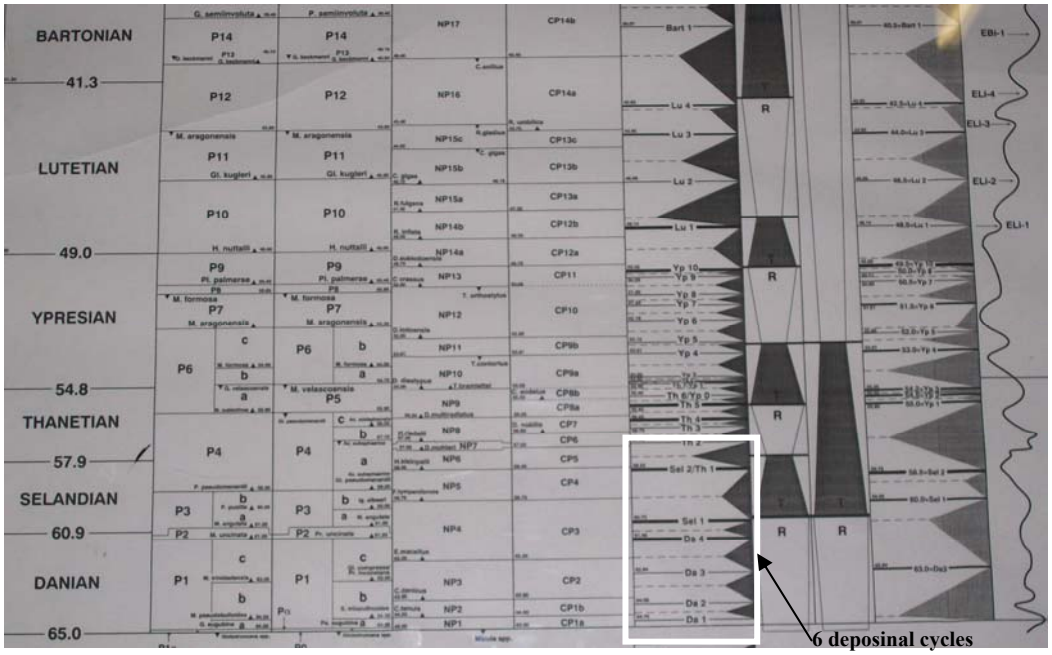

Figure 23. Cenozoic sequence chronostratigraphic chart (after De Graciansky, 1998).

CHAPTER 4

PETROGRAPHIC ANALYSIS OF THE STUDIED SAMPLES

Petrographic analysis of studied samples comprise sedimentogical and paleontological data which can be recognized from the thin-section of the rock samples. The purpose of petrographic analysis is to classify the rock facies and test the statistical measuring of distributary percentage of benthonic, planktonic foraminifers and ostracoda in all 106 collected samples. Petrographic analysis has been performed by examing the main components, fossil associations of the samples. Lithological variation observed in the outcrop during the field study have also been considered. Standard petrographical techniques using a polarising microscope were used to describe sedimentologic features of two sandstone samples (HEA - 102, 103) through their thin sections.

Quantitative analysis of planktonic, benthonic foraminifers and ostracoda revealed that in general amount of planktonic foraminifers increase in mudstone and wackestone microfacies and amount of benthonic foraminifers and ostracoda increase in packstone and grainstone microfacies (Appedix A). The rest of thin sections were point-counted using a Swift automatic point counter in order to define their sedimentological and mineralogical properties. Per every 106 thin sections a total of 1500 points were counted.

4.1 Classification of Lithofacies

One hundred six thin sections were examined in detail for the petrographic study. These semi-quantitative data were used to classify the rocks. According to field and laboratory analysis of rock samples four types of rocks were defined in the studied sequence. These are 1) limestones; 2) mudstones; 3) marls and 4) sandstones (classified as litharenites).

4.1.1 Limestones

Limestones which were recognized in 25 samples (HEA-110, 119, 121, 123, 125, 127, 131, 133, 1, 2, 3, 4, 8, 16, 17, 18, 29, 44, 46, 47, 48, 49, 51, 52 and 53) were classified by using only Dunham's classification due to time saving (Tucker, 2001) (Figure 24). Dunham (1962) divides limestones on the basis of texture into: lime mudstone (micrite with grains less than 10%), wackestone (more than 10% grains floating in a matrix), packstone (grains in contact with matrix, grain supported) and grainstone (lacks mud and is grain supported) (Figure 24). By using this classification, limestone intervals in the the measured section, was classified as lime mudstone, wackestone, packstone and grainstone (Appendix B), for detailed explanation see subchapters below.

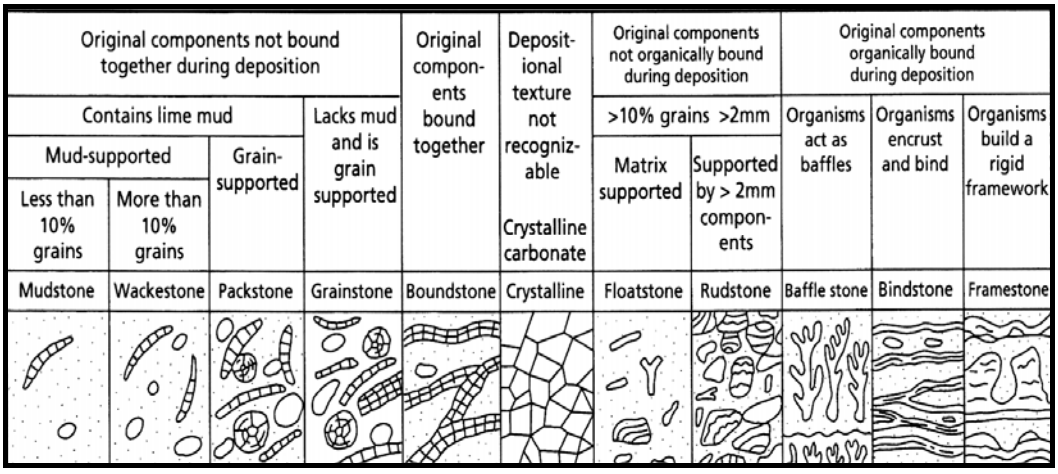

Figure 24. Classification of limestones based on depositional texture, Embry and Klovan, 1971 (after Dunham, 1962).

4.1.1.1 Lime mudstones

This microfacies type was recognized in only 2 levels (samples HEA-8, 29) and contains an average of 94.1% and a maximum of 95.1% matrix (Appendix B). Bioclasts constitute less than 3% and an averaging 2.8% of the rock volume. Quartz grains constitutes 1.9-3.7% of the rock volume (Appendix B). In general,

this microfacies is matrix supported and grains less than 10% are floating in the matrix (Figure 25).

4.1.1.2 Wackestones

This microfacies type was recorded in 11 levels (samples HEA-44, 46, 49, 52, 119, 121, 123, 125, 127, 131, 133) and contains an average of 80.25% and a maximum of 84.7% matrix, which is mainly composed of the lime mud. Bioclasts constitute 11.9-19.7% of the rock volume, which are commonly represented by benthonic foraminifers. Quartz grains constitute 1.8-6.3% of the rock volume (Appendix B). This microfacies is matrix supported and grains more than 10% are floating in the matrix (Figure 26).

4.1.1.3 Packstones

This microfacies type was determined in 6 levels (samples HEA-2, 47, 48, 51, 53, 110) and contains an average of 61.41% of matrix, which is again composed of lime mud. Bioclasts constitute less than 39.9% and an averaging 35.33% of the rock volume. Quartz grains constituting 0.2-5% of the rock volume (Appendix B). In general, under a microscope grains are in contact with matrix in this microfacies (Figure 27).

4.1.1.4 Grainstone

This microfacies type was recognized in only 2 levels (samples HEA-1, 3, 4, 16, 17, 18) and contains an average of 22.35% of matrix. Bioclasts constitute less than 73.2% and an averaging 69.01% of the rock volume. Calcite cement constitutes an averaging 8.31% of the rock volume. Quartz grains constituting 0.4-0.6% of the rock volume (Appendix B). Grainstone lacks lime mud and is grain supported in this microfacies (Figure 28).

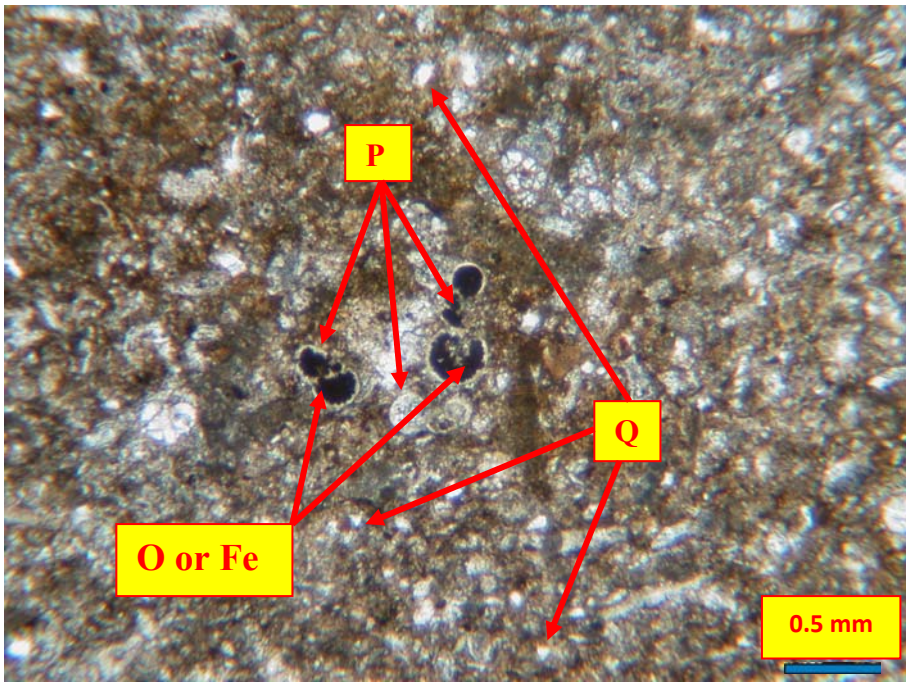

Figure 25. Photomicrograph of the muddy or clayey limestone (lime mudstone), (O or Fe - oil impregnation or Fe, P-planktonic foraminifera), Q-quartz), (HEA-8).

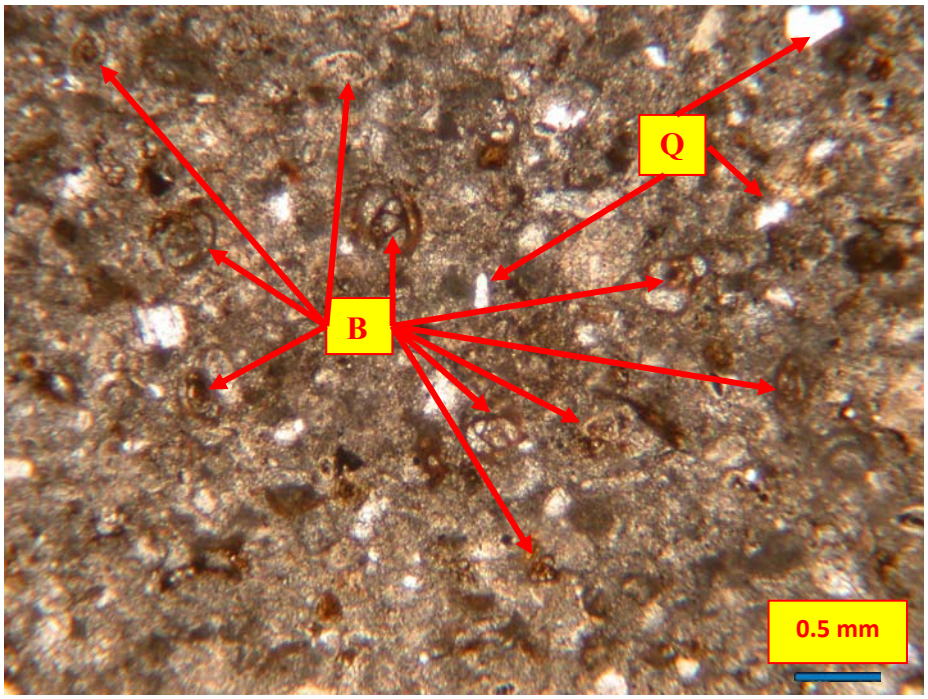

Figure 26. Photomicrograph of the limestone (wackestone), (B-benthonic foraminifers), Q-quartz), (HEA-46).

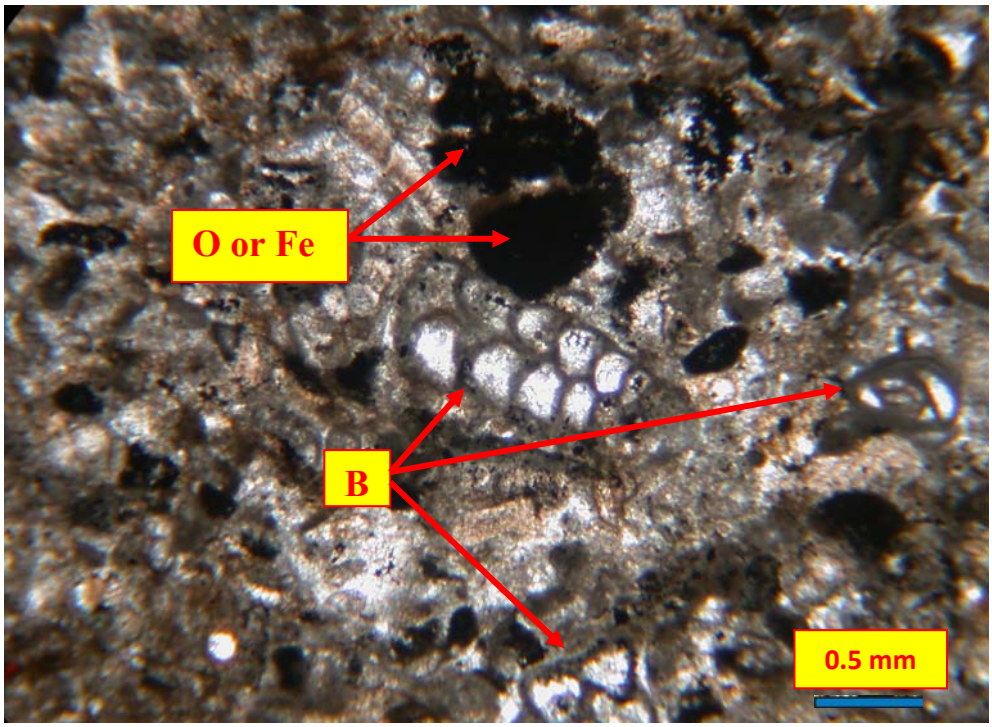

Figure 27. Photomicrograph of the muddy or clayey limestone (packstone),(O or Fe - oil impregnation or Fe, B-benthonic foraminifers), (HEA-110).

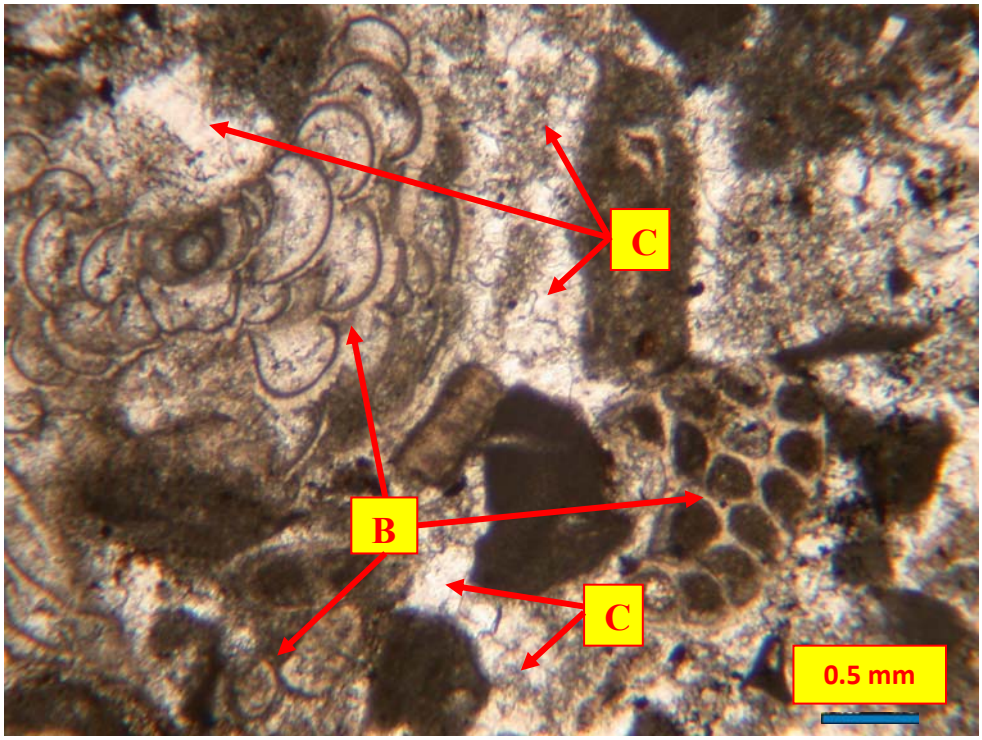

Figure 28. Photomicrograph of the limestone (grainstone), (B-benthonic foraminifers), C-calcite cement), (HEA-3).

4.1.2 Mudstones

Mudstones are very abundant throughout the measured section (samples HEA-101, 104, 105, 109, 111, 113, 115, 116, 118, 120, 122, 124, 126, 129, 130, 132, 134, 135, 137, 138, 144, 146, 148, 150, 152, 5, 14, 21, 22, 24, 27, 30, 31, 32, 33, 37, 39, 40, 41 and 42), from bottom to the top of the succession, mainly with intercalation of marl and limestone. Mudstones were classified during the field works by visual estimation and using hand lens. Mudstones have been defined by its indurate, massive and non-fissile structure.

The facies containing matrix between 33-65% have been defined as a mudstone facies according to Potter *et al*. (1980) classification. Twenhofel (1939) defines mud as a general term that includes clay, silt, claystone, siltstone, shale, and argillite, and that should be used only when the amounts of clay and silt are not known or specified or cannot be precisely identified: or "when a deposit consists of an indefinite mixture of clay and silt, and sand particles, the proportions varying from place to place, so that a more precise term is not possible". Potter *et al*. (2005) identifies mud as a field term for any soft plastic, silt-clay mixture with more than 50% of its size fraction smaller than four micrometers.

No sedimentary structures (lamination) are observed in mudstone facies. They are all massive, from thin to medium thick mudstone layers intercalated with other layers with no discordance. Their thicknesses vary between 10cm-15m ranges. This facies is very rich in microfossils, namely with the planktonic foraminifers and ostracoda.

Classifation of McKee and Weer (1952) was applied for mudstone (Figure 29, Figure 30). According to McKee and Weer's classification (1952) based on the quarts percentage within a rock, mudstones along the studied succession were defined as very fine (Samples HEA-104, 109, 111, 113, 115, 116, 118, 120, 122, 124, 126, 129, 130, 132, 134, 135, 137, 138, 144, 146, 148, 150, 152, 5, 14, 21, 22, 24, 27, 30, 32, 33 and 37) and just in few samples as fine (Samples HEA-101, 105, 31, 39, 40 and 42). In studied section there was not any coarse mudstone. Mudstones facies in the studied succession contain an average of 89 % and a

maximum of 96.9 % matrix, which is mainly consist quartz and clay minerals and sometimes stained with iron oxide. Quartz is the most common mineral and observed throughout the succession, in all mudstone facies (Appendix B). Quartz grains comprise of average of 6.13 % and their percentage value ranges between 1.2-18.3%, but mostly they are above 3% (Appendix B). At the lower mudstone layers they have higher values than in the upper layers, they show general decrease towards the top of the succession. Second most common mineral in mudstone facies is muscovite mineral. They are observed mostly in all mudstone layers and their value ranges between 0.1-2.1% (Appendix B). Their percentage does not show any change along the succession. Mudstone also is very rich with bioclasts, namely with planktonic and benthonic foraminifers. Bioclasts comprise of average of 4 % and their percentage value ranges between 0.4-14.2%, but mostly they are above 3% (Appendix B).

Quartz content	Mudrocks	
	fissile	non-fissile
>40% quartz	flaggy siltstone	massive siltstone
30-40% quatz	very coarse shale	very coarse mudstone
20-30% quartz	coarse shale	coarse mudstone
10-20% quartz	fine shale	fine mudstone
<10% quartz	very fine shale	very fine mudstone

Figure 29. McKee and Weir classification based on the amount of quartz components within a mudrock (1952).

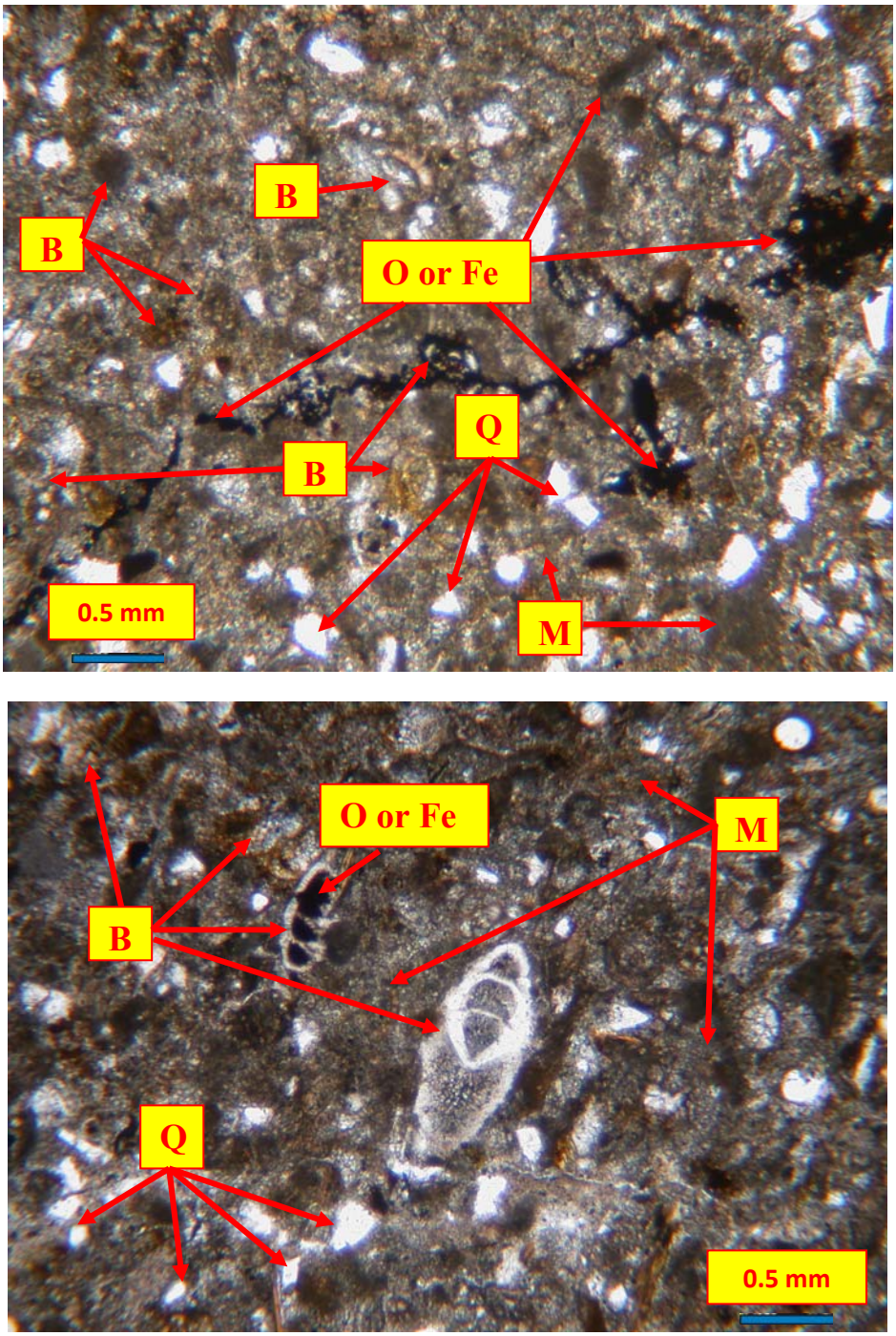

Figure 30. Photomicrographs of the mudstone, (M-matrix, O or Fe-oil impregnation or Fe, Q-quartz, B-benthonic foraminifers), (HEA-33).

4.1.3 Marls

Hubbard *et al*. (1990) define marl as a soft, loose, earthy, material that consists of varying amounts of calcium carbonate, clay and silt size material. Potter *et al*. (2005) also defines marl as fine grained sediment and rock that is composed of 50% or more carbonate. Pettijohn (1957) indicates that marl is an old term loosely applied to a variety of materials, most of which occurs as loose, earthy deposits consisting chiefly of an intimate mixture of clay and calcium carbonate, formed under marine conditions, specifically an earthy substance containing 35-65% clay and 65-35% carbonate.

Marls are the most abundant lithofacies in the studied succession (samples HEA-106, 107, 108, 112, 114, 117, 128, 136, 139, 140, 141, 142, 143, 145, 147, 149, 151, 153, 6, 7, 9, 10, 11, 12, 13, 15, 19, 20, 23, 25, 26, 28, 34, 35, 36, 38, 43, 45, 50) and contains an average of 85% of matrix. Bioclasts constitute less than 39% and an averaging 12.44% of the rock volume. Silt to clay size quartz fragments are constituting 0.1-5.2% of the rock volume (Appendix B). This facies was easily recognized in the field work. They are mainly yellowish and even sometimes light to dark grey colored, containing mainly clay, silt size materials and bioclasts (Figure 31, Appendix B). This facies as marl was recognized in the field by using HCl acid for proving its calcium carbonate content (Appendix B).

4.1.4 Sandstones

Sandstones in studied section (samples HEA-102, 103) were classified as litharenite by using Pettijohn *et al*. (1987) classification (Figure 32; Appendix - B). The classification scheme is based on a triangular diagram with end members of quartz (Q), feldspar (F) and rock fragments (L). Sandstones are divided into two major groups based on relative amount of grains and matrix, that is, whether the sandstones are composed of grains only, the *arenites*, or contain more than 15% matrix, forming the *wackes*. Litharenite is applied where the rock - fragments content exceeds 25% and is greater than feldspar as in our case (samples HEA-102 and HEA-103, Appendix B).

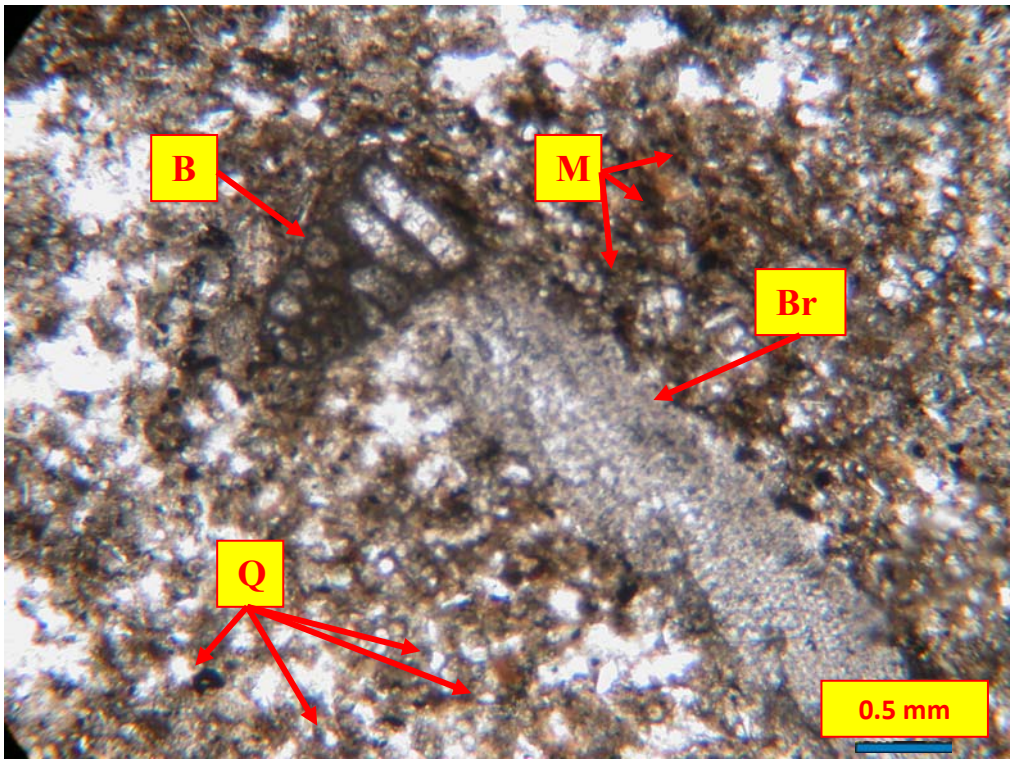

Figure 31. Photomicrograph of the marl (wackestone), (M-matrix, Q-quartz, B-benthonic foraminifers, Br-bryozoan fragment), (HEA-106).

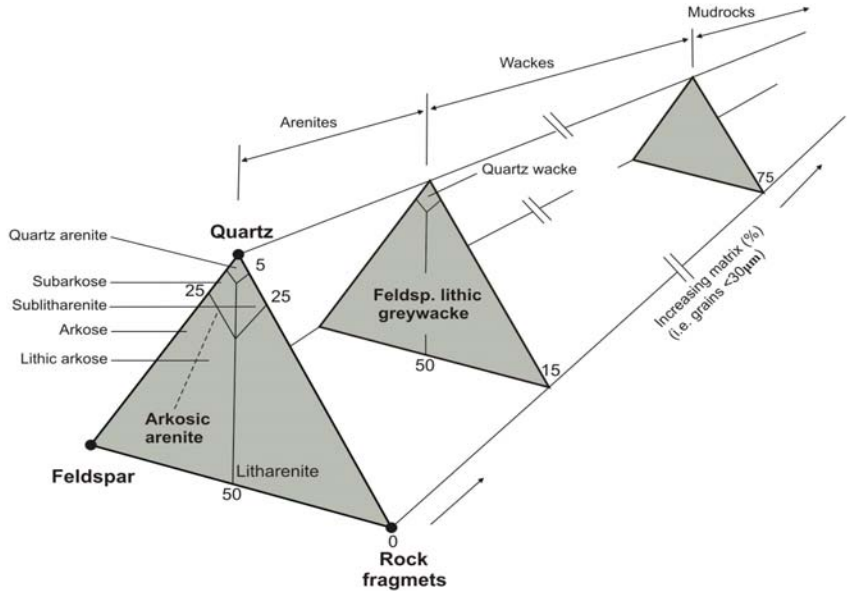

Figure 32. Classification of sandstones after Pettijohn *et al*. (1987).

Minerals or mineral groups, identified in the sandstones, are quartz (polycrystalline was common with minor monocrystalline), calcite (mainly as cement), feldspar and mica. The quartz component of these 2 samples is an average of 30.75% and a maximum of 40.5% and dominated by mainly polycrystalline and some monocrystalline quartz showing straight extinction (Appendix B). The grains are sub-angular to angular with angularity increasing from sample HEA-102 to HEA-103. Mica minerals are dominated by biotite and muscovite which contains an average 0.6% and maximum 0.9% (Figure 33, Figure 34, Appendix B). Plagioclase feldspar comprises the majority of the feldspar component which contains an average 2.2% and maximum 3% (Figure 35). The carbonate cement is a calcite comprising an average 10.15% of the whole rock volume (Figure 33, Figure 34, Figure 35). The rock fragments are comprising an average 49.15% and maximum 63.3% (Figure 33, Figure 34, Figure 35, Appendix B).

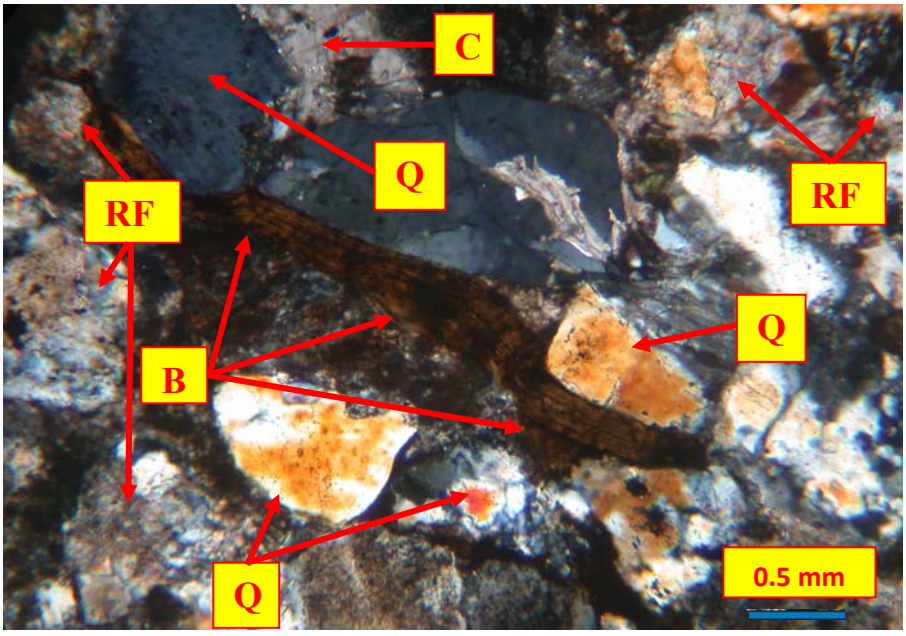

Figure 33. Photomicrographs of sandstone (B – biotite, RF-rock fragments, C-calcite cement, Q- quartz, HEA – 102).

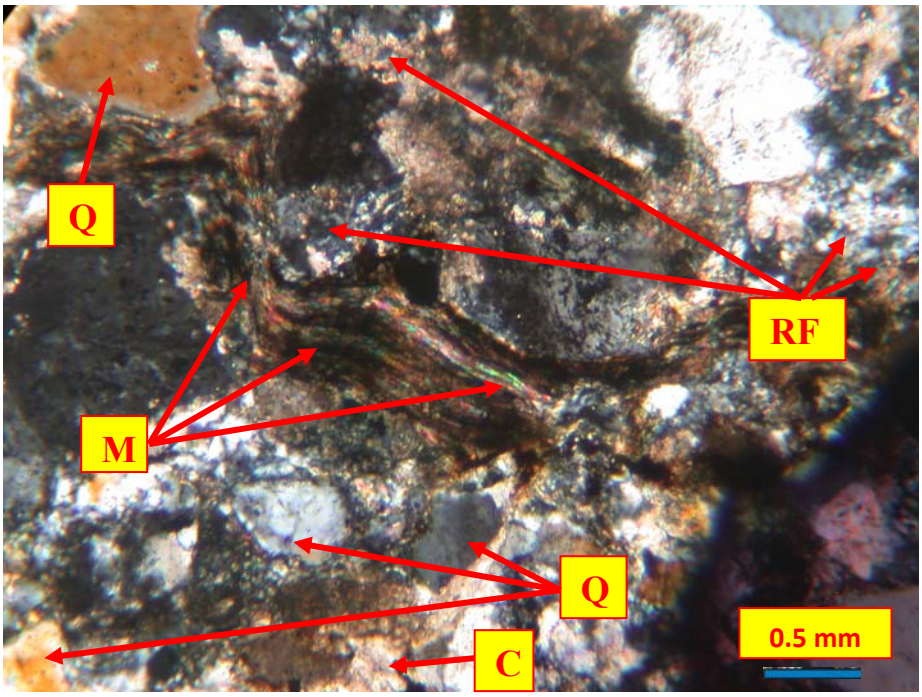

Figure 34. Photomicrographs of sandstone (M – muscovite, RF-rock fragments, C-calcite cement, Q- quartz, HEA – 102).

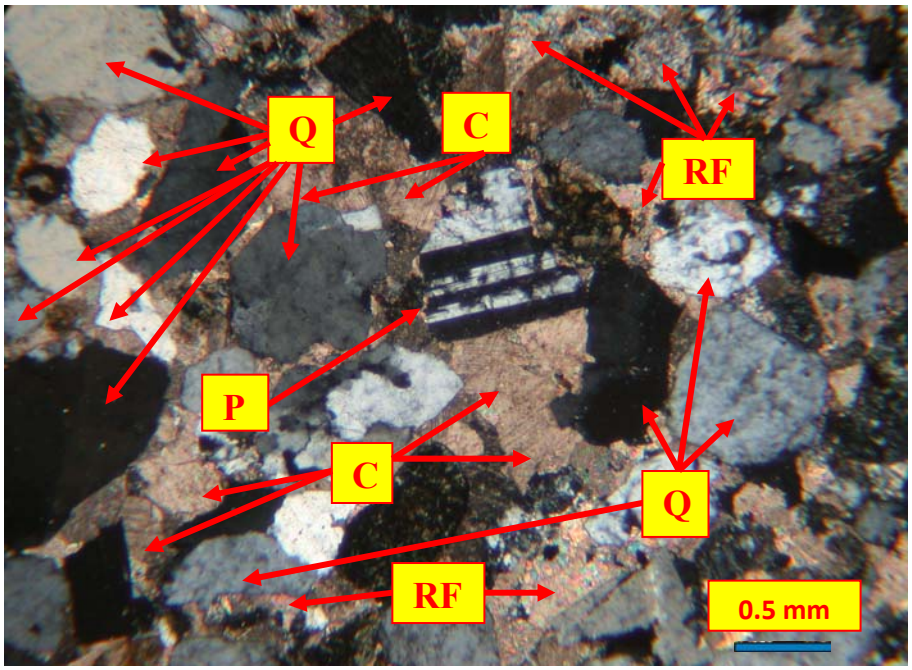

Figure 35. Photomicrographs of sandstone (P – plagioclase, RF-rock fragments, C-calcite cement, Q- quartz, HEA – 103).

To infer the tectonic setting of the basin and source rocks the modal compositions can be used for the sandstone samples (Dickinson and Suczek, 1979). Thin-section analysis of two sandstone samples (HEA-102 and HEA-103) shows that they are mainly composed of polycrystalline quartz, rock fragments and minor quantity of feldspars. The percentages of these grains were plotted on a triangular diagram of Dickinson (1985) (Figure 36), which is a plot of Qm (monocrystalline quartz), F (total feldspar), Lt (total lithic fragment), include Qp (polycrystalline quartz) with lithic grains (Figure 36). The results of the samples fall into section related recycled orogen terranes. It should be noted that precise results can be only obtained by measuring at least 300 samples from different places within one layer.

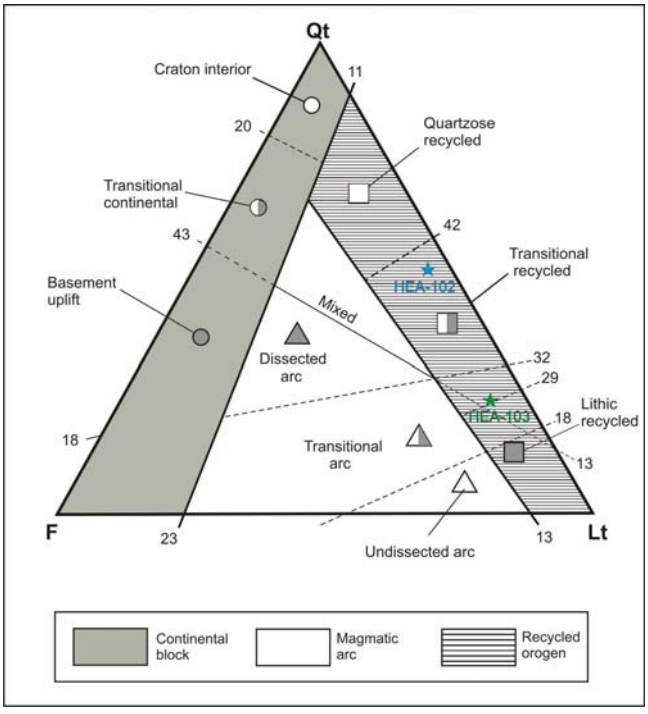

HEA-102	
Quartz	40,5%
Rock fragments	35%
Cement (Calcite)	9,8%
Plagioclase	1,4%
Matrix	11,4%
Muscovite	0,9%
Biotite	0,7%
HEA-103	
Quartz	21%
Rock fragments	63,3%
Cement (Calcite)	10,5%
Plagioclase	3%
Matrix	0,8%
Muscovite	0,7%
Biotite	0,4%

Figure 36. Triangular diagram showing average compositions of sand derived from different provenance terranes (after Dickinson, 1985).

4.2 Quantitative Analysis

In order to bring up the response of microfossils to sedimentary cyclicity, the relative abundances of all planktonic, benthonic foraminifers and ostracod individuals were collected and counted from each samples (20 gr). The planktonic, benthonic foraminifers and ostracods start to decrease on K/P boundary from the sample HEA-101 to 109 which correspond to transition from the transgressive system tract (TST) to the highstand system tract (HST) (Figure 37, Appendix A). The number of individuals of these microfossils drastically decreases towards the K/P boundary because of the mass extinction event. Planktonic foraminifers are very abundant in the Creataceous samples HEA-101, 104 and 105, which corresponds to *Pseudoguembelina hariaensis* Zone. Abrupt change in amount of planktonic foraminifers can be seen in the first Paleocene samples HEA-106, 107 and 108, this interval corresponds to the Pα Zone (Figure 37, Appendix A). Benthonic foraminifers and ostracods also drastically decrease in the first Paleocene samples HEA-106, 107 and 108 (Figure 37, Appendix A). Increasing of planktonic foraminifers starts firstly from the sample HEA-115, which corresponds to the TST (the P1b Zone) (Figure 37, Appendix A). Up in the succession the amount of foraminifers again starts to decrease from the samples HEA-117 to 131. After this level from the sample HEA-132 to HEA-138 the amount of planktonic and benthonic foraminifers starts to increase drastically, this interval corresponds to the P2 Zone (Figure 37, Appendix A). Increasing in the number of ostracoda shells can be seen in samples HEA-117, 118, 121, 123 and 137, this interval corresponds to the P2 Zone. In general it was revealed that after the mass extinction event, the relative abundance of planktonic, benthonic foraminifers and ostracods starts to increase mainly in the P2 Zone.

According to obtained data it was possible to reveal that the average abundance and number of planktonic individuals increase in the TST and decrease in the HST (Figure 37). The maximum relative abundance of planktonic foraminifers was observed in the sample HEA-115 which is the TST and minimum in the sample HEA-121 which is the HST. It should be noted that benthonic foraminifers and ostracods in general showed different trend of response to sedimentary cyclicity in the Haymana basin.

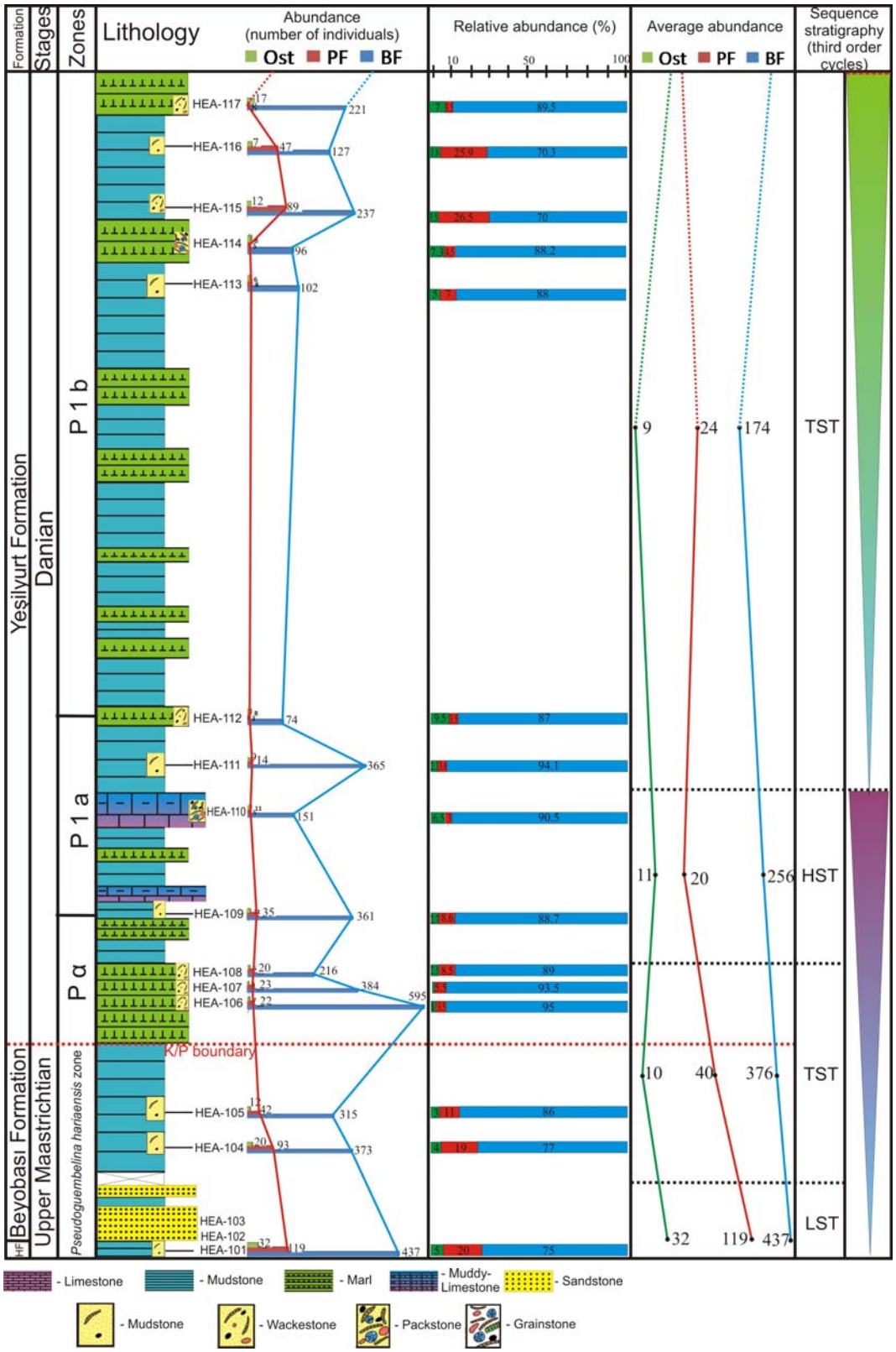

Figure 37. Quantitative analysis of planktonic (PF), benthonic foraminifers (BF) and ostracods (Ost) along studied succession.

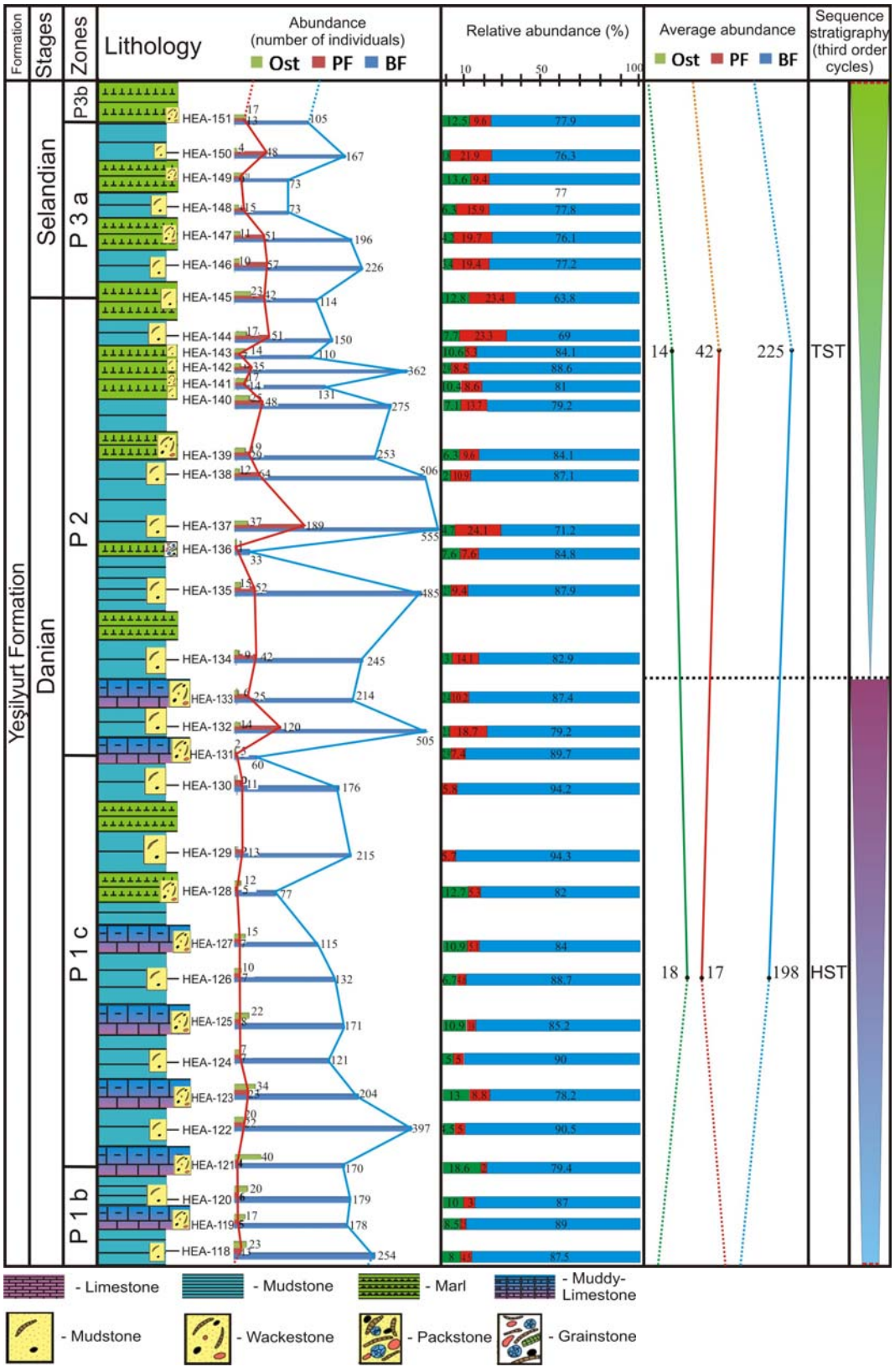

Figure 37. Continued.

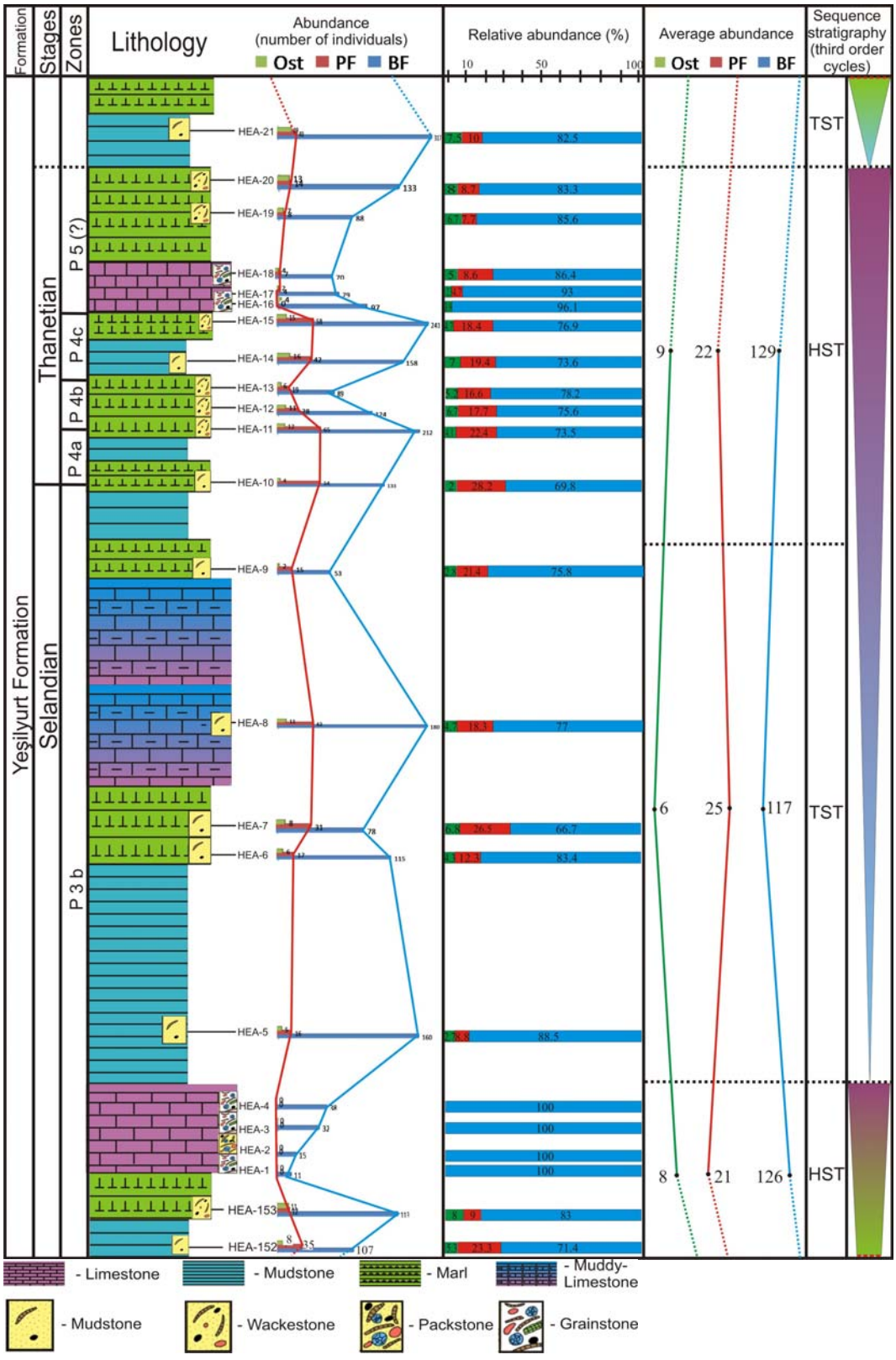

Figure 37. Continued.

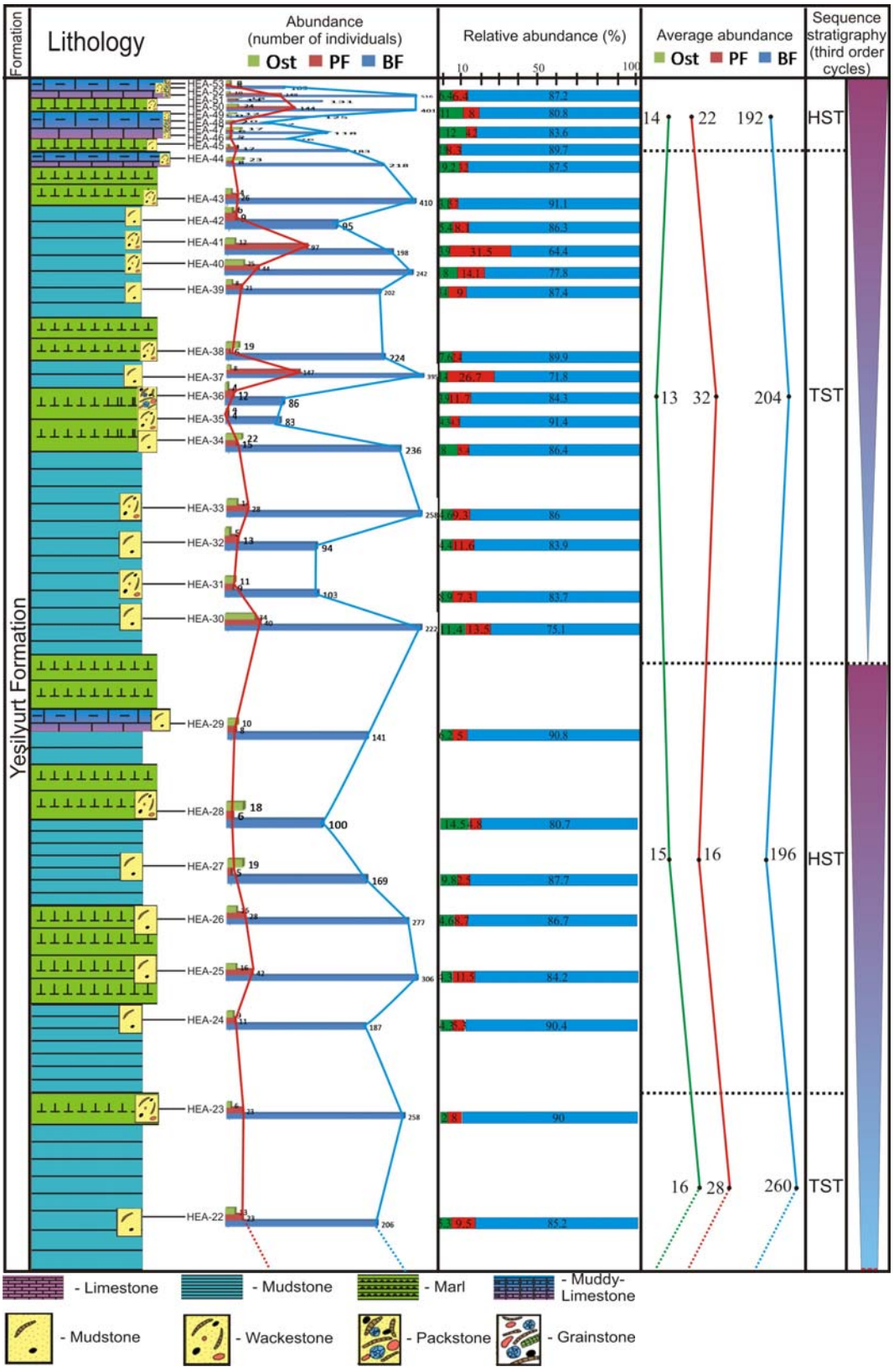

Figure 37. Continued.

For instance average abundance of benthonic foraminifers and ostracods at the lower part of the measured section increases in the HST and decreases in the TST (the P1b Zone, Figure 37). However, up in the studied succession the opposite results have been recorded. Ostracods in the TST are represented mainly by the pelagic forms, the wall of their shells is thin, fragile and ornamented (Figure 38). In the HST shallow-water (neritic) ostracods mainly represented by a robust and thick walled shells without any obvious ornamentation (Figure 39). Benthonic foraminifers in the HST are mainly represented by a miliolid type forms (Figure 40). Echinoid spines are also abundant along with benthonic foraminifers and ostracods in the HST (Figure 40).

As mentioned before the petrographical analysis along the succession was also carried out and the studied section mainly consists of mudstone, wackestone and packstone microfacies alternation. It was revealed that the relative abundance of planktonic foraminifers increases in the mudstone microfacies and decrease in the wackestone, packstone, grainstone and boundstone microfacies. However, the relative amount of benthonic foraminifers and ostracods mainly increases in the wackestone, packstone and grainstone microfacies and decreases in the mudstone microfacies (Figure 37).

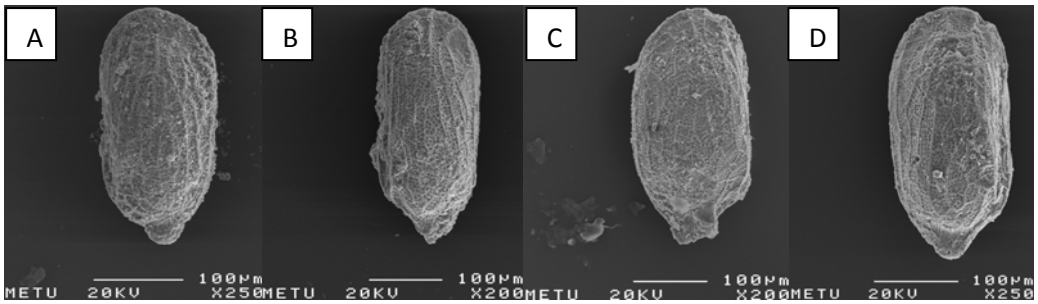

Figure 38. Photomicrograph of deep water (pelagic) ostracods (A: HEA-122; B: HEA-132; C: HEA-135; D: HEA-137).

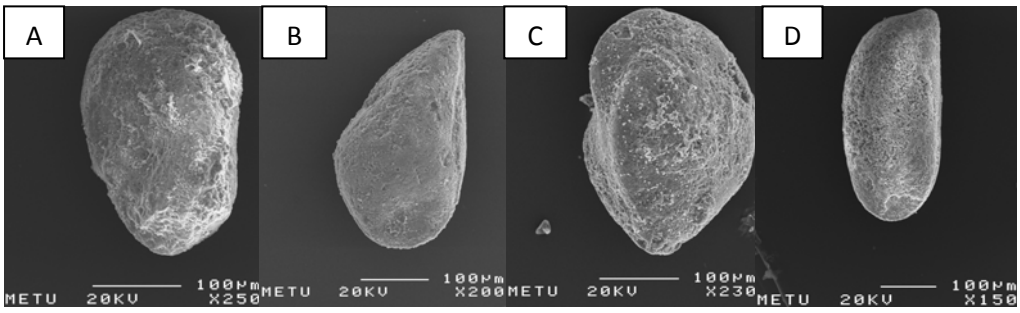

Figure 39. Photomicrograph of the shallow water ostracods (A: HEA-110; B: HEA-117; C: HEA-131; D: HEA-142).

Figure 40. Photomicrograph of the benthonic shallow-water foraminifers and echinoid spine (A and B: Miliolid forms, HEA-110; C: echinoid spine, HEA-127).

CHAPTER 5

SYSTEMATIC PALEONTOLOGY

This chapter includes a detailed taxonomic account of all the planktonic foraminifers observed during this study. Since most species are well documented in the literature, this taxonomy section was kept to a minimum. The taxonomy of the Cretaceous species has been carried out by considering the definitions from the taxonomic literature, such as Bolli *et al*. (1957), Postuma (1971), Robaszynski *et al*. (1984), Loeblich and Tappan (1988), Nederbraght (1991), Premoli Silva and Verga (2004). For the Paleocene species, the study of Postuma (1971) and the Atlas of Paleocene Planktonic Foraminifera (Olsson *et al*., 1999) have been used. The species characteristics that have been observed in this study will be explained and discussed as remarks for each form separately. There are some problems in the recognition of the some species because of absence of some characteristic morphological and wall-structural features such as pustules, costae, microperforations, cancelate structure, apertural structures (tegilla, portici, apertural flanges, etc.). These features could not be recognized easily because of poor preservation of forms.

For each species, the species epithet is followed by the original author(s) who propoesed the preferred combination. References to original descriptions and illustrations, and consequent changes of the taxonomic position and one or more reference(s) to illustrations that most closely approximate the species concepts used in this study are given. Range of the species are given from the literature. The term occurrence is used for stratigraphic distribution data in the studied section.

In the classification of the planktonic foraminifers; wall structure, wall composition, chamber architecture, presence or absence of keel(s) and

ornamentations and position of primary aperture designate the subfamily level. The category of protection of primary aperture (portici or tegilla), degree of trochospire and presence or absence of adumbilical ridges is used in genera descriptions, whereas shape of chambers, number of chambers in last whorl, rate of increase of chamber size, diameter of umbilicus, degree of peripheral angle, symmetry of profile, width of keel band, character of spiral suture and inflation of chambers are needed for identification of the species. In the present study, based on the criteria above, 29 genera and 67 species have been identified (Appendix C).

Order Foraminiferida EICHWALD, 1830

Suborder Globigerinina DELAGE and HEROURARD, 1896

Superfamily Globotruncanacea BROTZEN, 1942

Family Globotruncanidae BROTZEN, 1942

Subfamily Abathomphalinae PESSAGNO, 1967

Genus *Globotruncanella* REISS, 1957

Type species: *Globorotalia pschadae* KELLER, 1946

***Globotruncanella minuta* KARON & GONZALEZ DONOSO, 1984**

Pl. 1, fig. 1

1984 *Globotruncanella minuta* KARON & GONZALEZ DONOSO, p. 266, pl. 43, figs. 5-8.

Remarks:

This form can be identified by having 4-5 chambers in its last whorl. Chambers increase rapidly in size as added. This is a biconvex form and periphery is broadly rounded. Main aperture extraumbilical-umbilical. Sutures strongly depressed. Chambers is very low trochospired, nearly flat. The main difference of

this species from *Globotruncanella pschadae* is the absence of keel and broadly rounded chambers.

Stratigraphic range: From middle to upper Maastrichtian (Robaszynski *et al.*, 1984).

Occurrence: It has been recognized from sample HEA-101 to HEA-105 (the lower part of the studied section, latest Maastrichtian).

***Globotruncanella pschadae* KELLER, 1946**

Pl. 1, fig. 2

1946 *Globorotalia pschadae* KELLER, p. 99, pl. 2, figs. 4-6.

1984 *Globotruncanella pschadae* KELLER, ROBASZYNSKI *et al*., p. 267, pl. 44, figs. 7.

1998 *Globotruncanella havanensis* KELLER, NEDERBRAGT, p. 401, pl .2, fig. 5.

2000 *Globotruncanella pschadae* KELLER, ROBASZYNSKI *et al*., p. 481, p. 20, fig. 14.

2004 *Globotruncanella pschadae* KELLER, PREMOLI-SILVA and VERGA, p. 114, p. 44, figs. 3, 4.

Remarks:

This form can be identified by having 4-5 chambers in its last whorl. Chambers increase rapidly in size as added. Chambers is very low trochospired and actually this is a biconvex form. Periphery angular with a keel. Main aperture extraumbilical-umbilical.

Stratigraphic range: From middle to upper Maastrichtian (Robaszynski *et al.*, 1984).

Occurrence: It has been recognized from sample HEA-101 to HEA-105 (the lower part of the studied section, latest Maastrichtian).

Subfamily Globotruncaninae BROTZEN, 1942

Genus *Contusotruncana* KORCHAGIN, 1982

Type species: *Pulvinulina arca contusa* CUSHMAN, 1926

Contusotruncana fornicata PLUMMER, 1931

Pl. 1, fig. 3

1931 *Contusotruncana fornicata* PLUMMER, p. 130, pl. 13, figs. 4 a-c.

1984 *Rosita fornicata* PLUMMER, ROBASZYNSKI *et al.*, p. 251, pl. 38, figs. 1-4.

1987 *Rosita fornicata* PLUMMER, ÖZKAN and ALTINER, p.275, pl. 4, figs. 1-3; p.277, pl. 5, fig 7.

1992 *Contusotruncana fornicata* PLUMMER, NORRIS, p. 171, pl. 2, figs. d-g.

1998 *Contusotruncana fornicata* PLUMMER, NEDERBRAGT, p. 399, pl. 1, fig. 3.

2000 *Contusotruncana fornicata* PLUMMER, ROBASZYNSKI *et al.*, p. 481, p. 20, fig. 3.

Remarks:

This form can be identified by having 4-6 crescentic chambers in its last whorl. Chambers increase slowly in size. This species has a moderately high (sometimes low) trochospiral coiling. It can be spiroconvex or biconvex in appearance. In this study, mostly the spiroconvex forms are observed and in these cases, *Contusotruncana fornicata* resembles *Globotruncana arca* in the lateral view. However, from the spiral and umbilical sides, these two forms can simply

be distiguished by their chamber shape and numbers. Here, in contrast to *Globotruncana arca*, the chambers of this form are clearly more elongated in spiral view. Also the lower chamber number (mostly 4 or 6) of *Contusotruncana fornicata* in its final whorl and its more closely spaced keels are other differences from *Globotruncana arca*.

Stratigraphic range: From the top of the Upper Santonian to the Maastrichtian (Robaszynski *et al.*, 1984).

Occurrence: It has been recognized from sample HEA-101 (the lower part of the studied section, latest Maastrichtian).

Genus *Gansserina* CARON *et al.*, 1984

Type Species: *Globotruncana gansseri* BOLLI, 1951

***Gansserina gansseri* BOLLI, 1951**

Pl. 1, fig. 4, 5

1951 *Globotruncana gansseri* BOLLI, pl. 35, figs. 1-3.

1984 *Gansserina gansseri* BOLLI, ROBASZYNSKI *et al.*, p. 295, pl. 52, figs. 1-4.

1987 *Gansserina gansseri* BOLLI, ÖZKAN and ALTINER, p.275, pl. 4, figs. 10-12.

1992 *Gansserina gansseri* BOLLI, NORRIS, p.169, pl. 1, figs. k-m.

1998 *Gansserina gansseri* BOLLI, CHUNGKHAM and JAFAR, p. 75, pl. 1, figs. 4 a-c.

1999 *Gansserina gansseri* BOLLI, ÖZKAN-ALTINER and ÖZCAN, p. 294, pl. 2, fig. 8, 10.

2000 *Gansserina gansseri* BOLLI, ROBASZYNSKI *et al.*, p. 473, p. 16, fig. 1-3; p. 479, p. 19, fig. 13.

2004 *Gansserina gansseri* BOLLI, CHACON *et al*., p. 589, fig. 3 D; p.590, fig. 4 G, H.

2005 *Gansserina gansseri* BOLLI, OBAIDALLA, p. 215, pl. 1, fig. 1.

Remarks:

This form can be identified by having 4-8 petaloid chambers in the final whorl. Chambers increase gradually in size and there are pustules developed on its surface. Test profile is asymmetrical and has one peripheral keel throughout the final whorl. It is plano-convex in appearance.

Stratigraphic range: Through Maastrichtian (Robaszynski *et al.*, 1984).

Occurrence: It has been recognized only from sample HEA-101 (the lower part of the studied section, latest Maastrichtian).

Gansserina wiedenmayeri GANDOLFI, 1955

Pl. 2, fig. 1

1955 *Globotruncana wiedenmayeri* GANDOLFI, p. 71, pl. 7, fig. 4

1955 *Globotruncana wiedenmayeri magdalenensis* GANDOLFI, p. 72, pl. 8, fig. 2

1966 *Globotruncana bahije* GANDOLFI, EL NAGGAR, p. 53, pl. 5, fig. 3

Remarks:

This form can be identified by having 5-8 petaloid chambers in its last whorl. Chambers increase gradually in size. This species is low trochospiral form. Test profile is asymmetrical. There are two peripheral keels on the last chambers of the final whorl. This feature let us to distinguish the *Gansserina wiedenmayeri* from *Gansserina gansseri*.

Stratigraphic range: From the Middle to Upper Maastrichtian (Robaszynski *et al.*, 1984).

Occurrence: It has been recognized from sample HEA-101 (the lower part of the studied section, latest Maastrichtian).

Genus *Globotruncana* CUSHMAN, 1927

Type species: *Pulvinulina arca* CUSHMAN, 1926

Globotruncana aegyptiaca NAKKADY, 1950

Pl. 2, fig. 2, 3

1950 *Globotruncana aegyptiaca* NAKKADY, p. 690, pl. 80, fig. 20.

1984 *Globotruncana aegyptiaca* NAKKADY, ROBASZYNSKI *et al*., p. 179, pl. 2, figs. 1–6; p. 181, pl. 3, figs. 1–4.

1984 *Globotruncana aegyptiaca* NAKKADY, ÖZKAN and ALTINER, p. 269, pl. 1, figs. 13-15.

1988 *Globotruncana aegyptiaca* NAKKADY, KELLER, p. 250, pl.1, fig. 6.

1992 *Globotruncana aegyptiaca* NAKKADY, NORRIS, p.181, pl. 7, figs. c, d.

1998 *Globotruncana aegyptiaca* NAKKADY, NEDERBRAGT, p. 399, pl .1, figs. 6, 7; p. 401, pl. 2, fig. 1.

1999 *Globotruncana aegyptiaca* NAKKADY, ÖZKAN-ALTINER and ÖZCAN, p. 292, pl. 1, fig. 11.

2000 *Globotruncana aegyptiaca* NAKKADY, ARENILLAS *et al.*, p. 43, pl. 1, fig. 11, 12.

2000 *Globotruncana aegyptiaca* NAKKADY, ROBASZYNSKI *et al.*, p. 465, p. 12, fig. 1, 2; p. 479, p. 19, fig. 12.

2004 *Globotruncana aegyptiaca* NAKKADY, CHACON *et al*., p. 589, fig. 3 E.

Remarks:

Globotruncana aegpytiaca has from 3 to 5 chambers in the final whorl. It is differentiated from the other species of *Globotruncana* by having relatively lower number of chambers. Chambers increase rapidly in size. It has two equally developed keels throughout the final whorl. Low trochospire spirally coiled, nearly flat resulting in a strongly asymmetrical test (spiral side is almost plane).

Stratigraphic range: Through Maastrichtian (Robaszynski *et al.*, 1984).

Occurrence: It has been recognized from sample HEA-101 to HEA-104 (the lower part of the studied section, latest Maastrichtian).

***Globotruncana arca* CUSHMAN, 1926**

Pl. 2, fig. 4

1926 *Globotruncana arca* CUSHMAN, p. 23, pl.3, fig.1.

1984 *Globotruncana arca* CUSHMAN, ROBASZYNSKI *et al.*, p. 183, pl. 3, figs. 1–3.

1988 *Globotruncana arca* CUSHMAN, KELLER, p. 250, pl.1, figs. 7, 8, 11.

1992 *Globotruncana arca* CUSHMAN, NORRIS, p. 175, pl. 4, fig. j, k; p. 181, pl. 7, fig. 8.

1998 *Globotruncana arca* CUSHMAN, NEDERBRAGT, p. 401, pl .2, fig. 2 (not 3, 4).

2000 *Globotruncana arca* CUSHMAN, ROBASZYNSKI *et al.*, p. 481, p. 20, fig. 4.

2004 *Globotruncana arca* CUSHMAN, CHACON *et al*., p. 589, fig. 3 F.

2005 *Globotruncana arca* CUSHMAN, OBAIDALLA, p. 217, pl. 2, fig. 1, 2.

Remarks:

In the final whorl this species has 5 to 8 chambers. Chambers increase slowly to moderately in size. Chambers are highly trochospired. This species is

characterized by wide imperforate peripheral band and widely spaced keels. By this property, detection of this form is very easy. This form has a wide stratigraphic range and in our samples it is observed only at the base of measured section (Uppermost Maastrichtian).

Stratigraphic range: From Campanian to Maastrichtian (Robaszynski *et al.*, 1984).

Occurrence: It has been recognized from sample HEA-101 (the lower part of the studied section, latest Maastrichtian).

Globotruncana linneiana D'ORBIGNY, 1839

Pl. 2, fig. 5

1839 *Rosalina linneiana* D'ORBIGNY, p. 101, pl 5, figs. 10-12.

1984 *Globotruncana linneiana* ROBASZYNSKI *et al*., p. 201, pl. 13, figs. 1–4; p. 203, pl. 14, figs. 1-5.

1987 *Globotruncana linneiana* ÖZKAN and ALTINER, p.271, pl. 2, figs. 1– 3.

1992 *Globotruncana linneiana* NORRIS, p.173, pl. 3, figs. c, d; p. 181, pl. 7, fig.a.

2000 *Globotruncana linneiana* ROBASZYNSKI *et al.*, p. 465, p. 12, fig. 4.

2001 *Globotruncana linneiana* PETRIZZO, p. 854, fig. 9. 6 a-c.

2004 *Globotruncana linneiana* PREMOLI-SILVA and VERGA, p. 109, p. 39, figs. 2-4.

Remarks:

Globotruncana linneiana has from 5 to 7 chambers in the final whorl. Chambers increase slowly in size and very low trochospired, nearly flat. It is a very distinctive form with its box-like shape due to very wide double keels and

chambers that are not inflated. This species has two peripheral keels on all the chambers of the final whorl, separated by a wide imperforate band.

Stratigraphic range: From Santonian to Maastrichtian (Robaszynski *et al.*, 1984).

Occurrence: It has been recognized from sample HEA-101 (the lower part of the studied section, latest Maastrichtian).

Globotruncana mariei BANNER and BLOW, 1960

Pl. 3, fig. 1; Pl. 7, fig. 2

1960 *Globotruncana mariei* BANNER and BLOW, pl. 11, figs.6 a-c.

1984 *Globotruncana mariei* BANNER and BLOW, ROBASZYNSKI *et al*., p. 205, pl. 15, figs. 1–6.

1987 *Globotruncana mariei* BANNER and BLOW, ÖZKAN and ALTINER, p. 271, pl. 2, figs. 13–15.

2004 *Globotruncana mariei* BANNER and BLOW, PREMOLI-SILVA and VERGA, p. 110, p. 40, figs. 1-3.

Remarks:

This species also has a low number of chambers from 4 to 5 in the final whorl. Chambers increase moderately in size. However, this species is distinguished by biconvex test from *Globotruncana aegyptiaca* and by the presence of two keels separated by a rather narrow imperforate band which present on all the chambers of the final whorl. Chambers low trochospired, test shape almost symmetrical in shape.

Stratigraphic range: From Santonian to Maastrichtian (Robaszynski *et al.*, 1984).

Occurrence: It has been recognized from sample HEA-101 (the lower part of the studied section, latest Maastrichtian).

Genus *Globotruncanita* REISS, 1957

Type species: *Rosalina stuarti* DE LAPPARENT, 1918

Globotruncanita conica WHITE, 1928

Pl. 3, fig. 2, 3

1928 *Globotruncana conica* WHITE, p. 285, pl. 38, figs. 7 a-c.

1984 *Globotruncanita conica* WHITE, ROBASZYNSKI *et al.*, p. 227, pl. 26, figs. 1–3.

1991 *Globotruncanita conica* WHITE, LONGORIA and VON FELDT, p. 223, pl. 2, figs. 1-6; p. 237, pl. 9, figs. 12-15; p. 239, pl. 10, fig. 1, 3, 9; p. 241, pl. 11, figs. 11, 16.

2004 *Globotruncanita conica* WHITE, CHACON *et al*., p. 589, fig. 3 J.

2005 *Globotruncanita conica* WHITE, OBAIDALLA, p. 217, pl. 2, figs. 4, 5.

Remarks:

This species has chambers from 6 to 9 in the final whorl. Chambers increase slowly in size. It can be differentiated by its single keel throughout the final whorl, its circular outline and conical form because of its highly trochospiral test. Test strongly convex, trochospire high, umbilical side almost flat.

Stratigraphic range: From Middle to Upper Maastrichtian (Robazynski *et al.*, 1984).

Occurrence: It has been recognized from sample HEA-101 to HEA-105 (the lower part of the studied section, latest Maastrichtian).

***Globotruncanita stuartiformis* DALBIEZ, 1955**

Pl. 3, fig. 4

1955 *Globotruncana elevata* (BROTZEN) subsp. *stuartiformis* DALBIEZ, p. 169, fig. 10 a-c.

1984 *Globotruncanita stuartiformis* DALBIEZ, ROBASZYNSKI *et al.*, p. 239, pl. 32, figs. 1–4.

1987 *Globotruncanita stuartiformis* DALBIEZ, ÖZKAN and ALTINER, p.273, pl. 3, figs. 7-9.

1991 *Globotruncanita stuartiformis* DALBIEZ, LONGORIA and VON FELDT, p. 231, pl. 6, figs. 1-12; p. 237, pl. 9, figs. 1-5; p. 239, pl. 10, figs. 2, 5, 8, 11, 16.

1992 *Globotruncanita stuartiformis* DALBIEZ, NORRIS, p.169, pl. 1, figs. c, d.

1998 *Globotruncanita stuarti* DALBIEZ, NEDERBRAGT, p. 403, pl .3, fig. 3, 4.

2000 *Globotruncanita stuartiformis* DALBIEZ, ROBASZYNSKI *et al.*, p. 467, p.13, fig.2; p. 479, pl.19, fig.6.

Remarks:

Test has 5-7 chambers in the final whorl. Chambers increase slowly in size. Chambers are moderately high trochospired and that is why there is a slightly asymmetrical test shape in edge view. It has also one peripheral keel throughout the final whorl. It is more abundant than *Globotruncanita conica* in our samples.

Stratigraphic range: From Uppermost Santonian to the end of Maastrichtian (Robaszynski *et al.,* 1984).

Occurrence: It has been recognized from sample HEA-101 to HEA-105 (the lower part of the studied section, latest Maastrichtian).

Family Rugoglobigerinidae SUBBOTINA, 1959

Genus Archaeoglobigerina PESSAGNO, 1967

Type species: *Archaeoglobigerina blowi* PESSAGNO, 1967

Archaeoglobigerina blowi PESSAGNO, 1967

Pl. 4, fig. 1

1967 *Archaeoglobigerina blowi* PESSAGNO, p. 316, pl. 59, figs. 5-7.

1984 *Archaeoglobigerina blowi* PESSAGNO, ROBASZYNSKI *et al.*, p. 277, pl. 47, figs. 1-2.

1992 *Archaeoglobigerina blowi* PESSAGNO, NORRIS, p. 173, pl. 3, fig. e.

2000 *Archaeoglobigerina blowi* PESSAGNO, ROBASZYNSKI *et al.*, p. 481, p. 20, fig. 10.

2004 *Archaeoglobigerina blowi* PESSAGNO, PREMOLI-SILVA and VERGA, p. 73, p. 3, figs. 1, 2.

Remarks:

Test has 4 chambers in the final whorl and they are low to flat trochospired. This form resembles *Rugoglobigerina macrocephala* at first sight. However, the pustulose structure of this form separates it from the highly costate *Rugoglobigerina macrocephala*.

Stratigraphic range: From Upper Coniacian to the end of Maastrichtian (Robaszynski *et al.,* 1984).

Occurrence: It has been recognized from sample HEA-101 (the lower part of the studied section, latest Maastrichtian).

Genus Rugoglobigerina BRONNIMANN, 1952

Type species: *Globigerina rugosa* PLUMMER, 1927

***Rugoglobigerina hexacamerata* BRONNIMANN, 1952**

Pl. 4, fig. 2

1952 *Rugoglobigerina hexacamerata* BRONNIMANN, pl. 2, figs. 10-12.

1955 *Globotruncana hexacamerata subhexacamerata* BRONNIMANN, GANDOLFI, pl. 4, figs. 7.

Remarks:

Test has 6 chambers in the final whorl. Chambers increase slowly in size. Trochospire is low to flat. Main aperture is umbilical.

Stratigraphic range: Through Maastrichtian (Robaszynski *et al.*, 1984).

Occurrence: It has been recognized from sample HEA-101 (the lower part of the studied section, latest Maastrichtian).

***Rugoglobigerina macrocephala* BRONNIMANN, 1952**

Pl. 4, fig. 3

1952 *Rugoglobigerina macrocephala macrocephala* BRONNIMANN, p. 25, pl. 2, figs. 1-3.

1984 *Rugoglobigerina macrocephala* BRONNIMANN, ROBASZYNSKI *et al.*, p. 283, pl. 49, fig. 7.

1988 *Rugoglobigerina macrocephala* BRONNIMANN, KELLER, p. 250, pl.1, fig. 3.

2004 *Rugoglobigerina macrocephala* BRONNIMANN, PREMOLI-SILVA and VERGA, p. 200, p. 130, figs. 1-4.

Remarks:

This form has 4 distinct chambers and they increase in size very rapidly. The last chamber of the form is approximately as large as the rest of whole test. Chambers low to flat trochospired. Surface of chamber highly costate and striations can be easily recognized. Primary aperture is umbilical.

Stratigraphic range: From Middle to Upper Maastrichtian (Robaszynski *et al.*, 1984).

Occurrence: It has been recognized from sample HEA-101 to HEA-104 (the lower part of the studied section, latest Maastrichtian).

Rugoglobigerina milamensis SMITH & PESSAGNO, 1973

Pl. 4, fig. 4

1973 *Rugoglobigerina milamensis* SMITH & PESSAGNO, p. 56, pl. 24, figs. 4-7.

Remarks:

Test has 5-6 chambers in the final whorl and highly trochospired. Chambers increase rapidly in size. Surface of the test covered with thin striations.

Stratigraphic range: From Campanian to Maastrichtian (Robaszynski *et al.*, 1984).

Occurrence: It has been recognized from sample HEA-101 to HEA-104 (the lower part of the studied section, latest Maastrichtian).

Rugoglobigerina rugosa PLUMMER, 1926

Pl. 4, fig. 5

1926 *Globigerina rugosa* PLUMMER, p. 38, pl. 2, fig. 10 a.

1984 *Rugoglobigerina rugosa* PLUMMER, ROBASZYNSKI *et al.,* p. 283, pl. 49, figs. 4, 6.

1988 *Rugoglobigerina rugosa* PLUMMER, KELLER, p. 252, pl. 2, fig. 14.

1992 *Rugoglobigerina rugosa* PLUMMER, NORRIS, p. 177, pl. 5, fig. h, i; p. 181, pl. 7, fig. b.

2004 *Rugoglobigerina rugosa* PLUMMER, CHACON *et al*., p. 590, fig. 4 L.

2005 *Rugoglobigerina rugosa* PLUMMER, OBAIDALLA, p. 217, pl. 2, fig. 3.

Remarks:

Rugoglobigerina rugosa has 4-5 chambers in its last whorl. It is differentiated form other *Rugoglobigerina* with its flatter outline, rapid increase in the chamber size and absence of the spines (Robaszynski *et al.,* 1984). It is very common all along the base of the measured section. Wall of test is macroperforate.

Stratigraphic range: From Campanian to Maastrichtian (Robaszynski *et al.,* 1984).

Occurrence: It has been recognized from sample HEA-101 to HEA-105 (the lower part of the studied section, latest Maastrichtian).

Genus *Trinitella* BRONNIMANN, 1952

Type species: *Trinitella scotti* BRONNIMANN, 1952

***Trinitella scotti* BRONNIMANN, 1952**

Pl. 5, fig. 1

1971 *Rugoglobigerina bronnimanni* EL NAGGAR, p.57, pl. 4, figs. 4-6.

1971 *Rugoglobigerina scotti* EL NAGGAR, BRONNIMANN, p.92-93, figs. 1-4.

1985 *Rugoglobigerina scotti* EL NAGGAR, BRONNIMANN, p.74-75, pl. 34. figs. 7-8.

Remarks:

Test very low trochospiral, arranged in 2-3 whorls, the last whorl consisting of 5-6 chambers. Spiral side almost flat, umbilical side moderately convex; equatorial periphery tabulate. Wall perforate, surface of the chambers strongly rugose (pustules and ridges), except the last one, which is mostly smooth. Chambers of the initial whorls and the first chambers of the last whorl are subglobular, gradually increasing in size, the last chambers becoming flattened on the spiral side and abruptly enlarged, about twice as large as the penultimate ones. Sutures depressed, on the spiral side strongly curved, on the umbilical side relatively straight to slightly curved. Some specimens show elevated sutures between the last chambers on the spiral side, in which case an indistinct pseudo-keel may be present. Umbilicus fairly wide.

Stratigraphic range: Upper Maastrichtian (Robaszynski *et al.*, 1984).

Occurrence: It has been recognized from sample HEA-101 (the lower part of the studied section, latest Maastrichtian).

Superfamily Heterohelicacea CUSHMAN, 1927

Family Heterohelicidae CUSHMAN, 1927

Subfamily Heterohelicinae CUSHMAN, 1927

Genus *Heterohelix* EHRENBERG, 1843

Type species: *Textilaria americana* EHRENBERG, 1843

Heterohelix globulosa EHRENBERG, 1840

Pl. 5, figs. 2, 3

1840 *Heterohelix globulosa* EHRENGERG, p. 135, pl. 4, figs. 2b, 4b, 5b, 7b, 8b.

1938 *Guembelina reussi* EHRENGERG, CUSHMAN, p. 11, pl. 2, figs. 6-9.

1991 *Heterohelix globulosa* EHRENGERG, NEDERBRAGT, p. 347, pl. 2, figs. 1a-2b.

1995 *Heterohelix globulosa* EHRENGERG, DE KLASZ *et al.*, p. 367, pl. 2, fig. 3.

2002 *Heterohelix globulosa* EHRENGERG, LUCIANI, p. 312, pl. 1, fig. 7-10.

2005 *Heterohelix globulosa* EHRENGERG, OBAIDALLA, p. 215, pl. 1, fig. 10.

Remarks:

Heterohelix globulosa is the simplest form of the genus *Heterohelix* with its globular chambers. The globular chambers increase gradually in size, except for the late chambers, which increase more rapidly. Faint costae are present on all chambers. In the description of Nederbragt (1991), it is said that this form may have an initial coiling part, but in the samples of the present study, such an observation hasn't been made. In our studied section, this form is observed in top part of the Maastrichtian.

Stratigraphic range: From Turonian to Maastrichtian (Nederbragt, 1991).

Occurrence: It has been recognized in the lower (Uppermost Maastrichtian) part of the studied section (from sample HEA-101 to HEA-105).

Heterohelix labellosa NEDERBRAGT, 1991

Pl. 5, fig. 4

1991 *Heterohelix labellosa* NEDERBRAGT, p. 347, pl. 2, figs. 4a-c, 3, 5 a-b.

2004 *Heterohelix labellosa* NEDERBRAGT, PREMOLI-SILVA and VERGA, p. 141, p. 71, figs. 1-3.

Remarks:

This form has many different morphotypes with variable chamber shape and strength of costae. In this study *Heterohelix* forms with reniform adult chambers and thinner chamber depth are accepted as the members of this form. While the sides of its juvenile part are widely flaring, sides of the adult part become nearly parallel. The ones strength of the observable costae is variable in this form. In this study, this form is not common and found only in sample HEA-101.

Stratigraphic range: Its range is stated from Campanian to Maastrichtian (Nederbragt, 1991).

Occurrence: It has been recognized in the lower (Latest Maastrichtian) part of the studied section (from sample HEA-101).

***Heterohelix planata* CUSHMAN, 1938**

Pl. 5, fig. 5

1938 *Heterohelix planata* CUSHMAN, p. 12, 13, pl. 2, figs. 13, 14.

1991 *Heterohelix planata* CUSHMAN, NEDERBRAGT, p. 349, pl. 3, figs. 3-4c.

2004 *Heterohelix planata* CUSHMAN, PREMOLI-SILVA and VERGA, p. 142, p. 72, figs.7-9.

Remarks:

In this form the chamber shape was defined as ovate (Nederbragt, 1991). However, in our samples the chamber shape can be described as globular to subglobular. Although it can be confused with *Heterohelix globulosa* with this

definition, it is differentiated from this form by its edge view which has a thin chamber depth similar with *Heterohelix labellosa*. Thin costae can be seen in some of the forms, while the other's costae were deformed because of bad preservation. In our case it is observed only in sample HEA-101.

Stratigraphic range: From Santonian to Maastrichtian (Nederbragt, 1991).

Occurrence: It has been recognized in the lower (Latest Maastrichtian) part of the studied section (from sample HEA-101).

***Heterohelix punctulata* CUSHMAN, 1938**

Pl. 5, figs. 6, 7, 8

1938 *Guembelina punctulata* CUSHMAN, p. 13, pl. 2, figs. 15, 16.
1959 *Pseudotextularia echevarriai* CUSHMAN, SEIGLIE p. 59, pl. 3, figs. 2-6.
1988 *Heterohelix punctulata* CUSHMAN, KELLER, p. 252, pl. 2, fig. 10.
1991 *Heterohelix punctulata* CUSHMAN, NEDERBRAGT, p. 349, pl. 3, figs. 6a-b.

Remarks:

This is also one of the rare forms observed in our samples. It resembles *Heterohelix globulosa* with the globular or subglobular chambers, but in the edge view, the shape of chambers of *Heterohelix punctulata* becomes ovate or rectangular, because this form has chambers that are deeper than width or height. It is characterized by rapidly flaring in the juvenile stage.

Stratigraphic range: From Santonian to Maastrichtian (Nederbragt, 1991).

Occurrence: It has been recognized in the lower (Latest Maastrichtian) part of the studied section (from sample HEA-101).

Heterohelix striata EHRENBERG, 1840

Pl. 5, figs. 9, 10

1840 *Textularia striata* EHRENBERG, p. 135, pl. 4, figs. 1a, 2a, 3a.
1967 *Heterohelix striata* EHRENBERG, p. 264, figs. 2a.

Remarks:

The globular chambers increase gradually in size, except for the late chambers, which increase more rapidly. The species differs from *H. globulosa* in possessing fewer and much more strongly developed costae.

Stratigraphic range: From Santonian to Maastrichtian (Nederbragt, 1991).

Occurrence: It has been recognized from sample HEA-101 to HEA-104 (the lower part of the studied section, latest Maastrichtian).

Genus *Laeviheterohelix* NEDERBRAGT, 1991

Type species: *Guembelina pulchra* BROTZEN, 1936

Laeviheterohelix dentata STENESTAD, 1968

Pl. 6, fig. 1, 2

1968 *Heterohelix dentata* STENESTAD, p.67, 68, pl. 1, figs. 3-6, 8, 9; pl. 2, figs. 1-3.
1991 *Laeviheterohelix dentata* STENESTAD, NEDERBRAGT, p. 353, pl. 5, figs. 1-2c.
2002 *Heterohelix dentata* STENESTAD, LUCIANI, p. 312, pl. 1, fig. 2.

Remarks:

This form can be defined by its smooth surface, which separates the genus from the other heterohelicids, its widely flaring sides, its reniform chambers and its very narrow edge view. The form has an initial spiral coiling part (Nederbragt, 1991). However, in our studied samples, this coiling cannot be observed in the initial part.

Stratigraphic range: From Middle Campanian to Maastrichtian (Nederbragt, 1991).

Occurrence: It has been recognized from sample HEA-101 to HEA-104 (the lower part of the studied section, latest Maastrichtian).

Genus *Planoglobulina* CUSHMAN, 1927

Type species: *Guembelina acervuloinides* EGGER, 1902

Planoglobulina acervulinoides EGGER, 1899

Pl. 6, fig. 3, 4

1899 *Guembelina acervuloinides* EGGER, p. 35, pl. 14, fig. 20.

1972 *Planoglobulina acervuloinides* EGGER, MARTIN, p. 81, pl. 3, figs. 3-6.

1991 *Planoglobulina acervuloinides* EGGER, NEDERBRAGT, p. 355, pl. 6, figs. 5 a-b; p. 357, pl. 7, figs. 1 a-b.

1999 *Planoglobulina acervuloinides* EGGER, ÖZKAN-ALTINER and ÖZCAN, p. 292, pl. 1, fig. 9.

2000 *Planoglobulina acervuloinides* EGGER, ROBASZYNSKI *et al.*, p. 481, p. 20, fig. 17.

Remarks:

This form is a *Planoglobulina* species with the biserial part followed by up to 6 sets of multiserial chamberlets. In the specimens observed in this study, the chamberlets are mostly 4 sets. Chambers and chamberlets are globular to subglobular. From the edge view, this form is compressed towards its both ends and inflated in the middle part. *Planoglobulina acervuloinides* is defined to be covered by distinct costae. In our specimens, the distinct costae that define the form can easily be observed. It is very common in all Cretaceous samples, while its abundance decreasing in the upper parts although it does not disappear up to the Cretaceous - Paleogene boundary.

Stratigraphic range: Through Maastrichtian (Nederbragt, 1991).

Occurrence: It has been recognized from sample HEA-101 to HEA-105 (the lower part of the studied section, latest Maastrichtian).

Genus *Pseudotextularia* RZEHAK, 1891

Type species: *Cuneolina elegans* RZEHAK, 1891

***Pseudotextularia elegans* RZEHAK, 1891**

Pl. 6, figs. 5, 6

1891 *Cuneolina elegans* RZEHAK, p. 4.

1988 *Pseudotextularia elegans* RZEHAK, KELLER, p. 250, pl.1, fig. 17.

1991 *Pseudotextularia elegans* RZEHAK, NEDERBRAGT, p. 363, pl. 10, figs. 1a-2b.

2000 *Pseudotextularia elegans* RZEHAK, ARENILLAS *et al.*, p. 43, pl. 1, fig. 7, 8.

2000 *Pseudotextularia elegans* RZEHAK, ROBASZYNSKI *et al.*, p. 481, p. 20, fig. 16.

Remarks:

Pseudotextularia is a genus that can simply be distinguished by its chambers distinctly deeper than wide and high and its compressed side view. The properties that differentiates *Pseudotextularia elegans* from the other species of this genus is its definitely bi-convex test in edge view and the thick, continuous costae which cover its surface. Chambers increase only slowly in size as added and are broader than high and finely costate.

Stratigraphic range: Throughout the Maastrichtian (Nederbragt, 1991).

Occurrence: It has been recognized from sample HEA-101 to HEA-105 (the lower part of the studied section, latest Maastrichtian).

***Pseudotextularia nuttalli* VOORWIJK, 1937**

Pl. 6, figs. 7 (a, b)

1937 *Guembelina nuttalli* VOORWIJK, p. 192, pl. 2, figs. 1-9.

1991 *Pseudotextularia nuttalli* VOORWIJK, NEDERBRAGT, p. 363, pl. 10, figs. 4 a-b, 6 a-b.

2004 *Pseudotextularia nuttalli* VOORWIJK, PREMOLI-SILVA and VERGA, p. 186, pl. 116, figs. 3-5.

Remarks:

Different than *Pseudotextularia elegans*, this form is biconvex in its edge view and its costae are finer. In our section, it is seen almost in all of the Cretaceous samples.

Stratigraphic range: From Coniacian to end of the Maastrichtian (Nederbragt, 1991).

Occurrence: It has been recognized from sample HEA-101 to HEA-105 (the lower part of the studied section, latest Maastrichtian).

Genus *Racemiguembelina* MONTANARO GALLITELLI, 1957

Type species: *Guembelina fructicosa* EGGER, 1902

Racemiguembelina fructicosa EGGER, 1899

Pl. 6, fig. 8

1899 *Racemiguembelina fructicosa* EGGER, p. 35, pl. 14, figs. 8, 9, 24.

1988 *Racemiguembelina fructicosa* EGGER, KELLER, p. 250, pl.1, fig. 15.

1991 *Racemiguembelina fructicosa* EGGER, NEDERBRAGT, p. 363, pl. 10, figs. 5 a-b.

1999 *Racemiguembelina fructicosa* EGGER, ÖZKAN-ALTINER and ÖZCAN, p. 292, pl. 1, fig. 10.

2000 *Racemiguembelina fructicosa* EGGER, ROBASZYNSKI *et al.*, p. 477, p. 18, fig. 3.

2004 *Racemiguembelina fructicosa* EGGER, CHACON *et al*., p. 590, fig. 4 M.

2005 *Racemiguembelina fructicosa* EGGER, OBAIDALLA, p. 215, pl. 1, fig. 4.

Remarks:

This readily recognizable species has a biserial early stage, which later becomes multiserial by development of supplementary, inflated and coarsely costate chambers. The test form is conical. Each terminal chamber possesses a basal arched aperture opening into the central cavity.

Stratigraphic range: Throughout Maastrichtian (Nederbragt, 1991).

Occurrence: It has been recognized from sample HEA-101 to HEA-105 (the lower part of the studied section, latest Maastrichtian).

Subfamily *Pseudoguembelina* ALIYULLA, 1977

Genus *Pseudoguembelina* BRONNIMANN and BROWN, 1953

Type species: *Guembelina excolata* CUSHMAN, 1926

***Pseudoguembelina hariaensis* NEDERBRAGT, 1991**

Pl. 6, fig. 9, 10 (a, b)

1991 *Pseudoguembelina hariensis* NEDERBRAGT, p. 359, pl. 8, figs. 6, 7 a-c; p. 361, pl. 9, figs. 1a-b, 2a-b.

2001 *Pseudoguembelina hariensis* NEDERBRAGT, PETRIZZO, p. 855, fig. 10. 12, 13.

2004 *Pseudoguembelina hariensis* NEDERBRAGT, PREMOLI-SILVA and VERGA, p. 180, pl. 110, figs. 1-4.

2005 *Pseudoguembelina hariensis* NEDERBRAGT, OBAIDALLA, p. 215, pl. 1, fig. 3.

Remarks:

The biserial part of its test is followed by one or two sets of multiserial chamberlets. It has ecliptic appearance in its edge view. This form has thin, discontinuous costae and it is lacking the accessory apertures. This form is the marker species that is used in the heterohelicid biozonation.

Stratigraphic range: Uppermost Maastrichtian (Nederbragt, 1991).

Occurrence: It has been recognized from sample HEA-101 to HEA-105 (the lower part of the studied section, latest Maastrichtian).

Superfamily Planomalinocea BOLLI, LOEBLICH and TAPPAN, 1957

Family Globigerinelloididae LONGORIA, 1974

Subfamily Globigerinelloidinae LONGORIA, 1974

Genus *Globigerinalloides* CUSHMAN and TEN DAM, 1948

Type species: *Globigerinelloides algeriana* CUSHMAN and TEN DAM, 1948

***Globigerinelloides prairiehillensis* PESSAGNO, 1967**

Pl. 7, fig. 1

1967 *Globigerinelloides prairiehillensis* PESSAGNO, p. 277, pl. 90, figs. 1-2.

Remarks:

Test has 5-7 inflated subglobular chambers in the final whorl and they increase slowly in size. Test has moderately wide umbilical area and deep depressed sutures. Test ultrastructure is the perforated cones.

Stratigraphic range: From Upper Santonian to the end of Maastrichtian (Robaszynski *et al.*, 1984).

Occurrence: It has been recognized from sample HEA-101 (the lower part of the studied section, latest Maastrichtian).

PALEOCENE PLANKTONIC FORAMINIFERS

Family Chiloguembelinidae REISS, 1963

Genus *Chiloguembelina* LOEBLICH and TAPPAN, 1956

Type species: *Chiloguembelina midwayensis* CUSHMAN, 1940

Chiloguembelina crinita GLAESSNER, 1937

Pl. 7, fig. 3

1937 *Gümbelina crinita* GLAESSNER, p. 383, pl. 4, figs. 34 a,b.

1957 *Chiloguembelina crinita* GLAESSNER; BECKMANN, p. 89, pl. 21, fig. 4.

Remarks:

Test small, built up with about 6-12 spherical or oval-shaped chambers. The spire of the initial chambers in existing specimens is not distinctly recognizable. The ratio of chamber width to the length varies strongly. The last chamber diagonally overlies the previous one. The test surface is covered by fine granulations, which are always found on the upper surface of the last chambers.

Stratigraphic range: From Thanetian to Ypresian (Olsson *et al*., 1999).

Occurrence: From sample HEA-10 to HEA-20.

Chiloguembelina midwayensis CUSHMAN, 1940

Pl. 7, fig. 4

1940 *Gümbelina midwayensis* CUSHMAN, p. 65, pl. 11, fig. 15.

1957 *Chiloguembelina midwayensis* CUSHMAN, LOEBLICH and TAPPAN, p. 179, pl. 41, fig. 3, pl. 43, figs. 7a-b, pl. 45, figs. 9a-b.

1957 *Chiloguembelina midwayensis* CUSHMAN, BECKMANN, p. 90, pl. 21, figs. 1a-b.

1957 *Chiloguembelina midwayensis strombiformis* BECKMANN, p. 90, pl. 21, figs. 6a-c.

Remarks:

Test small, built up with about 8-15 spherical or oval-shaped chambers, compressed, usually twice as long as broad, rapidly tapering, with the greatest breadth formed by the last pair of chambers, periphery rounded throughout, lobulate, slightly overlapping, inflated, increasing rapidly in height as added; sutures distinct, depressed, very slightly curved, wall spinose and microperforate.

Stratigraphic range: From Lower Danian to Upper Thanetian (Olsson *et al*., 1999).

Occurrence: From sample HEA-109 to HEA-16.

***Chiloguembelina morsei* KLINE, 1943**

Pl. 7, figs. 5, 6, 7

1943 *Gümbelina morsei* KLINE, p. 44, pl. 7, fig. 12.

1957 *Chiloguembelina morsei* KLINE; LOEBLICH and TAPPAN, p. 179, pl. 40, figs. 2a-b, pl. 41, fig. 4, pl. 42, figs. 1a-b, pl. 43, figs. 2, 6a-b.

1993 *Chiloguembelina midwayensis* CUSHMAN; MACLEOD, p. 66, pl. VI, figs. 3-4.

Remarks:

Test small built up with about 10-15 spherical or oval-shaped chambers, about twice as long as broad, regularly tapering, with greatest breadth at apertural end. The test is biserial throughout. Sutures are distinct and depressed. The initial chambers are sub-spherical. The surface of the holotype test is marked by numerous small pustules.

Stratigraphic range: From Lower Danian to Upper Danian (Olsson *et al*., 1999).

Occurrence: From sample HEA-106 to HEA-123.

Chiloguembelina subtriangularis Beckmann, 1957

Pl. 8, figs. 1, 2 (?)

1957 *Chiloguembelina subtriangularis* BECKMANN, p. 91, pl. 21, fig. 5, text-fig. 15.

Remarks:

Test small, biserial with a subangular periphery, subtriangular in side view. Chambers slightly overlapping the previous chambers, sutures depressed. The specimen which is shown in the Plate 8, fig. 2 could not be defined clearly because of its bad preservation. Subtriangular appearance of this specimen could be interpreted as *Chiloguembelina subtriangularis.*

Stratigraphic range: From Upper Danian to Selandian (Olsson *et al*., 1999).

Occurrence: From sample HEA-122 to HEA-152.

Family Globigerinidae CARPENTER, PARKER and JONES, 1862

Genus *Eoglobigerina* MOROZOVA, 1959

Type species: *Globigerina (Eoglobigerina) eobulloides* MOROZOVA, 1959

Eoglobigerina edita SUBBOTINA, 1953

Pl. 8, fig. 3

1953 *Globigerina edita* SUBBOTINA, p. 62, pl. 2, fig. 1a-c.

1961 *Globigerina hemisphaerica* MOROZOVA, p. 11, pl. 1, fig. 4.

1961 *Globigerina tetragona* MOROZOVA, p. 13, pl. 1, fig. 2.

1961 *Globigerina pentagona* MOROZOVA, p. 13, pl. 1, fig. 3.

1962 *Globorotalia edita* SUBBOTINA; HILLEBRANDT, p. 130, pl. 11, figs. 14, 15.

1992 *Eoglobigerina edita polycamera* KHALILOV; OLSSON, HEMLEBEN, BERGGREN and LIU, p. 197, pl. 2, fig. 6.

1996 *Eoglobigerina edita* SUBBOTINA; KOUTSOUUKOS, p. 331, figs. 6, 7, 8.

2005 *Eoglobigerina edita* SUBBOTINA; OBAIDALLA, p. 219, pl. 3, fig. 17.

Remarks:

Test small, rounded, with high spiral consisting of 3 whorls. The species is characterized by a moderately high trochospiral test with 6 globular chambers which increase gradually in size in the ultimate whorl, and a strongly lobulate peripheral margin. The chambers of the early whorls are compactly arranged and closely packed together. The ventral side is weakly convex compared with the dorsal. The umbilicus is small, shallow and distinct. Sutures deep, slightly curved. The wall is cancellate and with small pores. The most characteristic feature of this species is the turret-like dorsal surface which is associated with the large size of the chambers in the earlier whorls.

Stratigraphic range: From Lower Danian to Upper Danian (Olsson *et al*., 1999).

Occurrence: From sample HEA-107 to HEA-132.

***Eoglobigerina eobulloides* MOROZOVA, 1959**

Pl. 8, fig. 4

1959 *Globigerina (Eoglobigerina) eobulloides* MOROZOVA, p. 1115, text-figs. 1a-c.

1973 *Globigerina fringa* PREMOLI SILVA and BOLLI, p. 541, pl. 7, figs. 6,9.

1979 *Eoglobigerina eobulloides eobulloides* MOROZOVA; BLOW, p. 1214, pl. 60, fig. 9 and pl. 61, fig. 1.

1982 *Eoglobigerina fringa* SMIT, p. 329, pl. 2, figs. 11a-c.

1990 *Eoglobigerina fringa* STOTT and KENNETT, p. 559, pl. 1, figs. 5,6.

1991 *Eoglobigerina eobulloides* MOROZOVA; HUBER, p. 461, pl. 2, figs. 9-11.

Remarks:

This species is characterized by a moderately elevated trochospiral test with 4 globular to oval chambers which increase moderately in size. Spiral side of the test is flattish. The cancellate wall texture is very weakly developed and difficult to view with the light microscope, especially where preservation of the wall is poor. The main difference of this species from *Eoglobigerina edita* is absence of turret-like dorsal surface and less amount of chambers.

Stratigraphic range: From Lower Danian to Middle Danian (Olsson *et al*., 1999).

Occurrence: From sample HEA-109.

***Eoglobigerina spiralis* BOLLI, 1957**

Pl. 8, fig. 5

1957 *Globigerina spiralis* BOLLI, p. 70, pl. 16, figs. 16-18.

1979 *Eoglobigerina spiralis* BOLLI; BLOW, p. 1222, pl. 79, figs. 5-9.

1991 *Igorina spiralis* BOLLI; HUBER, p. 461, pl. 3, figs. 13-15.

Remarks:

This species has an about 15 chambers (arranged in 3 whorls) with a distinct elevated spire with 6 inflated, globular and slightly laterally compressed chambers in the ultimate whorl. Chambers increase moderately in size. Shape of test is

medium trochospiral, spiral side distinctly convex and umbilical side nearly flat. The umbilicus is very small and is often overlapped by the ultimate chamber. Sutures on spiral side radial, slightly curved and depressed; on umbilical side radial, depressed. The wall texture is perforate and more strongly developed than in the ancestral species such as *Eoglobigerina edita* and *Eoglobigerina eobulloides*.

Stratigraphic range: Upper Danian (Olsson *et al*., 1999).

Occurrence: From sample HEA-132 to HEA-145.

Genus *Parasubbotina* OLSSON, HEMLEBEN, BERGGREN & LIU, 1992

Type species: *Globigerina pseudobulloides* PLUMMER, 1926

Parasubbotina pseudobulloides PLUMMER, 1926

Pl. 9, fig. 1

1926 *Globigerina pseudo-bulloides* PLUMMER, p. 133, pl. 8, figs. 9a-c.

1950 *Globigerina pseudobulloides* PLUMMER; SUBBOTINA, p. 106, pl. 4, figs. 8-10.

1957 *Globorotalia pseudobulloides* PLUMMER; BOLLI, p. 72, pl. 17, figs. 19-21.

1962 *Globorotalia (Globorotalia) pseudobulloides* PLUMMER; HILLEBRANDT, p. 124, pl. 12, figs. 2a-c.

1979 *Globorotalia (Turborotalia) pseudobulloides* PLUMMER; BLOW, p. 1096, pl. 69, figs. 2,3.

1992 *Subbotina pseudobulloides* PLUMMER; BERGGREN, p. 563, pl. 1, figs. 7,8.

1992 *Parasubbotina pseudobulloides* PLUMMER; OLSSON, HEMLEBEN, BERGGREN and LIU, p. 197, pl. 3, figs. 1-7.

Remarks:

Test of this species is rotaliform, very low trochospired and has about 10-12 chambers with 5 highly ventricose (inflated) chambers in the ultimate whorl. Inflated and globular chambers which are slightly ovoid in shape increase rapidly in size. Periphery broadly rounded and lobate. Wall of shell distinctly punctate and finely reticulate (see second and third chambers). The umbilicus is narrow and deep.

Stratigraphic range: From Lower Danian to Selandian (Olsson *et al*., 1999).

Occurrence: From sample HEA-121 to HEA-153.

***Parasubbotina variospira* BELFORD, 1984**

Pl. 9, figs. 2, 3

1984 *Globorotalia* (*Turborotalia*) *variospira* BELFORD, p. 18, pl. 24, figs. 15-17; pl. 25; figs. 1-7.

1984 *Morozovella variospira* BELFORD, p. 113, pl. 5, figs. 1-8; text-figs. 26.

Remarks:

Test large, consisting of about 9-12 chambers arranged in three whorls, usually 4 but sometimes 5 chambers visible in the last whorl. Chambers increasing slowly in size. Sutures on both dorsal and ventral sides narrow, deeply depressed, radial. Test wall is perforate, with small pustules.

Stratigraphic range: From Selandian to Lower Thanetian (Olsson *et al*., 1999).

Occurrence: From sample HEA-146 to HEA-11.

Genus *Subbotina* BROTZEN and POZARYSKA, 1961

Type species: *Globigerina triloculinoides* PLUMMER, 1926

Subbotina cancellata BLOW, 1979

Pl. 10, fig. 1

1953 *Globigerina fringa* SUBBOTINA, p. 62, pl. 3, fig. 3.

1979 *Subbotina triangularis cancellata* BLOW, p. 1284, holotype: pl. 80, fig. 7.

Remarks:

Test of this species is tightly coiled with 3 chambers in the ultimate whorl. The test is compact, rounded in outline and slightly lobulate. Wall on all chambers of the test is a very coarse cancellate. This wall structure allows to easily differentiate this species from other *Subbotina* species.

Stratigraphic range: From Upper Danian to Thanetian (Olsson *et al*., 1999).

Occurrence: From sample HEA-128 to HEA-13.

Subbotina triangularis WHITE, 1928

Pl. 10, fig. 2

1928 *Globigerina triangularis* WHITE, p. 195, pl. 28, figs. 1a-c.

1957 *Globigerina inaequispira* LOEBLİCH and TAPPAN, p. 181, pl. 52, figs. 1a-2c.

1957 *Globigerina triloculinoides* LOEBLICH and TAPPAN, p. 183, pl. 62, figs. 3a-c.

1970 *Globigerina pseudotriloba* SHUTSKAYA, p. 85, pl. 2, figs. 7a-c.

1970 *Globigerina uruchaensis* SHUTSKAYA, p. 87, pl. 2, figs. 6a-c.

1970 *Globigerina gerpegensis* SHUTSKAYA, p. 104, pl. 3, figs. 3a-c.

1977 *Subbotina patagonica*/*triangularis* group TJALSMA, p. 510, pl. 4, fig. 2.

1979 *Subbotina triangularis triangularis* WHITE; BLOW, p. 1281, pl. 91, figs. 7,9.

Remarks:

Test a somewhat loose coil of 3-4 chambers in the ultimate whorl, with a narrow, deep and small umbilicus which is sometimes obscured by an overlapping ultimate chamber. Test triangular, composed of about two whorls arranged in a low trochoid spire. Chambers inflated, somewhat appressed and sutures deep. Shape of test triangular in umbilical view as well. The wall of test is moderately cancellate.

Stratigraphic range: From Upper Danian to Ypresian (Olsson *et al*., 1999).

Occurrence: From sample HEA-135 to HEA-20.

***Subbotina triloculinoides* PLUMMER, 1926**

Pl. 10, fig. 3

1926 *Globigerina triloculinoides* PLUMMER, p. 134, pl. 8, figs. 10 a-b.

1928 *Globigerina pseudotriloba* WHITE, p. 194, pl. 27, figs. 17 a,b.

1952 *Globigerina stainforthi* BRANNIMANN, p. 171, pl. 3, figs. 10-12.

1961 *Globigerina (Globigerina) microcellulosa* MOROZOVA, p. 14, pl. 1, fig. 11.

1961 *Subbotina triloculinoides* PLUMMER; BROTZEN and POZARYSKA, p. 160, pl. 4, fig. 4; p. 160, text-fig. 2.

1979 *Subbotina triloculinoides triloculinoides* PLUMMER; BLOW, p. 1287, pl.74, fig. 6.

Remarks:

Test spiral, trochoid, composed of about 2 whorls, the last of which is composed of 3 very rapidly increasing and highly globose chambers. Periphery very broadly rounded and distinctly lobate. Shell surface moderately reticulate. The main difference of this species from *Subbotina cancellata* is the less obvious cancellate structure of the wall. Umbilicus narrow and deep. Aperture is umbilical.

Stratigraphic range: From Danian to Thanetian (Olsson *et al*., 1999).

Occurrence: From sample HEA-115 to HEA-11.

***Subbotina trivialis* SUBBOTINA, 1953**

Pl. 11, fig. 1

1953 *Globigerina trivialis* SUBBOTINA, p. 64, pl. 4, figs. 4a-c; paratypes: figs. 5a-7c.

1979 *Eoglobigerina trivialis* SUBBOTINA; BLOW, p. 1224, pl. 65, figs. 1-3, pl. 66, figs. 4,7.

1991 *Subbotina trivialis* SUBBOTINA; HUBER, p. 461, pl. 3, figs. 16, 17.

Remarks:

A low trochospiral, tightly coiled test with 3 1/2 chambers in the ultimate whorl. The ultimate chamber is equal to the penultimate one. The chambers are closely packed together and partially overlap each other. Because of this the shell is very compact. Shell inflated with tall first whorls which are 2 in number and large in size. The wall is moderately cancellate with relatively large pores and a cellular pattern. The umbilicus is very small. Septal sutures curved, deeply incised as is characteristic of species with strongly inflated shells.

Stratigraphic range: From Lower Danian to Upper Danian (Olsson *et al*., 1999).

Occurrence: From sample HEA-106 to HEA-135.

Subbotina velascoensis CUSHMAN, 1925

Pl. 11, fig. 2

1925 *Globigerina velascoensis* CUSHMAN, p. 19, pl. 3, figs. 6a-c.
1928 *Globigerina velascoensis* CUSHMAN var. *compressa* WHITE, p. 196, pl. 28, figs. 3a,b.
1956 *Globigerina triloculinoides* PLUMMER *nana* KHALILOV, p. 236, pl. 1, figs. 4a-c.
1956 *Globigerina quadritriloculinoides* KHALILOV, p. 237, pl. 1, figs. 5a-c.

Remarks:

A tightly coiled test with compressed 3 chambers and a subquadrate test shape. The ultimate chamber is much compressed, an elongate oval shape that makes up about half of the test and typically overhangs the earlier chambers. The test of wall is coarsely cancellate. Periphery broadly rounded, chambers distinct.

Stratigraphic range: From Selandian to Ypresian (Olsson *et al*., 1999).

Occurrence: From sample HEA-152 to HEA-20.

Family Guembelitriidae MONTANARO GALLITELLI, 1957

Genus *Globoconusa* KHALILOV, 1956

Type species: *Globoconusa conusa* KHALILOV, 1956.

Globoconusa daubjergensis BRONNIMANN, 1952

Pl. 11, fig. 3

1952 *Globigerina daubjergensis* BRONNIMANN, p. 340, text-fig. 1.

1956 *Globoconusa conusa* KHALILOV, p. 249, pl.5, figs. 2a-c.

1957 *Globigerinoides daubjergensis* BRONNIMANN; LOEBLICH and TAPPAN, p. 184, pl. 40, figs. 1a-c.

1961 *Globoconusa kozlowskii* BROTZEN and POZARYSKA, p. 162, pl. 1, figs. 1-14, pl. 2, figs. 1-17, pl. 3, figs. 1a-2c.

1961 *Globigerina (Eoglobigerina) trifolia* MOROZOVA, p. 12, pl. 1, fig. 1.

1967 *Globoconusa tripartita* MOROZOVA *et al*., p. 193, pl. 5, figs. 4-6.

1969 *Globoconusa daubjergensis gigantea* BANG, p. 65, pl. 4, figs. 1-3b.

1970 *Globoconusa daubjergensis* BRONNIMANN; OLSSON, p. 601, pl. 92, figs. 2 a, b.

1979 *Globastica daubjergensis* BRONNIMANN; BLOW, p. 1235, pl. 74, figs. 7-9.

1999 *Globastica daubjergensis* BRONNIMANN; PARDO *et al*., p. 260, pl. 4, fig. 10.

2002 *Globoconusa daubjergensis* BRONNIMANN; KAROUI-YAAKOUB *et al*., p. 242, pl. 2, fig. 14-15.

Remarks:

The final whorl, the dominant portion of the test, consists of 3 gradually increasing in size subglobular chambers. *Globoconusa daubjergensis* is characterized by a extremely small size. Its outer surface is covered by abundant small pustules. The species exhibits wide variation in spire height; some specimens are marked by a relatively low trochospire, whereas others display a relatively high spire (similar to short-spired *Guembelitria cretacea*). In our case this is low trochospired form. The outline of the trochoid test is distinctly lobulate. The sutures of the final whorl are strongly incised, those of the early test are not clearly visible.

Stratigraphic range: From Lower Danian to Upper Danian (Olsson *et al*., 1999).

Occurrence: From sample HEA-106 to HEA-126.

Genus *Guembelitria* CUSHMAN, 1933

Type species: *Guembelitria cretacea* CUSHMAN, 1933.

***Guembelitria cretacea* CUSHMAN, 1933**

Pl. 11, figs. 4, 5

1933 *Guembelitria cretacea* CUSHMAN, p. 37, pl. 4, figs. 12 a, b.
1961 *Guembelitria irregularis* MOROZOVA, p. 17, pl. 1, fig. 9.
1978 *Chiloguembelitria danica* HOFKER, p. 60, holotype, pl. 4, fig. 14.
1986 *Guembelitria azzouzi* SALAJ, p. 49, pl. 1, figs. 1-6, pl. 2, fig. 1.
1986 *Guembelitria besbesi* SALAJ, p. 50, pl. 1, figs. 7-9.
1988 *Guembelitria cretacea* CUSHMAN; KELLER, p. 252, pl. 2, fig. 1.
1989 *Guembelitria trifolia* KELLER, p. 319, fig 3 - 3, 4.
2003 *Guembelitria cretacea* CUSHMAN; ABDELGHANY, p. 399, figs. 8, 12.
2004 *Guembelitria cretacea* CUSHMAN; ARENILLAS *et al*., p. 82, fig. 4.

Remarks:

The test is small, triserial, and composed of globular chambers with strongly depressed sutures. The wall structure is microperforate.

Stratigraphic range: From Maastrichtian to Middle Danian (Olsson *et al*., 1999).

Occurrence: From sample HEA-104 (the lower part of the studied section, latest Maastrichtian) to HEA-116 (Danian, P1b Zone).

Genus *Parvularugoglobigerina* HOFKER, 1978

Type species: *Globigerina eugubina* LUTERBACHER and PREMOLI SILVA, 1964.

Parvularugoglobigerina alabamensis LIU and OLSSON, 1992

Pl. 12, fig. 1

1992 *Guembelitria alabamensis* LIU and OLSSON, p. 341, pl. 2, figs. 1-7, figs. 1-3.

Remarks:

Globular or spherical chambers arranged in a high trochospire with 3 chambers in the last formed whorls. Sutures deeply incised. Test of wall microperforate.

Stratigraphic range: From Lower Danian to Selandian (Olsson *et al*., 1999).

Occurrence: From sample HEA-107 to HEA-152.

Parvularugoglobigerina eugubina LUTERBACHER and PREMOLI SILVA, 1964

Pl. 12, figs. 2, 3; pl. 13, fig. 1

1964 *Globigerina eugubina* LUTERBACHER and PREMOLI SILVA, p. 105, pl. 2, figs. 8a-c.

1964 *Globigerina umbrica* LUTERBACHER and PREMOLI SILVA, p. 106, pl. 2, figs. 2a-c.

1964 *Globigerina anconitana* LUTERBACHER and PREMOLI SILVA, p. 107, pl. 2, figs. 3a-c.

1964 *Globigerina sabrina* LUTERBACHER and PREMOLI SILVA, p. 108, pl. 2, figs. 6a-c.

1979 *Globorotalia (Turborotalia) longiapertura* BLOW, p. 1085, pl. 56, figs. 3, 4.

1986 *Postrugoglobigerina hariana* SALAJ, p. 53, pl. 3, figs. 1-3, 5.

1988 *Globigerina* cf. *edita* SUBBOTINA; KELLER, p. 257, pl. 3, fig. 18.

1991 *Parvularugoglobigerina eugubina* LUTERBACHER and PREMOLI SILVA; D'HONDT AND KELLER, p. 96, pl. 4, figs. 4-6.

1997 *Parvularugoglobigerina eugubina* LUTERBACHER and PREMOLI SILVA; LUCIANI, p. 811, figs. 1-7.

1999 *Parvularugoglobigerina eugubina* LUTERBACHER and PREMOLI SILVA; PARDO, p. 260, pl. 4, figs. 1,2.

2000 *Parvularugoglobigerina eugubina* LUTERBACHER and PREMOLI SILVA; ARENILLAS, p. 208, pl. 1, figs. 9, 10.

2007 *Parvularugoglobigerina eugubina* LUTERBACHER and PREMOLI SILVA; MACLEOD *et al*., p. 107, figs, 5, D, E.

Remarks:

Parvularugoglobigerina eugubina exhibits extremely variable morphology and it should be noticed that preservation of this species in studied samples is not very good. The test is a low trochospire with 2 1/2 whorls, each composed of 4 1/2 to 8 inflated subglobular chambers, increasing slowly in size. The test of wall is microperforate.

Stratigraphic range: Throughout Lower Danian (Olsson *et al*., 1999).

Occurrence: From sample HEA-106 to HEA-109.

***Parvularugoglobigerina extensa* BLOW, 1979**

Pl. 13, fig. 2

1979 *Eoglobigerina extensa* BLOW, p. 1220, pl. 69, fig. 7.

1979 *Eoglobigerina fodina* BLOW, p. 1221, pl. 57, figs. 5-6.

1982 *Globigerina minutula* LUTERBACHER and PREMOLI SILVA; SMIT, p. 338, pl. 3, figs. 3-6.

1988 *Globoconusa conusa* KHALILOV; KELLER, p. 257, pl. 3, figs. 12-14.

Remarks:

The small test is coiled in a distinct trochospire with 9-10 inflated subglobular chambers comprising the spire and 3-4 chambers in the last whorl. In spiral side, the chambers are inflated and closely appressed. The spiral sutures are depressed and moderately incised. The wall is very finely perforate.

Stratigraphic range: Throughout Lower Danian (Olsson *et al*., 1999).

Occurrence: From sample HEA-106 to HEA-109.

Genus *Woodringina* LOEBLICH and TAPPAN, 1957

Type species: *Woodringina claytonensis* LOEBLICH and TAPPAN, 1957

Woodringina claytonensis LOEBLICH and TAPPAN, 1957

Pl. 13, figs. 3, 4, 5, 6

1957 *Woodringina claytonensis* LOEBLICH and TAPPAN, p. 39, figs. 1a-d.

1988 *Woodringina hornerstownensis* KELLER, p. 257, pl.3, fig. 15.

1993 *Woodringina kelleri* MACLEOD, p. 63, pl. 4, figs. 1-3.

1993 *Woodringina* cf. *kelleri* MACLEOD, p. 63, pl. 3, figs. 4, 5, 12.

1996 *Woodringina claytonensis* LOEBLICH and TAPPAN; KOUTSOUUKOS, p. 327, figs. 1-3,6.

2004 Chiloguembelina *claytonensis* LOEBLICH and TAPPAN; KELLER and PARDO, p. 97, pl. 1, fig. 15.

2005 *Woodringina claytonensis* LOEBLICH and TAPPAN; OBAIDALLA, p. 219, pl. 3, fig. 5.

Remarks:

Test free, tiny, subglobular, flaring rapidly, early stage with weakly observable single whorl of three chambers (reduced "triserial"), followed by three, rarely up to five pairs of biserial sometimes slightly twisted chambers in development. Sutures are distinct and constricted. Wall of test is calcareous, finely perforate and very finely hispid.

Stratigraphic range: From Lower Danian to Middle Danian (Olsson *et al*., 1999).

Occurrence: From sample HEA-106 to HEA-116.

***Woodringina hornerstownensis* OLSSON, 1960**

Pl. 13, figs. 7, 8

1960 *Woodringina hornerstownensis* OLSSON, p. 29, pl. 4, figs. 18, 19.

1988 *Chiloguembelitria taurica* KELLER, p. 257, pl. 3, fig. 3.

1996 *Woodringina hornerstownensis* OLSSON; KOUTSOUUKOS, p. 327, figs. 6-13.

1999 *Woodringina hornerstownensis* OLSSON; PARDO *et al*., p. 254, pl. 1, fig. 16.

2004 *Woodringina hornerstownensis* OLSSON; KELLER and PARDO, p. 97, pl. 1, fig. 16.

Remarks:

Test small, biserial, elongate, slightly twisted, rather rapidly tapering, about twice as long as broad. Initial end consists of whorl of weakly observable 3 chambers, rest of test consists of biserial arrangement of chambers. The test of wall is microperforate. Sutures are distinctly depressed. *Woodringina hornerstownensis* is distinguished from *W. claytonensis* by the elongate tapering test and the almost straight sutures. Moreover, *Woodringina hornerstownensis* often has six or more pairs of biserial chambers, while *W. claytonensis* is usually limited to five or fewer.

Stratigraphic range: From Lower Danian to Middle Selandian (Olsson *et al*., 1999).

Occurrence: From sample HEA-109 to HEA-122.

Family Hedbergellidae LOEBLICH & TAPPAN, 1961
Subfamily Hedbergellinae LOEBLICH & TAPPAN, 1961

Genus *Globanomalina* HAQUE, 1956

Type species: *Globanomalina ovalis* HAQUE, 1956

***Globanomalina chapmani* PARR, 1938**

Pl. 13, fig. 9

1938 *Globorotalia chapmani* PARR, holotype: pl. 3, figs. 9 a,b.
1951 *Anomalina luxorensis* NAKKADY, p. 691, pl. 90, figs. 39-41.
1956 *Globanomalina ovalis* var. *lakiensis* HAQUE, p. 149, pl. 14, figs. 2a-c.
1953 *Globorotalia membranacea* EHRENBERG; SUBBOTINA, p. 205, pl. 16, figs. 12 a-c.
1957 *Globorotalia elongata* BOLLI, p. 77, pl. 20, figs. 11-13.

1957 *Globorotalia troelseni* LOEBLICH and TAPPAN, p. 196, pl. 60, figs. 4 a-c.

1962 *Globorotalia ehrenbergi* HILLEBRANDT, p. 126, pl. 12, figs. 3 a-c.

1987 *Planorotalites chapmani* PARR; NEDERBRAGT and VAN HINTE, p. 586, pl. 2, figs. 3-10.

Remarks:

This species is identified by its compressed, biconvex test and the rapidly enlarging chambers. The number of chambers in the ultimate whorl is 4-5 but can range up to 6. The wall of test is smooth with a silvery lustre and in some chambers is punctate. Sutures are depressed, gently recurved on both sides of the test.

Stratigraphic range: From Middle Selandian to Upper Thanetian (Olsson *et al*., 1999).

Occurrence: From sample HEA-8 to HEA-20.

***Globanomalina compressa* PLUMMER, 1926**

Pl. 14, fig. 1

1926 *Globigerina compressa* PLUMMER, p. 135, pl. 8, figs. 11 a-c.

1953 *Globigerina compressa* var. *compressa* PLUMME; SUBBOTINA, p. 63, pl. 2, figs. 2a-6c.

1962 *Globorotalia compressa* PLUMMER; HILLEBRANDT, p. 125, pl.12, figs. 1a-c.

1979 *Globorotalia (Turborotalia) compressa compressa* PLUMMER; BLOW, p. 1062, pl. 75, figs. 10, 11.

1991 *Planorotalites compressus* PLUMMER; HUBER, p. 461, pl. 3, figs. 1, 2.

1992 *Globanomalina compressa* PLUMMER; BERGGREN, p.563, pl. 1, figs. 14-16.

Remarks:

Test has 5 moderately inflated and gradually increasing chambers which is rotaliform, closely coiled, somewhat compressed and equally bioconvex. Sutures distinctly depressed and strongly curved on the spiral side. The wall of test is thin, smooth and finely punctate.

Stratigraphic range: From Upper Danian to Selandian (Olsson *et al*., 1999).

Occurrence: From sample HEA-125 to HEA-144.

***Globanomalina ehrenbergi* BOLLI, 1957**

Pl. 14, fig. 2

1949 *Globorotalia membranacea* CUSHMAN and BERMUDEZ, p. 34, pl. 6, figs. 16-18.

1957 *Globorotalia ehrenbergi* BOLLI, p. 77, pl. 20, figs. 18-20.

1963 *Globorotalia haunsbergensis* GOHRBANDT, p. 53, pl. 6, figs. 10-12.

1979 *Globorotalia (Turborotalia) haunsbergensis* GOHRBANDT; BLOW, p. 1075, pl. 88, figs. 6,8.

Remarks:

Test has about 12-15 chambers which arranged in 2-3 whorls. The 5 chambers of the last whorl increasing fairly rapidly in size. Shape of test low trochospiral, nearly biconvex and compressed. Wall calcareous, perforate and surface smooth. Sutures on spiral side slightly curved, distinctly depressed; on umbilical side radial, depressed. Umbilicus is a shallow and open.

Stratigraphic range: From Upper Danian to Thanetian (Olsson *et al*., 1999).

Occurrence: From sample HEA-133 to HEA-148.

Globanomalina imitata SUBBOTINA, 1953

Pl. 14, fig. 3

1953 *Globorotalia imitata* SUBBOTINA, p.259, pl. 16, figs. 14a-c, 15a-c, 16a-c.

Remarks:

Test has 4 chambers in the last whorl and these show a rapid increase in dimensions. Shell rotaliform, strongly convoluted with a broadly oval outline. Dorsal side flattened, ventral side convex, subconical. The sutures are almost straight and slightly curved in some chambers on both the dorsal and the ventral sides. Attention should be paid to the shortness of the sutures on the spiral side as compared with the rather long sutures on the ventral side. The wall is thin, smooth and perforated by many small pores.

Stratigraphic range: From Upper Danian to Upper Thanetian (Olsson *et al*., 1999).

Occurrence: From sample HEA-122 to HEA-15.

Globanomalina ovalis HAQUE, 1956

Pl. 15, fig. 1

1956 *Globanomalina ovalis* HAQUE, p. 147, pl. 14, figs. 3a-c.

1958 *Globigerina pseudoiota* HORNIBROOK, p. 34, pl. 1, figs. 16-18.

1979 *Pseudohastigerina wilcoxensis* CUSHMAN and PONTON; BLOW, pl. 111, fig. 5.

Remarks:

Test has 5 inflated, globose, somewhat overlapping chambers. Chambers rapidly increasing in size as added. Last 2 chambers occupy more than half of the test. Some chambers are oval, longer than broad, biconvex, nearly bilaterally symmetrical. Spiral side is flat, showing all the chambers. Sutures distinct, depressed, somewhat curved on the spiral side, radial on the ventral. Wall calcareous, smooth, shiny and very finally microperforate.

Stratigraphic range: From Upper Thanetian to Ypresian (Olsson *et al*., 1999).

Occurrence: From sample HEA-14 to HEA-20.

***Globanomalina planocompressa* SHUTSKAYA, 1965**

Pl. 15, fig. 2

1965 *Globorotalia planocompressa planocompressa* SHUTSKAYA, p. 179, pl. 1, figs. 6a-c.

1957 *Globorotalia compressa* PLUMMER; LOEBLICH and TAPPAN, p. 188, pl. 40, figs. 5a-c.

1979 *Globorotalia (Turborotalia) compressa planocompressa* SHUTSKAYA; BLOW, p. 1067, pl. 68, figs. 4, 8-10.

1992 *Globanomalina planocompressa* SHUTSKAYA; OLSSON, HEMLEBEN, BERGGREN and LIU, p. 207, pl. 7, figs. 6-8.

Remarks:

Test has 4-5 inflated subspherical chambers, rapidly and uniformly increasing in size and arranged freely. Sutures are deep and straight. Umbilicus narrow. The wall of test is smooth and finely perforate.

Stratigraphic range: From Lower Danian to Upper Danian (Olsson *et al*., 1999).

Occurrence: From sample HEA-107 to HEA-122.

Globanomalina pseudomenardii BOLLI, 1957

Pl. 15, fig. 3

1953 *Globorotalia membranacea* SUBBOTINA, p. 258, pl. 16, figs. 13a-c.
1957 *Globorotalia pseudomenardii* BOLLI, p. 77, pl. 20, figs. 14-16.
1962 *Globorotalia pseudomenardii* BOLLI; HILLEBRANDT, pl. 12, figs. 5a-6b.
1987 *Planorotalites pseudomenardii* BOLLI; NEDERBRAGT and VAN HINTE, p. 587, pl. 1, figs. 1-16.

Remarks:

Chambers strongly compressed. Test has about 15 chambers, which arranged in 3 whorls. The 5 chambers of the last whorl increasing rapidly in size. Shape of test very low trochospiral and periphery angular with distinct keel. Wall of the test is calcareous, perforate and in some chambers smooth. Sutures on spiral side strongly curved, especially between last chambers.

Stratigraphic range: From Lower Thanetian to Upper Thanetian (Olsson *et al*., 1999).

Occurrence: From sample HEA-10 to HEA-15.

Genus *Hedbergella* BRONNIMANN & Brown, 1958

Type species: *Anomalina lorneiana trocoidea* GANDOLFI, 1942

Hedbergella holmdelensis OLSSON, 1964

Pl. 16, fig. 1

1964 *Hedbergella holmdelensis* OLSSON, p. 160, pl. 1, figs. 1a-c, 2a-c.

1999 *Hedbergella holmdelensis* OLSSON; PARDO *et al*., p. 258, pl. 3, fig. 13, 14.

2004 *Hedbergella holmdelensis* OLSSON; ARENILLAS *et al*., p. 82, fig. 4.

2004 *Muricohedbergella holmdelensis* OLSSON, PREMOLI-SILVA and VERGA, p. 166, pl. 96, figs. 3-5, p. 260, pl. 30, figs. 6-8.

Remarks:

Chambers represented from 5 to 6 in the final whorl, increase rapidly in size as added. Test is trochospirally coiled. Sutures distinct and radial. Wall of the test calcareous and perforated. Stratigraphic range of this form is Lower Maastrichtian to Lowermost Paleocene (P0 Zone) (Olsson *et.al*., 1999) but our precise research have been revealed that this species became extinct in Pα Zone.

Stratigraphic range: From Lower Maastrichtian to Lower Danian (Olsson *et al*., 1999).

Occurrence:

It has been recognized from last Cretaceous sample HEA-105 (Uppermost Maastrichtian) and first Paleocene sample HEA-106 (the lower part of the studied section, Danian).

Family Heterohelicidae CUSHMAN, 1927

Genus *Zeauvigerina* FINLAY, 1939

Type Species: *Zeauvigerina zelandica* FINLAY, 1939

Zeauvigerina waiparaensis JENKINS, 1966

Pl. 16, fig. 2, 3, 4

1966 *Chiloguembelina waiparaensis* JENKINS, p. 1095, pl. 1, figs. 1-6.

1973 *Heterohelix glabrans* CUSHMAN; WEBB, p. 543, pl. 1, fig. 4.

1994 *Zeauvigerina waiparaensis* JENKINS; HUBER and BOERSMA, p. 276-278, pl. 1, figs. 1-10.

1999 *Chiloguembelina waiparaensis* JENKINS; PARDO *et al*., p. 256, pl. 2, figs. 1-4.

2004 *Chiloguembelina waiparaensis* JENKINS; KELLER and PARDO, p. 97, pl. 1, figs. 11, 12.

Remarks:

Test has 10-15 subglobular, biserial, small and elongate chambers, the first chambers increase slowly in size and the last chambers increase more rapidly in size. Wall of the test is calcareous and finely perforate. Sutures slightly depressed and distinct.

Stratigraphic range: From Maastrichtian to Upper Thanetian (Olsson *et al*., 1999).

Occurrence: From sample HEA-106 to HEA-152.

Zeauvigerina virgata KHALILOV, 1967

Pl. 16, figs. 5, 6

1967 *Heterohelix virgata* KHALILOV, p. 174-175, figs. 9a, 9b.

1994 *Zeauvigerina virgata* KHALILOV; HUBER and BOERSMA, p. 279-280, pl. 2, figs. 9a-c, 11a-c.

Remarks:

Test has long 10-12 spherical chambers, compressed bilaterally, slowly becoming broader toward the apertural end. Chambers alternating in two rows,

forming moderate zigzags along the depressed spiral suture. Chambers gradually increase in size toward the apertural end. Wall calcareous with pustules and microperforate.

Stratigraphic range: From Middle Danian to Upper Thanetian (Olsson *et al*., 1999).

Occurrence: From sample HEA-115 to HEA-152.

Family Truncorotaloididae LOEBLICH and TAPPAN, 1961

Genus *Igorina* DAVIDZON, 1976

Type species: *Igorina tadjikistanensis* BYKOVA**,** 1953

Igorina albeari CUSHMAN AND BERMUDEZ, 1949

Pl. 16, fig. 7

1949 *Globorotalia albeari* CUSHMAN and BERMUDEZ, p. 33, pl. 6, figs. 13-15.

1957 *Globorotalia pusilla laevigata* BOLLI, p. 78, pl. 20, figs. 5-7.

1979 *Globorotalia albeari* CUSHMAN and BERMUDEZ; BLOW, p. 883, pl. 92, figs. 4, 8, 9; pl. 93, figs; 1-4.

Remarks:

It is difficult to count number of chambers, but it seems that there are 6 or 8 chambers in the last whorl. Test moderately biconvex, essentially circular, cancellate and increasing very gradually in size as added.

Stratigraphic range: From Selandian to Upper Thanetian (Olsson *et al*., 1999).

Occurrence: From sample HEA-152 to HEA-15.

Igorina tadjikistanensis BYKOVA, 1953

Pl. 17, fig. 1

1953 *Globorotalia tadjikistanensis* BYKOVA, p. 86, pl. 3, figs. 5a-c.

1984 *Globorotalia* (*Morozovella*) *tadjikistanensis* BYKOVA; BELFORD, p. 10, pl. 18, figs. 18-23.

1953 *Globorotalia convexa* SUBBOTINA, p. 209, 210, pl. 1, figs. 2a-c.

1990 *Morozovella convexa* SUBBOTINA; STOTT and KENNETT, p. 560, pl. 3, figs. 5, 6.

Remarks:

Test rounded in outline, spiroconvex, ovate to subcircular, moderately lobulate, densely and finely praemuricate. It is also difficult to count amount of chambers but it should be 5-7 chambers in last whorl. Umbilicus small, shallow as a result of tight coiling mode.

Stratigraphic range: From Selandian to Ypresian (Olsson *et al*., 1999).

Occurrence: From sample HEA-152 to HEA-20.

Genus *Morozovella* MCGOWRAN AND LUTERBACHER, 1964

Type species: *Pulvinulina velascoensis* CUSHMAN, 1925.

Morozovella angulata WHITE, 1928

Pl. 17, fig. 2

1928 *Globigerina angulata* WHITE, p. 27, fig. 13.

1937 *Globorotalia angulata* WHITE; GLAESSNER, p. 383, pl. 4, figs. 35a-c.

1962 *Globorotalia* (*Truncorotalia*) *angulata* WHITE; HILLEBRANDT, p. 131, 132, pl. 13, figs. 14a-15c.

1979 *Globorotalia* (*Morozovella*) *angulata* WHITE; BLOW, p. 984, pl. 86, figs. 7-9.

1989 *Morozovella protocarina* CORFIELD, p. 98, pl. 1, figs. 1-12.

Remarks:

Test has 10-12 chambers arranged in 2 whorls, 4-6 chambers in final whorl rapidly increasing in size. Spiral side flat, umbilical side convex, early chambers slightly elevated. Sutures depressed, strongly recurved on spiral side and radial on umbilical side. Wall of the test is perforate.

Stratigraphic range: From Selandian to Thanetian (Olsson *et al.*, 1999).

Occurrence: From sample HEA-146 to HEA-152.

***Morozovella praeangulata* BLOW, 1979**

Pl. 17, fig. 3

1964 *Acarinina quadratoseptata* DAVIDZON and MOROZOVA, p. 28, 30, pl. 2, figs. 1a-c.

1979 *Globorotalia* (*Acarinina*) *praeangulata* BLOW, p. 942-944, pl. 82, figs. 5, 6.

Remarks:

The test is comprised of about 10-12 trochospirally coiled chambers with 5-6 chambers visible in the last whorl of the test. The umbilicus is open and deep.

Sutures are radially disposed and quite deeply incised. Wall of the test is perforate with pustules.

Stratigraphic range: From Upper Danian to Selandian (Olsson *et al*., 1999).

Occurrence: From sample HEA-132 to HEA-146.

Genus *Praemurica* OLSSON, HEMLEBEN, BERGGREN, AND LIU, 1992

Type species: *Globigerina (Eoglobigerina) taurica* Morozova, 1961.

Praemurica inconstans SUBBOTINA, 1953

Pl. 18, figs. 1, 2

1953 *Globigerina inconstans* SUBBOTINA, p. 58, pl. 3, figs. 1,2.

1956 *Globigerina schachdagica* KHALILOV, p. 246, pl. 1, fig. 3.

1957 *Acarinina praecursoria* MOROZOVA, p. 111, text-fig. 1.

1957 *Globorotalia trinidadensis* BOLLI, p. 73, figs. 19-21.

1961 *Globorotalia* (*Acarinina*) *inconstans* SUBBOTINA; LEONOV and ALIMARINA, pl. 3, figs. 1-3.

1962 *Globorotalia* (*Globorotalia) inconstans* SUBBOTINA; HILLEBRANDT, p. 130, pl. 12, figs. 7,8.

1964 *Globorotalia inconstans* SUBBOTINA; LUTERBACHER, p. 650, figs. 19-23.

1966 *Globigerina arabica* EL NAGGAR, p. 157, 158, pl. 18, fig. 6.

1970 *Acarinina inconstans inconstans* SUBBOTINA; SHUTSKAYA, p. 108, pl. 6, figs., 4, 5.

1979 *Globorotalia* (*Turborotalia*) *inconstans* SUBBOTINA; BLOW, p. 1080, pl. 71, figs. 6, 7.

1990 *Subbotina inconstans* SUBBOTINA; STOTT and KENNETT, p. 559, pl. 2, figs. 5, 6.

1992 *Morozovella inconstans* SUBBOTINA; BERGGREN, p. 564, pl. 1, figs. 12, 13.

Remarks:

Test has 6 chambers in the final whorl. Peripheral margin rounded to weakly subangular, chambers in early whorls tightly coiled, rapidly expanding in final whorl. Sutures radial, strongly curved and deeply incised. There is a well-defined, shallow umbilicus in the middle of the umbilicus side. Chambers spherical, closely packed together. Wall of the test is cancellate.

Stratigraphic range: Upper Danian to Selandian (Olsson *et al*., 1999).

Occurrence: From sample HEA-122 to HEA-150.

***Praemurica pseudoinconstans* BLOW, 1979**

Pl. 18, fig. 3

1979 *Globorotalia (Turborotalia) pseudoinconstans* BLOW, p. 1105, pl. 67, fig. 4.

1991 *Morozovella inconstans* HUBER, p. 461, pl. 3, figs. 11, 12.

1992 *Praemurica pseudoinconstans* BLOW; OLSSON, HEMLEBEN, BERGGREN and LİU, p. 202. pl. 6, figs. 1, 4.

1996 *Praemurica pseudoinconstans* BLOW; KOUTSOUUKOS, p. 331, figs. 1, 8.

Remarks:

The comparatively small test is coiled in a low trochospire with 5-6 complete chambers visible in the last whorl of the test and about 12-14 chambers comprising the all spire. Ultimate whorl increase gradually in size at first but then more rapidly in the final few chambers. The ultimate chamber is offset slightly

towards the umbilical side. Sutures deep and curved on the spiral side and radial on the umbilical side. Wall of the test is cancellate.

Stratigraphic range: From Lower Danian to Upper Danian (Olsson *et al*., 1999).

Occurrence: From sample HEA-109 to HEA-137.

***Praemurica uncinata* BOLLI, 1957a**

Pl. 18, fig. 4

1957 *Globorotalia uncinata* BOLLI, p. 74, pl. 17, figs. 13-15.

1966 *Globorotalia uncinata uncinata* BOLLI; EL NAGGAR, p. 240, pl. 18, figs. 1a-c.

1970 *Acarinina inconstans uncinata* BOLLI; SHUTSKAYA, p. 110, pl. 6, fig. 1a-c.

1979 *Globorotalia (Acarinina) praecursoria praecursoria* MOROZOVA; BLOW, p. 944-947, pl. 76, figs. 4,8,9 and pl. 81, fig. 3.

Remarks:

Test weakly cancellate, elongate-oval, plano-convex, moderately lobulate test with 8 chambers in last whorl. Sutures on umbilical side radial, depressed, on spiral side incised and strongly recurved yielding typically trapezoidal shaped chambers. Umbilicus is narrow and deep.

Stratigraphic range: From Upper Danian to Selandian (Olsson *et al*., 1999).

Occurrence: From sample HEA-135 to HEA-150.

CHAPTER 6

CONCLUSION

Regarding to the scope of the study, a 162 m thick stratigraphic section from Upper Cretaceous (uppermost Maastrichtian) to Paleocene sedimentary sequence was measured through the Haymana, Beyobası and Yeşilyurt formations in the Haymana basin (Central Anatolia, Turkey), which is mainly composed of limestone, mudstone and marl alternations and a total of 106 samples were analyzed.

1. The methods of study included the identification of planktonic foraminifers in the thin sections and washed samples, petrographic analysis, provenance analysis and SEM analysis. Different washing methods were applied on all 106 samples for extracting the individual planktonic foraminifers from the samples. Namely, standard washing techniques, such as hydrogen peroxide treatment, were applied to extract the individual forms. Since this method was not become successful in some lithology (marl and limestone) of the studied samples, different washing methods were applied. The best results were obtained when limestone and marl samples kept in 50% of acetic acid (CH_3COOH) solution for 12 hours, whereas mudstone samples kept in 50% of hydrogen peroxide (H_2O_2) for 72 hours. After all tests of planktonic and benthonic foraminifers and ostracods were picked up from washing residue and collected in microfossil holders and counted one by one in order to reveal their response to sedimentary cyclicity.

2. First of all, a detailed taxonomic study were carried out based on wall structure, wall composition, chamber architecture, position of primary aperture, presence or absence of keel(s) and ornamentations. As a result 29 genera

and 67 species were identified. The species were compared and the criteria used in distinguishing the forms in this study were explained in detail.

3. This study was conducted to establish the detailed biostratigraphic framework and to construct the biozonal scheme for the Maastrichtian, Danian, Selandian and Thanetian intervals and to delineate the uppermost Maastrichtian-Danian in other words Cretaceous-Paleogene boundary. For the first time very detailed biozonation for Paleocene was established by means of planktonic foraminifers in the Haymana Region (Central Anatolia, Turkey). This biozonation for Paleocene includes 6 different planktonic foraminiferal zones and 8 Subzones, which are Pα Zone, P1 Zone (Subzones-P1a, P1b, P1c), P2 Zone, P3 Zone (Subzones-P3a, P3b), P4 Zone (Subzones-P4a, P4b, P4c) and P5 Zone. It should be noted that this study is the one of the detailed biostratigraphical study of the Paleocene in Turkey and all Paleocene zones (except P0) defined for the first time. By investigation and determination of foraminifers genera under the microscope, the K/P boundary in the studied succession was pinpointed in transition from mudstone to marl facies, which indicates the mass extinction of large, ornamented and keeled Cretaceous foraminifers such as *Globotruncana, Globotruncanita, Pseudoguemelina, Pseudotextularia, Planoglobulina, Racemiguembelina, Rugoglobigerina, Trinitella* and appearance new delicate, minute and non-keeled ones in the Paleocene such as *Eoglobigerina, Chiloguembelina, Globanomalina, Parasubbotina, Praemurica, Parvularugoglobigerina, Igorina, Globoconusa, Woodringina* and etc. The interval between the sample HEA-105 and the sample HEA-106 where K/P boundary was pinpointed is 4.75 m in thickness. As a result of precise conducted research the significant bioevent has been revealed, namely that in studied section *Hedbergella holmdelensis* became extinct in Pα Zone instead of P0 Zone defined by Olsson *et al*. (1999).

4. In the sequence-stratigraphic study of the studied section it was possible to recognize the A, B, C and D-type meter-scale cycles, six depositional sequences, six third and two second order cycles which coincide fairly well with the Global Sea Level Change Curve. The first depositional sequence is complete

and represented by LST, TST and HST and composed of A, B and C-type meter-scale cycles. A-type is only seen at the base of the section and is basically composed of mudstones which overlain by a sandstone lithology. B-type cycle is characterized by mudstones capped by marls. C-type is the combination of mudstone and muddy-limestone association, this means that the accommodation space started to decrease in the carbonate generating areas of the basin and limestone (muddy-limestone) deposits started to prograde towards the basin. The second depositional sequence is composed of TST and HST deposits, consisting of B and C-type cycles. The third depositional sequence consists of the TST and HST deposits made up of B-type meter-scale cycles. The TST of the third depositional sequence started to get deposited above the second depositional sequence and is characterized by B-type meter-scale cycles. The HST deposits of the third depositional sequence are characterized by a D-1-type meter-scale cycle which is capped by a prominent limestone level. Meter-scale cycles of the fourth depositional sequence are mainly composed of D-2, D-3 and B-type meter-scale cycles. The TST of the fifth depositional sequence is represented by a B-type meter-scale cycles and the HST is composed of D-3-type meter-scale cycle. The sixth depositional sequence again represented by the TST and HST deposits, consisting of B and D-type cycles. Sequence architecture of the measured section is constructed by the stacking pattern of these meter-scale cycles which are basically characterized by capping limy facies at their tops, which indicate the highstand conditions during the sea level oscillations.

5. During the detailed petrographic analysis, several minerals or mineral groups were recognized in the studied samples. These are quartz, plagioclase, muscovite and biotite. Cement is commonly calcite. The quantitative data of minerals and rock fragments was used for classification of the studied samples.

6. Quantitative analysis of the planktonic, benthonic foraminifers and ostracods was carried out and as a result it was possible to figure out the response of foraminifers to sedimentary cyclicity in the Haymana basin. The best response to sedimentary cyclicity was revealed for planktonic foraminifers. Namely, the

average abundance of planktonic foraminifers increases in the transgressive systems tract (TST) and decreases in the highstand systems tract. Benthonic foraminifers and ostracods showed different trend of response to sedimentary cycles. For instance average abundance of benthonic foraminifers and ostracods at the lower part of the measured section increases in the HST and decreases in the TST but up in the studied succession the opposite result was recognized. This means that planktonic foraminifers showed the best response to sedimentary cyclicity in the studied section.

REFERENCES

Abdelghany, O., 2003. Late Campanian-Maastrichtian foraminifera from the Simsima Formation on the western side of the Northern Oman Mountains. Cretaceous Research, 24, pp. 391-405.

Arenillas, I., Arz, J. A., Molina, E. and Dupuis, C., 2000. An independent test of planktic foraminiferal turnover across the Cretaceous/Paleogene (K/P) boundary at El Kef, Tunusia: Catastrophic mass extinction and possible survivorship. Micropaleontology, vol. 46, no. 1, pp. 31-49.

Arenillas, I., Arz, J. A., Molina, E., 2004. A new high-resolution planktic foraminiferal zonation and subzonation for the lower Danian, Lethaia, 37, pp. 79-95.

Arıkan, Y., 1975. Tuzgölü havzasının jeolojisi ve petrol imkanları. MTA Bülteni, 85, pp. 17-38.

Bailey, E. B. and Mc Callian, W. J, 1953. Serpentine lavas, the Ankara Melange and the Anatolian Thrust. Phil. Trans. R. Soc. London. no. LXII, pp. 404-442.

Bang, I, 1969. Planktonic Foraminifera and Biostratigraphy of the Danian. In P. Brönnimann and H.H. Renz, editors, Proceedings of the First International Conference on Planktonic Microfossils, 1, Geneva, pp. 58-65.

Banner, F.T. and Blow, W.H., 1959. The classification and stratigraphic distribution of the Globigerinaceae. Paleontology, 2 (1), pp. 1-27.

Beckmann, J. P., 1957. Chiloguembelina Loeblich and Tappan and Related Foraminifera from the Lower Tertiary. In A.R. Loeblich, Jr., and collaborators, Studies in Foraminifera, United States National Museum. Bulletin, 215, pp. 83-95.

Belford, D.J., 1984. Tertiary Foraminifera and Age of Sediments, Ok Tedi-Wabag, Papua, New Guinea. Bureau Mineral Resources, Geology and Geophysics, Australia Bulletin, 216, pp. 1-52.

Berggren, W.A., 1992. Paleogene Planktonic Foraminifera Magnetobiostratigraphy of the Southern Kerguelen Plateau (Sites 747-749). In S.W. Wise, Jr., R. Schlich, *et al*., Proceedings of the Ocean Drilling Program, Scientific Results, 120, College Station, Texas: Ocean Drilling Program, pp. 551-569.

Berggren, W. A., Kent D. V., Swisher C. C., Aubry M. P., 1995. A revised Cenozoic geochronology and chronostratigraphy. In: W.A., Berggren, D.V., Kent, C.J. Dabrio, (eds), Tertiary Basin of Spain, Cambridge Univ. Pres, chapter E 11, pp. 129-212.

Blow, W.H., 1979. The Cainozoic Globigerinida. Leiden: E.J. Brill. 1413 p.

Bolli, H. M., Loeblich, A. R. Jr. and Tappan, H., 1957. Planktonic foraminiferal families Hantkeninidae, Orbulinidae, Globorotaliidae and Globotruncanidae, Bull. U. S. Natl. Mus., 215, pp. 3-50.

Bolli, H. M., 1966. Zonation of Cretaceous to Paleocene marine sediments based on planktonic foraminifera. Boletino Informativo Asociacion Venezolana de Geologiya, Mineria y Petroleo, 9, pp. 3-32.

Bronnimann, P., 1952. Globigerinidae from the Upper Cretaceous (Cenomanian - Maestrichtian) of Trinidad, B. M. I., Bull., Am. Paleontol., 34, pp.: 5-71.

Brotzen, F., and K. Pozaryska, 1961. Foraminifères du Paléocène et de l'Eocène inférieur en Pologne septentrionale; remarques paléogéographiques. Revue de Micropaléontologie, 4, pp. 155-166.

Bykova, N.K., 1953. Foraminifery suzakskogo yarusa Tadzhikskoi depressii. Trudy VNIGRI, nov. ser. v. 69, Mikrofauna SSSR, Sbornik 6, pp. 5-103.

Canudo, J. I., 1997. El Kef blind test I results. Marine Micropaleontology, vol. 29, pp. 73-76.

Canudo, J. I., Keller, G., Molina, E., 1991. Cretaceous-Tertiary boundary extinction pattern and faunal turnover at Agost and Caravaca, SE Spain. Mar. Micropaleontol., 17, pp. 319-341.

Caron, M., 1985. Cretaceous planktonic foraminifera. In: Bolli, H.M., Saunders, J.B. and Perch Nielsen, K. Editors, 1985. Plankton Stratigraphy, Cambridge University Press, New York, USA, pp. 17-86.

Chacon, B., Martin-Chivelet, J. and Grafe, K. U., 2004. Latest Santonian to latest Maastrichtian planktic foraminifera and biostratigraphy of the hemipelagic successions of the Prebetic Zone (Murcia and Alicante provinces, south-east Spain). Cretaceous Research, vol. 25, pp. 585-601.

Chungkham, P. and Jafar, S. A., 1998. Late Cretaceous (Santonian-Maastrichtian) integrated Coccolith – Globotruncanid biostratigraphy of pelagic

limestones from the accretionary prism of Manipur, northeastern India. Micropaleontology, vol. 44, no. 1, pp. 69-83.

Corfield, R.M., 1989. Morozovella protocarina: a New Species of Palaeocene Planktonic Foraminferida. Journal of Micrpaleontology, 8, pp. 97-102.

Cox, R. & Lowe, D.R. 1996. Quantification of the effect of secondary matrix on the analysis of sandstone compositional and a petrographic - chemical technique for retrieving original framework grain models of altered sandstones. Journal of Sedimentology Research, 66, pp. 548-558.

Cushman, J.A., 1925. Some New Foraminifera from the Velasco Shale of Mexico. Contributions from the Cushman Laboratory for Foraminiferal Research, 1, pp. 18-23.

Cushman, J. A., 1927. An outline for a re-classification of the Foraminifera. Contr. Cush. Lab. Res., vol. 3, pp. 1-105.

Cushman, J.A., 1933. Some New Foraminiferal Genera. Contributions from the Cushman Laboratory for Foraminiferal Research, 9, pp. 32-38.

Cushman, J.A., 1940. Midway Foraminifera from Alabama. Contributions from the Cushman Laboratory for Foraminiferal Research, pp. 51-73.

Cushman, J.A., and P.J. Bermudez, 1949. Some Cuban Species of Globorotalia. Contributions Cushman Laboratory Foraminiferal Research, 25, pp. 26-45.

Çiner, A., 1996. Distribution of Small Scale Sedimentary Cycles Throughout Several Selected Basins. Turkish J. of Earth Sciences, 5, pp. 25-37.

Çiner, A., Deynoux, M., Ricou, S. and Koşun, E. 1996. Cyclicity in the middle Eocene Cayraz carbonate formation, Haymana basin, Central Anatolia, Turkey, Paleogeography, Paleoclimatology, Paleoecology, 121, pp. 313-329.

Davidzon, R.M., and V.G. Morozova, 1964. Planktonic and Benthonic calcareous Foraminifera of the Bukhara Beds (Paleocene) of the Tadzhik Depression. Paleontologicheskiy Zhurnal, 3, pp. 23-29.

De Graciansky, 1998. Mesozoic and Cenozoic sequence chronostratigraphic framework of Europeau basins. In: P.C. de, HARDENBOL, J., JACQUIN, T. & VAIL, P.R. (eds): Mesozoic and Cenozoic sequence stratigraphy of European basins. - SEPM Spec. Publ. no 60, pp. 3-5.

D'Hondt, S., and G. Keller, 1991. Some Patterns of Planktic Foraminiferal Assemblage Turnover at the Cretaceous-Tertiary Boundary. Marine Micropaleontology 17, pp. 77-118.

Dickinson, W.R. 1985. Interpreting provenace relations from detrital modes of sandstones. In: Provenance of Arenites (Ed. G.G. Zuffa). Reidel, Dordrecht, pp. 333-361.

Dickinson, W.R. and Selly, D. R., 1979. Structure and stratigraphy of forearc regions. Bull. Am. Assoc. of Pet. Geol., 63, 1, pp. 2-31.

Dickinson, W. and Suczek, C., 1979. Plate tectonics and sandstone compositions, The American Journal of Petroleum Geologists Bulletin, 63, pp. 2164-2182.

Dunham, R., 1962. Classifications of carbonate rocks according to depositional texture. In: Ham, W. E. (ed.), Classification of carbonate rocks. American Association of Petroleum Geologist Memoir, pp. 108-121.

El-Naggar, Z.R., 1966. Stratigraphy and Planktonic Foraminifera of the Upper Cretaceous-Lower Tertiary. Bulletin of the British Museum (Natural History), Geology, London, Supplement 2, 291 p.

Embry, A.F. and Klovan, J.E., 1971. A Late Devonian reef tract on the Northeastern Banks Island, NWT: Canadian Petroleum Geology Bulliten, vol.19, p. 730.

Felix, M., Ogg, J. and Smith, G., 2004. A geologic time scale. Printed in the United Kingdom at the University Press, Cambridge, pp. 385-390.

Forquin, C., 1975, North-West Anatolia, Tectonic evolution of the south margin of the European continent during Tertiary time. Bulletin of the Geological Society of France, vol..17. pp. 1058-1070. (In french).

Gardin, S., Del Panta, F., Monechi, S. and Pozzi, M., 2001. A tethyan reference record for the Campanian and Maastrichtian stages: the Bottaccione section (Central Italy); review of data and new calcareous nannofossil results. In: Odin, G. S. (ed.) The Campanian-Maastrichtian Boundary. 2001 Elsevier Science B. V., Chapter E4, pp. 745-757.

Ginsburg, R. N., 1997. An attempt to resolve the controversy over the end-Cretaceous extinction of planktic foraminifera at El Kef, Tunisia using a blind test. Marine Micropaleontology, vol. 29, pp. 65-103.

Ginsburg, R. N., 1997. Not so blind El Kef Test – Reply. Marine Micropaleontology, vol. 32, 399 p.

Glaessner, M.F., 1937. Planktonische Foraminiferen aus der Kreide und dem Eozan und ihre stratigraphische Bedeutung. Studies in Micropaleontology, Publications of the Laboratory of Paleontology, Moscow University, pp. 27-52.

Gohrbandt, K.H.A., 1963. Zur Gliederung der Paläogen im Helvetikum nördlich Salzburg nach planktonischen Foraminiferen. I. Teil: Paleozän und tiefstes Untereozän. Mitteilungen der Geologischen Gesellschaft in Wien, 56, pp. 1-16.

Görür, N., Oktay, F.Y., Seymen, I., Sengör, A.M.C., 1984. Paleotectonic evolution of the Tuzgölü basin complex, Central Turkey: sedimentary record of a Neo - Tethyan closure. In: Dixon, J.E., Robertson, A.H.F., (eds) The geological evolution of the eastern Mediterranean. Geol Soc Lond, pp. 467-482.

Görür, N., Derman, A.S., 1978. Stratigraphic and tectonic analysis of the Tuzgölü-Haymana basin (In turkish). TPAO report, No, 1514 (non published).

Haque, A.F.M.M., 1956. The Foraminifera of the Ranikot and the Laki of the Nammal Gorge, Salt Range. Pakistan Geological Survey, Paleontologia Pakistanica, 1, pp. 1-300.

Hillebrandt, A.V., 1962. Das Paleozän und seine Foraminiferenfauna im Becken von Reichenhall und Salzburg. Bayerische Akademie der Wissenschaften, 108, 181 p.

Hofker, J., 1978. Analysis of a Large Succession of Samples through the Upper Maastrichtian and the Lower Tertiary of Drill Hole 47.2, Shatsky Rise, Pacific, Deep Sea Drilling Project. Journal of Foraminiferal Research, 8, pp. 46-75.

Hornibrook, 1958. New Zealand Upper Cretaceous and Tertiary Foraminiferal Zones and some Overseas Correlations. Micropaleontology, 4, pp. 25-38.

Hubbard D, Herman J, and Bell P. 1990. Speleogenesis in a travertine scarp: observations of sulphide oxidation in the subsurface. In: Herman J, Hubbard D, editors: Travertine-marl: Streamdeposits in Virginia. Pub 101. Charlottesville, VA. Virginia Division of Mineral Resources, pp. 177-184.

Huber, B.T., 1991. Planktonic Foraminifer Biostratigraphy of Campanian-Maestrichtian Sediments from Sites 698 and 700, Southern South Atlantic. In P.F. Ciesielski, Y. Kristoffersen, *et al*., Proceedings of the Ocean Drilling Program, Scientific Results, 114, College Station, Texas: Ocean Drilling Program, pp. 281-298.

Huber, B.T., and A. Boersma, 1994. Cretaceous Origin of Zeauvigerina and its Relationship to Paleocene Biserial Planktonic Foraminifera. Journal of Foraminiferal Research, 24, pp. 268-287.

Hüseynov, A., 2007. Sedimentary cyclicity in the Upper Cretaceous successions of the Haymana basin (Turkey): depositional sequences as response to relative sea-level changes. M. Sc. Thesis, Middle East Technical University, 120 p.

Jenkins, D.G., 1966. Planktonic Foraminiferal Zones and New Taxa from the Danian to Lower Miocene of New Zealand. New Zealand Journal of Geology and Geophysics, 8, pp. 1088-1126.

Karoui-Yaakoub, N., Zaghbib-Turki, D., Keller, G., 2002. The Cretaceous-Tertiary (K-P) mass extinction in planktic foraminifera at Elles I and El Melah, Tunisia. Palaeogeography, Palaeclimatology, Palaeoecology, 178, pp. 233-255.

Keller, G., 1988. Extinction, survivorship and evolution of planktic foraminifera across the Cretaceous/Tertiary boundary at El Kef Tunisia. Marine Micropaleontology 13, pp. 239-263.

Keller, G., 1989. Extended Cretaceous/Tertiary Boundary Extinctions and Delayed Population Change in Planktonic Foraminifera from Brazos River, Texas, Paleoceanography, 4, pp. 287-332.

Keller, G., 1997. Analysis of El Kef blind test I. Marine Micropaleontology, vol. 29, pp. 89-93.

Keller, G., 2001. The end-cretaceous mass extinction in the marine realm: year 2000 assessment. Planetary and Space Science, vol. 49, pp. 817-830.

Keller, G., 2002. Guembelitria-dominated late Maastrichtian planktic foraminiferal assemblages mimic early Danian in Central Egypt. Marine Micropaleontology 47, pp. 71-99.

Keller, G., Adattei T., Stinnesbeck, W., Luciani, V., Karoui-Yaakoub, N. and Zaghbib-Turki, D., 2002. Paleoecology of the Cretaceous-Tertiary mass extinction in planktonic foraminifera. Palaeogeography, Palaeoclimatology, Palaeoecology, vol. 178, pp. 257-297.

Keller, G., Li, L., MacLeod, N., 1995. The Cretaceous/Tertiary boundary stratotype section at El Kef, Tunisia: how catastrophic was the mass extinction? Palaeogeogr. Palaeoclimatol. Palaeoecol., 119, pp. 221-254.

Keller, G., Pardo, A., 2004. Disaster opportunists Guembelitrinidae: index for environmental catastrophes. Marine Micropaleontology, 53, pp. 83-116.

Kline, V.H., 1943. Clay County Fossils: Midway Foraminifera and Ostracoda, Mississippi, Geological Survey Bulletin, 53, pp. 1-98.

Khalilov, D.M., 1956. O pelagicheskoy faune foraminifer Paleogenovykh otlozheniy Azerbaydzhana. Trudy Instituta Geologii, Akademiya Nauk Azerbaydzhanskoy SSR, 17, pp. 234-255.

Khalilov, D.M., 1967. Mikrofauna i stratigrafiya paleogenovykh otlozheniy Azerbaydzhana, chast' II [Microfauna and stratigraphy of Paleogene strata of Azerbaydzhan, Part 2]. Akademiya Nauk Azerbaydzhanskoy SSR Instituta Geologii, Baku, 216 p.

Knitter, H., 1979. Eine verbesserte methode zur gewinnung von mikrofosilien aus harten, nicht schlammbaren kalken. Geol. Bl. Nor-Bayern, 29, pp. 182-186.

Koutsoukos, E.A.M., 1996. Phenotypic experiments into new pelagic niches in early Danian planktonic foraminifera: aftermath of the K/P boundaryevent. In: M.B. Hart (Editor), Biotic Recovery from Mass Extinction Events, Geological Society, Special Publication, London, 102, pp. 319-335.

Kouwenhoven, T., 1997. El Kef blind test : How blind was it? - Comment. Marine Micropaleontology, vol. 32, pp. 397-398.

Koçyiğit, A., 1991. An example of an accretionary fore–arc basin from northern Central Anatolia and its implications for the history of subduction of Neo-Tethys in Turkey. Geol Soc Am Bull, 103, pp. 22-36.

Koçyiğit, A., Özkan, S., Rojay, F.B., 1988. Examples from the fore-arc basin remnants at the active margin of northern Neo-Tethys; development and emplacement ages of the Anatolian nappe, Turkey. Journal Pure Applied Science Ankara, vol. 21, p. 183-210.

Leonov, G.P. and V.P. Alimarina, 1961. Stratigrafiya i planktonnye foraminifery "perekhodnykh" ot mela k paleogeny sloev tsentral'nogo Predkavkazya. In: Problema V: Granitsa melovoi i paleogenovoi sistem. Mezhdunarodnyi geologicheskii kongress, XXI sessiya Doklady sovetskikh geologov, Izdalstvo Akademiya Nauk, pp. 29-60.

Li, L. and Keller, G., 1998. Maastrichtian climate, productivity and faunal turnovers in planktic foraminifera in South Atlantic DSDP sites 525A and 21. Marine Micropaleontology, vol. 33, pp. 55-86.

Lipps, J. H., 1997. The Cretaceous-Tertiary boundary: the El Kef blind test. Marine Micropaleontology, vol. 29, pp. 65-66.

Liu, C., and R.K. Olsson, 1992. Evolutionary Adaptive Radiation of Microperforate Planktonic Foraminifera following the K/T Mass Extinction Event. Journal of Foraminiferal Research, 22, pp. 328-346.

Loeblich, A.R, Jr., and H. Tappan, 1957. Planktonic Foraminifera of Paleocene and Early Eocene Age from the Gulf and Atlantic Coastral Plains. In A.R. Loeblich, Jr., and collaborators, Studies in Foraminifera, United States National Museum Bulletin 215, pp. 173-198.

Longoria, J. F. and VonFeldt, A. E., 1991. Taxonomy, phylogenetics and biochronology of single-keeled globotruncanids (Genus *Globotruncanita* Reiss). Micropaleontology, vol. 37, no. 3, pp. 197-243.

Luciani, V., 1997. Planktonic foraminiferal turnover across the Cretaceous-Tertiary boundary in the Vajont valley (Southern Alps, northern Italy). Cretaceous Research, 18, pp. 799-821.

Luciani, V., 2002. High-resolution planktonic foraminiferal analysis from the Cretaceous-Tertiary boundary at Ain Settera (Tunisia): Evidence of an extended mass extinction. Palaeogeography, Palaeoclimatology, Palaeoecology, vol. 178, pp. 299-319.

Luterbacher, H.P., 1964. Studies in some Globorotalia from the Paleocene and Lower Eocene of the Central Apennines. Eclogae geologicae Helvetiae, 57, pp. 631-730.

Luterbacher, H. P., and I. Premoli Silva, 1964. Biostratigrafia del limite Cretaceo-Terziario nell'Appenino centrale. Rivista Italiana di Paleontologia e Stratigrafia, 70, pp. 67-128.

MacLeod, N., 1993. The Maastrichtian-Danian Radiation of Triserial and Biserial Planktic Foraminifera: testing Phylogenetic and Adaptational Hypotheses in the (Micro)fossil Record. Marine Micropaleontology, 21, pp. 47-100.

MacLeod, N., Whitney, D. L., Huber, B. T., Koeberl, C., 2007. Impact and extinction in remarkably complete Cretaceous-Tertiary boundary sections from Demerara Rise, tropical western North Atlantic. Geological Society of America Bulletin, 119, pp. 101-105.

Masters, B. A., 1997. El Kef blind test II results. Marine Micropaleontology, vol. 29, pp. 77-79.

McKee, E. D., Weir, G. W., 1953, Terminology for stratification and cross-stratification in sedimentary rocks: Geological Society of America, vol. 64, 90 p.

Mithchum, R. M., Vail, P. R. and Thomson, S. 1977. Seismic stratigraphy and global changes of sea level, part 2: The depositional sequences as a basic unit of for stratigraphic analysis. Applications to Hydrocarbon Exploration: *Association of Petroleum Geologist Memoir,* 26, pp. 53-62.

Morozova, V.G., 1959. Stratigrafiya Datsko-Montskikh otlozhenii Kryma po foraminiferam. Doklady Akademiya Nauk SSSR, 124, pp. 1113-1116.

Morozova, V.G., 1961. Datsko-Montskie planktonnye foraminifery yuga SSSR [Dano-Montian planktonic foraminifera of the southern USSR], Paleontologicheskiy Zhurnal. 2, pp. 8-19.

Morozova, V.G., G.E. Kozhevnikova, and A.M. Kuryleva, 1967. Datsko-Paleotsenovye Raznofatsial'nye otlozheniya Kopet-Daga i metody ikh korrelyatsii po foraminiferam [Danian-Paleocene Heterofacial Deposits of Kopet-Dag and Methods of their Correlation according to the Foraminifers], Trudy Geologicheskogo Instituta, Akademiya Nauk SSSR, 157, pp. 1-208.

Nakkady, S.E., 1951. A New Foraminiferal Fauna from the Esna Shales and Upper Cretaceous Chalk of Egypt. Journal of Paleontology, 24, pp. 675-692.

Nederbragt, A. J., 1991. Late Cretaceous biostratigraphy and development of Heterohelicidae (planktic foraminifera). Micropaleontology, vol. 37, no. 4, pp. 329-372.

Nederbragt, A. J., 1998. Quantitative biogeography of late Maastrichtian planktic foraminifera. Micropaleontology, vol. 44, no. 4, pp. 385-412.

Nederbragt, A.J., and J.E. Van Hinte, 1987. Biometric Analysis of Planorotalites pseudomenardii (Upper Paleocene) at Deep Sea Drilling Site 605, Northwestern Atlantic. In J.E., Van Hinte, S.W. Wise, *et al*., Initial Reports of the Deep Sea Drilling Project, 93, Washington, D.C.: U.S. Government Printing Office, pp. 577-592.

Norris, R. D., 1992. Umbilical structures in Late Cretaceous planktonic foraminifera. Micropaleontology, vol. 38, no. 2, pp. 165 - 181.

Obaidalla, N. A., 2005. Complete Cretaceous/Paleogene (K/P) boundary section at Wadi Nukhul, southwestern Sinai, Egypt: inference from planktic foraminiferal biostratigraphy. Revue de Paléobiologie, 24 (1), pp. 201-224.

Olsson, R.K., 1960. Foraminifera of Latest Cretaceous and Earliest Tertiary Age in the New Jersey Coastal Plain. Journal of Paleontology, 34, pp. 1-58.

Olsson, R.K., 1964. Late Cretaceous Planktonic Foraminifera from New Jersey and Delaware. Micropaleontology, 10, pp. 157-188.

Olsson, R.K., 1970. Planktonic Foraminifera from Base of Tertiary, Millers Ferry, Alabama. Journal of Paleontology, 44, pp. 598-604.

Olsson, R. K, 1997. El Kef blind test III results. Marine Micropaleontology, vol. 29, pp. 80-84.

Olsson, R. K, Hemleben, C., Berggen, W.A., and Huber, B.T., 1999. Atlas of Paleocene planktonic foraminifera. Washington, D.C.: Smithsonian Institution Press, pp. 1-197.

Orue-etxebarria, X., 1997. El Kef blind test IV results. Marine Micropaleontology, vol. 29, pp. 85-88.

Özcan, E., Özkan, S.A., 1997. Late Campanian – Maastrichtian evolution of orbitoidal foraminifera in Haymana basin successions (Ankara, Central Turkey). Revue Paleobiol., Geneve, 16, (1), pp. 271-290.

Özcan, E., Özkan, S.A., 1999. The Genus Lepidorbitoides: Evolution and Stratigraphic Significance in some Anatolian Basins (Turkey). Revue de Micropaleontologie, 42, pp. 111-131.

Özcan, E., Özkan, S.A., 2001. Description of an early ontogenetic evolutionary step in Lepidorbitoides: Lepidorbitoides bisambergensis asymmetrica subsp. n., Early Maastrichtian (Central Turkey) Rivista Italiana di Paleontologia e Stratigrafia, 107, pp. 137-144.

Özcan, E., Sirel, E., Özkan, S.A. and Çolakoğlu, S., 2001. Late Paleocene Orthophragminae (foraminifera) from the Haymana – Polatli Basin, (Central Turkey) and description of a new taxon, *Orbitoclypeus haymanaenis* Micropaleontology, 47, pp. 339-357.

Özkan, S. and Altıner, D., 1987. Maastrichtian planktonic foraminifera from the Germav Formation in Gercüş area (SE Anatolia, Turkey), with notes on the suprageneric classification of globotruncanids. Revue de Paléobiologie, vol. 6, no. 2, pp. 261-277.

Özkan, S., Özcan, E., 1999. Upper Cretaceous planktonic foraminiferal biostratigraphy from NW Turkey: calibration of the stratigraphic ranges of larger benthonic foraminifera Geological Journal, 34, pp. 287-301.

Pardo, A., Adatte, T., Keller, G., Oberhansli, H., 1999. Paleoenvironmental changes across the K-T transition in Koshak (Kazakstan) based on planktic foraminifera and clay minerals. Palaeogeogr. Palaeoclimat. Palaeoecol., 154, pp. 247-273.

Parr, W.J., 1938. Upper Eocene Foraminifera from Deep Borings in King's Park, Perth, Western Australia. Journal of the Royal Society of Western Australia, 24, pp. 69-101.

Pessagno, E. A. Jr., 1967. Upper Cretaceous Planktonic Foraminifera from the western Gulf Coastal Plain. Pal. Amer., vol. 5, no. 37, pp. 245-445.

Pettijohn, F., 1957. Sedimentary rocks. 2nd ed. Harper & Bros., New York, 718 p.

Pettijohn, F., Potter, P., & Siever, R. 1987. Sand and sandstone. Springer - Verlag, New York.

Petrizzo, M. R., 2001. Late Cretaceous planktonic foraminifera from Kerguelen Plateau (ODP Leg 183): new data to improve the Southern Ocean biozonation. Cretaceous Research, Volume 22, pp. 829-855.

Plummer, H.J., 1926. Foraminifera of the Midway Formation in Texas. University of Texas Bulletin, 2644, pp. 1-206.

Posamentier, H. W., Jervey, M. T. and Vail, P. R. 1988. Eustatic controls on clastic Deposition I-Conceptual framework. Sea-Level Changes-An Integrated Approach. *The Society of Economic Paleontologist and Minaralogist,* Special Publication , 42, pp. 109-124.

Postuma, J., 1971. Manual of planktonic foraminifera. Amsterdam, New York, Elsevier Pub. Co., pp. 113-215.

Potter P. E., Maynard B. J., and Pryor W. A., 1980. Sedimentology of Shale: Study Guide and Reference Source. Springer-Verlag, 310 p.

Potter P., Maynard B., and Depetris P., 2005. Mud and Mudstones: Introduction and Overview. Springer, 297 p.

Premoli Silva, I., and H.M. Bolli, 1973. Late Cretaceous to Eocene Planktonic Foraminifera and Stratigraphy of Leg 15 sites in the Caribbean Sea. In N.T. Edgar, J.B. Saunders, *et al*., Initial Reports of the Deep Sea Drilling Project, 15, Washington, D.C.: U.S. Government Printing Office, pp. 499-547.

Premoli Silva, I. and Sliter, W. V., 1999. Cretaceous paleoceanography: Evidence from planktonic foraminiferal evolution. In: Geological Society of America, Special Paper 332, pp. 301-328.

Premoli Silva, I. and Verga, D., 2004. Practical manual of Cretaceous planktonic foraminifera. International School an planktonic foraminifera, 3° Course: Cretaceous. Verga and Retteri (eds) Universites of Perugia and Milan, Tipografia Pontefelcino, Perugia (Italy), 283 p.

Robaszynski, F., Caron, M., Gonzalez Donoso, J.M. and Wonders, A. H., 1984. Atlas of Late Cretaceous Globotruncanids. Revue de Micropaléontologie, 26 (3-4), pp. 145-305.

Robaszynski, F. 1998. Cretaceous planktonic foraminiferal biozonation. Exxon chart 2000.

Robasyznski, F., Gonzales Donoso, J. M., Linares, D., Amedro, F., Caron, M., Dupuis, C., Dhondt, A. V. and Gartner, S., 2000. Le Crétacé supéerieur de la Région de Kalaat Senan, Tunisie Centrale. Lithobiostratigraphie intégrée: Zones d' ammonites, de foraminifers planctoniques et de nannofossiles du Turonien supérieur au Maastrichtien. Bull. Centres Rech. Explor.-Prod. Elf-Aquitaine, vol. 22, no. 2, pp. 359-490.

Salaj, J., 1986. The new Postrugoglobigerina praedaubjergensis Zone at the Base of the Stratotype of the Marine Paleocene (El Kef, Tunisia). Geologicky sbornik, Geologica carpathica, 37, pp. 35-58.

Sarg, J. F., 1988. Carbonate sequence stratigraphy. In: Sea-level Changes: An integrated approach. Wilgus, C. K., Hastings, B. S. *et al*. (eds.), The Society of Economic Paleontologist and Mineralogist, Special Publication, 42, 163 p.

Shutskaya, E.K., 1965. Filogeneticheskie vzaimootnoscheniya vidov gruppy Globorotalia compressa Plummer v datskom vekhe i paleotzenovoi epokhe. Akademiya Nauk SSSR; Voprosyi Mikropaleontologii, 9, pp. 173-188.

Shutskaya, E.K., 1970. Morfologicheskie grupirovki vidov rodov Globigerina i Acarinina v nizhnei chasti paleogena Kryma, Predkavkazya i zapada Srednei Azii i ipisanie vidov. In E.K. Shutskaya, editor, Stratigrafiya i paleontologiya Mezozoiskikh i Paleogenovykh otlozhenii Srednei Azii. Vsesoyuznyi Naucho-Issledovatel'skii Geologorazvedochnyi Nefyanoi Institut (VNIGNI), Trudy, vyp., 69, pp. 79-134.

Sirel, E., 1999. Four new genera (*Haymanella, Kayseriella, Elazigella and Orduella*) and one new species of *Hottingerina* from the Paleocene of Turkey Micropaleontology, 42, pp. 113-137.

Sirel, E., Gündüz, H., 1976. Description and stratigraphical distrubition of the some species of the genera Nummulites, Assilina and Alveolina from the Ilerdian, Cuisian and Lutetian of the Haymana region. Bull Geol Soc Turkey 19, pp. 31-44 (in Turkish).

Sloss, L. L. 1963. Sequences in the cratonic interior of North America. *Geological Society of America Bull.,* 74, pp. 93-114.

Smit, J., 1982. Extinction and Evolution of Planktonic Foraminifera after a Major Impact at the Cretaceous/Tertiary Boundary. Geological Society of America Special Publication, 190, pp. 329-352.

Smit, J. and Nederbragt, A., 1997. Analysis of the El Kef blind test II. Marine Micropaleontology, vol. 29, pp. 94-100.

Stott, L.D., and J.P. Kennett, 1990. Antarctic Paleogene Planktonic Foraminifer Biostratigraphy: ODP Leg 113, Sites 689 and 690. In P.F. Barker, J.P. Kennett, *et al*., Proceedings of the Ocean Drilling Program, Scientific Results, 113, College Station, Texas: Ocean Drilling Program, pp. 549-569.

Subbotina, N.N., 1950. Mikrofauna i stratigrafiya Elburganskogo Gorozonta Goriathego Klyitcha; Mikrofauna SSSR, sbornik 4. Trudy Vsesoyuznego Nauchno-Issledovatels'logo Geologo-razvedochnogo Institut (VNIGRI), new series, 51, pp. 5-112.

Subbotina, N.N., 1953. Iskopaemye foraminifery SSSR (Globigerinidy, Khantkenininidy i Globorotaliidy). Trudy Vsesoyznogo Nauchno-Issledovatel'skogo Geologo-razvedochnogo Instituta (VNIGRI), vyp. 76, 296 p.

Şengör, A.M.C. and Yılmaz, Y., 1981. Tethyan evolution of Turkey: A plate tectonic approach. Tectonophysics 75, pp. 181-241.

Tjalsma, R.C., 1977. Cenozoic Foraminifera from the South Atlantic, DSDP Leg 36. In P.F. Barker, I.W.D. Dalziel, *et al*., Initial Reports of the Deep Sea Drilling Project, 36:493-518. Washington, D.C.: U.S. Government Printing Office.

Toker, V., 1979. Upper Cretaceous Planktonic Foraminifera and the biostratig-raphic investgations of the Haymana area. Bulliten of the Geological Society of Turkey, 22, pp. 121-132.

Tucker, E., 2001. Sedimentary petrography. Blackwell Publishing, 262 p.

Tur, N. A., Smirnov, J. P. and Huber, B. T., 2001. Late Albian-Coniacian planktic foraminifera and biostratigraphy of the northeastern Caucasus. Cretaceous Research, Volume 22, pp. 719-734.

Twenhofel, W. H. 1939. Principles of sedimentation. New York, McGraw-Hill Book Co., 610 p.

Ünalan, G., Yüksel, V., Tekeli, T., Gonenç, O., Seyirt, Z., Hüseyn, S., 1976. Upper Cretaceous -Lower Tertiary stratigraphy and paleogeographic evolution of Haymana – Polatli region (SW Ankara). Turkish Geol Soc Bull 19, pp. 159-176 (in Turkish).

Vail, P. R., and Mitchum, JR. 1977. Seismic stratigraphy and global changes of sea level, Part 1: Overview-Applications to Hydrocarbon Exploration. *Am.Association of Petroleum Geologists. Memoir,* 26, pp. 63-81.

Vail, P.R., Michum, R. M. Jr., Todd, R.G., Widmier, J.M., Thompson, S., Sangree, J.B., Budd, J.B., Hatlied, W.G., 1977. Seismic stratigraphy and global changes of sea level. American Association of Petroleum Geologists Memoir, vol. 26, pp. 47-212

Wagoner, Van J.C., H.W. Posamentier, R.M. Mitchum, P.R. Vail, J.F. Sarg, T.S. Loutit, and J. Hardenbol, 1988. An overview of the fundamentals of sequence stratigraphy and key definitions. In C.K. Wilgus, B.S. Hastings, C.G.St.C. Kendall, H.W. Posamentier, C.A. Ross, J.C. Van Wagoner, eds., Sealevel changes: an integrated approach. Society of Economic Paleontologists and Mineralogists Special Publication No. 42, pp. 39-45.

Webb, P. N., 1973. Upper Cretaceous-Paleocene Foraminifera from Site 208 (Lord Howe Rise, Tasman Sea), DSDP, Leg 21. In R. E. Burns, J. E. Andrews, *et al*., Initial Reports of the Deep Sea Drilling Project, 21, Washington, D.C.: U.S. Government. Printing Office, pp. 541-573.

Weber, M.E., Fenner, J., Thies, A. and Cepek, P., 2001. Biological response to Milankovitch forcing during the Late Albian (Kirchrode I borehole, northwestern Germany). Palaeogeography, Palaeoclimatology, Palaeoecology, vol. 174, pp. 269-286.

White, M.P., 1928. Some Index Foraminifera of the Tampico Embayment of Mexico, Pt. 1. Journal of Paleontology, 2, pp. 177-215.

Yang, W., Kominz, M.A., Major, R.P. 1998. Distinguishing the roles of autogenic versus allogenic processes in cyclic sedimentation, Cisco Group (Virgilian and Wolfcampanian), north-central Texas. *GSA Bulletin*, 110, 10, pp.1333-1353.

Yüksel, S., 1970. Etude geologique de la region d'Haymana (Turquie Centrale). These Univ Nancy, 179 p.

APPENDIX A

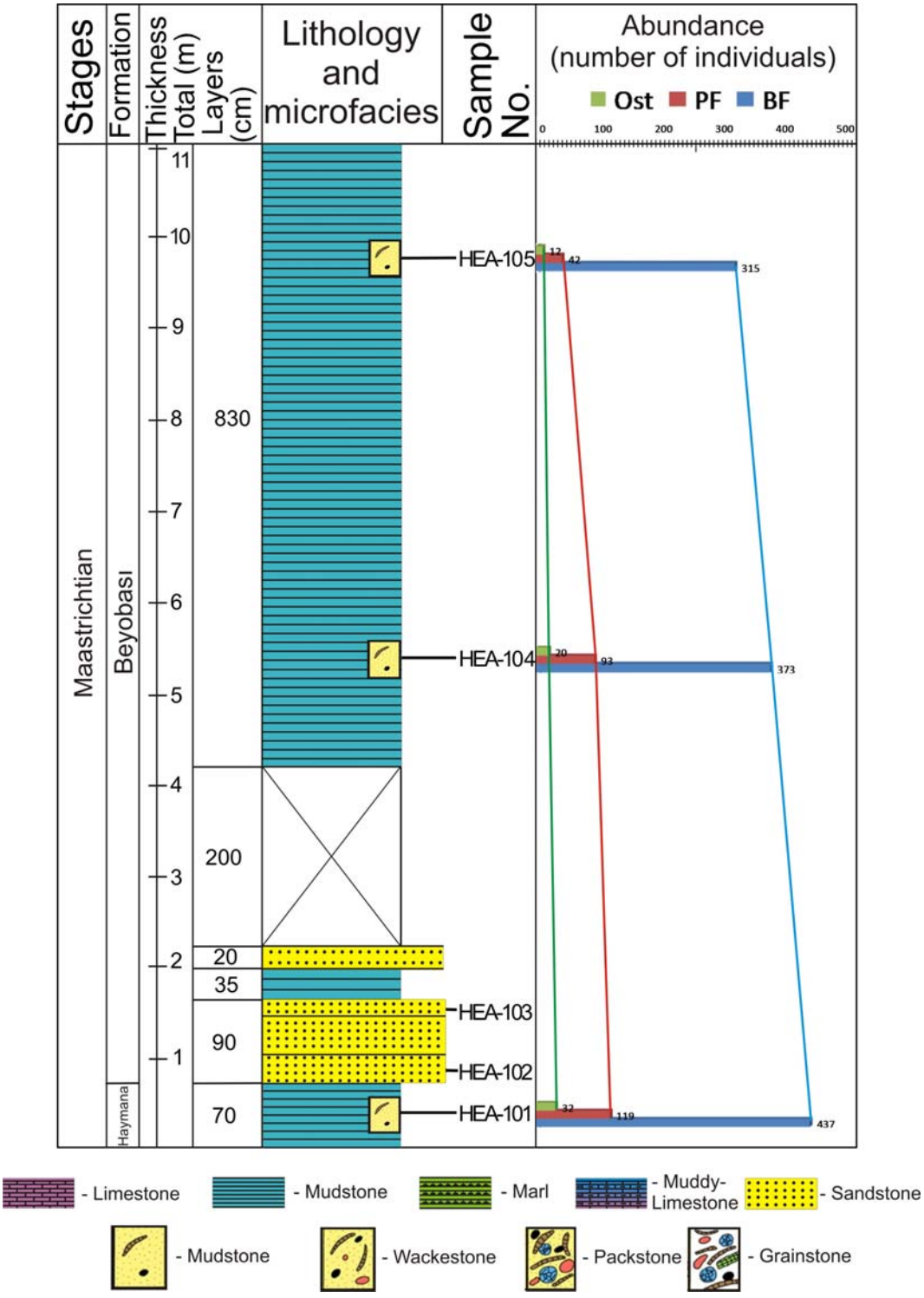

Figure A1. Detailed measured section.

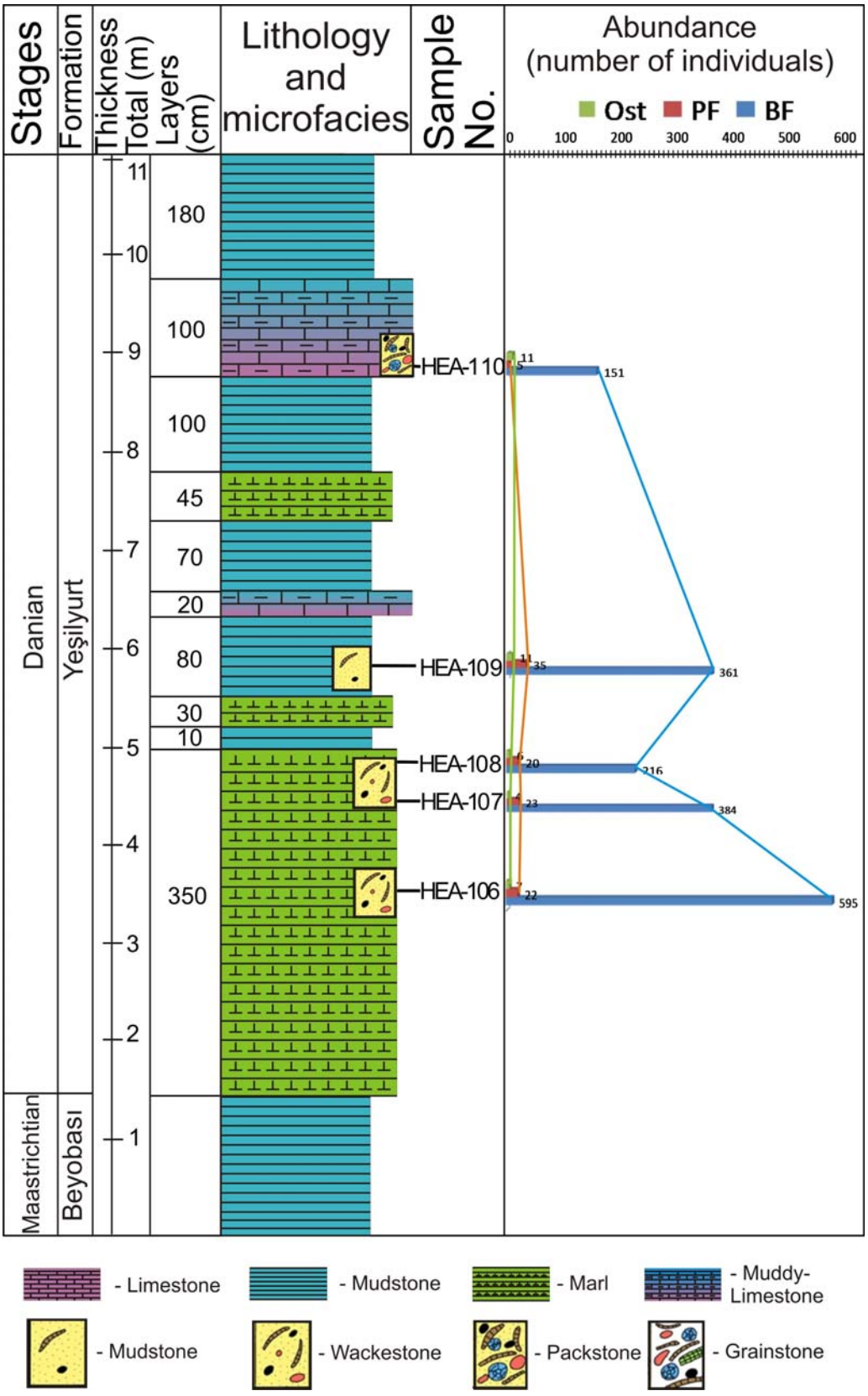

Figure A2. Detailed measured section (continued).

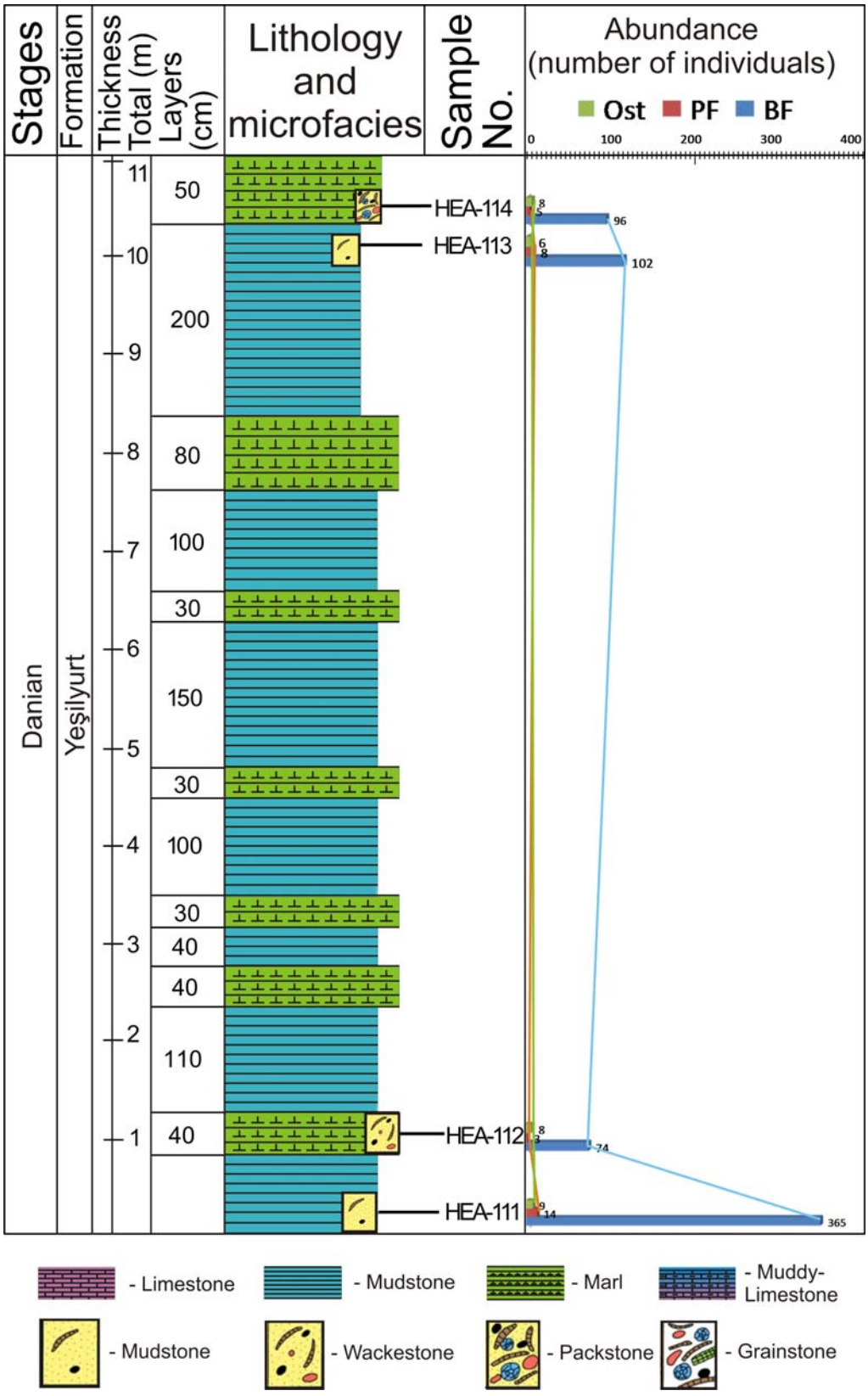

Figure A3. Detailed measured section (continued).

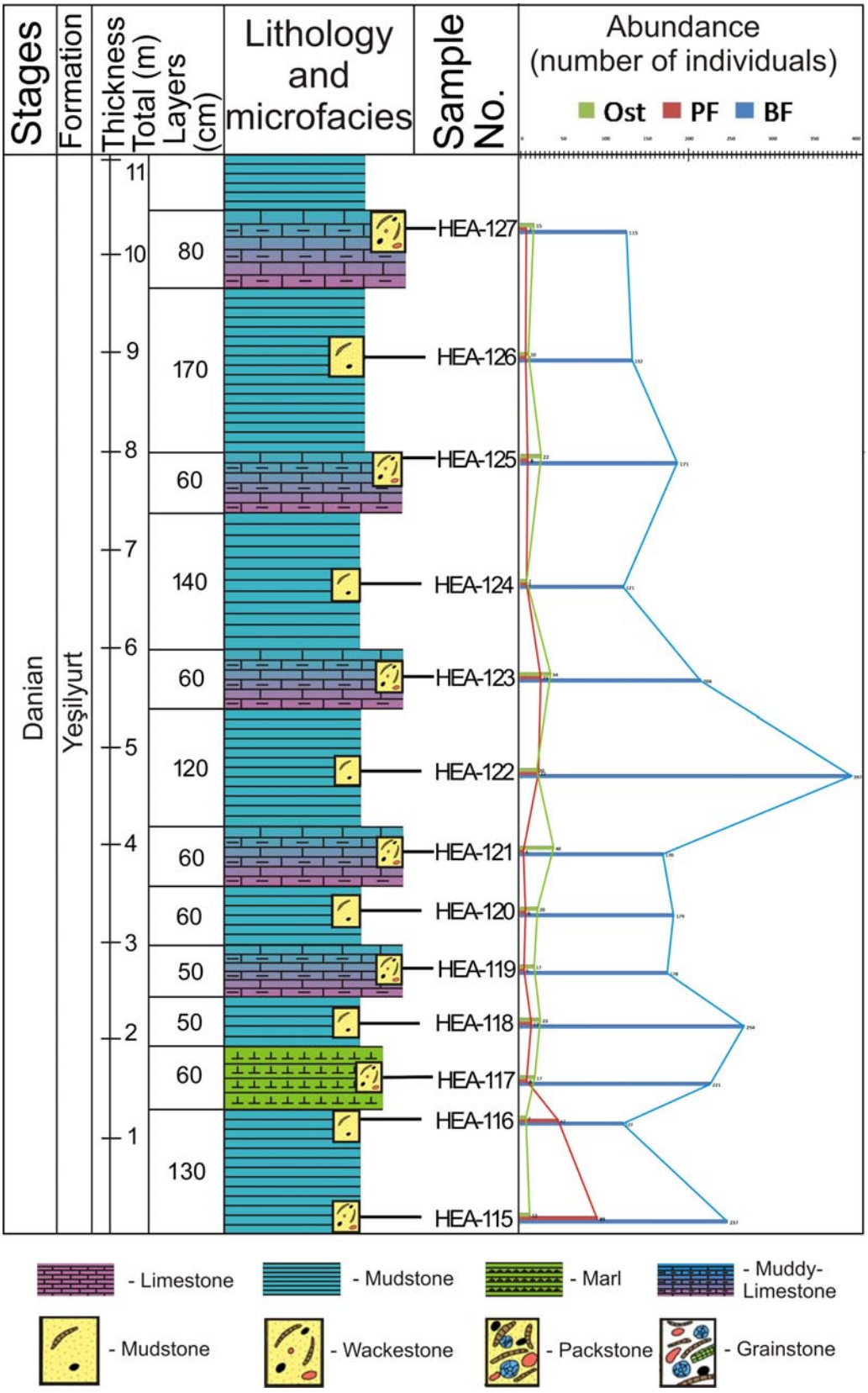

Figure A4. Detailed measured section (continued).

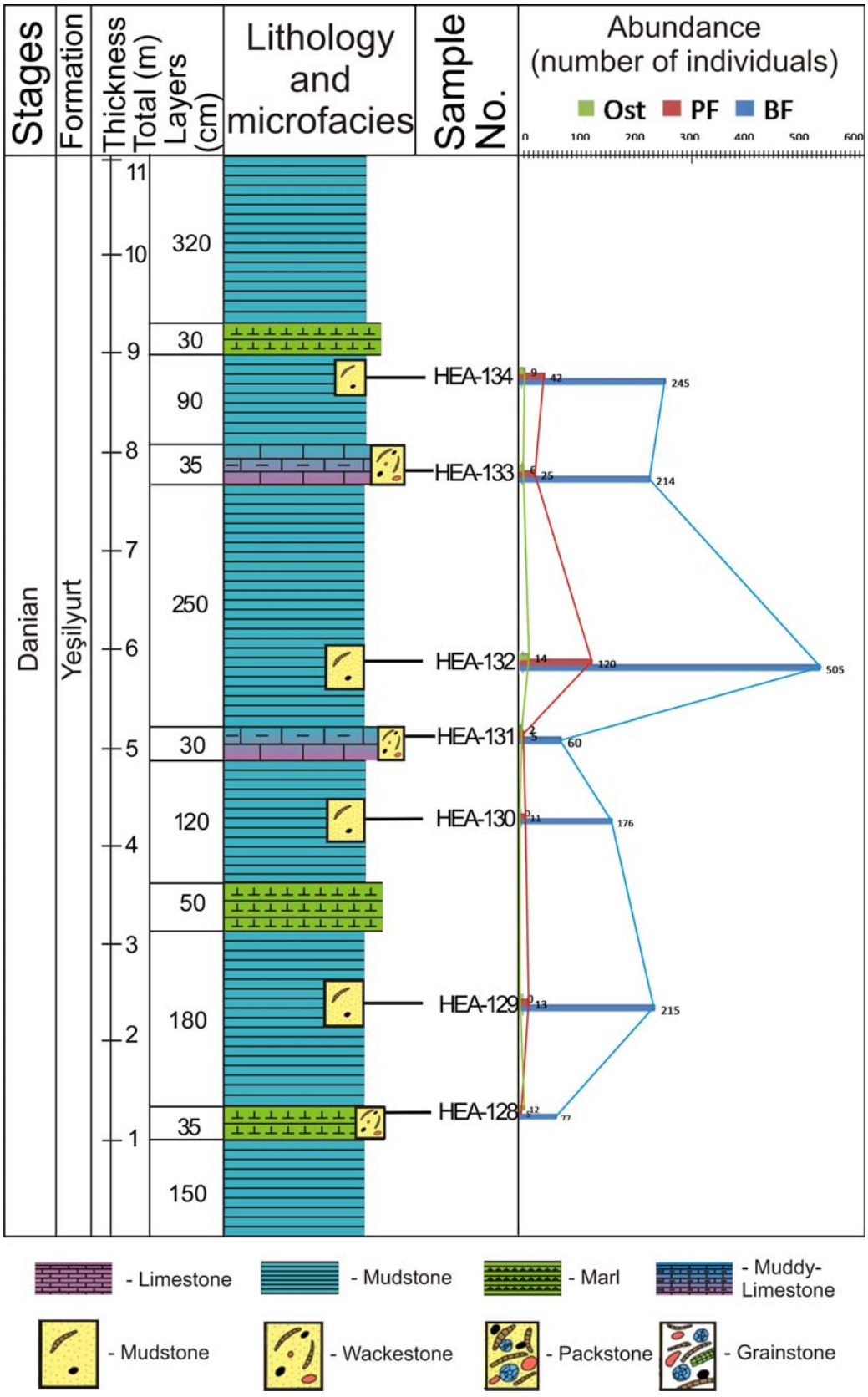

Figure A5. Detailed measured section (continued).

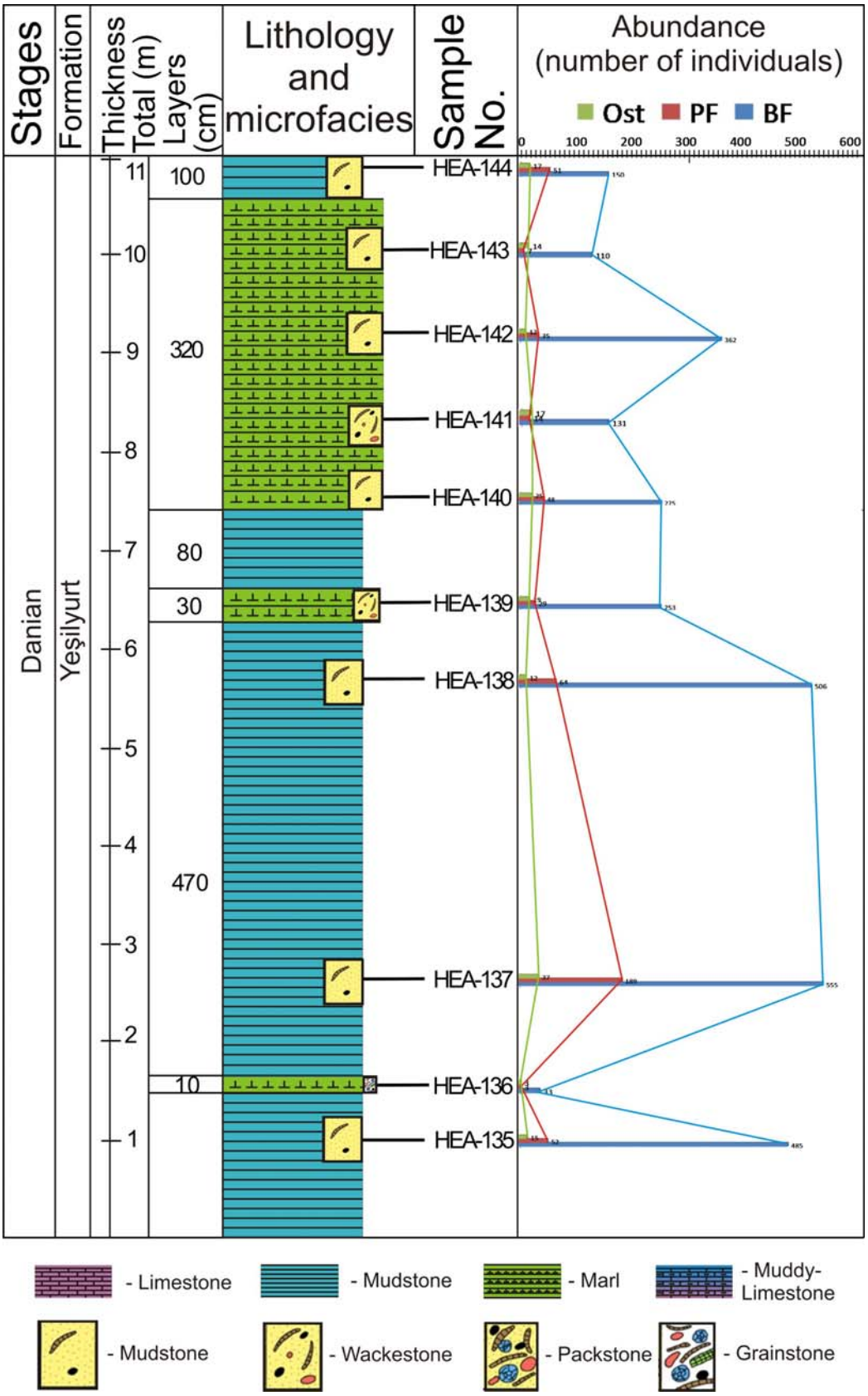

Figure A6. Detailed measured section (continued).

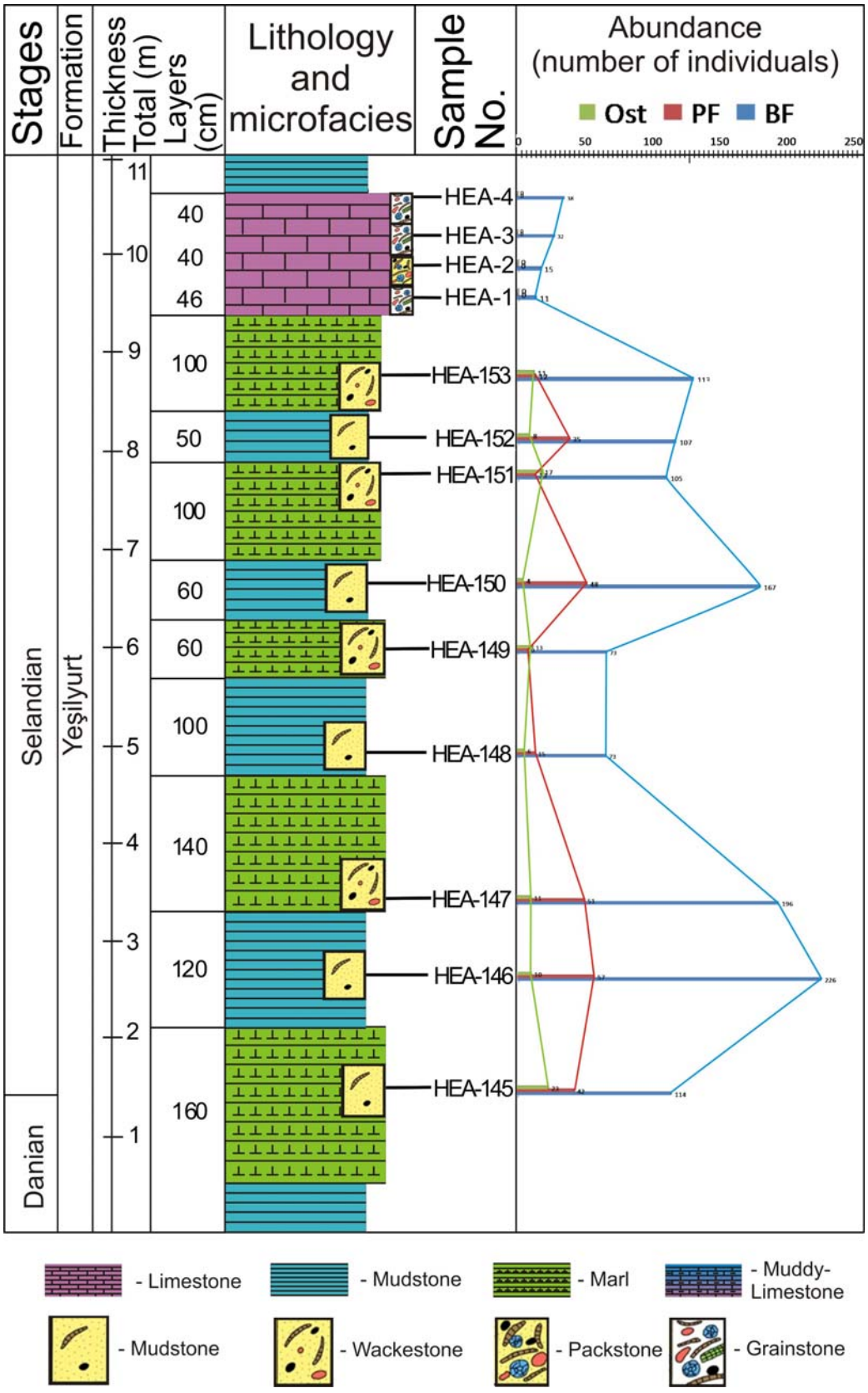

Figure A7. Detailed measured section (continued).

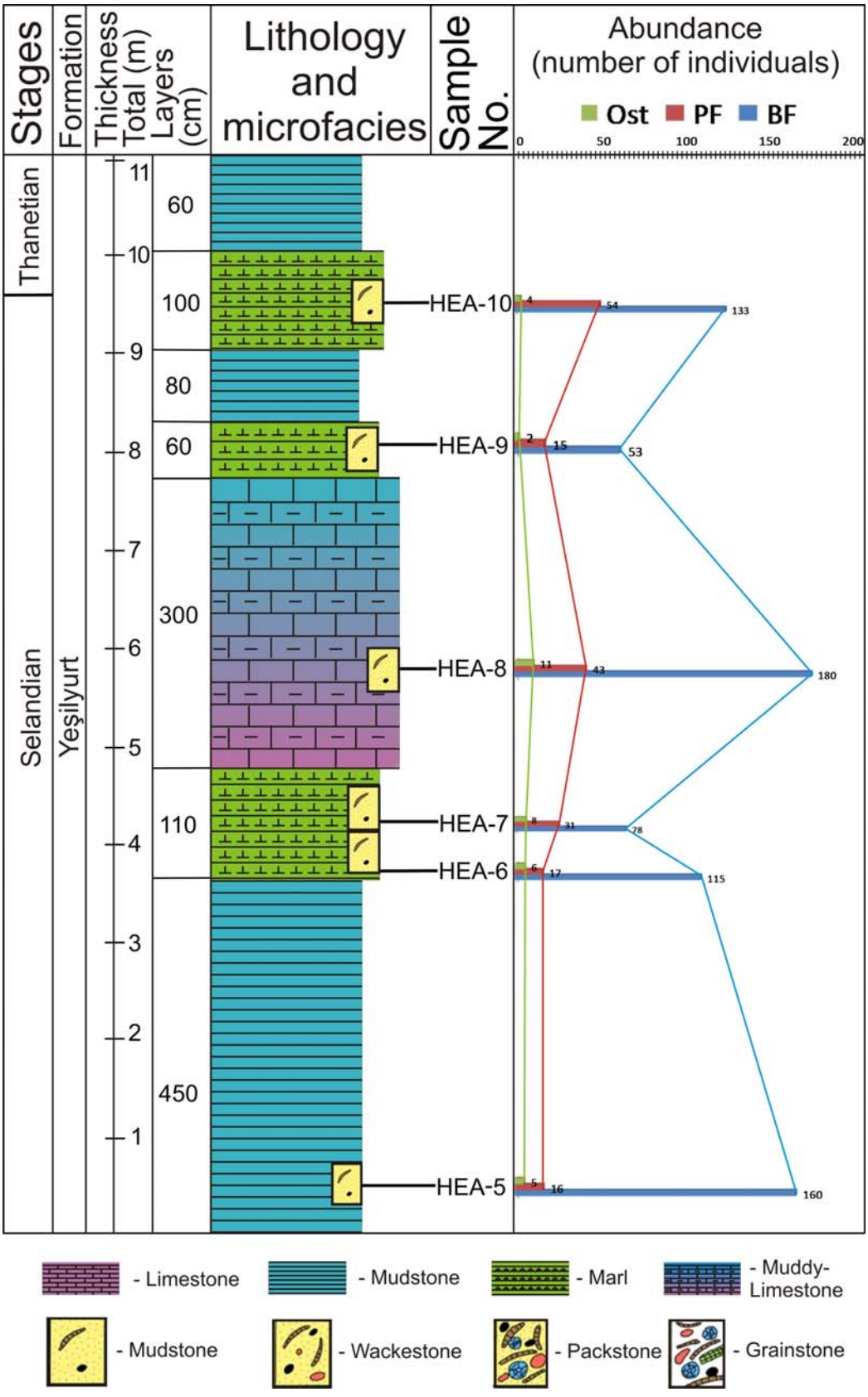

Figure A8. Detailed measured section (continued).

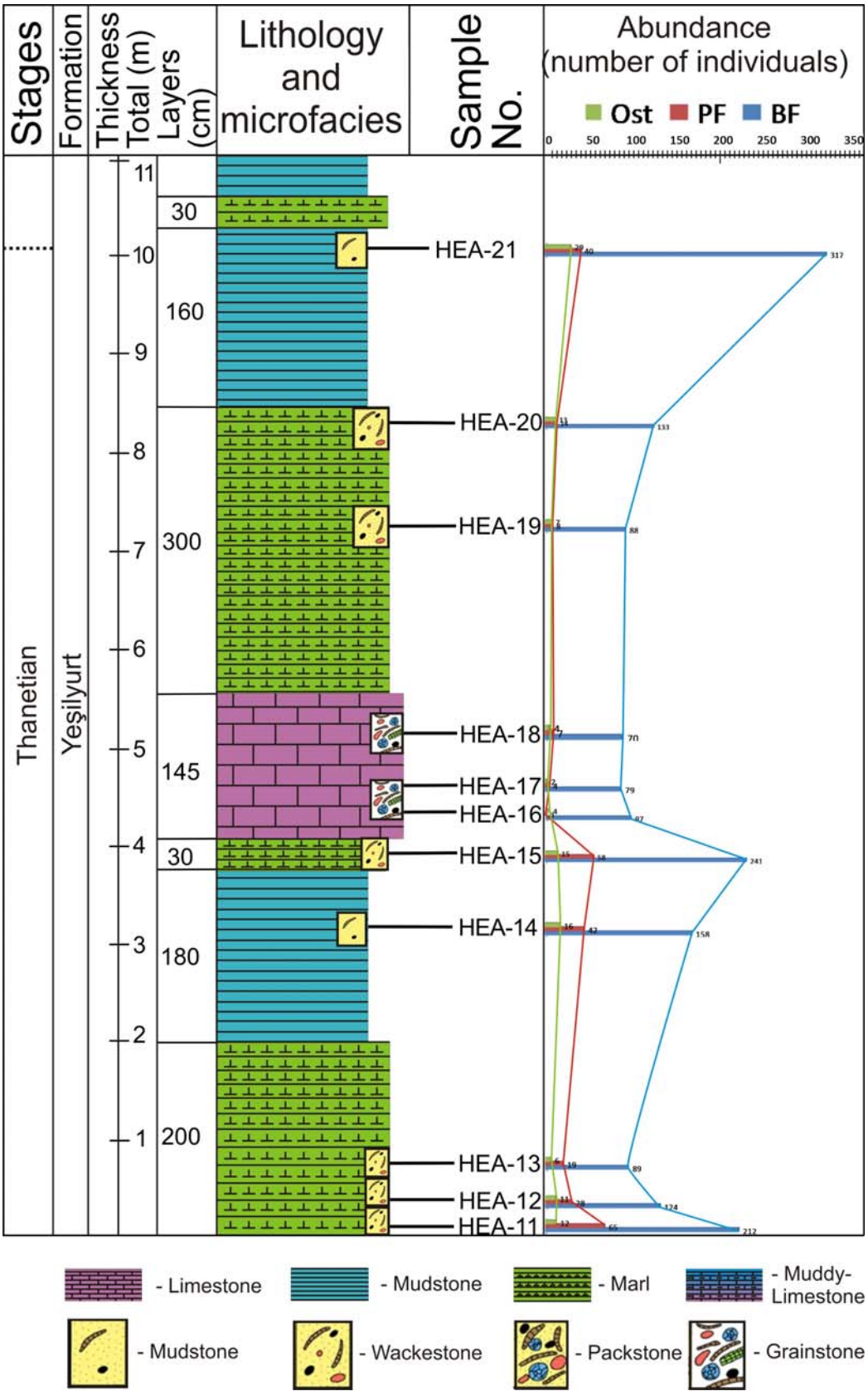

Figure A9. Detailed measured section (continued).

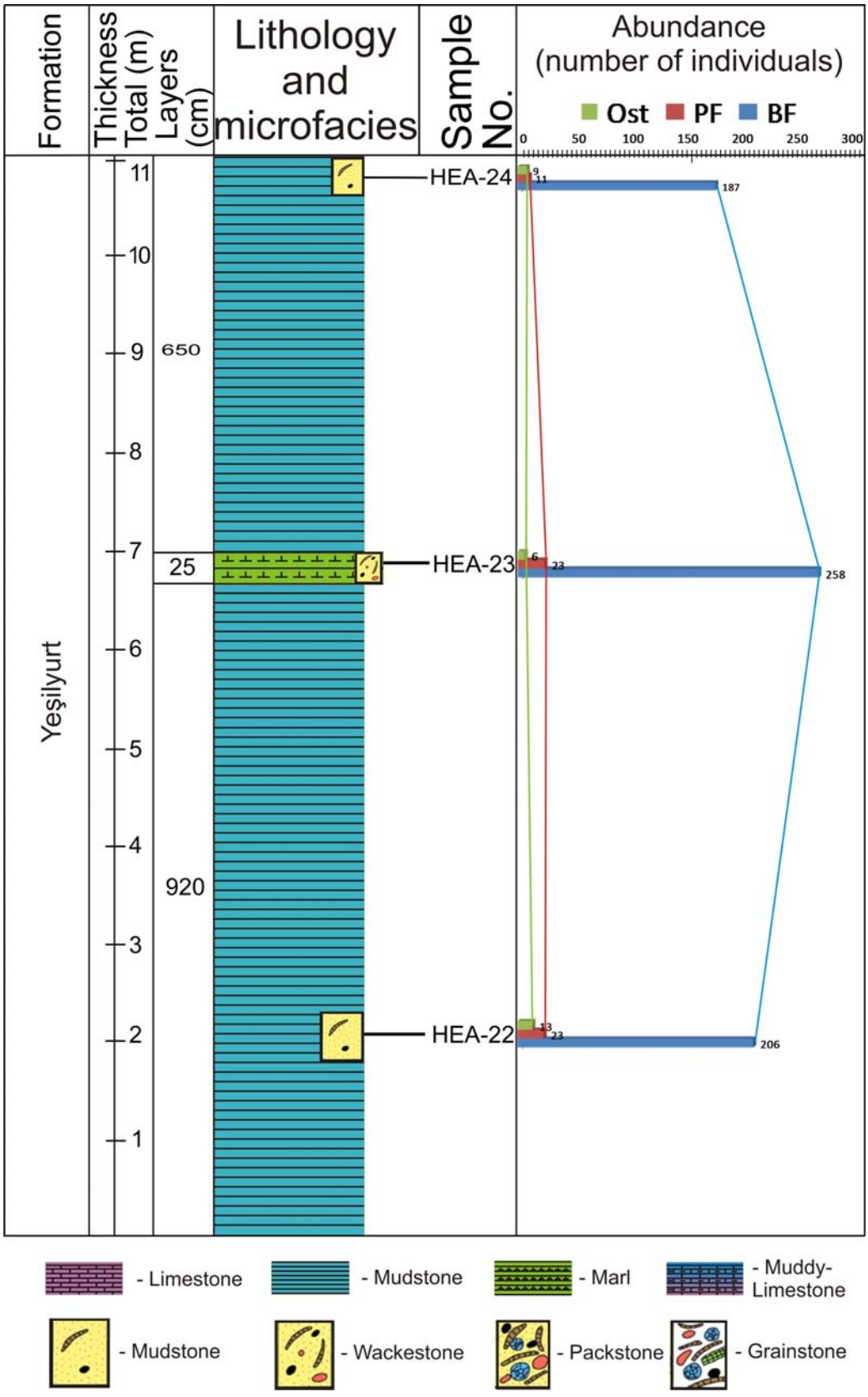

Figure A10. Detailed measured section (continued).

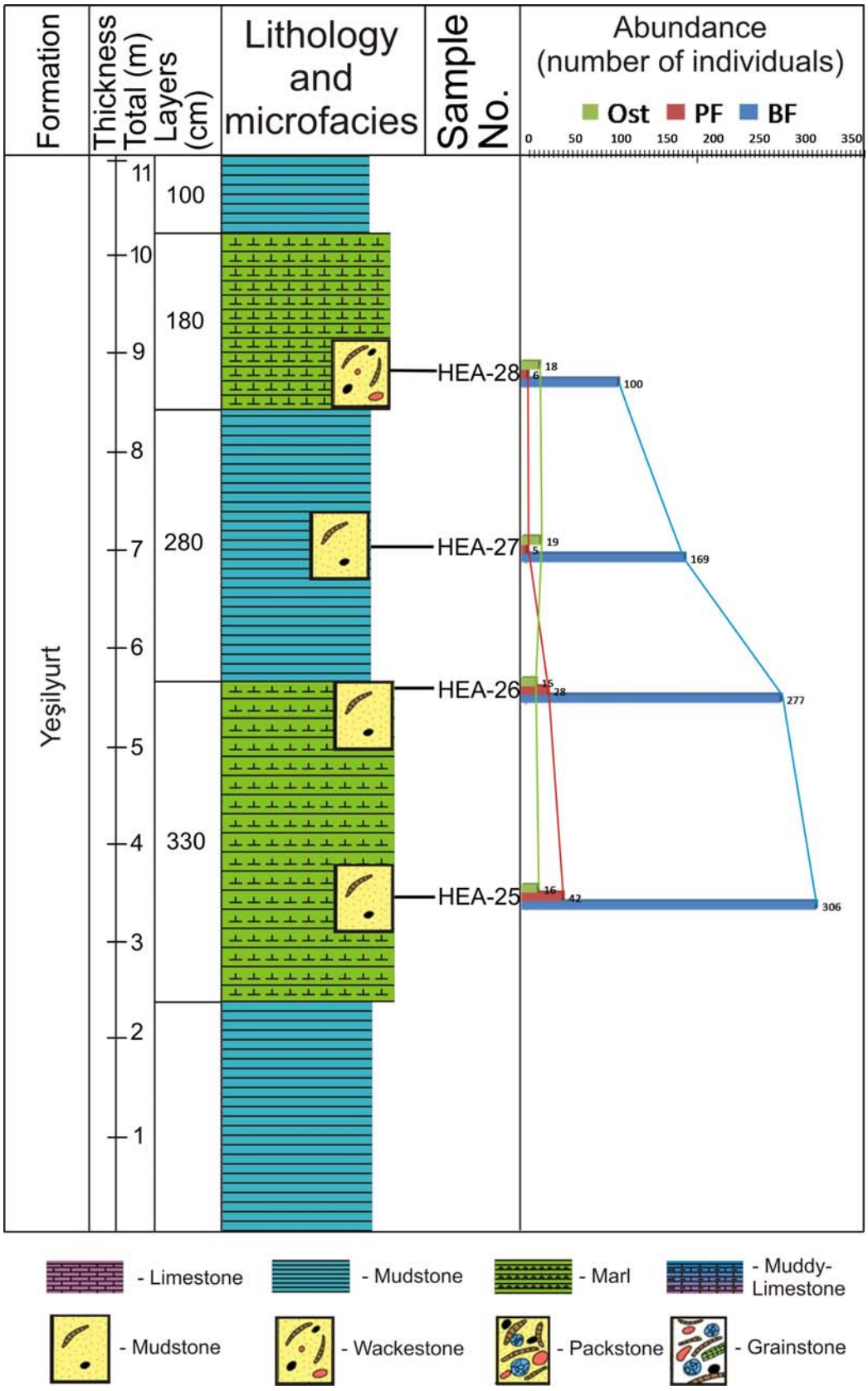

Figure A11. Detailed measured section (continued).

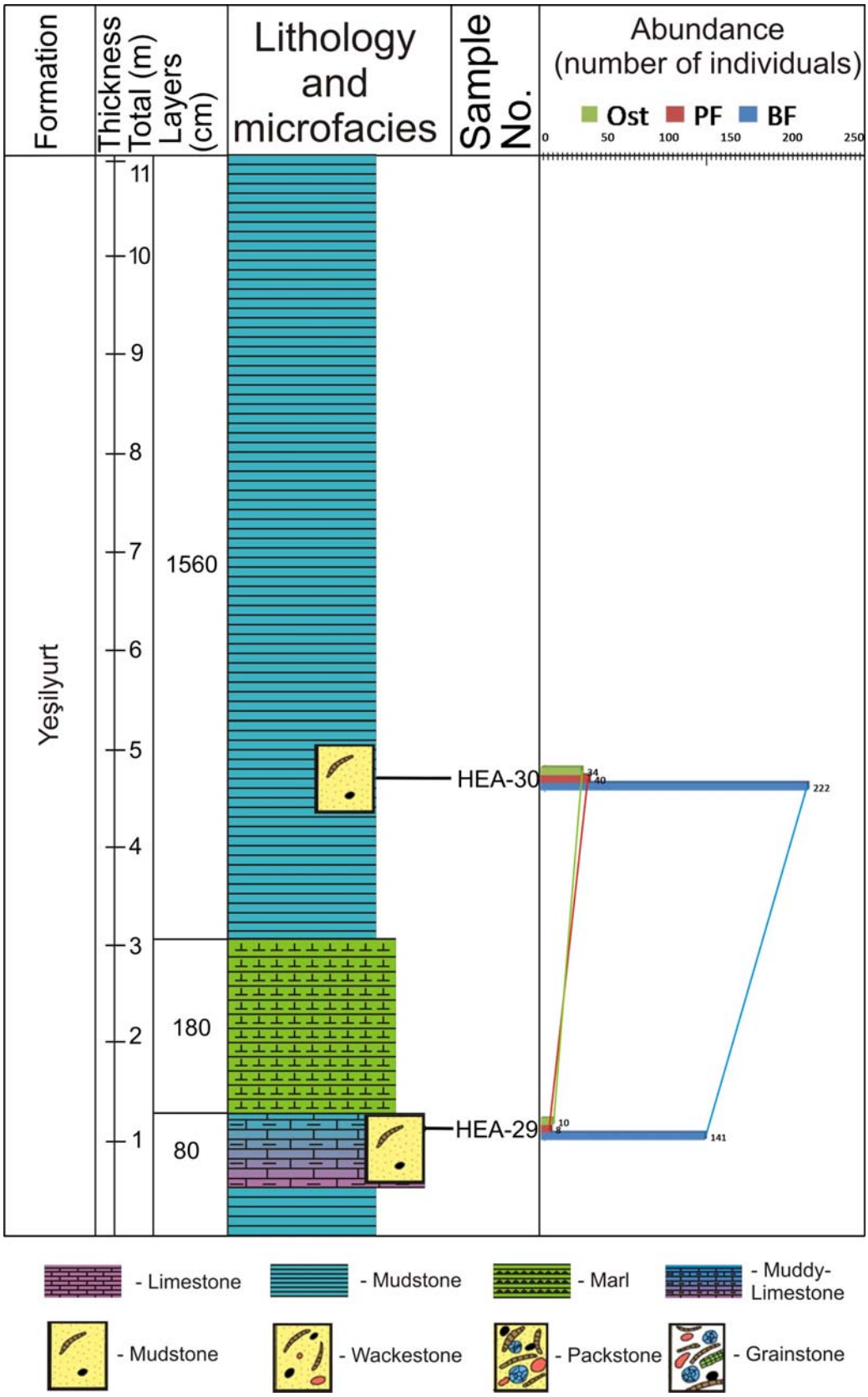

Figure A12. Detailed measured section (continued).

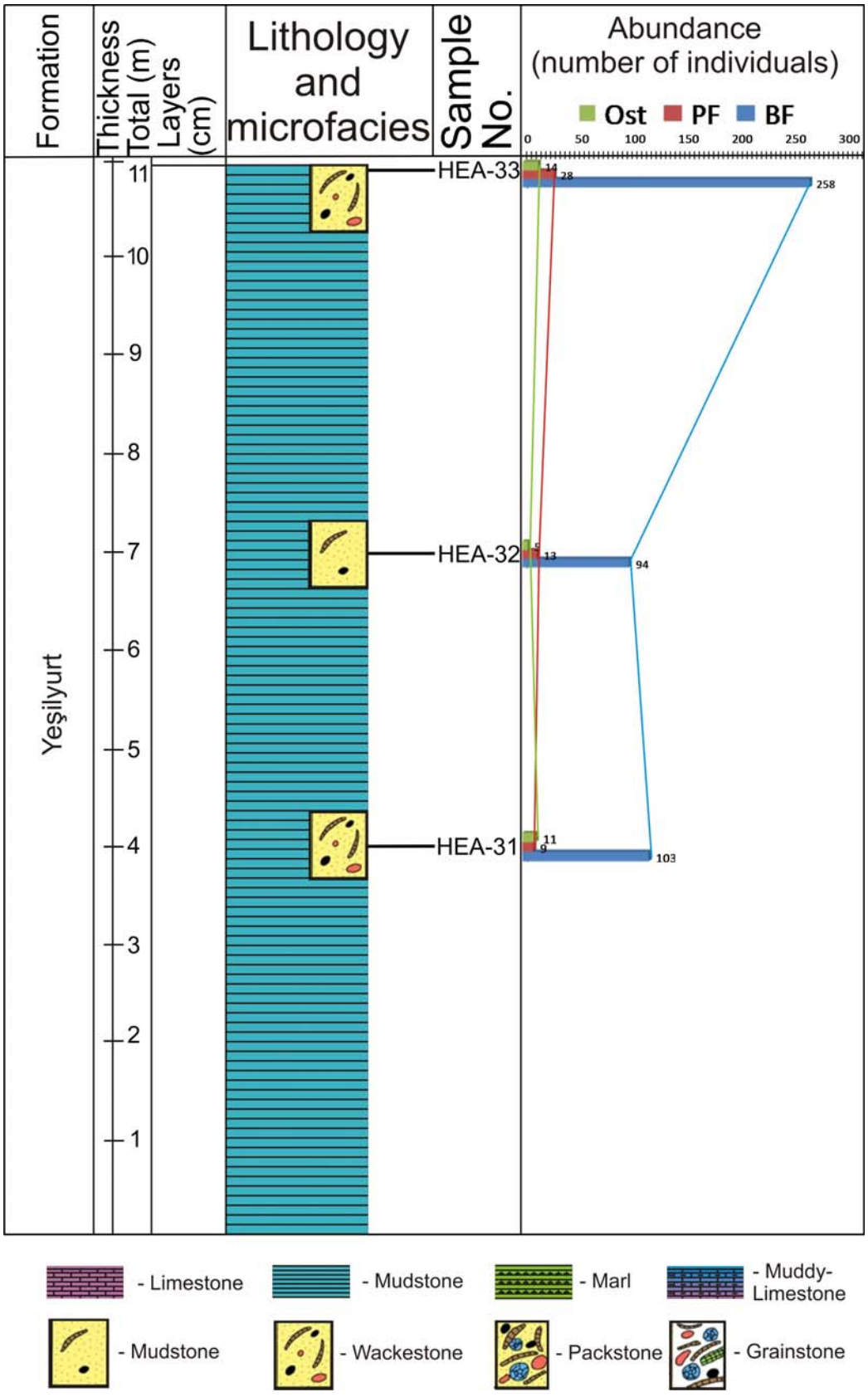

Figure A13. Detailed measured section (continued).

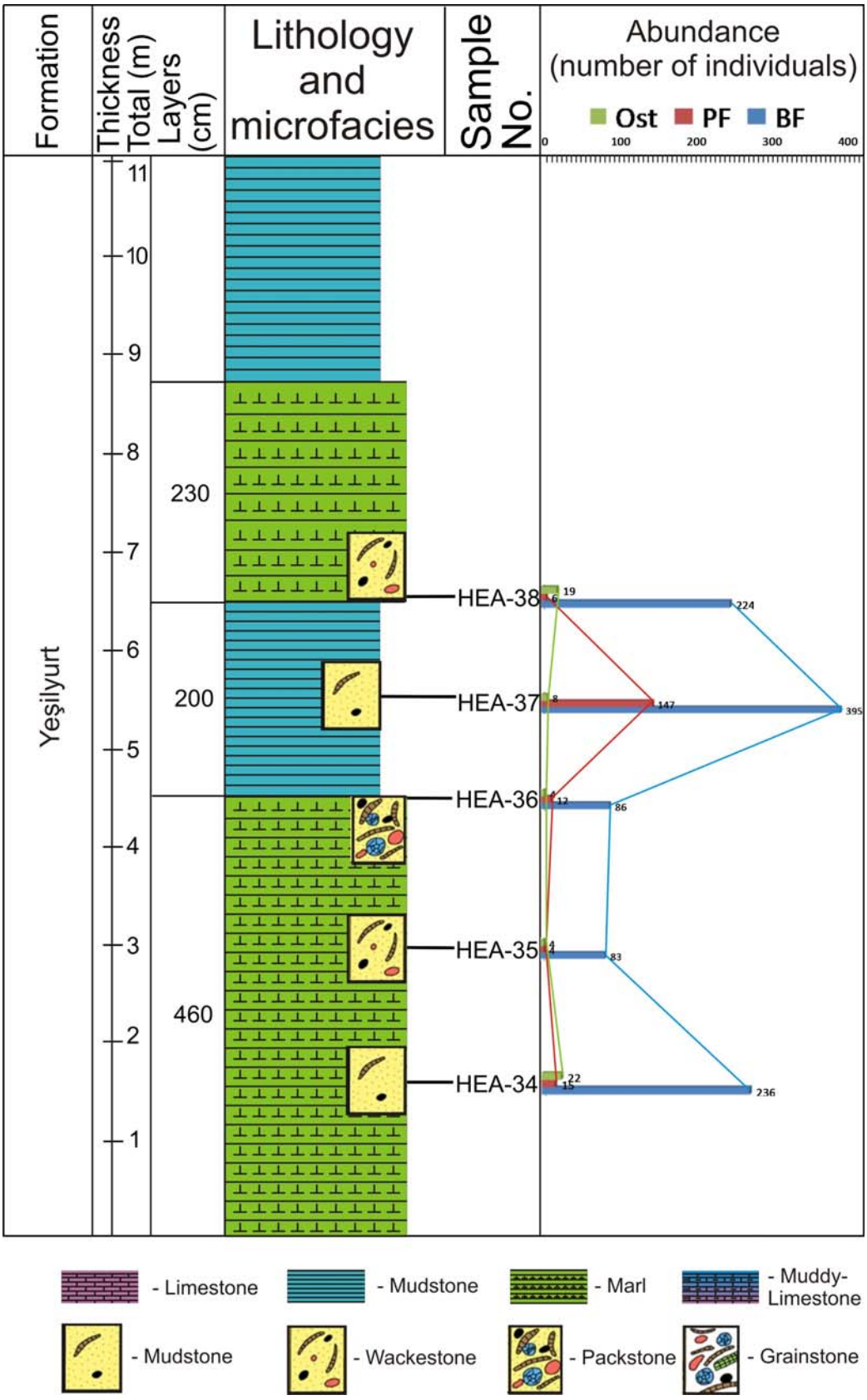

Figure A14. Detailed measured section (continued).

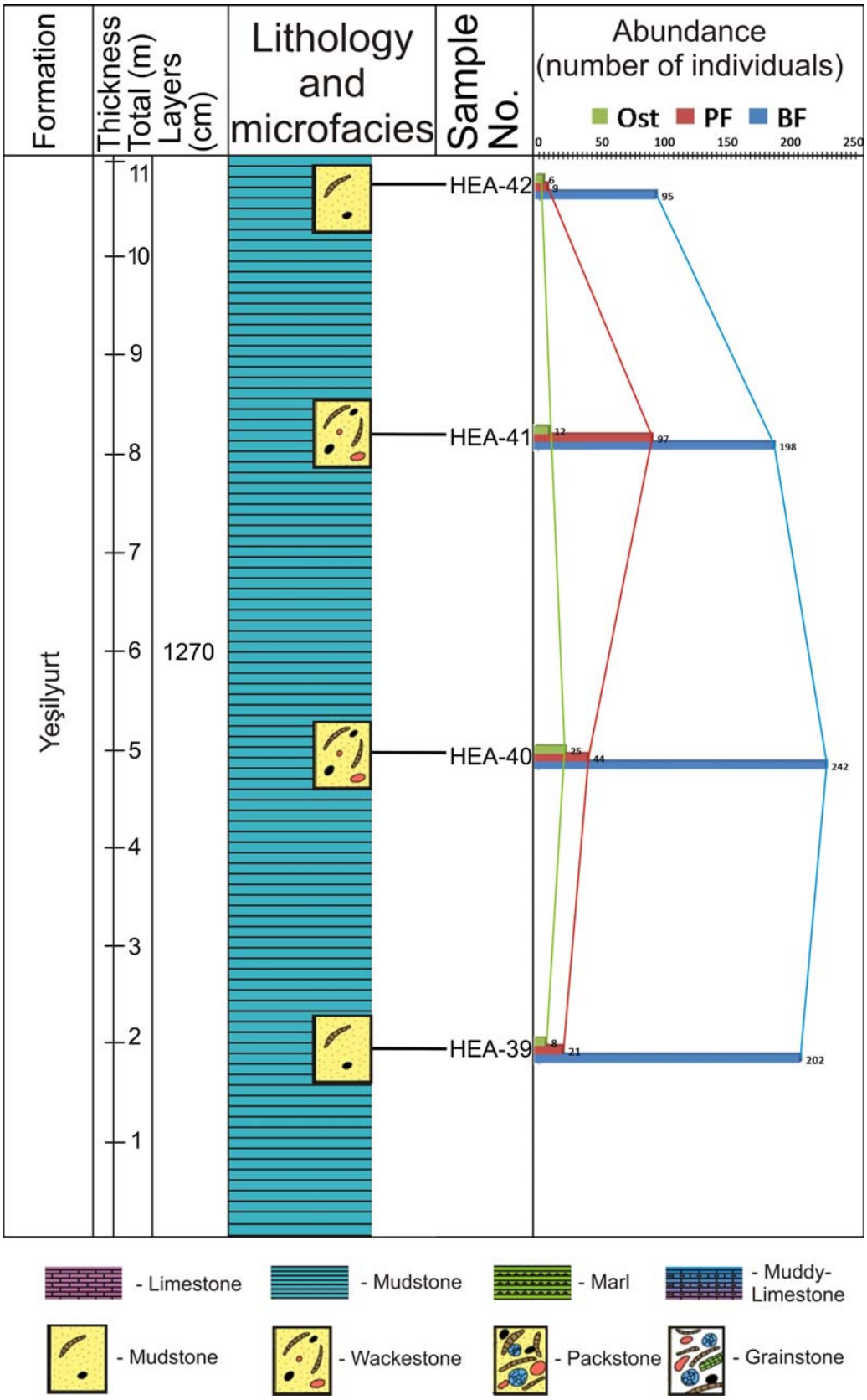

Figure A15. Detailed measured section (continued).

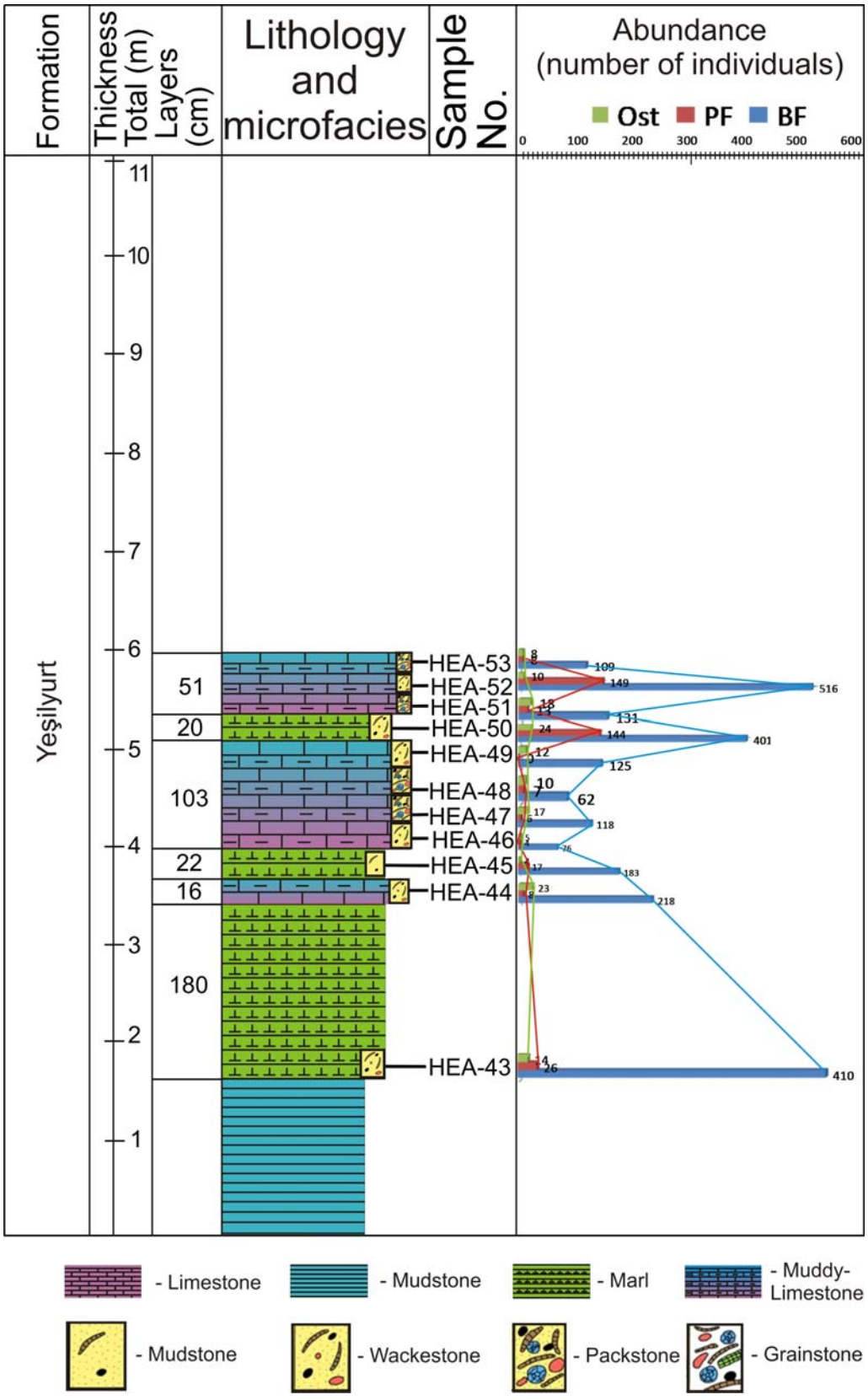

Figure A16. Detailed measured section (continued).

LIMESTONES

Samples No	Quartz	Rock fragments	Cement	Plagioclase	Matrix	Muscovite	Opaque	Chlorite	FF/Bioclast	Biotite	Facies	Classification
	%	%	%	%	%	%	%	%	%	%		
HEA-1	0.6	-	7.1	-	37.1	-	-	-	55.2	-	Limestone	Grainstone
HEA-2	0.2	-	2.3	-	58.8	0.4	-	-	38.3	-	Limestone	Packstone
HEA-3	0.4	-	14.3	-	38.6	-	-	-	46.5	-	Limestone	Grainstone
HEA-4	-	-	4	-	26.6	-	-	-	69.3	-	Limestone	Grainstone
HEA-16	-	-	8.8	-	17	0.2	-	-	73.8	-	Limestone	Grainstone
HEA-17	-	-	15.1	-	11.6	-	-	-	73.2	-	Limestone	Grainstone
HEA-18	-	-	0.6	-	3.2	-	-	-	96.1	-	Limestone	Grainstone
HEA-8	1.9	-	-	-	95.1	0.2	-	-	2.6	-	Muddy-Limestone	Mudstone
HEA-29	3.7	-	-	-	93.1	0.1	-	-	3	-	Muddy-Limestone	Mudstone
HEA-44	6.3	-	-		75.2	0.8	-	-	17.4	-	Muddy-Limestone	Wackestone
HEA-46	4	-	-	-	81.1	1	-	-	13.8	-	Muddy-Limestone	Wackestone
HEA-47	1.3	-	-	-	67.9	0.5	-	-	30.1	-	Muddy-Limestone	Packstone
HEA-48	0.9	-	-	-	65.1	0.3	-	-	33.7	-	Muddy-Limestone	Packstone
HEA-49	3.6	-	-	-	77.6	0.2	-	-	18.4	-	Muddy-Limestone	Wackestone
HEA-51	5	-	-	-	61.5	0.1	-	-	33	-	Muddy-Limestone	Packstone
HEA-52	2.8	-	-	-	80.7	1	-	-	15.4	-	Muddy-Limestone	Wackestone
HEA-53	2.4	-	2.4	-	58.1	-	-	-	37	-	Muddy-Limestone	Packstone
HEA-110	0.4	-	2.1	-	57.1	0.3	-	-	39.9	-	Muddy-Limestone	Packstone
HEA-119	4.4	-	-	-	81.7	1.7	-	-	12.2	-	Muddy-Limestone	Wackestone
HEA-121	3.3	-	-	-	79.5	0.6	-	-	16.6	-	Muddy-Limestone	Wackestone
HEA-123	2.7	-	-	-	77.6	-	-	-	19.7	-	Muddy-Limestone	Wackestone
HEA-125	3.8	-	-	-	83.9	0.4	-	-	11.9	-	Muddy-Limestone	Wackestone
HEA-127	1.8	-	-	-	84.7	0.7	-	-	12.8	-	Muddy-Limestone	Wackestone
HEA-131	2.6	-	-	-	78.4	0.1	-	-	18.9	-	Muddy-Limestone	Wackestone
HEA-133	4.1	-	-	-	82.4	0.2	-	-	13.3	-	Muddy-Limestone	Wackestone

Table B1. Point counting data derived from the samples of studied section (limestones).

MARLS

Samples No	Quartz	Rock fragments	Cement	Plagioclase	Matrix	Muscovite	Opaque	Chlorite	FF/Bioclast	Biotite	Facies	Classification
	%	%	%	%	%	%	%	%	%	%		
HEA-6	0.5	-	-	-	94.8	0.1	-	-	4.6	-	Marl	Mudstone
HEA-7	0.7	-	-	-	93.6	0.5	-	-	5.2	-	Marl	Mudstone
HEA-9	0.2	-	-	-	94.9	-	-	-	4.9	-	Marl	Mudstone
HEA-10	0.8	-	-	-	95.4	0.1	-	-	3.7	-	Marl	Mudstone
HEA-11	0.9	-	-	-	87.8	-	-	-	11.3	-	Marl	Wackestone
HEA-12	0.2	-	-	-	86.3	-	-	-	13.5	-	Marl	Wackestone
HEA-13	1.4	-	-	-	83	0.1	-	-	15.5	-	Marl	Wackestone
HEA-15	1.1	-	-	-	83.8	0.4	-	-	14.7	-	Marl	Wackestone
HEA-19	0.1	-	-	-	82.7	-	-	-	17.2	-	Marl	Wackestone
HEA-20	0.5	-	-	-	88.5	0.2	-	-	10.8	-	Marl	Wackestone
HEA-23	2.1	-	-	-	85.9	0.7	-	-	11.3	-	Marl	Wackestone
HEA-25	1.2	-	-	-	93.1	0.2	-	-	5.5	-	Marl	Mudstone
HEA-26	0.3	-	-	-	96.1	0.1	-	-	3.5	-	Marl	Mudstone
HEA-28	0.2	-	-	-	89.9	-	-	-	9.9	-	Marl	Wackestone
HEA-34	3.1	-	-	-	92.4	0.2	-	-	4.3	-	Marl	Mudstone
HEA-35	1.8	-	-	-	92.9	-	-	-	5.3	-	Marl	Wackestone
HEA-36	0.8	-	-	-	69.4	-	-	-	29.8	-	Marl	Packestone
HEA-38	0.3	-	-	-	79.3	-	-	-	20.4	-	Marl	Wackestone
HEA-43	2	-	-	-	84.7	0.2	-	-	13.1	-	Marl	Wackestone
HEA-45	2.8	-	-	-	96.1	0.4	-	-	0.7	-	Marl	Mudstone
HEA-50	0.9	-	-	-	88.9	-	-	-	10.2	-	Marl	Wackestone

Table B2. Point counting data derived from the samples of studied section (marls).

MARLS

Samples No	Quartz	Rock fragments	Cement	Plagioclase	Matrix	Muscovite	Opaque	Chlorite	FF/Bioclast	Biotite	Facies	Classification
	%	%	%	%	%	%	%	%	%	%		
HEA-106	2.4	-	-	-	83.7	0.7	-	-	13.2	-	Marl	Wackestone
HEA-107	3.1	-	-	-	84.4	0.2	-	-	12.3	-	Marl	Wackestone
HEA-108	4.5	-	-	-	79.7	0.5	-	-	15.3	-	Marl	Wackestone
HEA-112	5.2	-	-	-	83.1	0.2	-	-	11.5	-	Marl	Wackestone
HEA-114	1.5	-	-	-	59.4	0.1	-	-	39	-	Marl	Packstone
HEA-117	2.7	-	-	-	84.1	0.3	-	-	12.9	-	Marl	Wackestone
HEA-128	3.6	-	-	-	82.1	0.2	-	-	14.1	-	Marl	Wackestone
HEA-136	0.1	-	31.7	-	17.5	-	-	-	50.7	-	Marl	Grainstone
HEA-139	1.5	-	-	-	87.6	-	-	-	10.9	-	Marl	Wackestone
HEA-140	2.9	-	-	-	95.5	-	-	-	1.6	-	Marl	Mudstone
HEA-141	1.7	-	-	-	88.5	0.3	-	-	9.5	-	Marl	Wackestone
HEA-142	0.5	-	-	-	95.2	0.1	-	-	4.2	-	Marl	Mudstone
HEA-143	1.7	-	-	-	90.8	0.2	-	-	7.3	-	Marl	Mudstone
HEA-145	0.4	-	-	-	94.8	-	-	-	4.8	-	Marl	Mudstone
HEA-147	2.7	-	-	-	82.5	0.9	-	-	13.9	-	Marl	Wackestone
HEA-149	1.8	-	-	-	83	0.2	-	-	15	-	Marl	Wackestone
HEA-151	1.2	-	-	-	82.7	0.3	-	-	15.8	-	Marl	Wackestone
HEA-153	0.3	-	-	-	81.6	-	-	-	18.1	-	Marl	Wackestone

Table B3. Point counting data derived from the samples of studied section (marls).

MUDSTONES

Samples No	Quartz	Rock fragments	Cement	Plagioclase	Matrix	Muscovite	Opaque	Chlorite	FF/Bioclast	Biotite	Facies	Classification
	%	%	%	%	%	%	%	%	%	%		
HEA-101	18.3	-	-	-	80.8	0.3	-	-	0.6	-	Mudstone	Fine
HEA-104	8.9	-	-	-	88.9	0.2	-	-	2	-	Mudstone	Very fine
HEA-105	15.3	0.2	-	-	83.5	0.1	-	-	0.9	-	Mudstone	Fine
HEA-109	6.4	-	-	-	93.1	0.1	-	-	0.4	-	Mudstone	Very fine
HEA-111	7.2	-	-	-	88.6	0.5	-	-	3.7	-	Mudstone	Very fine
HEA-113	8.4	-	-	-	88.9	0.2	-	-	2.5	-	Mudstone	Very fine
HEA-115	2.7	-	-	-	85.4	0.1	-	-	11.8	-	Mudstone	Very fine
HEA-116	8.2	-	-	-	90	0.4	-	-	1.4	-	Mudstone	Very fine
HEA-118	4.5	-	-	-	92.4	0.2	-	-	2.9	-	Mudstone	Very fine
HEA-120	3.7	0.1	-	-	91.9	0.1	-	-	4.2	-	Mudstone	Very fine
HEA-122	5.1	-	-	-	90.9	0.7	-	-	3.3	-	Mudstone	Very fine
HEA-124	6.2	-	-	-	89.8	0.4	-	-	3.6	-	Mudstone	Very fine
HEA-126	2.2	0.2	-	-	94.1	0.3	-	-	3.2	-	Mudstone	Very fine
HEA-129	6	0.1	-	-	91	0.1	-	-	2.8	-	Mudstone	Very fine
HEA-130	3.1	-	-	-	96.1	-	-	-	0.8	-	Mudstone	Very fine
HEA-132	2.8	-	-	-	95.1	0.1	-	-	2	-	Mudstone	Very fine
HEA-134	5.5	-	-	-	90.2	0.5	-	-	3.8	-	Mudstone	Very fine
HEA-135	2.1	-	-	-	93.1	0.3	-	-	4.5	-	Mudstone	Very fine
HEA-137	3.3	-	-	-	93.2	-	-	-	3.5	-	Mudstone	Very fine
HEA-138	5.1	-	-	-	90.3	0.5	-	-	4.1	-	Mudstone	Very fine
HEA-144	3.2	-	-	-	94.9	0.2	-	-	1.7	-	Mudstone	Very fine
HEA-146	5.7	-	-	-	93.3	0.3	-	-	0.7	-	Mudstone	Very fine
HEA-148	5.3	-	-	-	93.5	0.1	-	-	1.1	-	Mudstone	Very fine
HEA-150	2.4	0.2	-	-	95.8	-	-	-	1.6	-	Mudstone	Very fine
HEA-152	1.9	-	-	-	91.4	0.3	-	-	6.4	-	Mudstone	Very fine

Table B4. Point counting data derived from the samples of studied section (mudstones).

MUDSTONES

Samples No	Quartz	Rock fragments	Cement	Plagioclase	Matrix	Muscovite	Opaque	Chlorite	FF/Bioclast	Biotite	Facies	Classification
	%	%	%	%	%	%	%	%	%	%		
HEA-5	1.5	-	-	-	92.9	0.4	-	-	5.2	-	Mudstone	Very fine
HEA-14	2.3	-	-	-	93.8	0.5	-	-	3.4	-	Mudstone	Very fine
HEA-21	6.7	0.2	-	-	87.8	0.8	-	-	4.5	-	Mudstone	Very fine
HEA-22	5.3	0.3	-	-	91.2	0.3	-	-	2.9	-	Mudstone	Very fine
HEA-24	8.5	0.1	-	-	85.7	0.1	-	-	5.6	-	Mudstone	Very fine
HEA-27	3.2	-	-	-	93.9	1.2	-	-	1.7	-	Mudstone	Very fine
HEA-30	9.1	0.5	-	-	83.3	0.3	-	-	6.8	-	Mudstone	Very fine
HEA-31	11.2	0.7	-	-	73.8	0.9	-	-	13.4	-	Mudstone	Fine
HEA-32	7.4	-	-	-	90.3	0.2	-	-	2.1	-	Mudstone	Very fine
HEA-33	2.8	-	-	-	84.6	0.1	-	-	12.5	-	Mudstone	Very fine
HEA-37	1.2	0.1	-	-	96.9	0.4	-	-	1.4	-	Mudstone	Very fine
HEA-39	14.3	0.4	-	-	79.1	2.1	-	-	4.1	-	Mudstone	Fine
HEA-40	10.9	-	-	-	74.7	0.2	-	-	14.2	-	Mudstone	Fine
HEA-41	5.9	-	-	-	84	1.4	-	-	8.7	-	Mudstone	Very fine
HEA-42	11.7	0.5	-	-	86.4	0.5	-	-	0.9	-	Mudstone	Fine

SANDSTONES

Samples No	Quarts	Rock fragments	Cement (Calcite)	Plagioclase	Matrix	Muscovite	Biotite	Facies	Classification
	%	%	%	%	%	%	%		
HEA-102	**40,5**	**35**	**9.8**	**1.4**	**11.4**	**0.9**	**0.7**	Sandstone	Litharenite
HEA-103	**21**	**63.3**	**10.5**	**3**	**0.8**	**0.7**	**0.4**	Sandstone	Litharenite

Table B5. Point counting data derived from the samples of studied section (mudstones and sandstones).

Samples No	Quartz	Rock fragments	Cement	Plagioclase	Matrix	Muscovite	Opaque	Chlorite	FF/Bioclast	Biotite	Facies	Classification
	%	%	%	%	%	%	%	%	%	%		
HEA-53	2.4	-	2.4	-	58.1	-	-	-	37	-	Muddy-Limestone	Packstone
HEA-52	2.8	-	-	-	80.7	1	-	-	15.4	-	Muddy-Limestone	Wackestone
HEA-51	5	-	-	-	61.5	0.1	-	-	33	-	Muddy-Limestone	Packstone
HEA-50	0.9	-	-	-	88.9	-	-	-	10.2	-	Marl	Wackestone
HEA-49	3.6	-	-	-	77.6	0.2	-	-	18.4	-	Muddy-Limestone	Wackestone
HEA-48	0.9	-	-	-	65.1	0.3	-	-	33.7	-	Muddy-Limestone	Packstone
HEA-47	1.3	-	-	-	67.9	0.5	-	-	30.1	-	Muddy-Limestone	Packstone
HEA-46	4	-	-	-	81.1	1	-	-	13.8	-	Muddy-Limestone	Wackestone
HEA-45	2.8	-	-	-	96.1	0.4	-	-	0.7	-	Marl	Mudstone
HEA-44	6.3	-	-	-	75.2	0.8	-	-	17.4	-	Muddy-Limestone	Wackestone
HEA-43	2	-	-	-	84.7	0.2	-	-	13.1	-	Marl	Wackestone
HEA-42	11.7	0.5	-	-	86.4	0.5	-	-	0.9	-	Mudstone	Fine
HEA-41	5.9	-	-	-	84	1.4	-	-	8.7	-	Mudstone	Very fine
HEA-40	10.9	-	-	-	74.7	0.2	-	-	14.2	-	Mudstone	Fine
HEA-39	14.3	0.4	-	-	79.1	2.1	-	-	4.1	-	Mudstone	Fine
HEA-38	0.3	-	-	-	79.3	-	-	-	20.4	-	Marl	Wackestone
HEA-37	1.2	0.1	-	-	96.9	0.4	-	-	1.4	-	Mudstone	Very fine
HEA-36	0.8	-	-	-	69.4	-	-	-	29.8	-	Marl	Packstone
HEA-35	1.8	-	-	-	92.9	-	-	-	5.3	-	Marl	Wackestone
HEA-34	3.1	-	-	-	92.4	0.2	-	-	4.3	-	Marl	Mudstone
HEA-33	2.8	-	-	-	84.6	0.1	-	-	12.5	-	Mudstone	Very fine
HEA-32	7.4	-	-	-	90.3	0.2	-	-	2.1	-	Mudstone	Very fine
HEA-31	11.2	0.7	-	-	73.8	0.9	-	-	13.4	-	Mudstone	Fine
HEA-30	9.1	0.5	-	-	83.3	0.3	-	-	6.8	-	Mudstone	Very fine
HEA-29	3.7	-	-	-	93.1	0.1	-	-	3	-	Muddy-Limestone	Mudstone
HEA-28	0.2	-	-	-	89.9	-	-	-	9.9	-	Marl	Wackestone
HEA-27	3.2	-	-	-	93.9	1.2	-	-	1.7	-	Mudstone	Very fine
HEA-26	0.3	-	-	-	96.1	0.1	-	-	3.5	-	Marl	Mudstone
HEA-25	1.2	-	-	-	93.1	0.2	-	-	5.5	-	Marl	Mudstone
HEA-24	8.5	0.1	-	-	85.7	0.1	-	-	5.6	-	Mudstone	Very fine
HEA-23	2.1	-	-	-	85.9	0.7	-	-	11.3	-	Marl	Wackestone
HEA-22	5.3	0.3	-	-	91.2	0.3	-	-	2.9	-	Mudstone	Very fine
HEA-21	6.7	0.2	-	-	87.8	0.8	-	-	4.5	-	Mudstone	Very fine
HEA-20	0.5	-	-	-	88.5	0.2	-	-	10.8	-	Marl	Wackestone
HEA-19	0.1	-	-	-	82.7	-	-	-	17.2	-	Marl	Wackestone
HEA-18	-	-	0.6	-	3.2	-	-	-	96.1	-	Limestone	Grainstone
HEA-17	-	-	15.1	-	11.6	-	-	-	73.2	-	Limestone	Grainstone
HEA-16	-	-	8.8	-	17	0.2	-	-	73.8	-	Limestone	Grainstone
HEA-15	1.1	-	-	-	83.8	0.4	-	-	14.7	-	Marl	Wackestone
HEA-14	2.3	-	-	-	93.8	0.5	-	-	3.4	-	Mudstone	Very fine
HEA-13	1.4	-	-	-	83	0.1	-	-	15.5	-	Marl	Wackestone
HEA-12	0.2	-	-	-	86.3	-	-	-	13.5	-	Marl	Wackestone
HEA-11	0.9	-	-	-	87.8	-	-	-	11.3	-	Marl	Wackestone
HEA-10	0.8	-	-	-	95.4	0.1	-	-	3.7	-	Marl	Mudstone
HEA-9	0.2	-	-	-	94.9	-	-	-	4.9	-	Marl	Mudstone
HEA-8	1.9	-	-	-	95.1	0.2	-	-	2.6	-	Muddy-Limestone	Mudstone
HEA-7	0.7	-	-	-	93.6	0.5	-	-	5.2	-	Marl	Mudstone
HEA-6	0.5	-	-	-	94.8	0.1	-	-	4.6	-	Marl	Mudstone
HEA-5	1.5	-	-	-	92.9	0.4	-	-	5.2	-	Mudstone	Very fine
HEA-4	-	-	4	-	26.6	-	-	-	69.3	-	Limestone	Grainstone
HEA-3	0.4	-	14.3	-	38.6	-	-	-	46.5	-	Limestone	Grainstone
HEA-2	0.2	-	2.3	-	58.8	0.4	-	-	38.3	-	Limestone	Packstone
HEA-1	0.6	-	7.1	-	37.1	-	-	-	55.2	-	Limestone	Grainstone
HEA-153	0.3	-	-	-	81.6	-	-	-	18.1	-	Marl	Wackestone
HEA-152	1.9	-	-	-	91.4	0.3	-	-	6.4	-	Mudstone	Very fine
HEA-151	1.2	-	-	-	82.7	0.3	-	-	15.8	-	Marl	Wackestone
HEA-150	2.4	0.2	-	-	95.8	-	-	-	1.6	-	Mudstone	Very fine
HEA-149	1.8	-	-	-	83	0.2	-	-	15	-	Marl	Wackestone
HEA-148	5.3	-	-	-	93.5	0.1	-	-	1.1	-	Mudstone	Very fine
HEA-147	2.7	-	-	-	82.5	0.9	-	-	13.9	-	Marl	Wackestone
HEA-146	5.7	-	-	-	93.3	0.3	-	-	0.7	-	Mudstone	Very fine
HEA-145	0.4	-	-	-	94.8	-	-	-	4.8	-	Marl	Mudstone
HEA-144	3.2	-	-	-	94.9	0.2	-	-	1.7	-	Mudstone	Very fine
HEA-143	1.7	-	-	-	90.8	0.2	-	-	7.3	-	Marl	Mudstone
HEA-142	0.5	-	-	-	95.2	0.1	-	-	4.2	-	Marl	Mudstone
HEA-141	1.7	-	-	-	88.5	0.3	-	-	9.5	-	Marl	Wackestone
HEA-140	2.9	-	-	-	95.5	-	-	-	1.6	-	Marl	Mudstone
HEA-139	1.5	-	-	-	87.6	-	-	-	10.9	-	Marl	Wackestone
HEA-138	5.1	-	-	-	90.3	0.5	-	-	4.1	-	Mudstone	Very fine
HEA-137	3.3	-	-	-	93.2	-	-	-	3.5	-	Mudstone	Very fine
HEA-136	0.1	-	31.7	-	17.5	-	-	-	50.7	-	Marl	Grainstone
HEA-135	2.1	-	-	-	93.1	0.3	-	-	4.5	-	Mudstone	Very fine
HEA-134	5.5	-	-	-	90.2	0.5	-	-	3.8	-	Mudstone	Very fine
HEA-133	4.1	-	-	-	82.4	0.2	-	-	13.3	-	Muddy-Limestone	Wackestone
HEA-132	2.8	-	-	-	95.1	0.1	-	-	2	-	Mudstone	Very fine
HEA-131	2.6	-	-	-	78.4	0.1	-	-	18.9	-	Muddy-Limestone	Wackestone
HEA-130	3.1	-	-	-	96.1	-	-	-	0.8	-	Mudstone	Very fine
HEA-129	6	0.1	-	-	91	0.1	-	-	2.8	-	Mudstone	Very fine
HEA-128	3.6	-	-	-	82.1	0.2	-	-	14.1	-	Marl	Wackestone
HEA-127	1.8	-	-	-	84.7	0.7	-	-	12.8	-	Muddy-Limestone	Wackestone
HEA-126	2.2	0.2	-	-	94.1	0.3	-	-	3.2	-	Mudstone	Very fine
HEA-125	3.8	-	-	-	83.9	0.4	-	-	11.9	-	Muddy-Limestone	Wackestone
HEA-124	6.2	-	-	-	89.8	0.4	-	-	3.6	-	Mudstone	Very fine
HEA-123	2.7	-	-	-	77.6	-	-	-	19.7	-	Muddy-Limestone	Wackestone
HEA-122	5.1	-	-	-	90.9	0.7	-	-	3.3	-	Mudstone	Very fine
HEA-121	3.3	-	-	-	79.5	0.6	-	-	16.6	-	Muddy-Limestone	Wackestone
HEA-120	3.7	0.1	-	-	91.9	0.1	-	-	4.2	-	Mudstone	Very fine
HEA-119	4.4	-	-	-	81.7	1.7	-	-	12.2	-	Muddy-Limestone	Wackestone
HEA-118	4.5	-	-	-	92.4	0.2	-	-	2.9	-	Mudstone	Very fine
HEA-117	2.7	-	-	-	84.1	0.3	-	-	12.9	-	Marl	Wackestone
HEA-116	8.2	-	-	-	90	0.4	-	-	1.4	-	Mudstone	Very fine
HEA-115	2.7	-	-	-	85.4	0.1	-	-	11.8	-	Mudstone	Very fine
HEA-114	1.5	-	-	-	59.4	0.1	-	-	39	-	Marl	Packstone
HEA-113	8.4	-	-	-	88.9	0.2	-	-	2.5	-	Mudstone	Very fine
HEA-112	5.2	-	-	-	83.1	0.2	-	-	11.5	-	Marl	Wackestone
HEA-111	7.2	-	-	-	88.6	0.5	-	-	3.7	-	Mudstone	Very fine
HEA-110	0.4	-	2.1	-	57.1	0.3	-	-	39.9	-	Muddy-Limestone	Packstone
HEA-109	6.4	-	-	-	93.1	0.1	-	-	0.4	-	Mudstone	Very fine
HEA-108	4.5	-	-	-	79.7	0.5	-	-	15.3	-	Marl	Wackestone
HEA-107	3.1	-	-	-	84.4	0.2	-	-	12.3	-	Marl	Wackestone
HEA-106	2.4	-	-	-	83.7	0.7	-	-	13.2	-	Marl	Wackestone
HEA-105	15.3	0.2	-	-	83.5	0.1	-	-	0.9	-	Mudstone	Fine
HEA-104	8.9	-	-	-	88.9	0.2	-	-	2	-	Mudstone	Very fine
HEA-103	21	63.3	10.5	3	0.8	0.7	-	-	-	0.4	Sandstone	Litharenite
HEA-102	40.5	35	9.8	1.4	11.4	0.9	-	-	-	0.7	Sandstone	Litharenite
HEA-101	18.3	-	-	-	80.8	0.3	-	-	0.6	-	Mudstone	Fine

Table B6. Point counting data derived from the samples of studied section (all samples).

APPENDIX C

EXPLANATION OF PLATES

PLATE I

(Scale bar = 100 & 10 μm)

Figure 1: *Globotruncanella minuta* KARON & GONZALEZ DONOSO; **a.** spiral side; **b.** side view; **c.** umbilical side, sample no.: HEA 101.

Figure 2: *Globotruncanella pschadae* KELLER; **a.** umbilical side; **b.** side view, sample no.: HEA 104.

Figure 3: *Contusotruncana fornicata* PLUMMER; **a.** spiral side; **b.** side view, sample no.: HEA 101.

Figure 4: *Gansserina gansseri* BOLLI; **a.** spiral side; **b.** side view, sample no.: HEA 101.

Figure 5: *Gansserina gansseri* BOLLI; **a.** spiral side; **b.** side view, sample no.: HEA 101.

PLATE I

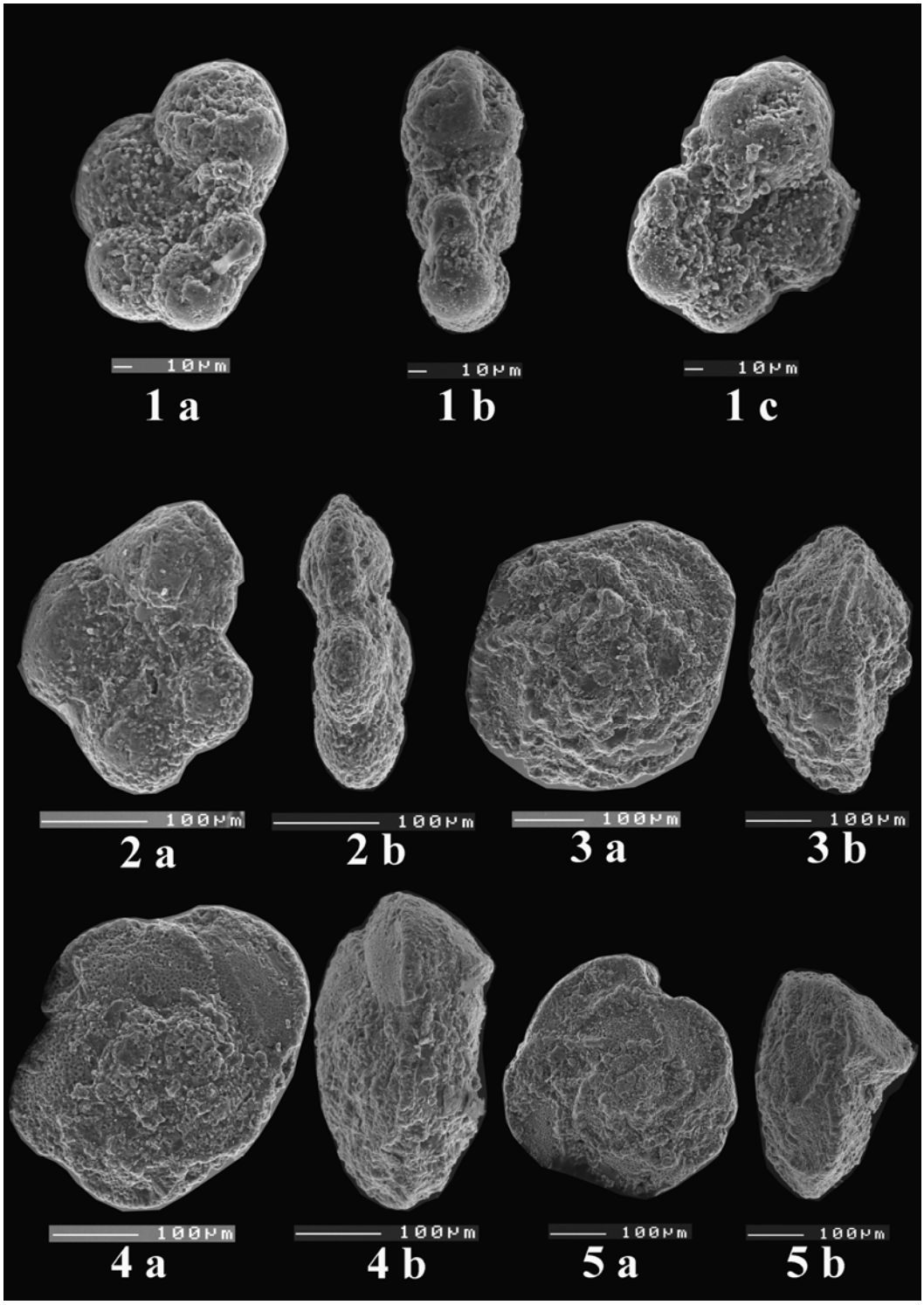
10µm
1 a
10µm
1 b
10µm
1 c
100µm
2 a
100µm
2 b
100µm
3 a
100µm
3 b
100µm
4 a
100µm
4 b
100µm
5 a
100µm
5 b

PLATE II

(Scale bar = 100 μm)

Figure 1: *Gansserina wiedenmayeri* GANDOLFI; **a.** spiral side; **b.** side view; **c.** umbilical side, sample no.: HEA 101.

Figure 2: *Globotruncana aegyptiaca* NAKKADY; **a.** spiral side; **b.** side view, sample no.: HEA 104.

Figure 3: *Globotruncana aegyptiaca* NAKKADY; **a.** spiral side; **b.** side view, sample no.: HEA 101.

Figure 4: *Globotruncana arca* CUSHMAN; **a.** spiral side; **b.** side view, sample no.: HEA 101.

Figure 5: *Globotruncana linneiana* D'ORBIGNY; **a.** spiral side; **b.** side view, sample no.: HEA 101.

PLATE II

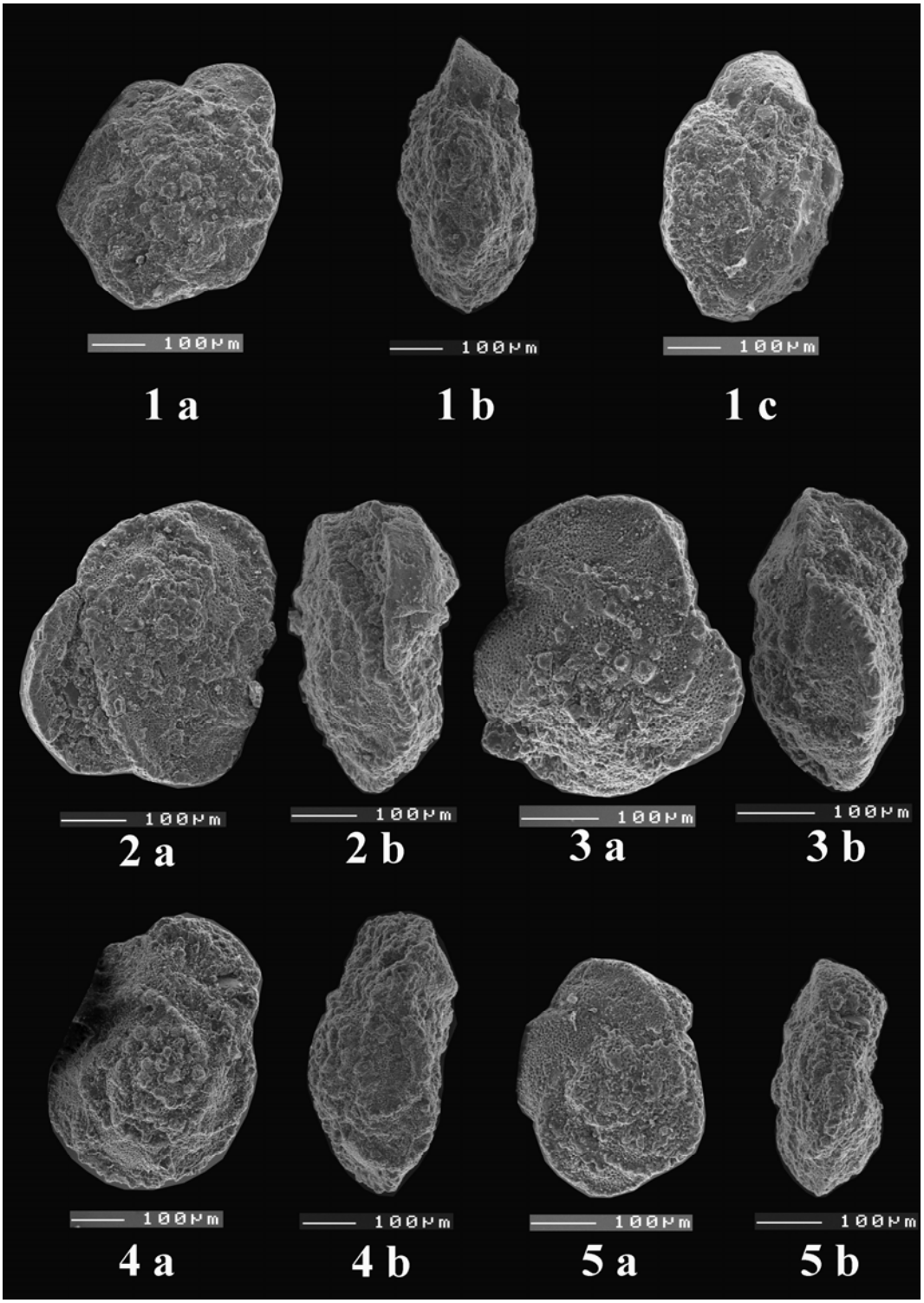
100µm
1 a
100µm
1 b
100µm
1 c
100µm
2 a
100µm
2 b
100µm
3 a
100µm
3 b
100µm
4 a
100µm
4 b
100µm
5 a
100µm
5 b

PLATE III

(Scale bar = 100 μm)

Figure 1: *Globotruncana mariei* BANNER and BLOW; **a.** spiral side; **b.** side view, sample no.: HEA 101.

Figure 2: *Globotruncanita conica* WHITE; **a.** spiral side; **b.** side view, sample no.: HEA 101.

Figure 3: *Globotruncanita conica* WHITE; **a.** spiral side; **b.** side view; **c.** umbilical side, sample no.: HEA 105.

Figure 4: *Globotruncanita stuartiformis* DALBIEZ; **a.** spiral side; **b.** side view; **c.** umbilical side, sample no.: HEA 105.

PLATE III

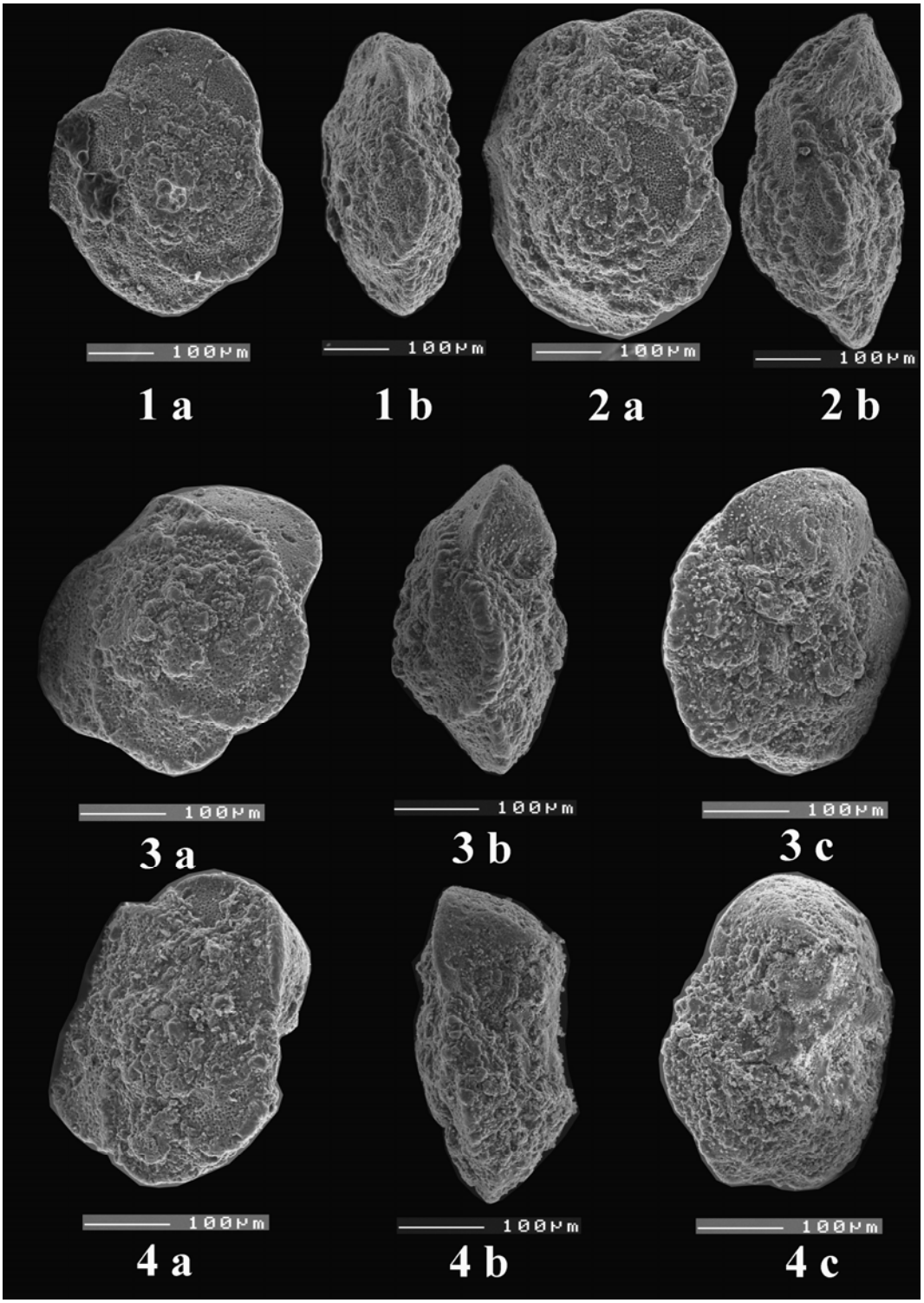
100µm
1 a
100µm
1 b
100µm
2 a
100µm
2 b
100µm
3 a
100µm
3 b
100µm
3 c
100µm
4 a
100µm
4 b
100µm
4 c

PLATE IV

(Scale bar = 100 μm)

Figure 1: *Archaeoglobigerina blowi* PESSAGNO; **a.** spiral side; **b.** side view, sample no.: HEA 101.

Figure 2: *Rugoglobigerina hexacamerata* BRONNIMANN; **a.** spiral side; **b.** side view, sample no.: HEA 101.

Figure 3: *Rugoglobigerina macrocephala* BRONNIMANN; **a.** spiral side; **b.** side view, sample no.: HEA 101.

Figure 4: *Rugoglobigerina milamensis* SMITH & PESSAGNO; **a.** spiral side; **b.** side view, sample no.: HEA 104.

Figure 5: *Rugoglobigerina rugosa* PLUMMER; **a.** spiral side; **b.** side view, sample no.: HEA 104.

PLATE IV

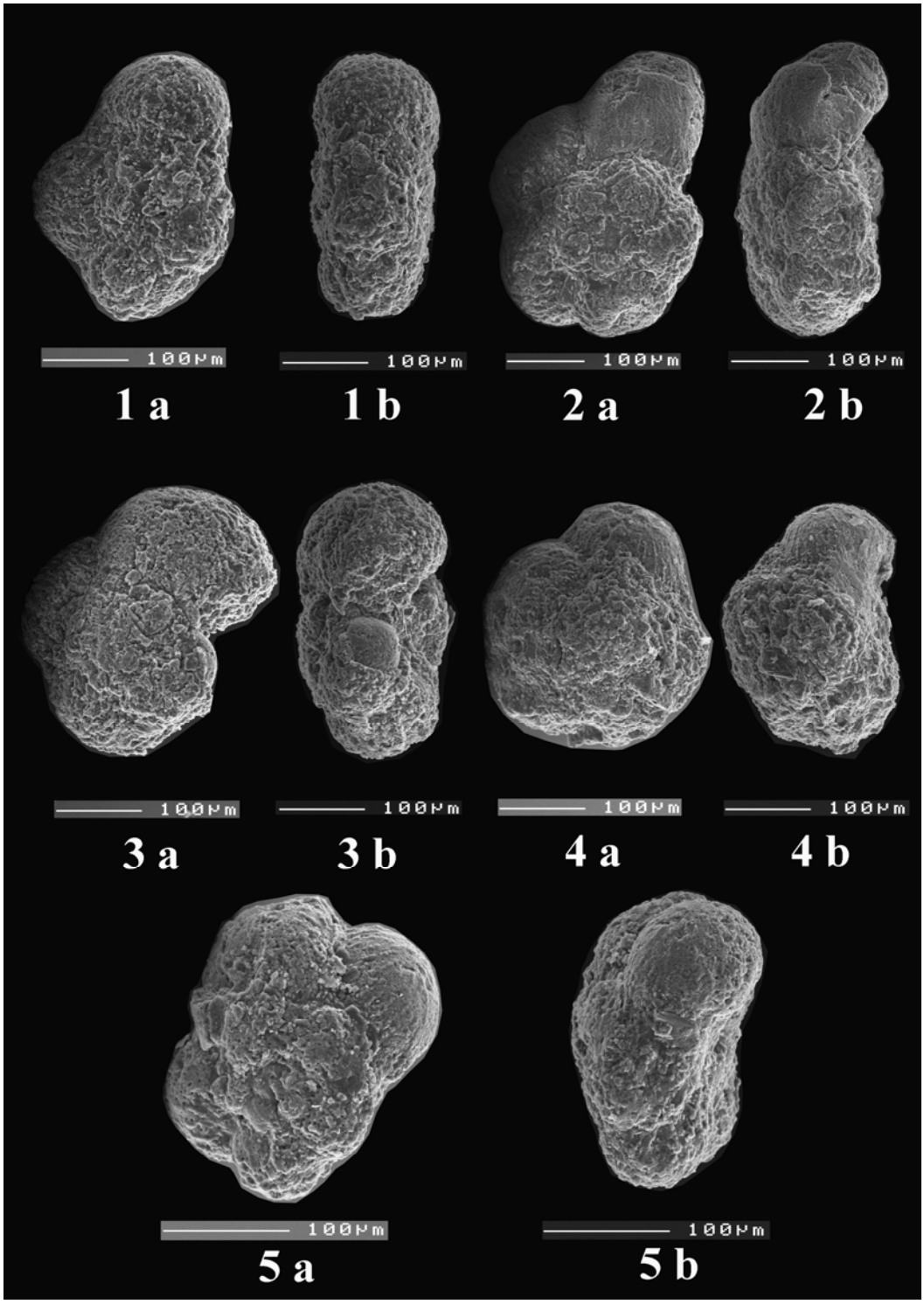
100µm
1 a
100µm
1 b
100µm
2 a
100µm
2 b
100µm
3 a
100µm
3 b
100µm
4 a
100µm
4 b
100µm
5 a
100µm
5 b

PLATE V

(Scale bar = 100 μm)

Figure 1: *Trinitella scotti* BRONNIMANN; **a.** spiral side; **b.** side view; **c.** umbilical side, sample no.: HEA 101.

Figure 2: *Heterohelix globulosa* EHRENBERG; sample no.: HEA 101

Figure 3: *Heterohelix globulosa* EHRENBERG; sample no.: HEA 101

Figure 4: *Heterohelix labellosa* NEDERBRAGT; sample no.: HEA 101

Figure 5: *Heterohelix planata* CUSHMAN; sample no.: HEA 101

Figure 6: *Heterohelix punctulata* CUSHMAN; sample no.: HEA 101

Figure 7: *Heterohelix punctulata* CUSHMAN; sample no.: HEA 101

Figure 8: *Heterohelix punctulata* CUSHMAN; sample no.: HEA 101

Figure 9: *Heterohelix striata* EHRENBERG; sample no.: HEA 104

Figure 10: *Heterohelix striata* EHRENBERG; sample no.: HEA 101

PLATE V

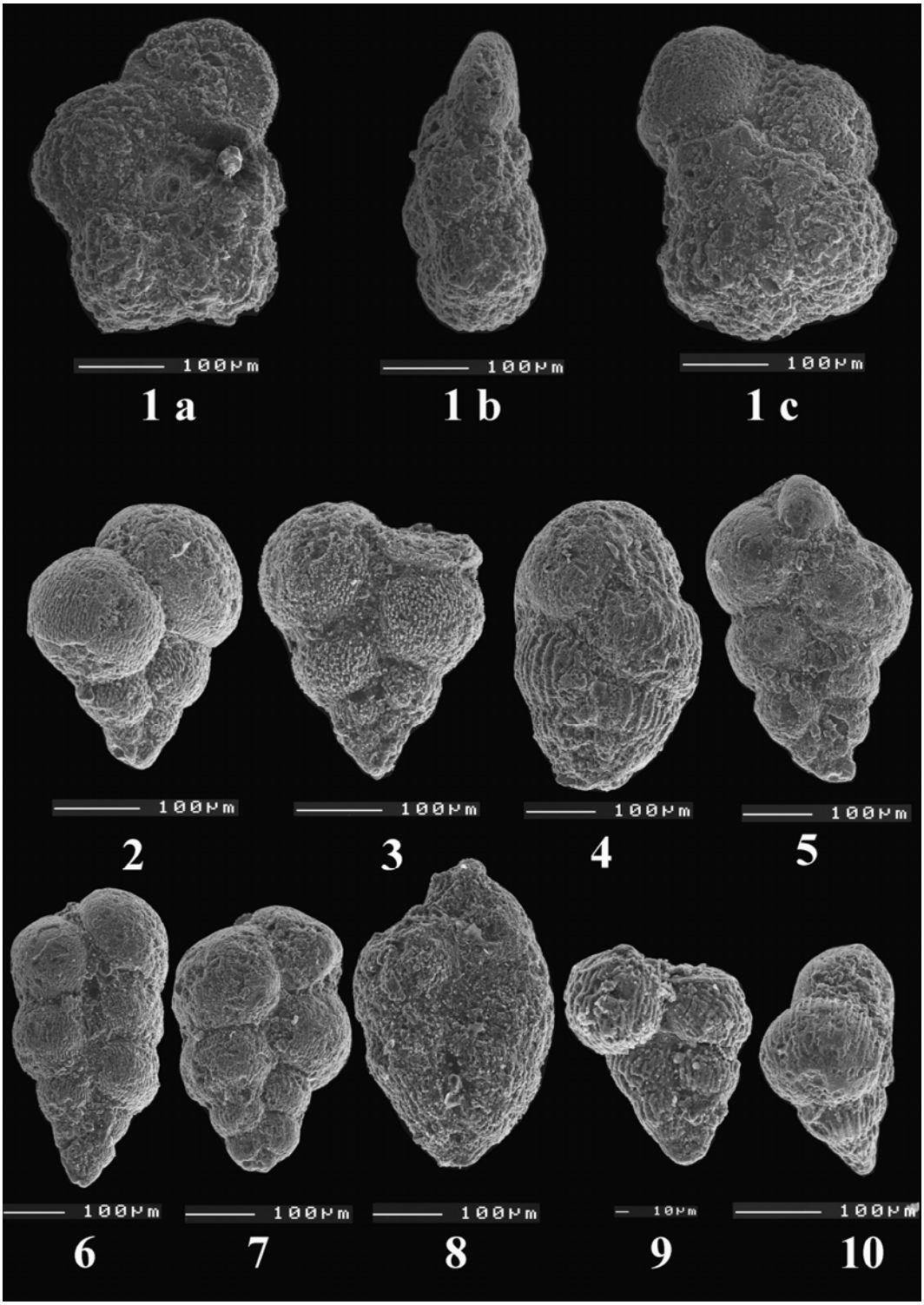
100µm
1 a
100µm
1 b
100µm
1 c
100µm
2
100µm
3
100µm
4
100µm
5
100µm
6
100µm
7
100µm
8
10µm
9
100µm
10

PLATE VI

(Scale bar = 100 μm)

Figure 1: *Laeviheterohelix dentata* STENESTAD; sample no.: HEA 101

Figure 2: *Laeviheterohelix dentata* STENESTAD; sample no.: HEA 104

Figure 3: *Planoglobulina acervulinoides* EGGER; sample no.: HEA 101

Figure 4: *Planoglobulina acervulinoides* EGGER; sample no.: HEA 101

Figure 5: *Pseudotextularia elegans* RZEHAK; sample no.: HEA 101

Figure 6: *Pseudotextularia elegans* RZEHAK; sample no.: HEA 101

Figure 7 (a, b): *Pseudotextularia nuttalli* VOORWIJK; sample no.: HEA 101

Figure 8: *Racemiguembelina fructicosa* EGGER; sample no.: HEA 101

Figure 9: *Pseudoguembelina hariaensis* NEDERBRAGT; sample no.: HEA 101

Figure 10 (a, b): *Pseudoguembelina hariaensis* NEDERBRAGT; sample no.: HEA 101

PLATE VI

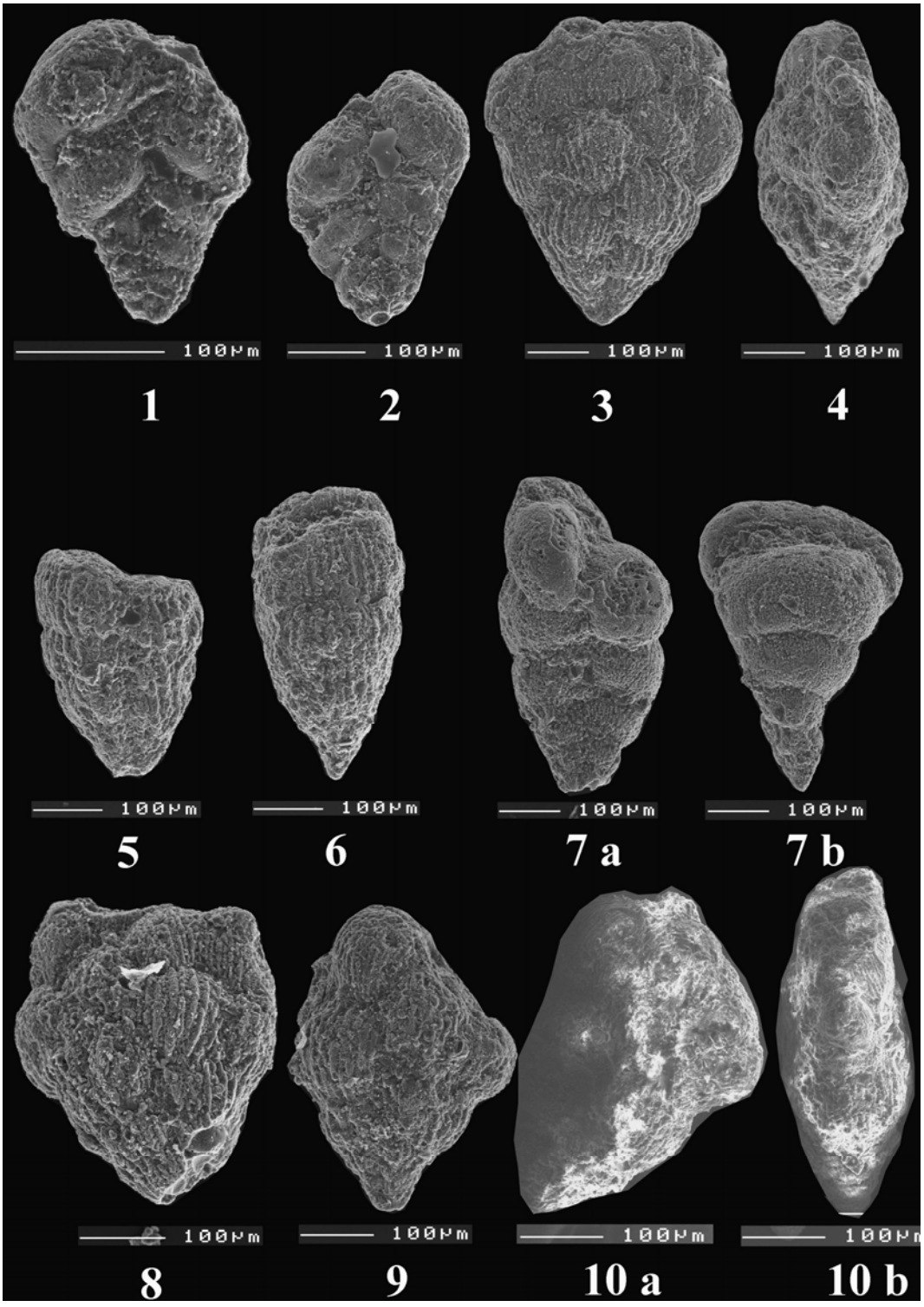

PLATE VII

(Scale bar = 100 μm)

Figure 1: *Globigerinelloides prairiehillensis* PESSAGNO; **a.** spiral side; **b.** side view, sample no.: HEA 101.

Figure 2: *Globotruncana mariei* BANNER and BLOW; **a.** spiral side; **b.** side view, sample no.: HEA 101.

Figure 3: *Chiloguembelina crinita* GLAESSNER; sample no.: HEA 10

Figure 4 (a, b): *Chiloguembelina midwayensis* CUSHMAN; sample no.: HEA 115

Figure 5: *Chiloguembelina morsei* KLINE; sample no.: HEA 106

Figure 6: *Chiloguembelina morsei* KLINE; sample no.: HEA 109

Figure 7: *Chiloguembelina morsei* KLINE; sample no.: HEA 111

PLATE VII

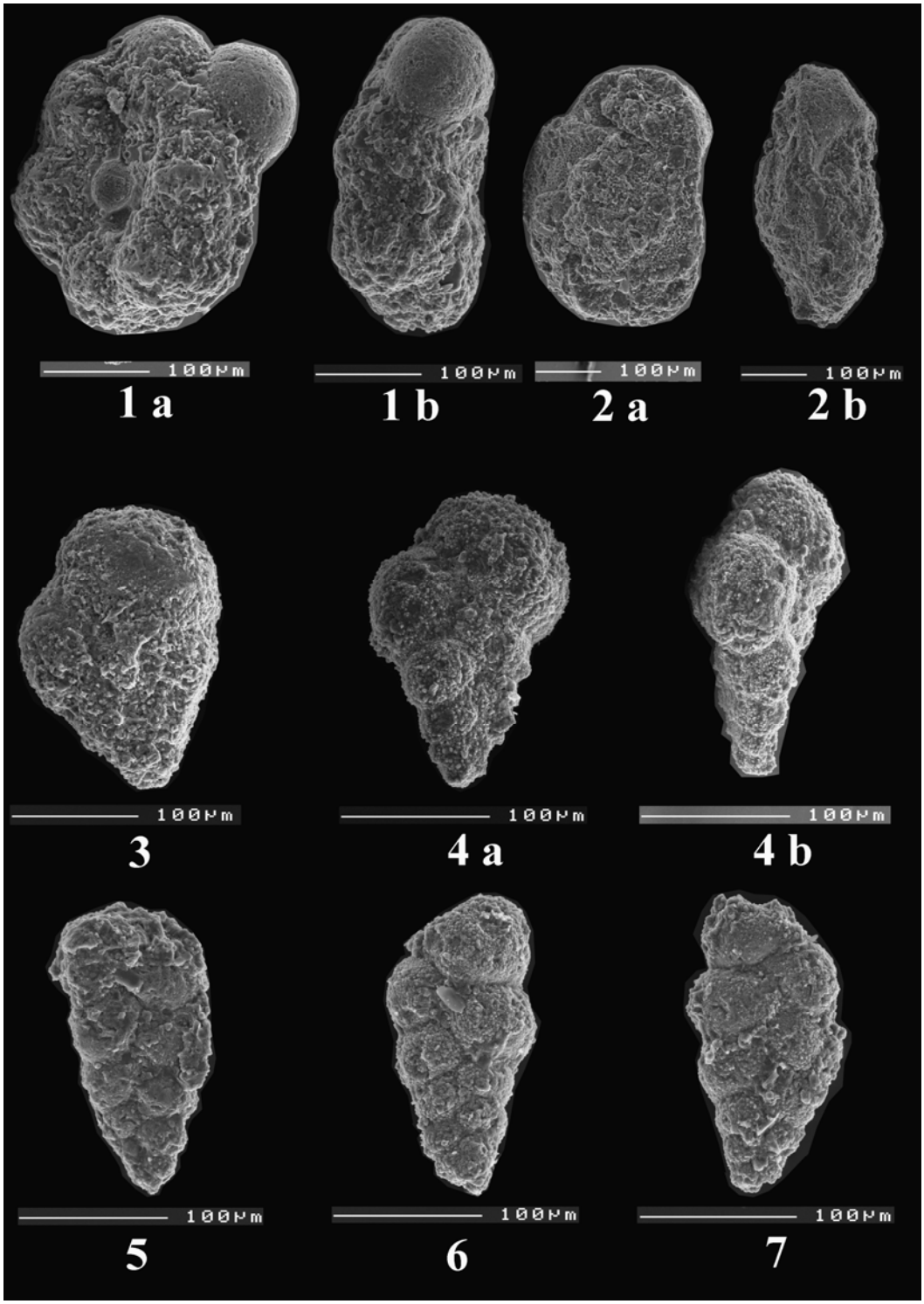
100µm
1 a
100µm
1 b
100µm
2 a
100µm
2 b
100µm
3
100µm
4 a
100µm
4 b
100µm
5
100µm
6
100µm
7

PLATE VIII

(Scale bar = 100 μm)

Figure 1: *Chiloguembelina subtriangularis* Beckmann; sample no.: HEA 122

Figure 2 (?): *Chiloguembelina subtriangularis* Beckmann; sample no.: HEA 132

Figure 3: *Eoglobigerina edita* SUBBOTINA; **a.** spiral side; **b.** side view; **c.** umbilical side, sample no.: HEA 109

Figure 4: *Eoglobigerina eobulloides* MOROZOVA; **a.** spiral side; **b.** side view; **c.** umbilical side, sample no.: HEA 122

Figure 5: *Eoglobigerina spiralis* BOLLI; **a.** spiral side; **b.** side view; **c.** umbilical side, sample no.: HEA 132

PLATE VIII

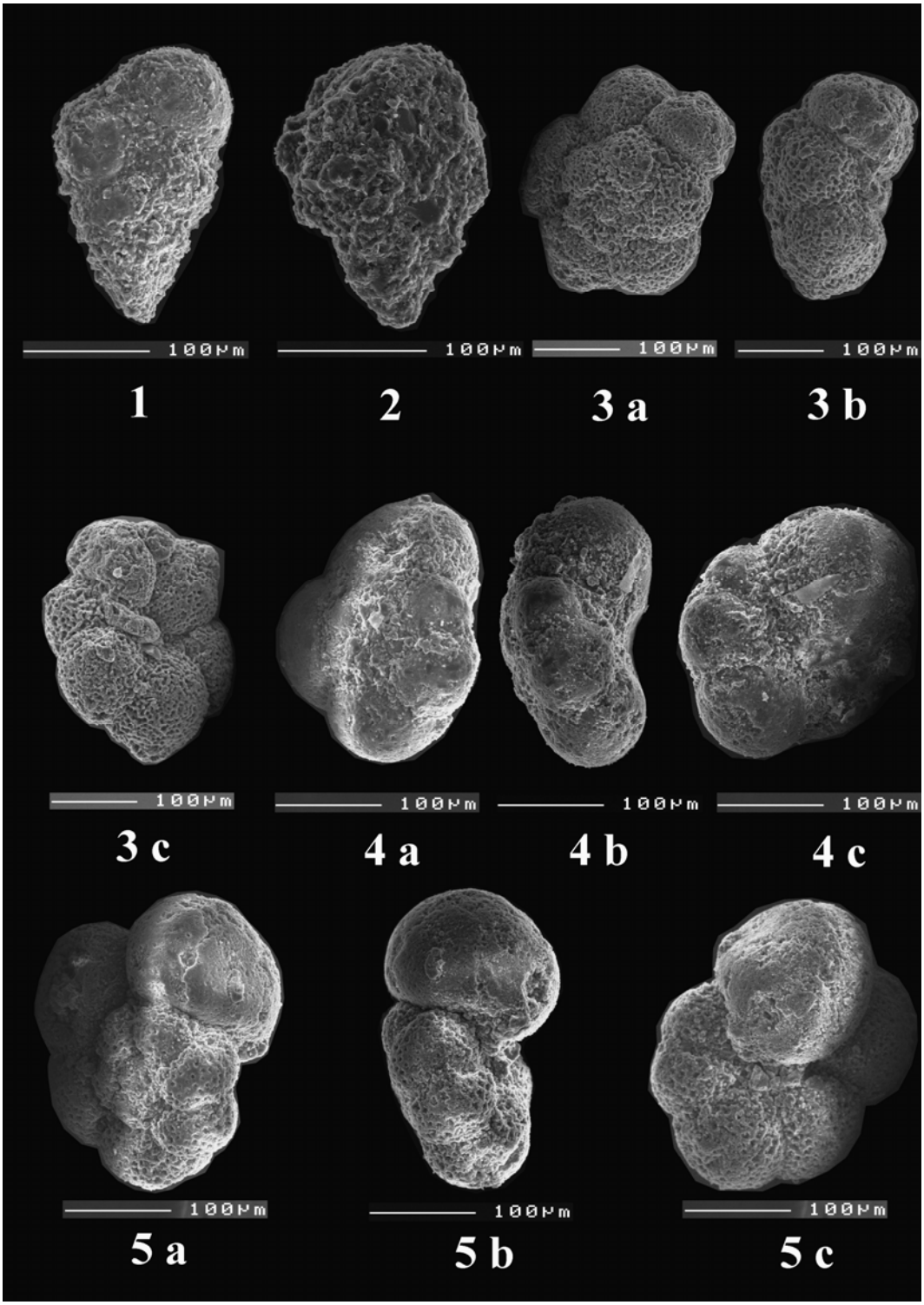

PLATE IX

(Scale bar = 100 μm)

Figure 1: *Parasubbotina pseudobulloides* PLUMMER; **a.** spiral side; **b.** side view; **c.** umbilical side, sample no.: HEA 132

Figure 2: *Parasubbotina variospira* BELFORD; **a.** spiral side; **b.** side view; **c.** umbilical side, sample no.: HEA 146

Figure 3: *Parasubbotina variospira* BELFORD; **a.** spiral side; **b.** side view; **c.** umbilical side, sample no.: HEA 146

PLATE IX

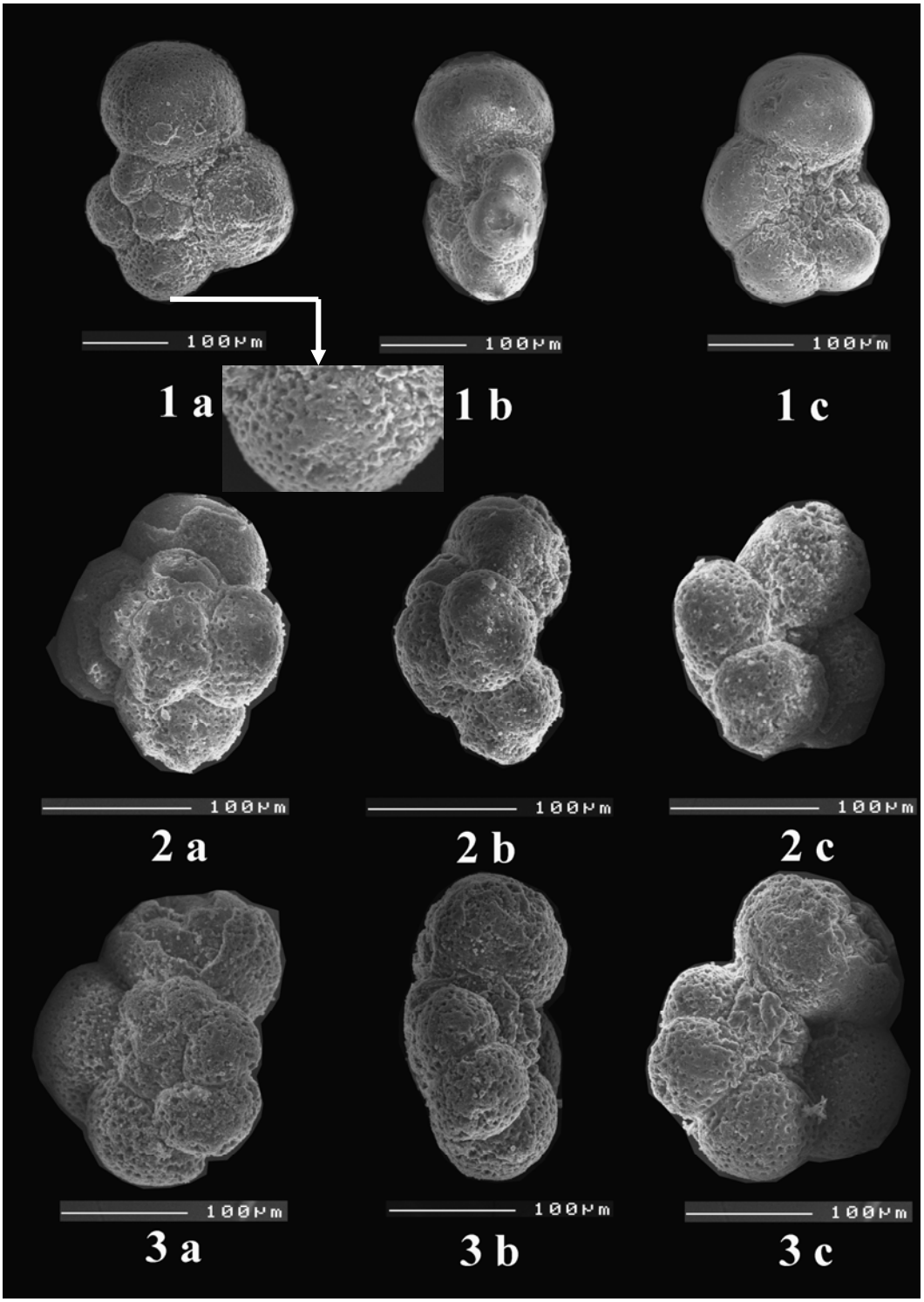

PLATE X

(Scale bar = 100 μm)

Figure 1: *Subbotina cancellata* BLOW; **a.** spiral side; **b.** side view; **c.** umbilical side, sample no.: HEA 132

Figure 2: *Subbotina triangularis* WHITE; **a.** spiral side; **b.** side view; **c.** umbilical side, sample no.: HEA 146

Figure 3: *Subbotina triloculinoides* PLUMMER; **a.** spiral side; **b.** side view; **c.** umbilical side, sample no.: HEA 132

PLATE X

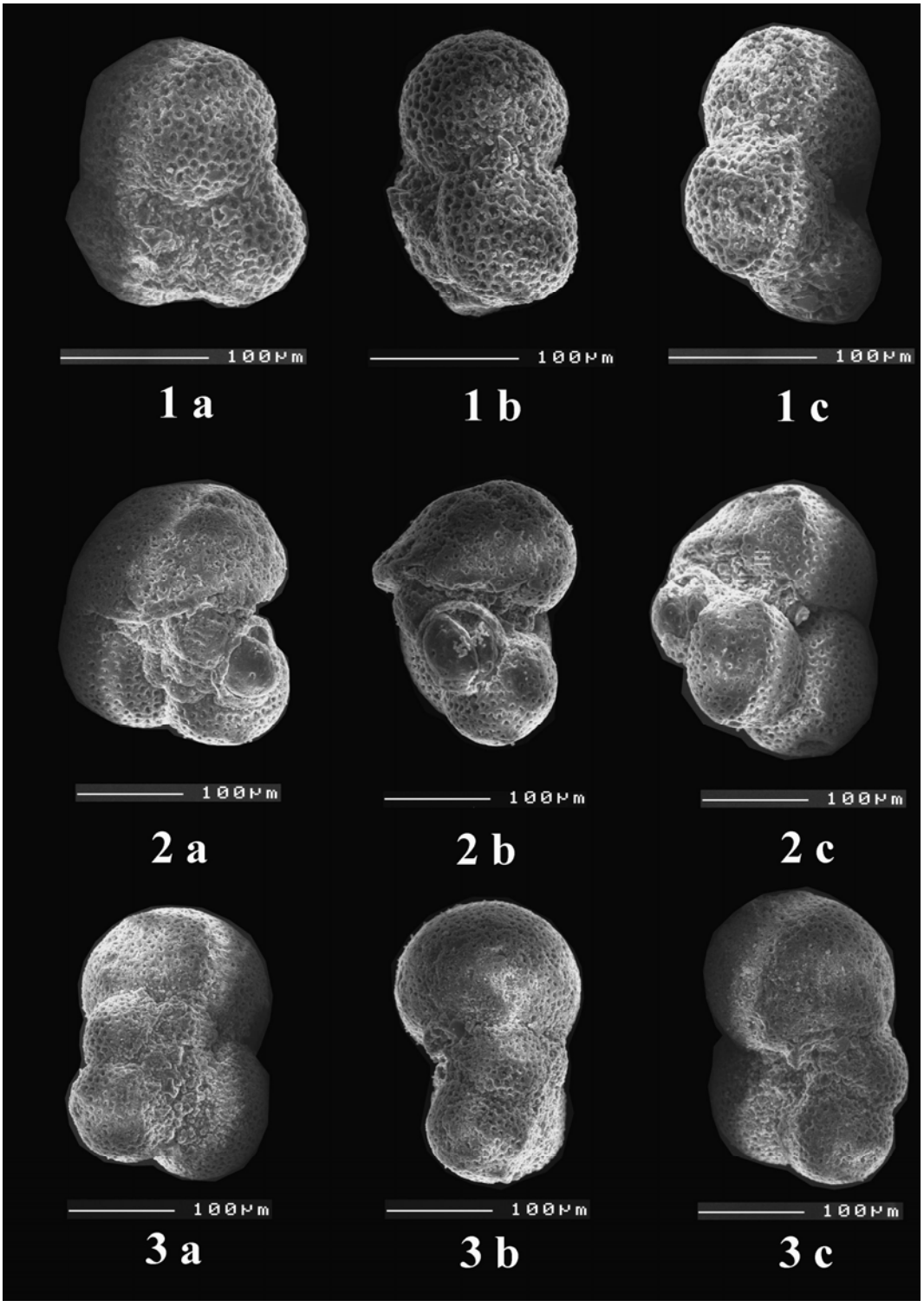
100µm
1 a
100µm
1 b
100µm
1 c
100µm
2 a
100µm
2 b
100µm
2 c
100µm
3 a
100µm
3 b
100µm
3 c

PLATE XI

(Scale bar = 100 & 10 μm)

Figure 1: *Subbotina trivialis* SUBBOTINA; **a.** spiral side; **b.** side view; **c.** umbilical side, sample no.: HEA 109

Figure 2: *Subbotina velascoensis* CUSHMAN; **a.** spiral side; **b.** side view; **c.** umbilical side, sample no.: HEA 152

Figure 3: *Globoconusa daubjergensis* BRONNIMANN; spiral side, sample no.: HEA 108

Figure 4: *Guembelitria cretacea* CUSHMAN; sample no.: HEA 107

Figure 5: *Guembelitria cretacea* CUSHMAN; sample no.: HEA 107

PLATE XI

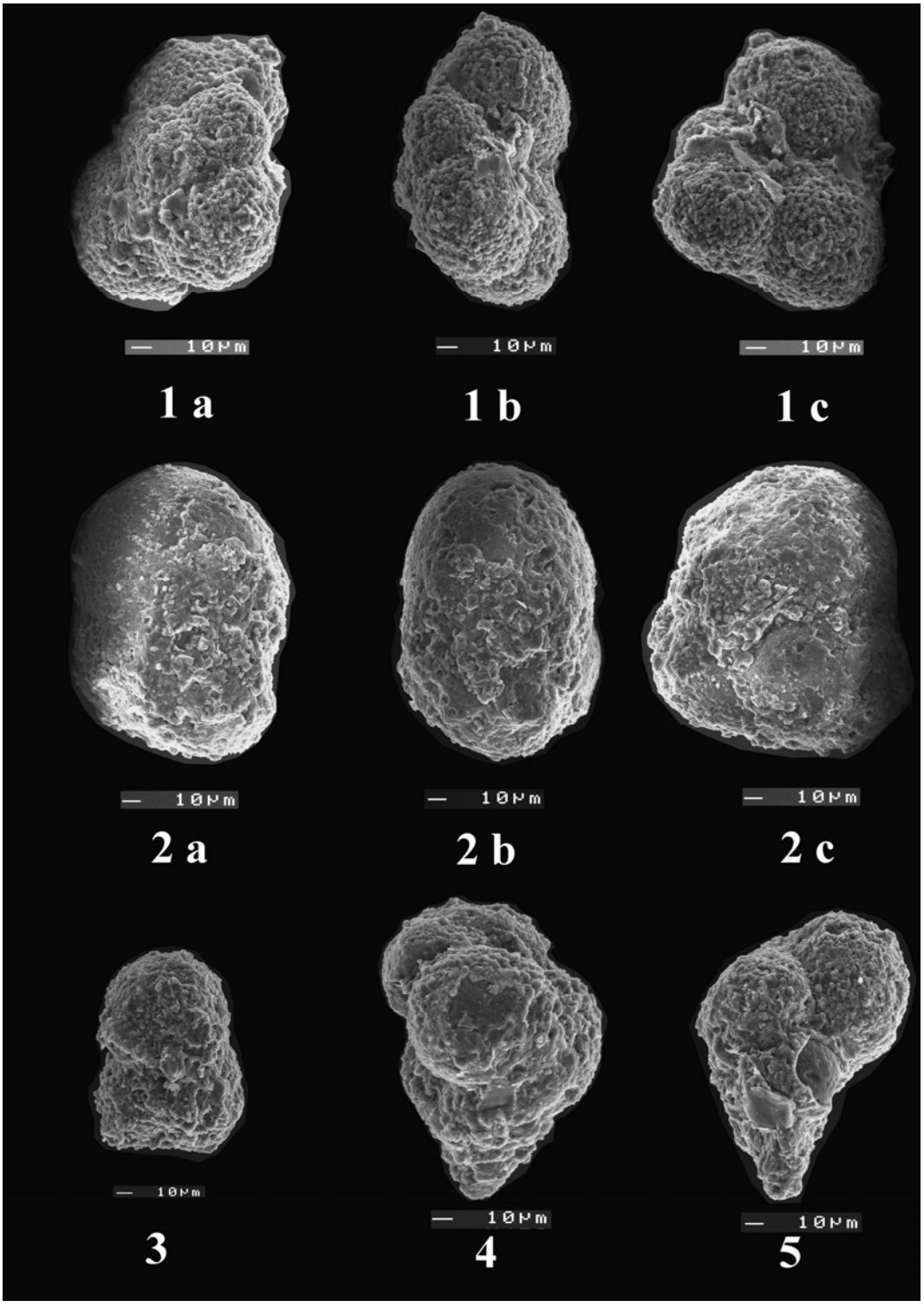
10µm
1 a
10µm
1 b
10µm
1 c
10µm
2 a
10µm
2 b
10µm
2 c
10µm
3
10µm
4
10µm
5

PLATE XII

(Scale bar = 100 & 10 μm)

Figure 1: *Parvularugoglobigerina alabamensis* LIU AND OLSSON; **a.** spiral side; **b.** side view, sample no.: HEA 126

Figure 2: *Parvularugoglobigerina eugubina* LUTERBACHER AND PREMOLI SILVA; **a.** spiral side; **b.** side view; **c.** umbilical side, sample no.: HEA 107

Figure 3: *Parvularugoglobigerina eugubina* LUTERBACHER AND PREMOLI SILVA; **a.** spiral side; **b.** side view; **c.** umbilical side, sample no.: HEA 106

PLATE XII

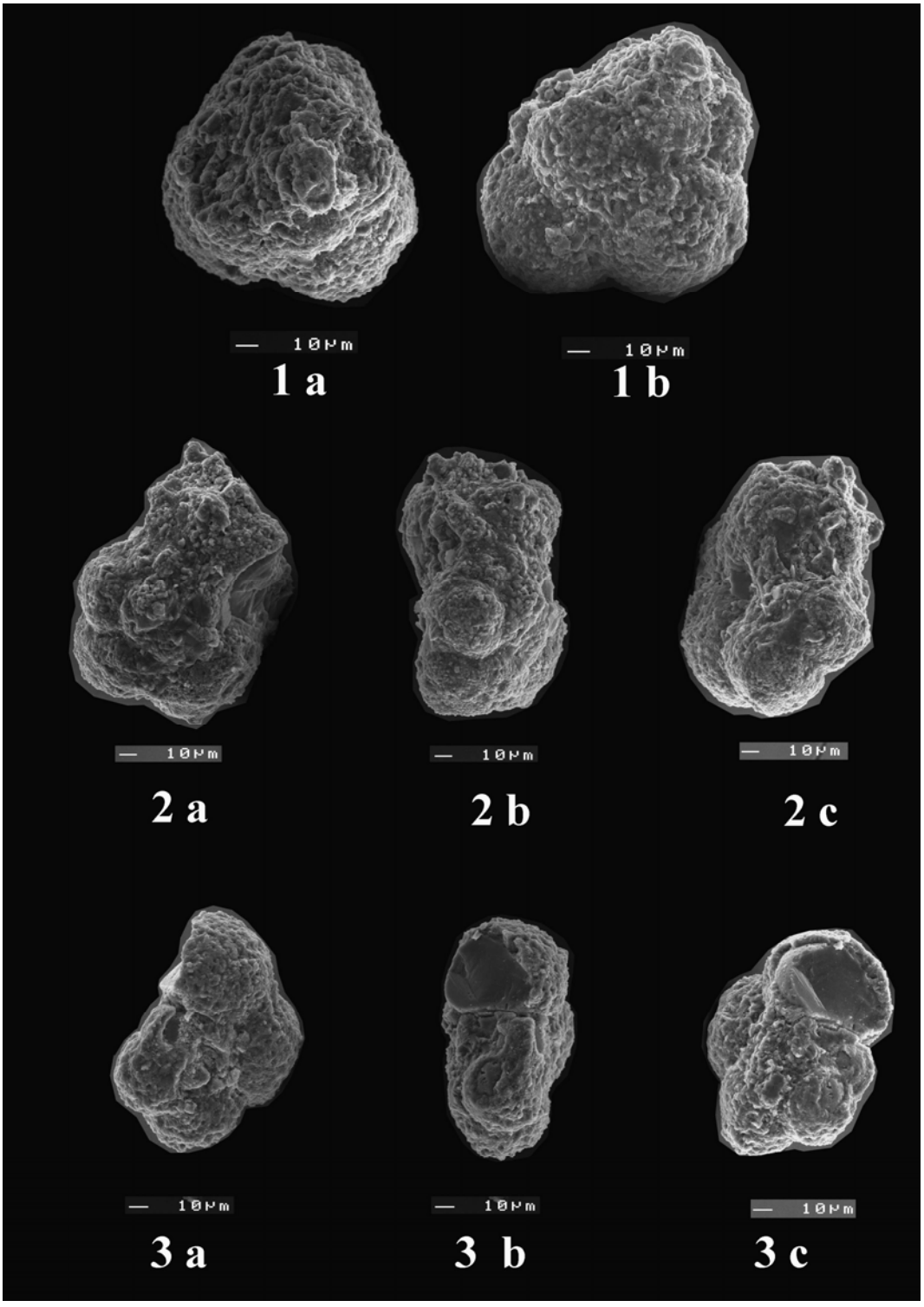

PLATE XIII

(Scale bar = 10 μm)

Figure 1: *Parvularugoglobigerina eugubina* LUTERBACHER AND PREMOLI SILVA; **a.** spiral side; **b.** side view; **c.** umbilical side, sample no.: HEA 107

Figure 2: *Parvularugoglobigerina extensa* BLOW; **a.** spiral side; **b.** side view; **c.** umbilical side, sample no.: HEA 109

Figure 3: *Woodringina claytonensis* LOEBLICH and TAPPAN; sample no.: HEA 106

Figure 4: *Woodringina claytonensis* LOEBLICH and TAPPAN; sample no.: HEA 108

Figure 5: *Woodringina claytonensis* LOEBLICH and TAPPAN; sample no.: HEA 108

Figure 6: *Woodringina claytonensis* LOEBLICH and TAPPAN; sample no.: HEA 109

Figure 7: *Woodringina hornerstownensis* OLSSON; sample no.: HEA 109

Figure 8: *Woodringina hornerstownensis* OLSSON; sample no.: HEA 109

Figure 9: *Globanomalina chapmani* PARR; **a.** spiral side; **b.** side view; **c.** umbilical side, sample no.: HEA 8

PLATE XIII

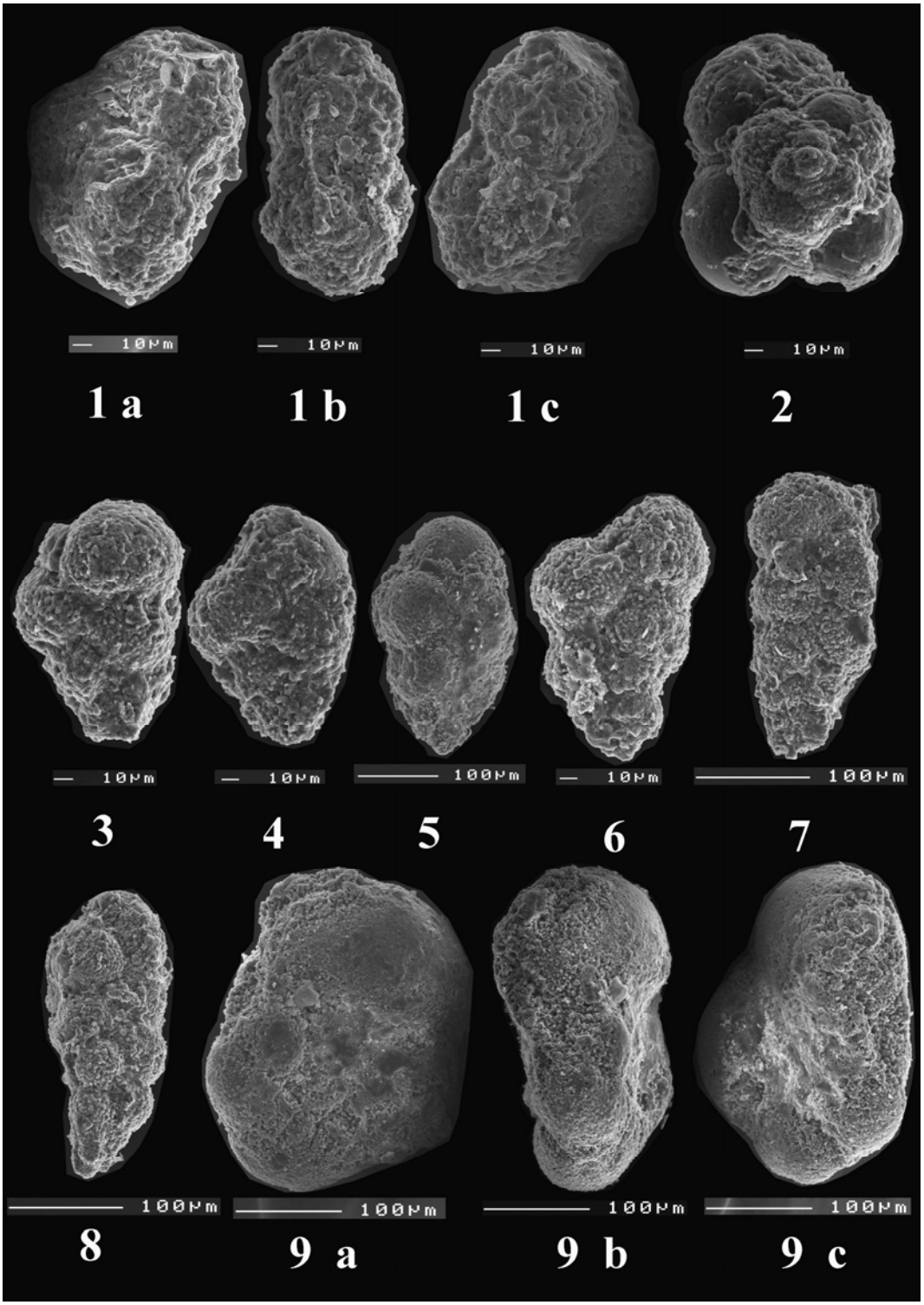
10µm
1 a
10µm
1 b
10µm
1 c
10µm
2
10µm
3
10µm
4
100µm
5
10µm
6
100µm
7
100µm
8
100µm
9 a
100µm
9 b
100µm
9 c

PLATE XIV

(Scale bar = 100 μm)

Figure 1: *Globanomalina compressa* PLUMMER; **a.** spiral side; **b.** side view; **c.** umbilical side, sample no.: HEA 137

Figure 2: *Globanomalina ehrenbergi* BOLLI; **a.** spiral side; **b.** side view; **c.** umbilical side, sample no.: HEA 137

Figure 3: *Globanomalina imitata* SUBBOTINA; **a.** spiral side; **b.** side view; **c.** umbilical side, sample no.: HEA 142

PLATE XIV

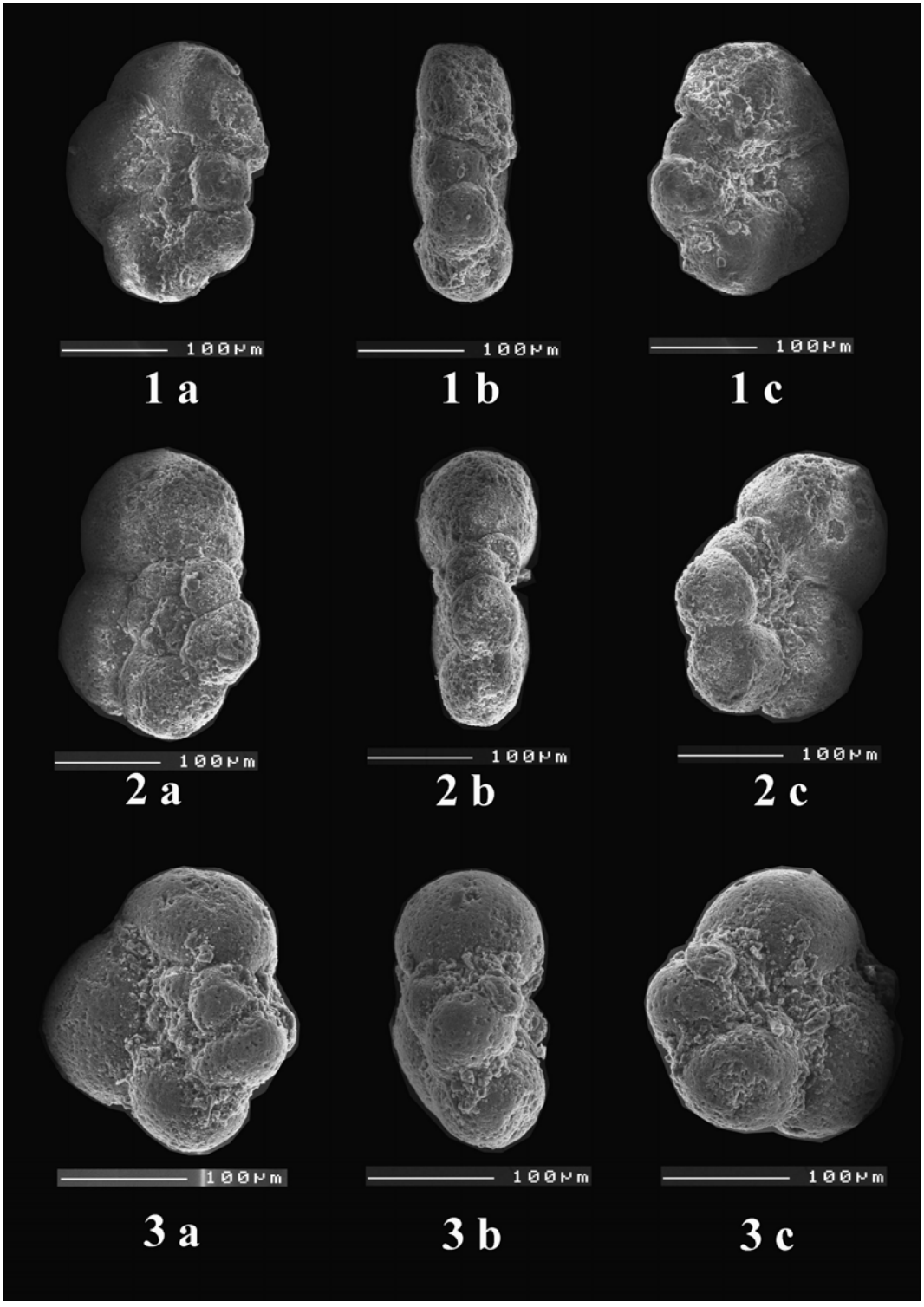
100µm
1 a
100µm
1 b
100µm
1 c
100µm
2 a
100µm
2 b
100µm
2 c
100µm
3 a
100µm
3 b
100µm
3 c

PLATE XV

(Scale bar = 100 μm)

Figure 1: *Globanomalina ovalis* HAQUE; **a.** spiral side; **b.** side view; **c.** umbilical side, sample no.: HEA 14

Figure 2: *Globanomalina planocompressa* SHUTSKAYA; **a.** spiral side; **b.** side view; **c.** umbilical side, sample no.: HEA 107

Figure 3: *Globanomalina pseudomenardii* BOLLI; **a.** spiral side; **b.** side view, sample no.: HEA 10

PLATE XV

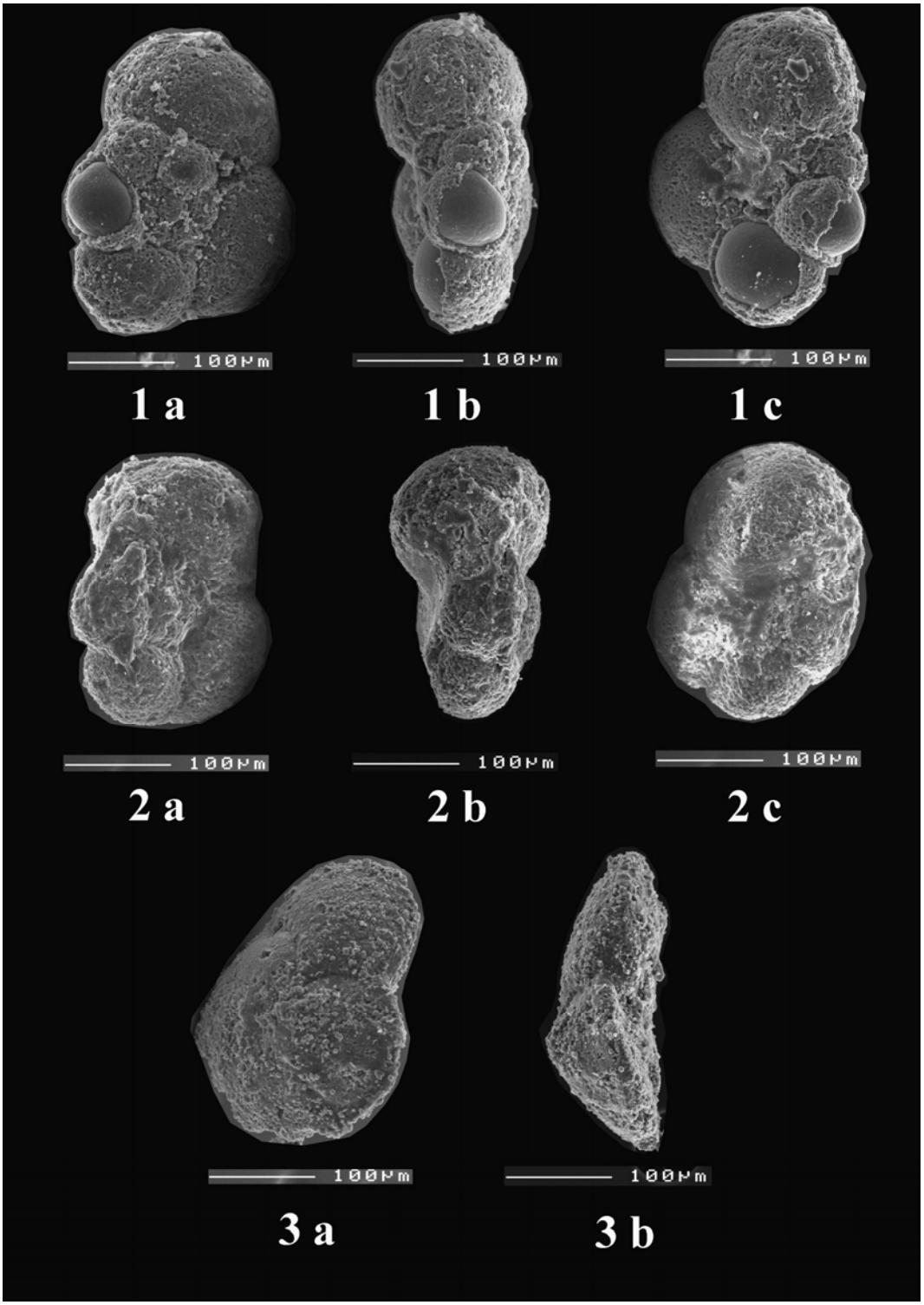
100µm
1 a
100µm
1 b
100µm
1 c
100µm
2 a
100µm
2 b
100µm
2 c
100µm
3 a
100µm
3 b

PLATE XVI

(Scale bar = 100 & 10 μm)

Figure 1: *Hedbergella holmdelensis* OLSSON; **a.** spiral side; **b.** side view; **c.** umbilical side, sample no.: HEA 106

Figure 2: *Zeauvigerina waiparaensis* JENKINS; sample no.: HEA 106

Figure 3: *Zeauvigerina waiparaensis* JENKINS; sample no.: HEA 106

Figure 4: *Zeauvigerina waiparaensis* JENKINS; sample no.: HEA 107

Figure 5: *Zeauvigerina virgata* KHALILOV; sample no.: HEA 116

Figure 6: *Zeauvigerina virgata* KHALILOV; sample no.: HEA 137

Figure 7: *Igorina albeari* CUSHMAN AND BERMUDEZ; **a.** spiral side; **b.** side view; **c.** umbilical side, sample no.: HEA 152

PLATE XVI

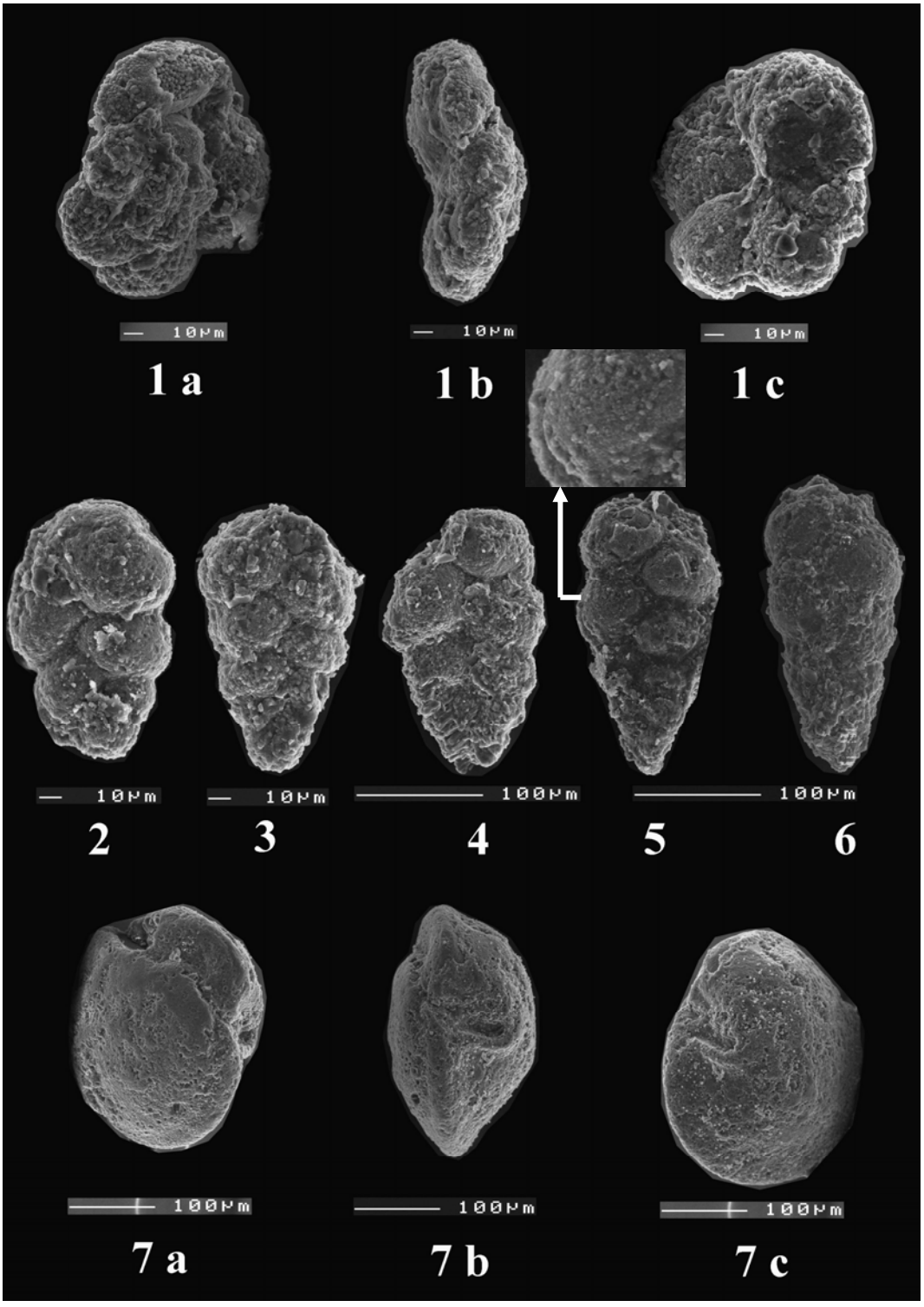
10µm
1 a
10µm
1 b
10µm
1 c
10µm
2
10µm
3
100µm
4
100µm
5
6
100µm
7 a
100µm
7 b
100µm
7 c

PLATE XVII

(Scale bar = 100 & 10 μm)

Figure 1: *Igorina tadjikistanensis* BYKOVA; **a.** spiral side; **b.** side view; **c.** umbilical side, sample no.: HEA 152

Figure 2: *Morozovella angulata* WHITE; **a.** spiral side; **b.** side view; **c.** umbilical side, sample no.: HEA 146

Figure 3: *Morozovella praeangulata* BLOW; **a.** spiral side; **b.** side view; **c.** umbilical side, sample no.: HEA 140

PLATE XVII

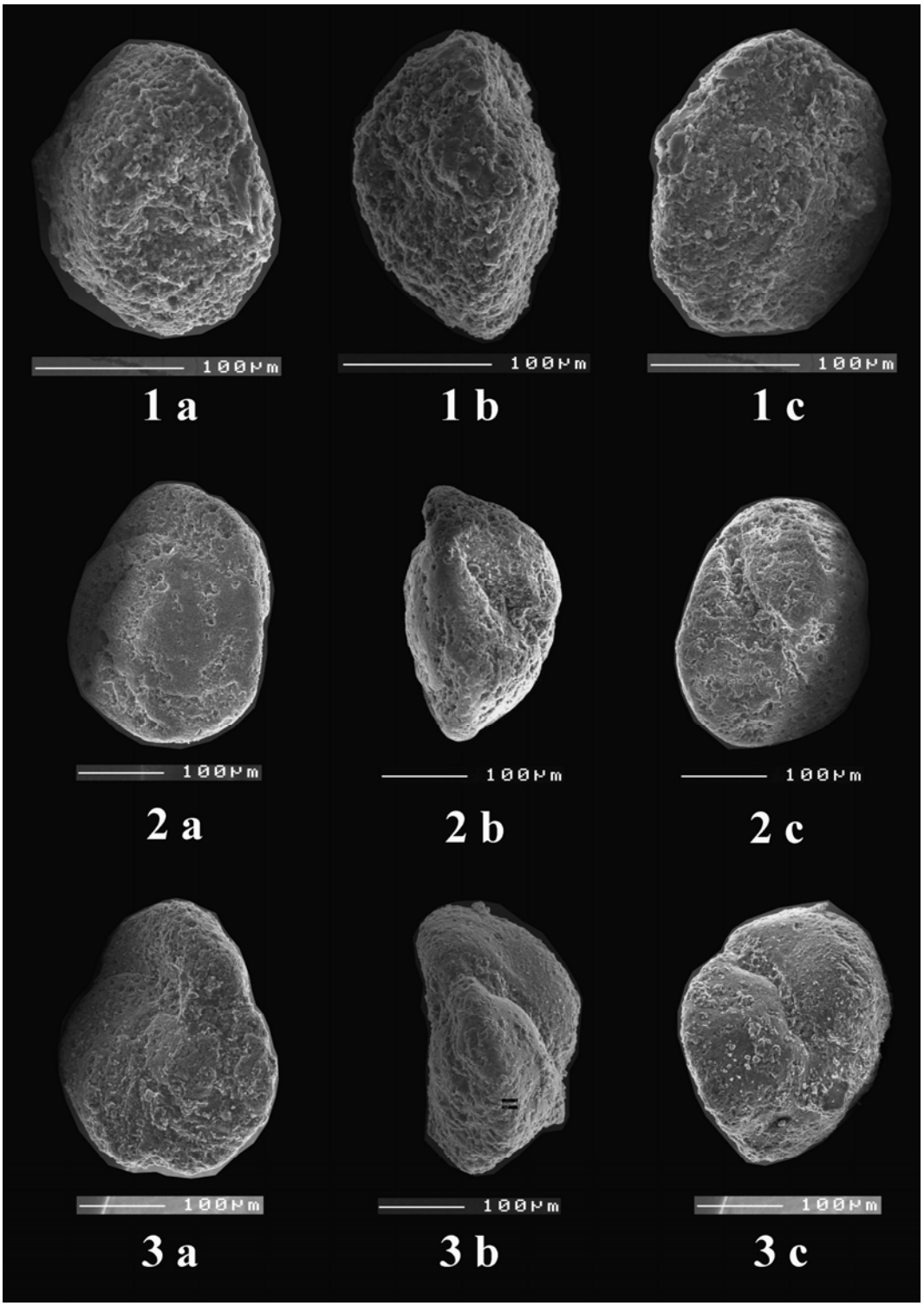
100µm
1 a
100µm
1 b
100µm
1 c
100µm
2 a
100µm
2 b
100µm
2 c
100µm
3 a
100µm
3 b
100µm
3 c

PLATE XVIII

(Scale bar = 100 & 10 μm)

Figure 1: *Praemurica inconstans* SUBBOTINA; **a.** spiral side; **b.** side view; **c.** umbilical side, sample no.: HEA 122

Figure 2: *Praemurica inconstans* SUBBOTINA; **a.** spiral side; **b.** side view; **c.** umbilical side, sample no.: HEA 144

Figure 3: *Praemurica pseudoinconstans* BLOW; **a.** spiral side; **b.** umbilical side, sample no.: HEA 109

Figure 4: *Praemurica uncinata* BOLLI; **a.** spiral side; **b.** side view; **c.** umbilical side, sample no.: HEA 142

PLATE XVIII

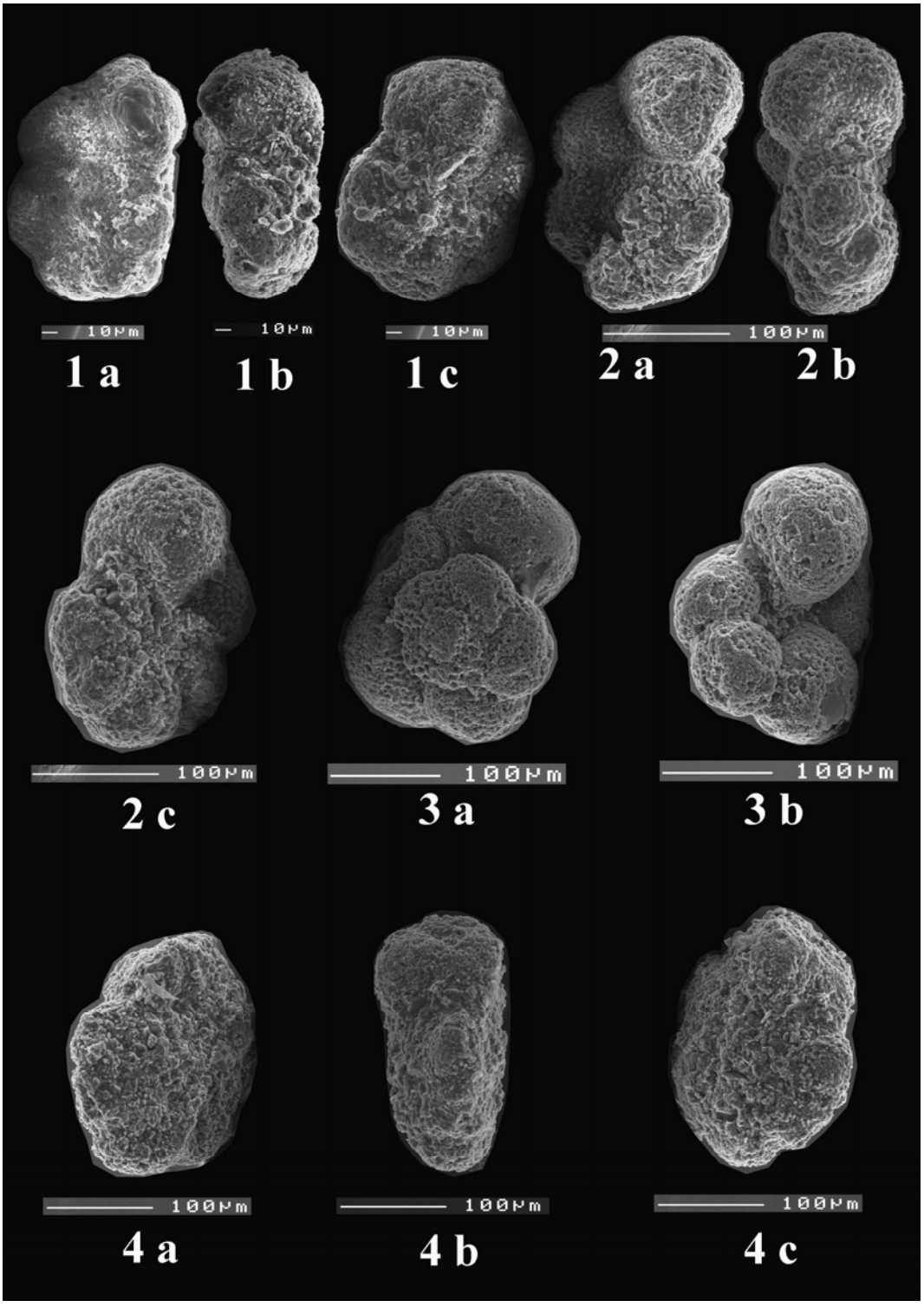
10µm
1 a
10µm
1 b
10µm
1 c
100µm
2 a
2 b
100µm
2 c
100µm
3 a
100µm
3 b
100µm
4 a
100µm
4 b
100µm
4 c